MONTPELLIER SUPAGRO
Ecole Doctorale SIBAGHE – Biologie Intégrative des Plantes

THESE DE DOCTORAT
présentée par :

François VASSEUR

Sous la direction de :
Denis VILE et Christine GRANIER

Réponses intégrées des plantes aux contraintes hydriques et thermiques : du gène au phénotype chez *Arabidopsis thaliana*

Soutenue le 18 décembre 2012

Jury

Oliver BRENDEL	Chargé de Recherche, INRA Nancy	Rapporteur
Pierre MARTRE	Chargé de Recherche, INRA Clermont-Ferrand	Rapporteur
Christine DILLMANN	Professeur, Université Paris Sud	Examinatrice
Evelyne COSTES	Directrice de Recherche, INRA Montpellier	Examinatrice
Frédéric GAYMARD	Directeur de Recherche, INRA Montpellier	Examinateur
Christine GRANIER	Chargée de Recherche, INRA Montpellier	Directrice de thèse
Denis VILE	Chargé de Recherche, INRA Montpellier	Encadrant de thèse

MONTPELLIER SUPAGRO
Doctoral School SIBAGHE – Plant Integrative Biology

Ph.D. THESIS
presented by:

François VASSEUR

supervised by:
Denis VILE and Christine GRANIER

Plant integrated responses to water deficit and high temperature: from gene to phenotype in *Arabidopsis thaliana*

Defended on December 18th, 2012

Jury

Oliver BRENDEL	Researcher, INRA Nancy	Main examiner
Pierre MARTRE	Researcher, INRA Clermont-Ferrand	Main examiner
Christine DILLMANN	Professor, University Paris Sud	Examiner
Evelyne COSTES	Senior Researcher, INRA Montpellier	Examiner
Frédéric GAYMARD	Senior Researcher, INRA Montpellier	Examiner
Christine GRANIER	Researcher, INRA Montpellier	Supervisor
Denis VILE	Researcher, INRA Montpellier	Supervisor

LABORATOIRE D'ACCUEIL

LEPSE

Laboratoire d'Ecophysiologie des Plantes sous Stress Environnementaux

UMR 759 INRA / Montpellier SupAgro

IBIP – Institut de Biologie Intégrative des Plantes

Bâtiment 7

2 place Viala

34060 Montpellier cedex 1

FRANCE

HOST LABORATORY

LEPSE

Laboratory of Plant Ecophysiology under Environmental Stresses

UMR 759 INRA / Montpellier SupAgro

IBIP – Institute for Plant Integrative Biology

Bâtiment 7

2 place Viala

34060 Montpellier cedex 1

FRANCE

Résumé

Les interactions entre les contraintes environnementales sur le phénotype rendent complexe l'étude des mécanismes d'adaptation et d'évolution des plantes. Aborder une telle question nécessite une approche intégrée de l'orchestration, à différentes échelles, des réponses des plantes à des stimuli environnementaux isolés et combinés. Nous avons utilisé *Arabidopsis thaliana* pour évaluer les bases génétiques des réponses à deux contraintes abiotiques majeures en forte interaction au champ : la sécheresse et les hautes températures. Grâce à des outils performants pour l'analyse du phénotype, une large gamme de traits a été mesurée sur de nombreux génotypes différant dans leur plasticité. Nous avons caractérisé la croissance et des traits d'histoire de vie, la morphologie et la structure foliaire, ainsi que les capacités d'acquisition et de conservation des ressources, en particulier l'eau et le carbone. Après une description des réponses phénotypiques et de leur architecture génétique, les conséquences de ces réponses dans une perspective écologique et évolutive ont été évaluées. En particulier, nous avons analysé les variations des stratégies fonctionnelles mises en relief par les covariations phénotypiques et génétiques. De plus, les processus responsables des réponses observées ont été examinés. Les résultats ont permis de mettre en évidence des variations génétiques associées à plusieurs régions génomiques dont l'influence est probablement majeure pour les mécanismes d'adaptation des plantes. Certaines de ces régions génomiques, de par leur effet sur la performance, sont porteuses d'intérêt dans une perspective d'amélioration des espèces cultivées face aux changements climatiques actuels.

Mots clefs : Allométrie, compromis physiologiques, espace phénotypique, génétique quantitative, plasticité multivariée, stress abiotique

Abstract

The mechanisms of plant adaptation and evolution are difficult to investigate since environmental constraints have interactive effects on plant phenotypes. Such study requires an integrated approach about the coordination, at different organizational levels, of the plant phenotypic responses to multiple environmental cues. Using the model plant *Arabidopsis thaliana*, we assessed the genetic bases of the integrated responses to two major abiotic constraints that strongly interact in the field: water availability and high temperature. Using powerful tools for the analysis of the phenotype, a large range of traits was measured in many genotypes that differ in their plasticity. We focused on the traits related to plant growth and life history, leaf structure and morphology, and to the acquisition and conservation of resources, specifically water and carbon. After a description of the phenotypic responses and their genetic architecture, the ecological and evolutionary consequences of these responses were evaluated. Specifically, we examined the variations in the functional strategies that are highlighted by phenotypic and genetic covariations. Moreover, the processes responsible of the observed phenotypic responses to environmental constraints were investigated. Strong genetic variability associated to particular genomic regions was identified. Such loci have presumably important influence on the mechanisms of plant adaption to fluctuating environments. Some of these genomic regions have a strong effect on plant performance in stressing conditions, and therefore offer promising avenues for crop improvement facing current global climate change.

Key words: Abiotic stress, allometry, multivariate plasticity, phenotypic space, physiological trade-offs, quantitative genetics

Remerciements

La préparation d'une thèse n'est pas le travail solitaire d'un étudiant. La préparation d'une thèse est un travail d'équipe, fait d'échanges, de collaborations, de réflexion, de remises en question et… de recadrages. Je tiens ici à remercier toutes les personnes qui ont participé, de près ou de loin, à ce travail. Par votre enthousiasme, vos conseils, votre soutien et votre disponibilité, vous avez tous et toutes contribué à transformer ce qu'on m'annonçait comme trois ans de galère en une aventure scientifique et humaine formidable. J'espère que cette thèse n'est pas une fin, mais seulement une étape, et que nous aurons bien d'autres occasions de travailler ensemble.

Plus particulièrement et avant tout, je tiens à remercier mon encadrant au quotidien, Denis. Maintenant que je suis à la fin de ces trois années, je m'aperçois ô combien ton encadrement m'a aiguillé et m'a permis d'enrichir mes connaissances et mon raisonnement scientifique. Ton sens critique et ton aptitude à remettre en cause les idées reçues ont été un apport inestimable. Merci pour la confiance que tu m'as témoigné tout au long de ces trois années. Et puis, je dois bien avouer que ta patience face à mes débordements ou à mon côté « brouillon » m'a toujours impressionné (surtout que tu n'es pas patient avec tout le monde…). La thèse n'aurait jamais été ce qu'elle a été sans ta complicité. Aurais-je pu imaginer me marrer autant avec mon encadrant ? Sans aucun doute non. Pour tous ces moments, de discussions enflammées devant un tableau, autour d'une bière le vendredi ou autour de plusieurs bières le samedi, un grand merci Denis. Mon seul regret est de me dire que j'aurai du mal à être un jour un aussi bon encadrant moi-même.

Je tiens aussi à remercier Christine, ma directrice de thèse. Christine, ton implication et ton soutien ont été la clef de voute de ce travail. Merci pour ton aide et ta disponibilité dans toutes les étapes de cette thèse, tes remarques pertinentes qui ont permis de réorienter mon travail lorsque je m'égarais, et merci pour ton enthousiasme dans les moments difficiles. Les soirées foot, à la Paillade ou sur grand écran (Montpellier champion !!), et le concours du mondial, sont autant de souvenirs que j'emporterai du LEPSE. Merci aussi d'avoir freiné, parfois, mon emportement excessif dans certaines situations. Plus généralement, je tiens à saluer le dynamisme avec lequel tu animes l'équipe SPIC depuis trois ans. Les projets, en cours ou à venir, autour de la station PHENOPSIS sont passionnants et je suis heureux d'y avoir pris part durant cette thèse.

Ils sont nombreux ceux et celles de l'équipe SPIC que je veux remercier ici. Mais avant tout, merci à l'équipe toute entière pour son accueil chaleureux et sa bonne humeur. Merci Myriam, évidemment, forcément, parce que les données acquises durant cette thèse l'ont été grâce à tes compétences et à ta disponibilité permanente. Tu peux être fière de tes enfants (je parle des PHENOPSIS ; P1, P2 et P3 pour les intimes), je leur dois ma thèse ! Merci à Alex et Fred. Votre patience pour analyser des centaines (que dis-je, des milliers !) de photos est extraordinaire, et elle a été un atout considérable dans mon travail. Alex, les « pause clope dans 5 minutes ? » ont toujours été agréables, je suis content de les avoir partagées avec toi. Merci aussi à Gaëlle pour son aide dans les opérations délicates de biochimie. Merci à Jessica pour son aide sur l'analyse des images infra-rouge, et pour son rire qui avait le don de redonner le sourire dans les plus grands moments de déprime. Merci à Florent avec qui j'ai partagé le bureau pendant deux ans. Florent, tes capacités d'analyse m'ont toujours bluffé, et elles ont été une source d'inspiration et de motivation dans mon travail. Merci aussi à tous les autres membres, présents ou passés, de l'équipe qui ont participé à cette thèse et ont contribué, par leurs échanges, à son bon déroulement : Marie B., Juliette, Séb, Harold, Cathy, Anne, Nathalie, Rémy, Mélanie, Cris, François B., Ravi (pardonnez-moi si j'en oublie). Merci aussi à Thibaut que j'ai eu le plaisir de co-encadrer durant son stage de M2.

Au-delà de l'équipe SPIC, je tiens à remercier l'ensemble du LEPSE non seulement pour leur accueil mais pour l'environnement scientifique et humain au sein de l'unité. La diversité des points de vue scientifiques, les débats et les discussions au sein du LEPSE ont été une source d'inspiration forte dans mon travail. Je tiens à remercier l'ensemble des chercheurs avec lesquels j'ai pu échangés au cours de ces trois ans et qui m'ont tous beaucoup apporté, en particulier Bertrand MULLER, François TARDIEU, Thierry SIMONNEAU, Claude WELCKER, Angélique CHRISTOPHE et Olivier TURC. Merci aussi à toute l'équipe technique du LEPSE. Comment oublier les après-midi pétanque ? Merci aussi aux soirées piscine organisées par Stéphane, au breakdance de Juliette dans la serre entre deux mesures au ciras, aux blagues de Suard & fils, aux débats politiques houleux avec Nico en fin de soirée, au tram qui accepte le vélo de Jo (et au passage, merci Doumé pour nous avoir conseillé de bons petits coins sur l'Ile !). Merci Cecilio et Llorenc pour nos soirées 'vin rouge/classico' (Llorenc merci aussi pour tes revendications indépendantistes et ta tequila mexicaine…). Merci Emilie pour ta bonne humeur en toute situation et pour les soirées crêpes. Merci Grégoire pour être l'autre thésard payé par le grand capital. Merci Vincent N. pour ta gaité permanente. Merci à Vincent O., Ivan et Marilyne pour nos échanges enflammés sur la politique et sur la société (je crois qu'on n'est définitivement pas d'accord, la faute à

Babylon, mais c'est pas grave, j'ai beaucoup aimé débattre avec vous et j'espère qu'on aura d'autres occasions). Merci aux deux Philippe, à Romain, à Carine, à Claudine, à Adel et à Abde pour leur diverses contributions, humaine ou scientifique, à ce travail. Merci à Marie-Claude et Marie-Françoise pour avoir réussi à déjouer les arcanes administratives inhérentes à toutes les thèses, et avoir participé au bon déroulement de celle-ci. Merci aussi pour leurs éclats de rire, communicatifs, que j'entendais depuis mon bureau. Merci à Martine BARRAUD pour m'avoir accompagné dans les procédures, pas toujours évidentes, d'inscription, de ré-inscription, et de formalités administratives en tout genre. Enfin merci à Hubert pour ses propriétés de rémanences improbables.

Je tiens aussi à remercier Cyrille VIOLLE que j'ai eu la chance de rencontrer grâce à Denis. Cyrille, merci pour nos discussions qui ont ouvert de nouvelles perspectives dans ma thèse, et de nouvelles conceptions dans mon esprit de scientifique débutant. J'espère qu'un jour on aura l'occasion de te faire boire une coupe de champagne, si tu vois ce que je veux dire… Merci aussi à Brian ENQUIST pour son soutien à nos travaux et nos discussions (même s'il ne liera probablement jamais ceci, je tenais à le remercier). Merci aussi à mon financeur, Bayer CropScience, pour avoir cru au projet et pour tout simplement… l'avoir financé. En particulier merci à Matthew HANNAH qui nous a fait confiance et nous as laissé la liberté scientifique nécessaire à la réalisation de ce projet. Cette expérience a été enrichissante en partie grâce à ces collaborations qui ont très bien fonctionné.

De façon plus personnelle, je souhaite remercier celle qui partage ma vie depuis deux ans. Justine, merci pour ton soutien permanent dans les meilleurs moments comme dans les pires. Merci d'être à mes côtés et d'avoir partagé cette aventure avec moi. Enfin, je tiens aussi à remercier mes parents et ma famille. Papa, maman, c'est grâce à vous que je peux aujourd'hui faire ce que j'ai toujours rêvé de faire et je vous en suis infiniment reconnaissant.

Avant-propos

L'esprit humain a besoin de filtres intellectuels pour lui permettre d'appréhender et d'intégrer la complexité des processus, des formes et des fonctions du vivant. Ces filtres peuvent être d'ordre matériel, il s'agit de la nécessité de partitionner l'organisme en un certain nombre de caractères phénotypiques mesurables et interprétables. Dans la pratique, ces caractères sont généralement considérés comme plus ou moins indépendants, bien qu'ils ne représentent que différentes mesures d'une même entité : l'organisme. Ces filtres sont aussi d'ordre conceptuel, il s'agit de définir un cadre d'analyse dans lequel se placer pour interpréter les données. Les approches diffèrent selon les questions adressées par les chercheurs, ce qui est occasionnellement la source de difficultés de communication entre les différentes disciplines scientifiques (Pigliucci 2003). Inversement, les moyens techniques sont aussi souvent un frein aux questions que souhaiteraient élucider les chercheurs, ce qui peut biaiser la démarche scientifique si elle ne s'interroge pas sur les approches et les méthodes. La première question que l'on peut se poser lorsqu'on observe une plante est : de quoi est-elle faite ? Cette question concerne l'étude de l'organisation et du déterminisme du phénotype, et elle est généralement adressée par les biologistes moléculaire et cellulaire, les généticiens et les physiologistes. La seconde question renvoie à une conception intellectuelle radicalement différente : pourquoi la plante est-elle comme ceci ? Cette question vise à comprendre l'origine évolutive d'un caractère phénotypique. Etant intimement liée aux mécanismes de la sélection naturelle, cette question est généralement adressée par les biologistes de l'évolution, les écophysiologistes et les écologues. Réconcilier ces deux approches conceptuelles est l'enjeu majeur de la biologie intégrative (Pigliucci 2003), ainsi que le souligne Ernst Mayr (1997) lorsqu'il définit la biologie : « the two major contributors to a new theory in the life sciences are the discovery of new facts (observations) and the development of new concepts »

Les filtres intellectuels indispensables pour transformer un organisme d'une très grande complexité en une série de mesures interprétables peuvent être illustrés par un exemple déjà utilisé pour représenter les filtres du langage lors de la transmission d'information dans la communication humaine (Culicover 2005). L'idée développée est que, dans le langage comme en biologie, les filtres opérés par l'esprit humain déterminent pour une large part le type de théories que nous sommes amenés à proposer. Pour illustrer son propos, l'auteur utilise le tableau de Salvador Dali représenté en Figure 1 (intitulé *Lincoln in Dalivision*). Ce tableau, œuvre de génie du maitre espagnol, nous offre différentes facettes suivant la distance

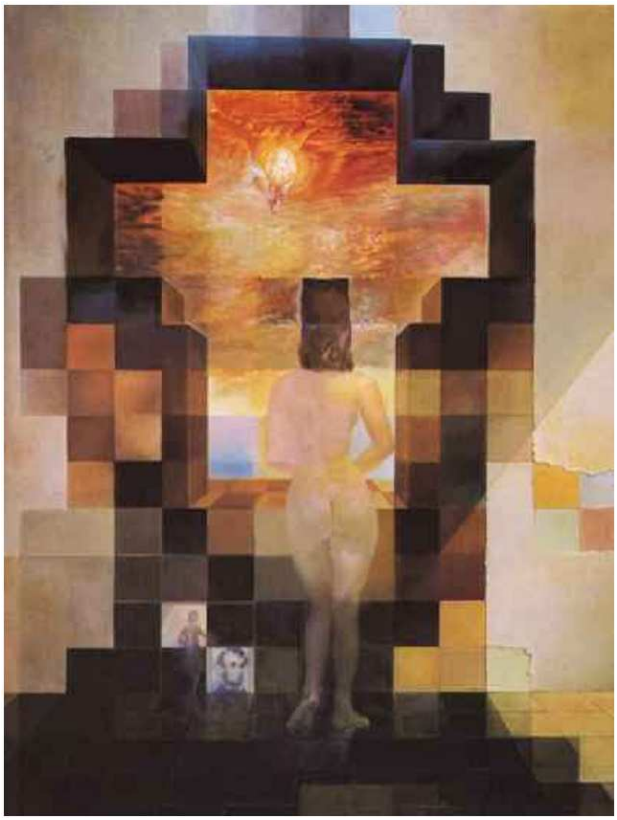

Figure 1. Lincoln in Dalivision de Salvador Dali

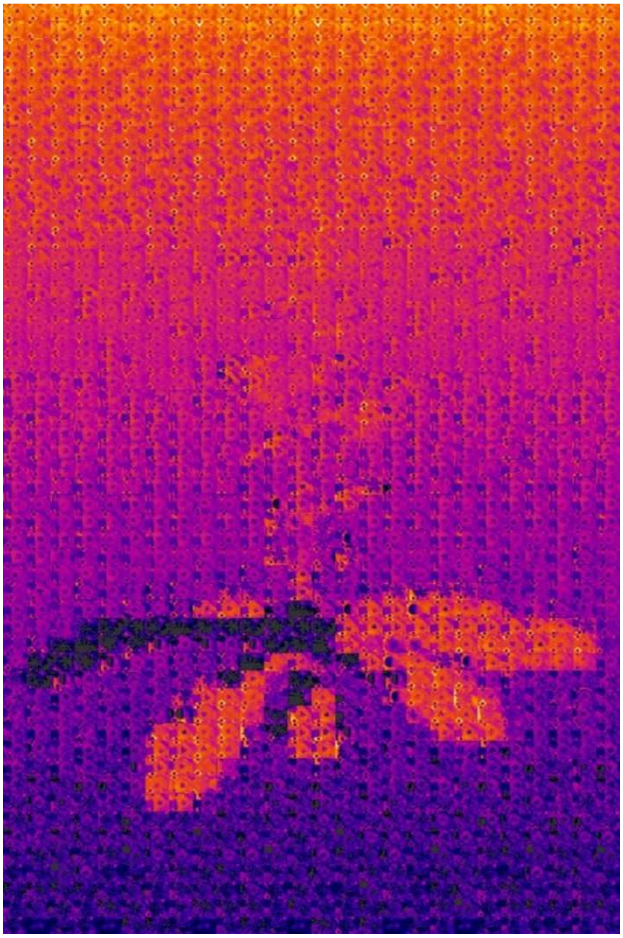

Figure 2. Composition Arabidopsis infra-rouge

à laquelle on l'observe. De près, on y voit la femme de Dali debout de dos. De loin, le tableau se transforme en un portrait d'Abraham Lincoln. Dans cet exemple, la distance opère sur l'objet d'observation de la même manière que le raisonnement scientifique opère sur la conceptualisation d'un organisme. Ainsi selon les angles et les points de vue, on peut avoir une vision complètement différente d'une même chose. Reprenons le même exemple, mais avec la composition mosaïque construite à partir des photos issues de cette thèse (Figure 2). Grâce à des variabilités de nuances parmi les centaines de photographies infra-rouge, on peut distinguer la forme d'une plante d'*Arabidopsis thaliana*. Cependant, si on souhaite regarder en détail l'une de ces photographies, le grossissement nécessaire fera perdre la vision d'ensemble de la figure. De la même manière, fragmenter l'information pour pouvoir la comprendre est inévitable en biologie même si cela conduit à perdre une partie de l'information initiale. Les disciplines scientifiques tentent de répondre à des questions différentes soulevées par leur approche et leur point de vue. Tenter d'établir des ponts entre ces disciplines scientifiques est crucial pour construire de nouvelles théories permettant de rendre compte de la diversité du vivant.

Les travaux menés au cours de cette thèse ont généré une grande quantité de données visant à caractériser le phénotype des plantes dans des conditions environnementales variées. Ils nous ont aidés à répondre, au moins en partie, à plusieurs des questions que nous nous sommes posées. La résolution de ces questions est passée par le développement d'approches originales de l'étude de l'interaction entre le génotype d'un organisme et l'environnement. Au terme de cette thèse, certains résultats demandent à être confirmés et de nouvelles questions se posent.

Références citées

Culicover, P. W. 2005. Squinting at Lincoln in Dalivision1. http://www.cogsci.msu.edu/DSS/2005-2006/Culicover/Dali_Lincoln.pdf.

Mayr, E. 1997. This is biology: The science of the living world. Universities Press.

Pigliucci, M. 2003. From molecules to phenotypes? – The promise and limits of integrative biology. Basic and Applied Ecology **4**:297-306.

Table des matières/Table of contents

Introduction générale

L'étude de la plasticité des plantes en réponse aux facteurs biotiques et abiotiques anime les botanistes et les biologistes depuis toujours, quels que soient leurs champs d'investigation et leurs spécialités. Dans un contexte de changements climatiques majeurs, la nécessité de trouver, parmi la diversité génétique végétale, des génotypes adaptés aux futures conditions climatiques apparaît plus cruciale encore. En 2012, la hausse des températures à l'échelle du globe n'est plus un sujet de débat au sein de la communauté scientifique (contrairement aux raisons de cette hausse). Par ailleurs, la diminution des ressources en eau a été recensée dans de nombreuses régions du monde (IPCC 2007). L'interaction d'épisodes de sécheresse et de forte chaleur a des conséquences importantes sur les écosystèmes. Ainsi au champ, ces deux contraintes environnementales sont déjà responsables de la majorité des diminutions de rendements à travers le monde (Boyer 1982, Ciais et al. 2005, Battisti and Naylor 2009). Plus inquiétant, leurs effets sont prévus en constante augmentation dans les décennies à venir (IPCC 2007). Un enjeu majeur des études actuelles vise à identifier les bases génétiques et physiologiques de la variabilité des réponses des plantes aux contraintes environnementales (Nicotra et al. 2010, Hansen et al. 2012). En effet, identifier des gènes ou des loci à caractère quantitatif (QTL) susceptibles d'améliorer les performances des espèces cultivées en condition de stress est un des défis de l'agronomie.

Parmi les espèces modèles qui ont émergé avec le développement de la biologie moléculaire, *Arabidopsis thaliana* (L.) Heynh (« l'Arabette des dames ») s'est rapidement imposée dans les laboratoires de recherche en tant que représentante des plantes à fleurs (Meinke et al. 1998). La raison de cet engouement tient principalement à la rapidité de son cycle de reproduction (permettant de multiplier les générations), à sa petite taille (permettant la culture de grandes populations dans un espace réduit), et à la relative simplicité de son génome (facilitant les études génétiques). Le nombre spectaculaire d'études sur cette espèce a permis de significativement améliorer nos connaissances sur la régulation génétique et moléculaire des principales fonctions des plantes (The Arabidospis Genome Initiative 2000). Présente des côtes méditerranéennes au cercle polaire, et des plaines d'Asie centrale aux iles du Cap Vert, cette petite plante rudérale a su s'adapter à des environnements très contrastés, notamment caractérisés par des différences importantes de précipitation et de température moyennes (Hoffmann 2002). La diversité des phénotypes rencontrés dans les populations naturelles d'*A. thaliana* est le reflet à la fois d'une variabilité génétique importante et de la

plasticité des caractères phénotypiques à l'environnement. Pour ces raisons, *A. thaliana* est rapidement devenue un organisme modèle non seulement en biologie moléculaire, mais aussi en écologie et en génétique des populations (Mitchell-Olds 2001, Weigel 2012). Cette thèse repose sur l'analyse (*i*) de plusieurs accessions issues de régions contrastées, (*ii*) d'une population de lignées recombinantes et de lignées introgressées issues d'un croisement entre une accession provenant du Cap Vert et une accession de laboratoire originaire de Pologne, et (*iii*) de mutants affectés dans des gènes spécifiques.

Les processus de croissance et de reproduction à l'échelle de la plante sont fortement coordonnés, ce qui implique l'existence de contraintes génétiques fortes limitant la variabilité des caractères individuels (Roff 2007, Wagner and Zhang 2011). Ces contraintes sont reflétées par les relations étroites liant entre eux les caractères relatifs à la taille et à l'âge, à la morphologie des feuilles et aux capacités d'acquisition du carbone et de conservation de l'eau. La diversité allélique induit néanmoins de la variabilité dans les combinaisons de traits, permettant l'existence de multiples stratégies fonctionnelles au sein d'une population (Grime 1988, Westoby et al. 2002). Plusieurs études durant la dernière décennie ont exploré le déterminisme génétique des réponses des plantes à la sécheresse et aux hautes températures, et ont permis d'identifier des QTL induisant des réponses contrastées à ces deux stress appliqués de manière isolée (e.g. McKay et al. 2003, Juenger et al. 2005, McKay et al. 2008 , Tonsor et al. 2008, Skirycz and Inze 2010 , Tisné et al. 2010). Ces loci sont porteurs d'intérêt en vue de comprendre et de prédire les capacités d'adaptation des plantes. Cependant, aucune étude ne s'est intéressée à la combinaison de ces deux stress, alors qu'ils interagissent très souvent au champ et qu'ils impactent les processus physiologiques majeurs comme la photosynthèse, la transpiration et la croissance (Mittler 2006). De plus, la plupart des études de génétique quantitative (sur *A. thaliana* comme sur d'autres espèces), se sont limitées à la mesure de quelques caractères phénotypiques d'intérêt simple à mesurer, comme le stade phénologique (e.g. Dorn and Mitchellolds 1991, El-Assal et al. 2001, Borevitz et al. 2002, Juenger et al. 2005, Mendez-Vigo et al. 2010). La variabilité et le déterminisme de caractères phénotypiques complexes, comme la vitesse de photosynthèse, le taux de transpiration et les dynamiques de croissance, ainsi que la morphologie des feuilles et l'allocation des ressources, restent encore peu étudiés (Pigliucci and Preston 2004, Nicotra et al. 2010). Cette limite est due à des raisons techniques évidentes étant donné le nombre importants d'individus nécessaires à une analyse statistique robuste, mais elle a été récemment dépassée grâce au développement des outils de phénotypage à haut débit (Houle et al. 2010 , Flood et al. 2011, Edwards et al. 2012). En associant ces outils aux capacités de régulation de l'environnement

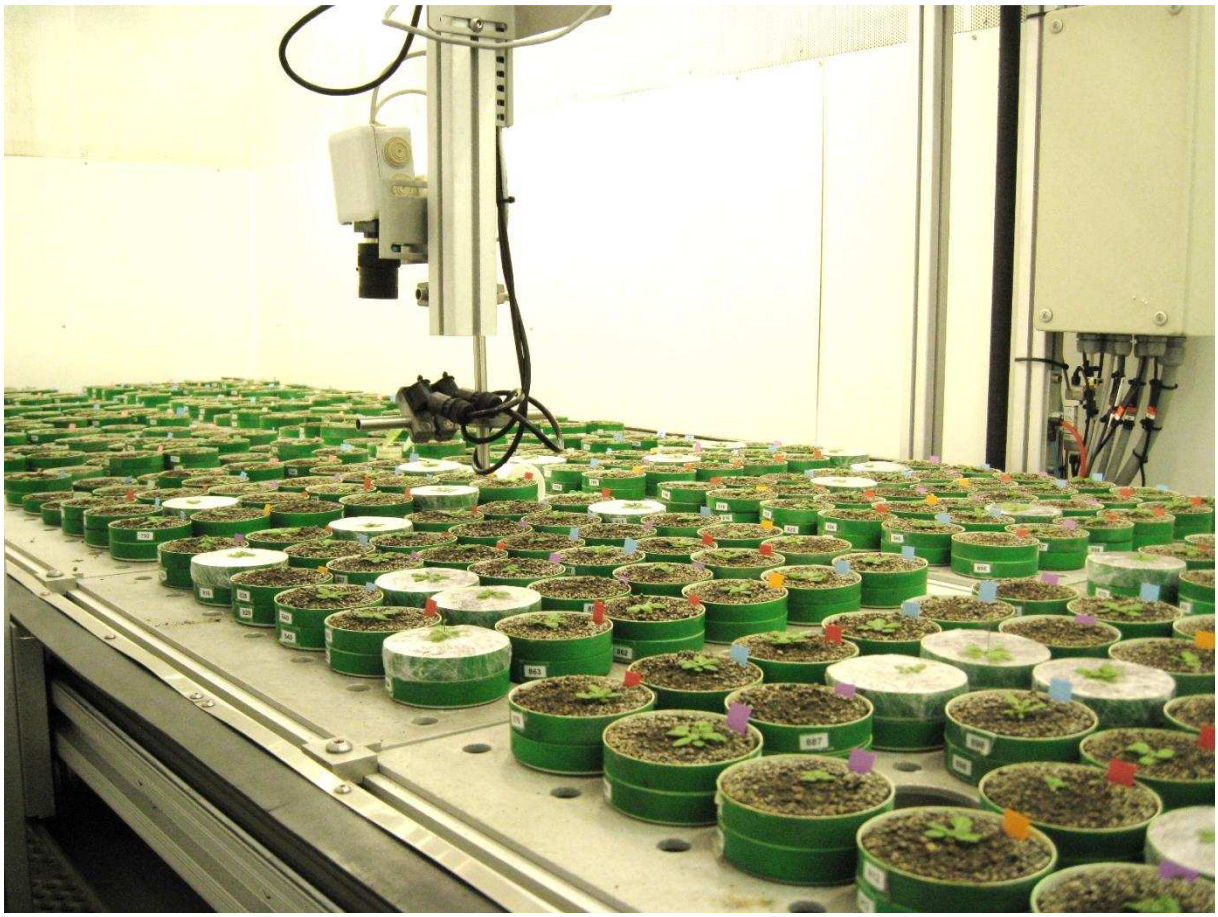

Figure 1. L'automate de phénotypage PHENOPSIS de la station 'Montpellier Plant Phenotyping Platform' (M3P).

de l'automate PHENOPSIS (Granier et al. 2006; Figure 1), nous avons analysé le déterminisme génétique de la plasticité d'*A. thaliana* aux stress hydrique et thermique à travers l'étude d'une large gamme de traits phénotypiques. Nous avons aussi participé à l'amélioration de ces outils pour la quantification de traits plus complexes comme la photosynthèse et l'architecture foliaire. Les objectifs de cette thèse ont été les suivants :

1. Examiner la variabilité naturelle des réponses des plantes aux stress hydrique et thermique isolés et combinés.
2. Identifier l'architecture génétique de ces réponses.
3. Proposer et tester des hypothèses évolutives à l'origine de ces réponses.

Nous avons fait le choix de mesurer tous les individus au même stade de développement (généralement à la floraison). Cela implique la comparaison de caractères intégrés sur l'ensemble du cycle de la croissance, tels que la taille de la plante et la morphologie des feuilles, à des mesures instantanées telles que la photosynthèse et la transpiration. L'influence de ce cadre d'analyse sur les résultats est importante (Coleman et al. 1994), elle sera discuté tout au long de la thèse, composée de trois chapitres indépendants suivis d'annexes.

Dans le premier chapitre de cette thèse, nous examinons la variabilité naturelle des réponses d'*A. thaliana* aux stress hydrique et thermique, isolés et combinés. La première partie de ce chapitre a été réalisée sur plusieurs écotypes issus de régions aux conditions climatiques contrastées (Vile et al. 2012). Nous y décrivons la plasticité des plantes, en mêlant des approches univariées et multivariées, et proposons des hypothèses adaptatives à l'origine des réponses observées. La seconde partie a été réalisée sur une population de lignées recombinantes dans le but de déterminer l'architecture génétique des réponses par une approche multivariée. Nous montrons que seuls quelques gènes pléiotropes sont impliqués dans la variabilité des phénotypes en réponse à l'environnement. De plus, le contrôle génétique du développement est indépendant de la disponibilité en eau et de la température alors que le contrôle génétique de la photosynthèse varie fortement en réponse aux stress.

Dans le deuxième chapitre, nous testons des hypothèses adaptatives à l'origine des réponses intégrées d'*Arabidopsis thaliana* aux hautes températures. Dans la première partie de ce chapitre, nous évaluons le rôle du statut carboné et des températures foliaires sur les réponses de plusieurs accessions naturelles et de mutants cultivés dans différentes conditions lumineuses à haute température (Vasseur et al. 2011). La plasticité de l'architecture foliaire suggère que le métabolisme carboné joue un rôle central à l'origine des réponses observées.

Dans la seconde partie de ce chapitrenous confrontons l'hypothèse métabolique à une hypothèse alternative : le refroidissement des tissus par la transpiration pourrait être la cause de la plasticité architecturale en réponse à la température (Pantin et al. soumis). Les résultats indiquent que des progrès significatifs peuvent être envisagés en agronomie en orientant les recherches vers l'optimisation de l'architecture foliaire en lien avec l'efficience d'utilisation de l'eau.

Dans le troisième chapitre, nous traitons les données obtenues sur la population de lignées recombinantes dans une perspective écologique. Dans la première partie de ce chapitre, nous détaillons l'importance des gènes pléiotropes à l'origine de la variabilité des stratégies fonctionnelles dans des conditions optimales d'irrigation et de température (Vasseur et al. 2012). Cette étude s'inscrit dans le cadre de la théorie métabolique de l'écologie qui fait l'hypothèse de contraintes évolutives fortes sur la relation entre les capacités métaboliques d'un organisme et sa taille (Brown et al. 2004). Dans la seconde partie de ce chapitre, nous explorons la plasticité des relations allométriques en réponse aux stress hydrique et thermique. A travers une approche de modélisation originale, nous mettons en évidence des interactions entre génotype et environnement associées à des différences de performance et de succès reproducteur. Les QTL responsables de ces interactions sont susceptibles d'avoir un rôle majeur dans les mécanismes d'adaptation des plantes dans leur milieu, et pourraient trouver des applications pour l'amélioration des espèces cultivées aux facteurs environnementaux.

Références

Battisti, D. S. and R. L. Naylor. 2009. Historical warnings of future food insecurity with unprecedented seasonal heat. Science **323**:240-244.

Borevitz, J. O., J. N. Maloof, J. Lutes, T. Dabi, J. L. Redfern, G. T. Trainer, J. D. Werner, T. Asami, C. C. Berry, D. Weigel, and J. Chory. 2002. Quantitative trait loci controlling light and hormone response in two accessions of Arabidopsis thaliana. Genetics **160**:683-696.

Boyer, J. S. 1982. Plant productivity and environment. Science **218**:443-448.

Brown, J. H., J. F. Gillooly, A. P. Allen, V. M. Savage, and G. B. West. 2004. Toward a metabolic theory of ecology. Ecology **85**:1771-1789.

Ciais, P., M. Reichstein, N. Viovy, A. Granier, J. Ogee, V. Allard, M. Aubinet, N. Buchmann, C. Bernhofer, A. Carrara, F. Chevallier, N. De Noblet, A. D. Friend, P. Friedlingstein, T. Grunwald, B. Heinesch, P. Keronen, A. Knohl, G. Krinner, D. Loustau, G. Manca, G. Matteucci, F. Miglietta, J. M. Ourcival, D. Papale, K. Pilegaard, S. Rambal, G. Seufert, J. F. Soussana, M. J. Sanz, E. D. Schulze, T. Vesala, and R. Valentini. 2005. Europe-wide reduction in primary productivity caused by the heat and drought in 2003. Nature **437**:529-533.

Coleman, J. S., K. D. McConnaughay, and D. D. Ackerly. 1994. Interpreting phenotypic variation in plants. Trends in Ecology & Evolution **9**:187-191.

Dorn, L. A. and T. Mitchellolds. 1991. Genetics of Brassica-Campestris .1. Genetic Constraints on Evolution of Life-History Characters. Evolution **45**:371-379.

Edwards, C. E., B. E. Ewers, C. R. McClung, P. Lou, and C. Weinig. 2012. Quantitative Variation in Water-Use Efficiency across Water Regimes and Its Relationship with Circadian, Vegetative, Reproductive, and Leaf Gas-Exchange Traits. Molecular Plant **5**:653-668.

El-Assal, S. E. D., C. Alonso-Blanco, A. J. M. Peeters, V. Raz, and M. Koornneef. 2001. A QTL for flowering time in Arabidopsis reveals a novel allele of CRY2. Nature Genetics **29**:435-440.

Flood, P. J., J. Harbinson, and M. G. Aarts. 2011. Natural genetic variation in plant photosynthesis. Trends in Plant Science **16**:327-335.

Granier, C., L. Aguirrezabal, K. Chenu, S. J. Cookson, M. Dauzat, P. Hamard, J. J. Thioux, G. Rolland, S. Bouchier-Combaud, A. Lebaudy, B. Muller, T. Simonneau, and F. Tardieu. 2006. PHENOPSIS, an automated platform for reproducible phenotyping of plant responses to soil water deficit in *Arabidopsis thaliana* permitted the identification of an accession with low sensitivity to soil water deficit. New Phytologist **169**:623-635.

Grime, J. P. 1988. Plant Strategies and the Dynamics and Structure of Plant-Communities - Tilman,D. Nature **336**:630-630.

Hansen, M. M., I. Olivieri, D. M. Waller, E. E. Nielsen, and M. W. G. The Ge. 2012. Monitoring adaptive genetic responses to environmental change. Molecular Ecology **21**:1311-1329.

Hoffmann, M. H. 2002. Biogeography of *Arabidopsis thaliana* (L.) Heynh. (Brassicaceae). Journal of Biogeography **29**:125-134.

Houle, D., D. R. Govindaraju, and S. Omholt. 2010. Phenomics: the next challenge. Nature Reviews Genetics **11**:855-866.

Initiative, T. A. G. 2000. Analysis of the genome sequence of the flowering plant *Arabidopsis thaliana*. Nature **408**:796-815.

IPCC. 2007. Climate Change 2007: The physical science basis. Contribution of Working Group I to the Fourth Assessment Report of the Intergovernmental Panel on Climate Change. Cambridge University Press, Cambridge, UK and New York, NY.

Juenger, T. E., S. Sen, K. A. Stowe, and E. L. Simms. 2005. Epistasis and genotype-environment interaction for quantitative trait loci affecting flowering time in *Arabidopsis thaliana*. Genetica **123**:87-105.

McKay, J. K., J. H. Richards, and T. Mitchell-Olds. 2003. Genetics of drought adaptation in *Arabidopsis thaliana*: I. Pleiotropy contributes to genetic correlations among ecological traits. Molecular Ecology **12**:1137-1151.

McKay, J. K., J. H. Richards, K. S. Nemali, S. Sen, T. Mitchell-Olds, S. Boles, E. A. Stahl, T. Wayne, and T. E. Juenger. 2008. Genetics of drought adaptation in *Arabidopsis thaliana* II. QTL analysis of a new mapping population, KAS-1 x TSU-1. Evolution **62**:3014-3026.

Meinke, D. W., J. M. Cherry, C. Dean, S. D. Rounsley, and M. Koornneef. 1998. *Arabidopsis thaliana*: A Model Plant for Genome Analysis. Science **282**:662-682.

Mendez-Vigo, B., M. T. de Andres, M. Ramiro, J. M. Martinez-Zapater, and C. Alonso-Blanco. 2010. Temporal analysis of natural variation for the rate of leaf production and its relationship with flowering initiation in *Arabidopsis thaliana*. J Exp Bot **61**:1611-1623.

Mitchell-Olds, T. 2001. Arabidopsis thaliana and its wild relatives: a model system for ecology and evolution. Trends in Ecology & Evolution **16**:693-700.

Mittler, R. 2006. Abiotic stress, the field environment and stress combination. Trends Plant Sci **11**:15-19.

Nicotra, A. B., O. K. Atkin, S. P. Bonser, A. M. Davidson, E. J. Finnegan, U. Mathesius, P. Poot, M. D. Purugganan, C. L. Richards, F. Valladares, and M. van Kleunen. 2010. Plant phenotypic plasticity in a changing climate. Trends Plant Sci **15**:684-692.

Pigliucci, M. and K. Preston. 2004. Phenotypic Integration: Studying the Ecology and Evolution of Complex Phenotypes. Oxford University Press.

Roff, D. A. 2007. Contributions of genomics to life-history theory. Nat Rev Genet **8**:116-125.

Skirycz, A. and D. Inze. 2010. More from less: plant growth under limited water. Curr Opin Biotechnol **21**:197-203.

Tisné, S., I. Schmalenbach, M. Reymond, M. Dauzat, M. Pervent, D. Vile, and C. Granier. 2010. Keep on growing under drought: genetic and developmental bases of the response of rosette area using a recombinant inbred line population. Plant Cell and Environment **33**:1875-1887.

Tonsor, S. J., C. Scott, I. Boumaza, T. R. Liss, J. L. Brodsky, and E. Vierling. 2008. Heat shock protein 101 effects in *A. thaliana*: genetic variation, fitness and pleiotropy in controlled temperature conditions. Molecular Ecology **17**:1614-1626.

Vasseur, F., F. Pantin, and D. Vile. 2011. Changes in light intensity reveal a major role for carbon balance in Arabidopsis responses to high temperature. Plant Cell and Environment.

Vasseur, F., C. Violle, B. J. Enquist, C. Granier, and D. Vile. 2012. A common genetic basis to the origin of the leaf economics spectrum and metabolic scaling allometry. Ecology Letters **15**:1149-1157.

Vile, D., M. Pervent, M. Belluau, F. Vasseur, J. Bresson, B. Muller, C. Granier, and T. Simonneau. 2012. Arabidopsis growth under prolonged high temperature and water deficit: independent or interactive effects? Plant Cell and Environment **35**:702-718.

Wagner, G. P. and J. Z. Zhang. 2011. The pleiotropic structure of the genotype-phenotype map: the evolvability of complex organisms. Nature Reviews Genetics **12**:204-213.

Weigel, D. 2012. Natural Variation in Arabidopsis: From Molecular Genetics to Ecological Genomics. Plant Physiology **158**:2-22.

Westoby, M., D. S. Falster, A. T. Moles, P. A. Vesk, and I. J. Wright. 2002. Plant ecological strategies: Some leading dimensions of variation between species. Annual Review of Ecology and Systematics **33**:125-159.

Chapter 1

Natural variability and genetic determinisms of Arabidopsis responses to water deficit and high temperature

"Quoi plus que l'organisme vivant fait voir et sentir le temps vrai? Pour une plante, une forme équivaut à un âge – la forme est liée à la grandeur. Le temps est inextricablement, corrélativement lié à l'être. Un an est un nœud, une couche, une masse séparée du milieu et annexée, surajoutée, exhaussée, digérée, ordonnées, classée, édifiée… »
Paul Valéry

Chapter objectives:

High temperature and water deficit are among the major stresses impairing plant growth and productivity. In this first chapter, we investigated the plasticity and the genetic determinisms of the integrated responses of *Arabidopsis thaliana* to these stresses. Specifically, we addressed the following questions:

- What is the natural variability of Arabidopsis responses to combined and isolated water deficit and high temperature?
- What are the genetic determinisms of these responses?

Combining uni- and multi-variate approaches, we quantified the traits related to plant development, growth and morphology in ten natural accessions originated from contrasted climatic conditions. The analysis of a RIL population revealed some QTL involved in the variability of plant development and life history traits whatever the environment and others involved in the plasticity of carbon metabolism to water deficit and high temperature. These data allowed proposing adaptive hypotheses to the origin of the responses observed.

Manuscript #1

Arabidopsis growth under prolonged high temperature and water deficit: independent or interactive effects?

Denis Vile[1], Marjorie Pervent[1], Michaël Belluau[1], François Vasseur[1], Justine Bresson[1], Bertrand Muller[1], Christine Granier[1] and Thierry Simonneau[1]

[1]Laboratoire d'Ecophysiologie des Plantes sous Stress Environnementaux (LEPSE), UMR 759, INRA-SUPAGRO, F-34060 Montpellier, France

Article first published online: 9 Nov 2011 in *Plant, Cell and Environment*
Volume 35, Issue 4, Pages 702-718, DOI: 10.1111/j.1365-3040.2011.02445.x
url: http://onlinelibrary.wiley.com/doi/10.1111/j.1365-3040.2011.02445.x/pdf

Abstract

High temperature and water deficit are frequent environmental constraints restricting plant growth and productivity. These stresses often occur simultaneously in the field but little is known about their combined impacts on plant growth, development, and physiology. We evaluated the responses of ten *A. thaliana* natural accessions to prolonged elevated air temperature (30°C) and soil water deficit applied separately or in combination. Plant growth was significantly reduced under both stresses and their combination was even more detrimental to plant performance. The effects of the two stresses were globally additive but some traits responded specifically to one but not the other stress. Root allocation increased in response to water deficit, while reproductive allocation, hyponasty and specific leaf area increased under high temperature. All the traits that varied in response to combined stresses also responded to at least one of them. Tolerance to water deficit was higher in small-sized accessions under control and high temperature and in accessions with high biomass allocation to root under control conditions. Accessions that originate from sites with higher temperature have less stomatal density and allocate less biomass to the roots when cultivated under high temperature. Independence and interaction between stresses as well as the relationships between traits and stress responses are discussed.

Key-words: *Arabidopsis thaliana*, growth, phenology, biomass allocation, leaf morphology, stomatal density, high temperature, water deficit.

Introduction

High temperature (HT) and water deficit (WD) are two important environmental constraints restricting plant growth and productivity in many areas of the world (Boyer 1982, Ciais et al. 2005). Global climate change will presumably increase the occurrence and extend the distribution of these constraints, leading to further reduction of productivity and shifts in biodiversity (Chaves et al. 2002, Lobell and Asner 2003, Porter 2005, Thuiller et al. 2005, IPCC 2007). The two stresses often occur simultaneously in the field but little is known about their combined effects on plant growth, development, and physiology (Machado and Paulsen 2001, Zhang et al. 2008).

Different mechanisms have been identified as ensuring plant survival and growth under elevated temperatures or water shortage. They include long-term evolutionary phenological and morphological adaptations and short-term avoidance or acclimation mechanisms. Even moderate increases in air temperature (Lafta and Lorenzen 1995, Loveys et al. 2002) or decreases in soil water availability (Passioura 1996) are responsible for impaired plant growth. Many elementary biological processes and morphological traits underlying plant growth are sensitive to temperature, and their responses repeatedly resemble a bell-shape curve. As temperature rises above a particular threshold, processes such as net photosynthetic rate are negatively affected (Körner 2006, Sage and Kubien 2007, Parent et al. 2010), ultimately leading to a decline in plant performance. Temperature is also the main determinant of plant phenology (Ritchie and NeSmith 1991), and moderate increases in air temperature generally accelerate the rate of developmental processes leading to early flowering in most wild and cultivated species (Johnson and Thornley 1985). Whereas the effects of water deficit on phenology remain elusive, delayed timing of reproduction is often observed in crop species (McMaster et al. 2009). The effects of these stresses also depend on the phenological stage at which they occur (Prasad et al. 2008). For instance, HT has greater impacts on seed yield during the reproductive phase (Jenks and Wood 2010). Therefore, accelerated reproduction in response to HT is generally viewed as an escape mechanism.

HT and WD have contrasted effects on patterns of biomass allocation to organs and tissues. For instance, allocation to roots rapidly increases in response to moderate soil water deficit (Boyer 1985), whereas leaf relative water content and specific leaf area decline in plants subjected to water stress (Poorter et al. 2009). Leaf structure is also affected by temperature but, in contrast with WD, higher temperature often leads to the production of thinner leaves with higher specific leaf area (Boese and Huner 1990, Loveys et al. 2002,

Luomala et al. 2005, Poorter et al. 2009). These morphological changes are accompanied by changes in leaf anatomy. Leaves developed under WD have generally smaller cells in the parenchyma and the epidermis (Lecoeur et al. 1995) and higher stomatal density (Aubert et al. 2010, Tisné et al. 2010). Wahid et al. (2007) reported similar effects of HT and WD on cell density, but limited data is available on changes in leaf anatomy in response to HT.

The effects of WD, particularly osmotic stresses or watering deprivation, and HT, particularly short periods of acute heat stress, have been mostly analysed separately. There is however strong evidence that HT and WD interact to influence plant functioning (Rizhsky et al. 2002, Rizhsky et al. 2004). For instance, WD induces stomatal closure and reduces transpiration fluxes (Hsaio 1973). This in turn can cause an increase in leaf temperature by reducing transpirational cooling (Cook et al. 1964), and potentially enhances plant susceptibility to higher air temperature. Increase in leaf temperature can also raises plant water loss through transpiration (Lafta and Lorenzen 1995), and decrease root growth (Kuroyanagi and Paulsen 1988), thus increasing plant susceptibility to water shortage. By contrast, changes in leaf orientation in response to elevated temperature (Fu and Ehleringer 1989) such as hyponasty (Koini et al. 2009, Van Zanten et al. 2009) modify the leaf energy balance and could contribute to water saving by limiting rises in leaf temperature and evaporative demand. Hyponasty could also increase water consumption if associated with increased transpiration. Lastly, effects of HT on growth could lead to reduced leaf area, limiting plant water losses and thus mitigating the effects of WD.

In the face of the multiplicity of interacting, sometimes opposite effects between these two stresses, it appears difficult to predict plant responses to combined HT and WD. The aim of this study was therefore to evaluate the responses to both isolated and combined HT and WD in natural accessions of the model plant *Arabidopsis thaliana*. The following questions were addressed: (1) how HT and WD interact on traits related to plant growth, morphology and development and to what extent do their combined effects differ from those of isolated stresses? (2) Is the variability of responses to isolated and combined HT and WD related to the climatic conditions at the accessions collection sites? (3) To what extent are these responses related to trait values exhibited in control conditions? A set of ten *Arabidopsis* accessions spanning nearly the entirety of the latitudinal range of this species was selected to identify common responses and explore the natural variation of *Arabidopsis* tolerance to both stresses. Controlled environmental conditions were applied in full factorial experiments and maintained constant from the seedling to the reproductive stage. Control air temperature was set to 20 °C, as in most experimental studies (Balasubramanian et al. 2006, Saidi et al. 2011),

Table 1. Origin of the accessions studied and climate at the collection sites. X indicate the experiments in which accessions were studied.

Accession	Latitude (°N)	Longitude (°E)	Country	Mean autumn-spring precipitations (mm)	Mean autumn-spring temperature (°C)	Diurnal temperature range	Relative humidity	Exp. 1	Exp. 2	Exp. 3
Cvi-0	15	-23.4	Cape Verde Island	0.36	21.8	5.52	74.4		X	X
Mt-0	32.6	22.8	Lybia	52.2	15.2	7.57	62.0		X	X
Ct-1	37	15	Italy	61.19	12.3	8.73	73.5		X	X
Sha	38	68	Tadjikistan	53.1	8.2	13.16	59.5	X	X	X
Bay-0	49		Germany	29	2.99	8.58	77.0	X		
An-1	51.2	4.4	Belgium	64.2	5.96	7.74	82.2		X	X
Col-0	53	10	Poland	52.9	3.96	7.59	86.3	X	X	X
L*er*	53	16	Poland	38.2	2.6	7.63	83.1	X	X	X
Lc-0	58	-5	UK	161.0	4.1	5.83	88.5		X	X
Est-1	59	28	Russia	48.7	-2.1	7.68	84.3		X	X

whereas HT was set to 30 °C. This HT level has been identified to be the basal thermotolerance, i.e. the highest temperature tolerated by a plant that has never encountered previous HT, of the *Arabidopsis* accession Col-0 (Ludwig-Muller et al. 2000a). Soil WD was maintained constant at a level previously shown to significantly decrease leaf water potential and impair plant growth, resulting in reduced plant size of Col-0 by half (Aguirrezabal et al. 2006).

Materials and methods

Plant material and growth conditions

Ten accessions of *Arabidopsis thaliana* were grown in 1 to 3 independent experiments depending on the accession (Table 1). Seeds of all genotypes were stored at 4 °C in the dark ensuring stratification. Five seeds from each genotype were directly sown at the soil surface in 225 mL culture pots filled with a mixture (1:1, v:v) of loamy soil and organic compost (Neuhaus N2). Pots were damped with sprayed deionized water three times a day and placed in two controlled growth chambers in darkness (20 °C, 65% air relative humidity) until germination. After germination, plants were cultivated with a daily cycle of 12 h light supplied from a bank of HQi lamps which provided 175 µmol m^{-2} s^{-1} photosynthetic photon flux density (PPFD) at plant height.

Soil water deficit (WD) and high temperature (HT) treatments were applied to half of the pots after emergence of the first two true leaves (stage 1.02 in Boyes et al. 2001) ensuring a good establishment of the seedlings. In the first growth chamber, control air temperature (CT) was set to 20/17°C day/night, while HT treatment was set to 30/25°C in the second one. Air relative humidity was adjusted to 65% under CT and 85% under HT in order to maintain equal water vapor pressure deficit at 0.9 kPa. This was set up in order to avoid the confounding effect of temperature on transpiration through increased vapour pressure deficit. Soil water content was controlled before sowing to estimate the amount of dry soil and water in each pot. Subsequent changes in pot weight were due to changes in water status. Soil water content was maintained at 0.35 and 0.20 g H_20 g^{-1} dry soil with a modified one-tenth-strength Hoagland solution (Hoagland and Arnon 1950) in the well-watered and WD treatments, respectively. The field capacity of the substrate was 0.78 g H_2O g^{-1} dry soil (Granier et al. 2006), therefore the well-watered and WD treatments represented 45% and 25% of the soil field capacity, respectively. Pot weight was precisely adjusted to reach the target soil water content by weighing and watering each individual pot every Monday, Wednesday and Friday. Other days, a standard volume of nutrient solution amounting to the mean volume of

previously weighed water applications for each treatment was added to the plants without weighing the pots.

Three consecutive experiments were carried out following the same experimental procedure (see Table 1). In experiments 1 and 2, only one plant per pot was maintained until first silique shattering, while one to three plants were maintained until inflorescence emergence in experiment 3 for photosynthesis measurements and ABA content determination (see below).

Measurement of plant traits

During the course of plant development the following stages were scored: germination, cotyledons fully opened, 2 rosette leaves >1 mm, inflorescence emergence, first flower open and first silique shattered (stages 0.7, 1.0, 1.02, 5.01, 6.00 and 8.00 of Boyes et al. (2001), respectively). Leaf number was determined for each plant at each precise adjustment of soil water content, i.e. three times a week, only in experiment 2 and 3.

Dynamics of leaf production

For each plant in experiment 2, a sigmoid curve was fitted to the relationship between total number of rosette leaves (LN) and time from stage 1.02 to stage 8.00 by the following 4-parameter logistic model:

$$LN = \frac{a}{1 + e^{\left(-\frac{(d-d_0)}{b}\right)}}$$

where d is the number of days after stage 1.02, a is the maximum vegetative leaf number, d_0 is the time when $a/2$ leaves have developed and b is the inverse of slope factor which refers to the steepness of the curve, and is thus a parameter related to the maximum rate of leaf production. In order to standardize between genotypes, we used an estimate of leaf production duration (days) as $d_0 - b \ln(0.05/0.95)$, that is the time period for vegetative leaf number to increase from 5% to 95% maximum number. The maximum rate of leaf production (R_{max}, leaf d^{-1}) was calculated from the first derivative of the logistic model at d_0 as $R_{max} = a/(4b)$.

In Experiment 3, since leaf emergence rate is maximal and nearly constant between stage 1.02 to stage 5.01, R_{max} was fairly well estimated by the slope of the relationship between LN and time during this period. R_{max} varied across genotypes and treatments with highly reproducible results between experiments (r = 0.85, P < 0.001). Most of the plants survived the HT and WD treatments, and reached the reproductive stage. Only a few plants did not survive the combined HTxWD treatment.

Whole plant and leaf traits

In experiment 2, 20 days after germination, tip height, total length and blade length of the youngest fully expanded leaf were measured on each plant with a digital caliper as described in Hopkins, Schmitt & Stinchcombe (2008). At this time, plants had 6 to 14 leaves depending on the genotype and inflorescence had not emerged. Measurements were taken in randomized order between 2 and 4 hours after lights went on in the chambers to avoid any effects associated with time of the day like endogenous rhythms. The proportion of leaf composed of blade was estimated by the blade ratio, the blade length divided by total leaf length. Leaf insertion angle (degree) was calculated as θ = arcsine(leaf tip height/leaf length).

Plants were harvested at stage 8.00, in the morning and after irrigation. Rosettes were cut, inflorescences were detached from the rosettes and their fresh weights (mg) were determined immediately. Leaf blades were separated from the rosette, and fresh weights of the sixth and ninth leaves were determined. Mean leaf thickness (LT) of these two leaves was determined with a linear variable displacement transducer (LVDT, Solartron) connected to a multimeter and previously calibrated with 5 µm accuracy. Depending on the size of the leaf, LT was measured on six to ten points per leaf blade, avoiding the mid-vein. All blades were then stuck on a sheet of paper, arranged by order of emergence on the rosette, and the sheet of paper was scanned for area measurements. Additionally, a transparent imprint of the adaxial epidermis of the sixth leaf was obtained by drying off a varnish coat spread on the surface of the leaf. Imprint was peeled off and then stuck on microscope slides with one-sided adhesive for further measurements. Roots were carefully extracted from the soil and gently washed in deionized water. Leaf blades, petioles, reproductive structures and roots were then separately oven-dried at 65 °C for at least 3 days, and dry masses were determined. Rosette area (RA, cm^2) was determined as the sum of individual leaf blade areas measured on the scans with an image-analysis software (Bioscan-Optimas 4.10, Edmond, WA). From these measurements, leaf dry matter content (LDMC, the ratio of dry mass to fresh mass, mg g^{-1}) and specific leaf area (SLA, the ratio of leaf area to leaf dry mass, m^2 kg^{-1}) were calculated at the rosette and leaf (for leaves 6 and 9) levels. Biomass allocation was assessed by the ratios of above-ground vegetative, reproductive and below-ground dry masses to total plant dry mass. Root-to-shoot ratio was calculated as the ratio of root to vegetative above-ground masses.

Leaf epidermal anatomy

Epidermal imprints of the sixth leaves were placed under a microscope (Leitz DM RB; Leica) coupled to an image analyzer. Mean cell and stomatal densities were determined by counting the number of cells and stomata in two 0.12 mm^2 zones in the middle part of the leaf

Table 2. Results of the partitioning of phenotypic variation among the natural genotypes grown in a full factorial design of contrasted soil relative water content (W, 0.35 and 0.20 g H_20 g^{-1} dry soil in well-watered and water deficit treatment, respectively) and air temperature (T, 20 °C and 30 °C in control and high temperature treatment, respectively). The percentage of variance explained (SS_x/SS_{total}) and the level of significance (*, $P < 0.05$; **, $P < 0.01$; ***, $P < 0.001$) for each factor and the interactions are indicated. Values are from the full model including all interactions. All nonsignificant terms are reported, but were removed from the final model. Hypothesis testing was based on Pillai-Bartlett statistic in the MANOVA and on *F*-ratios from type III mean squares for all ANOVAs. R^2 is the proportion of total variance absorbed by the final model. All traits but R_{max} and leaf blade ratio were ln-transformed to fulfil ANOVA requirements. Net photosynthetic rate was not measured in WD conditions. [§]Data not available for Bay-0 and traits not included in the MANOVA.

Trait	Genotype (G)	Soil water content (W)	Temperature (T)	WxT	GxW	GxT	GxWxT	R^2 (%)
Df	9	1	1	1	9	9	9	
MANOVA	18.1***	0.5	32.7***	0.5	6.7**	3.4	1.9	57.5
Plant growth and final size, and biomass allocation								
R_{max} (leaf d^{-1})[§]	19.5***	31.9***	14.2***	0.0	3.1**	5.2***	0.8	73.9
Growth duration (days)[§]	44.9***	2.6***	8.6***	0.0	2.1	8.9***	6.2***	73.3
Leaf number at flowering (leaf)	46.6***	1.2***	19.1***	0.1	2.1*	6.7***	3.0***	78.7
Total dry mass (mg)	33.4***	18.3***	19.3***	0.0	3.1***	6.3***	3.4***	83.8
Reproductive allocation	31.5***	0.01	16.1***	0.1	2.3	5.3**	4.6*	59.8
Root allocation	10.2***	9.1***	0.5	1.2	6.3*	4.2	4.2	25.6
Leaf allocation	35.6***	1.0**	21.8***	0.3	2.2	7.4***	2.8*	70.8
Root to shoot ratio	19.2***	6.0***	1.1*	0.4	7.3**	4.0	3.8	33.6
Leaf structure, anatomy and physiology								
Leaf insertion angle (°)[§]	4.2***	0.3	69.4***	0.1	0.6	1.8	1.1	76.6
Leaf blade ratio (%)[§]	18.9***	10.5***	29.5***	2.1*	2.1	3.1*	1.5	64.1
Specific leaf area (cm^2 g^{-1})	27.5***	4.0***	18.1***	5.3***	4.7**	3.2*	4.8**	67.6
Leaf dry matter content (mg g^{-1})	14.4***	13.9***	1.7**	6.5***	7.6***	2.3	6.0*	52.4
Leaf thickness (µm)	45.8***	0.9*	10.7***	0.1	1.0	9.0***	2.3	66.4
Cell density (cell mm-^{2})	46.5***	15.2***	6.8***	0.2	6.6***	6.9***	1.3	82.0
Stomatal density (st. mm-^{2})	29.9***	14.9***	24.8***	0.0	4.1***	3.0**	0.9	76.7
Stomatal index (% st. $cell^{-1}$)	7.4**	1.1*	29.3***	0.1	3.6*	11.2***	3.4	52.6
ABA content (ng g^{-1} FW)	9.8	20.2***	8.4***	0.7	17.3*	6.1	14.6*	60.5
Net photosynthetic rate (µmol CO_2 s^{-1} m^{-2})	23.2**	-	23.3***	-	-	1.5	-	48.0

blade distributed on both sides of the mid-vein halfway from the margins. Stomatal index was calculated as 100 x stomatal number / (stomatal number + stomatal number x 2 + epidermal cell number).

Net photosynthetic rate

Net photosynthetic rate was measured using a single leaf chamber designed for *Arabidopsis* connected to an infrared gas analyzer system (CIRAS 2, PP systems, Amesbury, MA, USA) in experiment 3. Carbon fluxes were determined at steady-state (approximately 15 min after light was switched on) under control temperature (20 °C) and HT (30 °C) but only in well-watered conditions, and under ambient CO_2 (390 ppm) and light intensity (175 µmol m^{-2} s^{-1} PPFD). Photosynthesis was measured on two to 15 plants at bolting on An-1, Col-0, Cvi-0, Ler, Mt-0 and Sha.

Leaf ABA content

Leaf abscisic acid content (ABA, ng g^{-1} FW) was determined by radioimmunoassay (Quarrie et al. 1988) as previously described (Barrieu and Simonneau 2000). Leaf samples were ground finely under liquid nitrogen, placed in distilled water (5 ml *per* mg fresh weight) and immediately warmed at 70 °C for 5 min before shaking at 4 °C overnight. Extracts were then centrifuged at 16 000 g for 10 min at 4 °C, the supernatant was conserved at -20 °C and used for radioimmunoassay.

Meteorological data at the geographical origin of the accessions

Meteorological data (temperature, precipitation, relative humidity, diurnal temperature range) at the geographical origin of the accessions was extracted from high-resolution gridded datasets of climate data (New et al. 2002). Mean monthly parameters were calculated for the main period of vegetative growth of *A. thaliana* from September to May (Hoffmann 2002).

Data analysis

Statistical significance of trait variation was tested by three-way multivariate and univariate analyses of variance (MANOVA and ANOVA) with genotype, soil water content and air temperature as fixed factors. Post-hoc comparison between treatments was performed with Kruskal-Wallis non parametric test. Principal component analyses (PCA) were performed to study the relationships between the traits and the effects of the temperature and soil water treatments. PCAs were performed on data from the experiment where higher number of both traits and genotypes were studied (experiment 2) and on standardized mean trait values by genotype and treatment (n = 36) because traits were measured in very different

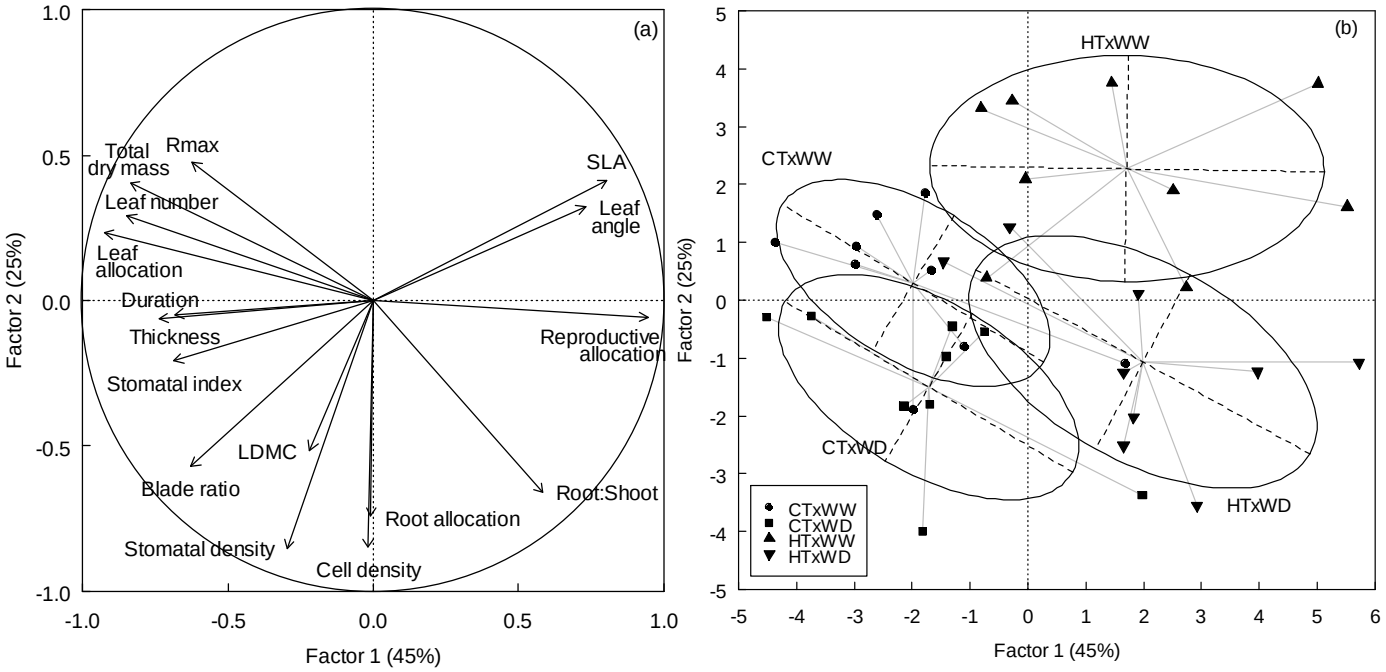

Figure 1. Principal component analysis on traits measured on nine Arabidopsis accessions grown under control (CT, 20/17 °C day/night) and high temperature (HT, 30/25 °C day/night), and in well-watered (WW, 0.35 g H20 g^{-1} dry soil) and water deficit (WD, 0.20 g H20 g^{-1} dry soil) conditions. HT and WD treatments were applied after emergence of the first two true leaves and plants were harvested at first visible pod. Only the first two axes are shown. (a) Representation of the variables; LDMC, leaf dry matter content; SLA, specific leaf area. (b) Representation of the accessions with centres of gravity and lines connected to each accession shown for each condition. CTxWW (circles), CTxWD (squares), HTxWW (triangles) and HTxWD (upside-down triangles). Ellipses represent inertia ellipses of each treatment. Each inertia ellipse is centered on the means, its width and height are given by 1.5 times the standard deviation of the coordinates on axes, and the covariance sets the slope of the main axis (Thioulouse et al. 1997).

units. Between- and within-treatment PCA analyses were performed on mean trait values to test for differences between treatments and focus on genotypic effects, respectively (Chessel et al. 2004). The null hypothesis that there is no difference between treatments was tested with a randomization test (*randtest.between* in the R/*ade4* package). The procedure checks that the observed value of the between/total inertia ratio is higher than expected under the null hypothesis. The distribution of the between/total inertia ratio is obtained by permuting the rows of the data frame, i.e. means per genotype and treatment (n = 999) and thus changing assignment to treatment group. Response ratios (R) between treated (T) and control (C) groups were calculated as $R_{T|C}$ = mean trait value$_T$/mean trait value$_C$ to quantify the effects of the treatments for each genotype. Five values of response ratios were calculated to obtain the response to water deficit according to the control conditions (WD-20 °C / WW-20 °C), the response to water deficit at high temperature (WD-30 °C / WW-30 °C), the response to high temperature in well-watered conditions (WW-30 °C / WW-20 °C), the response to high temperature in water deficit conditions (WD-30 °C / WD-20 °C), and the response to the combination of high temperature and water deficit compared to the control conditions (WD-30 °C / WW-20 °C). The response ratio quantifies the proportionate change that results from an experimental manipulation (Hedges et al. 1999). Response ratios were log-transformed in the statistical analyses. We tested the significance of the relationships between traits, response ratios, coordinates of the genotypes of the PCA axes, and climatic descriptors with correlation coefficients. All statistical tests were performed using R v.2.10 (R Development Core Team 2009).

Results

Analysis of multiple plant traits reveals significant genotype by environment effects but predominant additive effects of high temperature and water deficit

ANOVAs explained from 25% to 85% of the total variance of 16 functional traits related to plant growth, structure and physiology, and the MANOVA explained 58% of the total variance in the multivariate dataset (Table 2) Across traits, there was a highly significant genotypic variability among accessions (18% of variance explained in the MANOVA; from 4% to 47% of variance explained across traits). Additionally, strong genotype by environment (soil water content, temperature, or both) interactions were detected for all traits as indicated by highly significant first and second order interaction terms, highlighting the large natural phenotypic variability in the responses to both isolated and combined high temperature (HT)

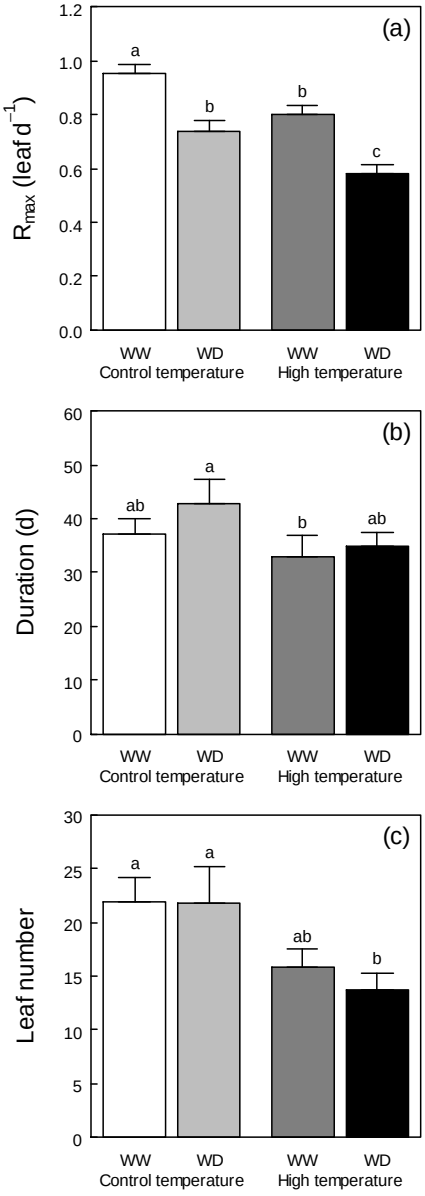

Figure 2. Dynamics of leaf production under control (CT, 20/17 °C day/night) and high temperature (HT, 30/25 °C day/night), and in well-watered (WW, 0.35 g H_20 g^{-1} dry soil) and water deficit (WD, 0.20 g H_20 g^{-1} dry soil) conditions. Maximum rate of leaf production (R_{max}) (a), duration of leaf production (b) and total leaf number (c). Bars are means + SE of nine accessions. Different letters indicate significant differences following Kruskal-Wallis test ($P < 0.05$).

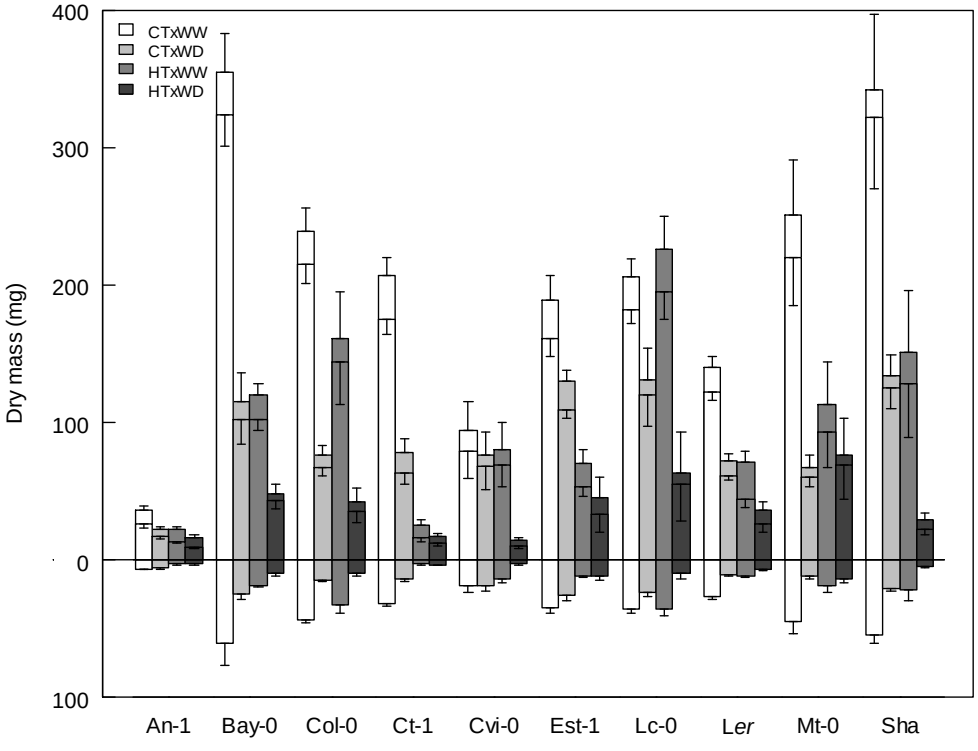

Figure 3. Plant dry mass under control (CT, 20/17 °C day/night) and high temperature (HT, 30/25 °C day/night), and in well-watered (WW, 0.35 g H_20 g^{-1} dry soil) and water deficit (WD, 0.20 g H_20 g^{-1} dry soil) conditions. Bars are means ± SE (n = 4 to 9) for the roots (below), vegetative leaves (intermediate) and reproductive stems (top) of ten Arabidopsis accessions.

and water deficit (WD). While significant for most of the traits, the effect of WD was not significant at the multivariate level. Interestingly, lack of significant interaction between water regime and temperature at the multivariate level and for most of the traits was indicative of prevailing additive effects of WD and HT (Table 2).

A principal component analysis (PCA) was performed in order to explore the multivariate pattern of effects of both isolated and combined HT and WD on the studied traits. First, second and third principal components (PC) explained 45%, 25% and 9% of the total variance, respectively (Fig. 1; see Supporting Information Table S1 for variable loadings). Size-related traits contributed most to PC1 which opposed large plants with numerous vegetative leaves and high rate of leaf production to plants that had high reproductive mass allocation and thinner, more erect leaves with high specific leaf area (Fig. 1a). Biomass allocation to the roots, epidermal cell density and stomatal density closely and negatively correlated with PC2. Leaf dry matter content contributed less to this axis but contributed to most of the variation on third axis.

Projection of the accessions (Fig. 1b) showed that the four temperature-by-soil water treatments were significantly discriminated in the first factorial plane ($P < 0.001$; permutation tests of between-treatments PCA) although the high genotypic variability was distinguishable as indicated by the distance of the accessions from the centroid of each treatment. Along PC1, plants grown under control conditions (20 °C air temperature; 0.35 g H_2O g^{-1} dry soil) were opposed to plants grown under combined HT and WD conditions (30 °C; 0.20 g H_2O g^{-1} dry soil). As indicated by the position of the centroid of each treatment along PC1, all treatments reduced plant performance compared to control conditions, and the combined stress was more detrimental to plants than isolated HT or WD. Isolated HT and WD treatments were significantly separated along PC2, indicating opposite effects of these stresses on traits related to this axis. Specifically, WD led to an increased biomass allocation to roots, a decrease in SLA and higher epidermal cell and stomata densities whereas HT had opposite effects.

The combination of high temperature and water deficit is more detrimental to plant development than isolated effects but differences between genotypes exist

As shown by the PCA, rosette development dynamics were significantly affected by HT, WD and their combination (Fig. 2; Table 2; Supporting Information Fig. S1). In control conditions, the average of maximum rate of leaf production (R_{max}, leaf d^{-1}) was 0.95 among genotypes and varied significantly from 0.75 in An-1 to 1.08 in Cvi-0 and Mt-0 (Supporting Information Fig. S2). The three treatments significantly reduced R_{max} (Fig. 2a; Table 2). Although the sensitivity of phenology to treatments varied significantly among *Arabidopsis*

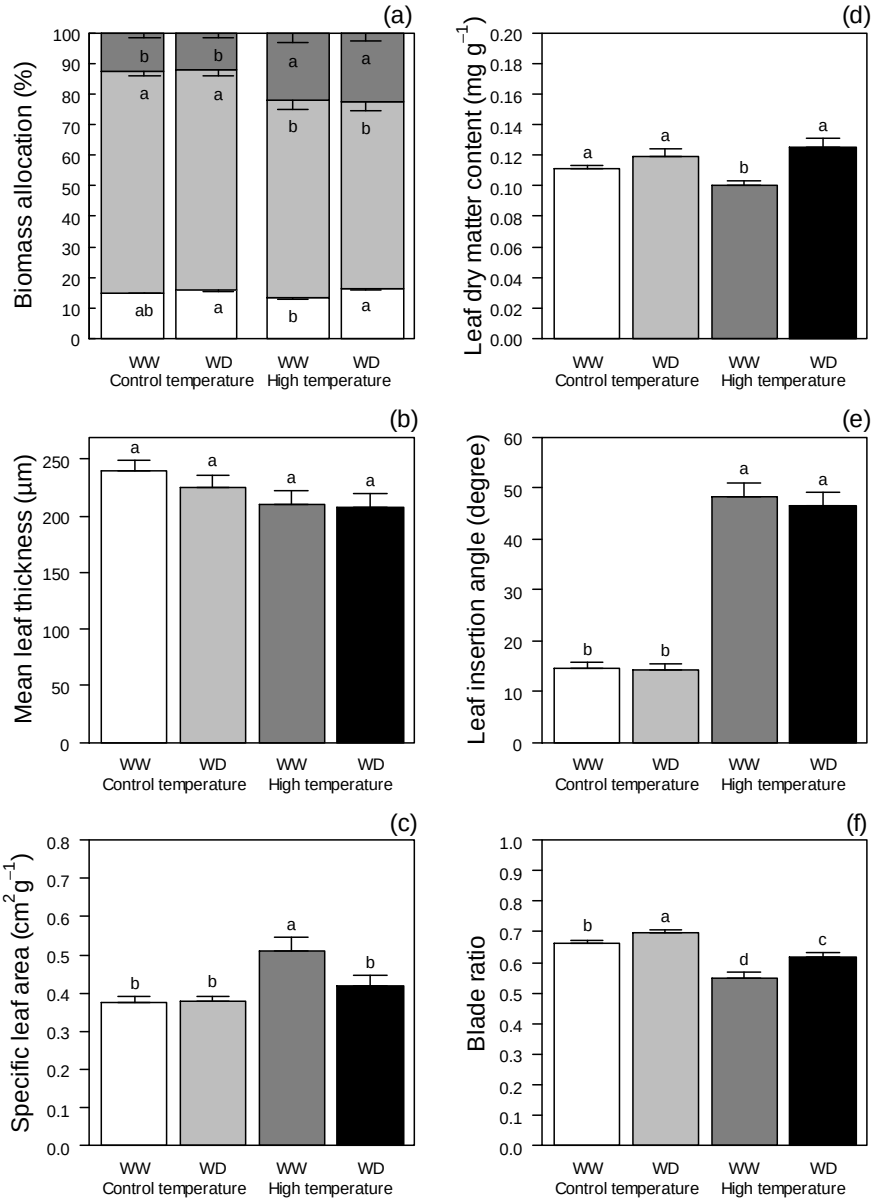

Figure 4. Biomass allocation and leaf morphology under control (CT, 20/17 °C day/night) and high temperature (HT, 30/25 °C day/night), and in well-watered (WW, 0.35 g H_20 g^{-1} dry soil) and water deficit (WD, 0.20 g H_20 g^{-1} dry soil) conditions. Dry mass allocation to the roots (below), vegetative leaves (intermediate) and reproductive stems (top) (a), leaf thickness (b), specific leaf area (c), leaf dry matter content (d), leaf insertion angle (e) and blade ratio (f). Bars are means ± SE of nine accessions. Different letters indicate significant differences following Kruskal-Wallis test ($P < 0.05$).

accessions, WD was on average more detrimental for leaf production (23% mean decrease) than HT (16% mean decrease; but see Lc-0 and Sha in Supporting Information Fig. S2a). Combining HT and WD had greater effects (40% mean decrease among genotypes) on R_{max} than isolated treatments (Fig. 2a). The duration of vegetative leaf production, which is highly related to flowering time in *A. thaliana*, also varied widely among accessions from 21 to 63 days in An-1 and Lc-0, respectively (Supporting Information Fig. S2b). Duration of leaf production and flowering time increased or decreased depending on accession and treatment leading to a highly significant 2nd order interaction term in the ANOVA (Table 2). While not significant in all accessions, WD tended to increase the duration of leaf production either at control or high temperature (nonsignificant water regime by temperature interaction in ANOVA; Table 2; Fig. 2b). By contrast, increasing air temperature tended to shorten the life cycle either in well-watered or WD conditions. As a result of their effects on plant growth dynamics, HT and WD significantly reduced total plant mass in all accessions but Cvi-0 and Lc-0 (Fig. 3; Table 2). On average, HT and WD similarly reduced total dry mass by 2-fold. Combining HT and WD (HTxWD) reduced plant size more severely than isolated stresses from 55% in An-1 to 91% in Ct-1 (Fig. 3; 85% mean decrease). In some genotypes plant dry mass tended to be less affected by isolated or combined HT and WD (An-1, Lc-0) while in others it was less reduced only under HT (Cvi-0) or WD (Est-1, L*er*). This resulted in weak relationships between response ratios to HT and WD for total dry mass (Supporting Information Fig. S3). However, the response ratio of HTxWD to control conditions ($R_{HTxWD|C}$) for the total dry mass was close to the sum of the response ratios of WD and HT to control conditions ($R_{WD|C} + R_{HT|C}$) suggesting nearly additive effects. This was true for all accessions except Cvi-0, Lc-0 and Mt-0. These accessions apart, clear additive effects were indicated by a significant relationship between $R_{HTxWD|C}$ and $R_{WD|C} + R_{HT|C}$ ($r = 0.82$; $P < 0.05$) with a slope not significantly different from one. Compared to other accessions, the growth of Mt-0 was less affected by the combination of HTxWD than by WD only (Fig. 3). To further investigate the genetic variability of responses to HT and WD we analysed the ranking of the genotypes from the PCA performed on trait values. The rankings were well conserved on PC1 and PC2. The Spearman's coefficients of rank correlation varied from 0.58 to 0.92 (Supporting Information Table S2). This indicated that accessions which exhibited higher value of a trait compared to other accessions in control conditions conserved this advantage when stressed.

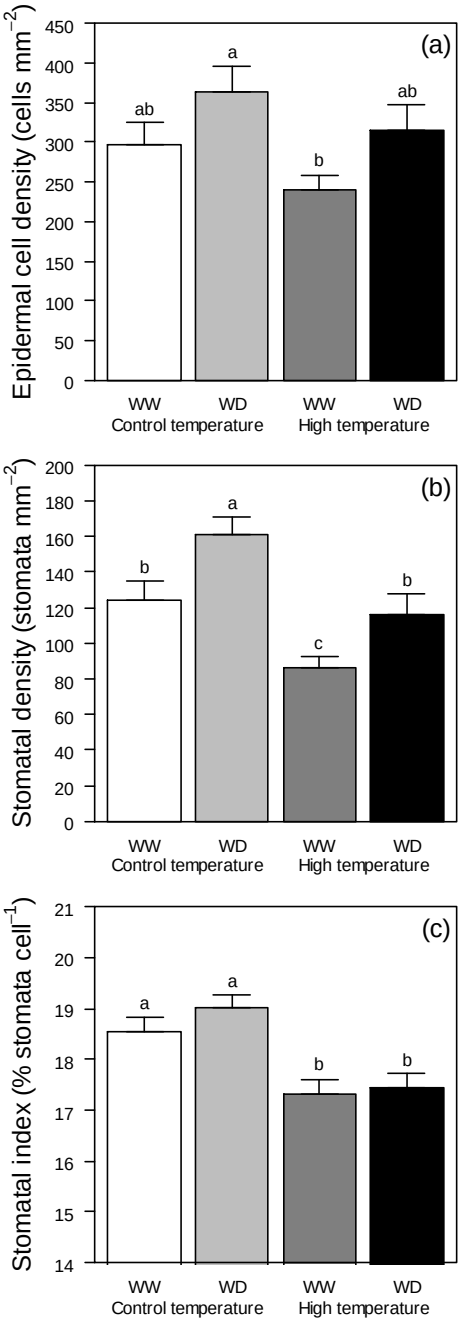

Figure 5. Leaf epidermal anatomy under control (CT, 20/17 °C day/night) and high temperature (HT, 30/25 °C day/night), and in well-watered (WW, 0.35 g H_20 g^{-1} dry soil) and water deficit (WD, 0.20 g H_20 g^{-1} dry soil) conditions. Cell density (a), stomatal density (b) and stomatal index (c). Bars are means + SE of nine accessions. Different letters indicate significant differences following Kruskal-Wallis test (P < 0.05).

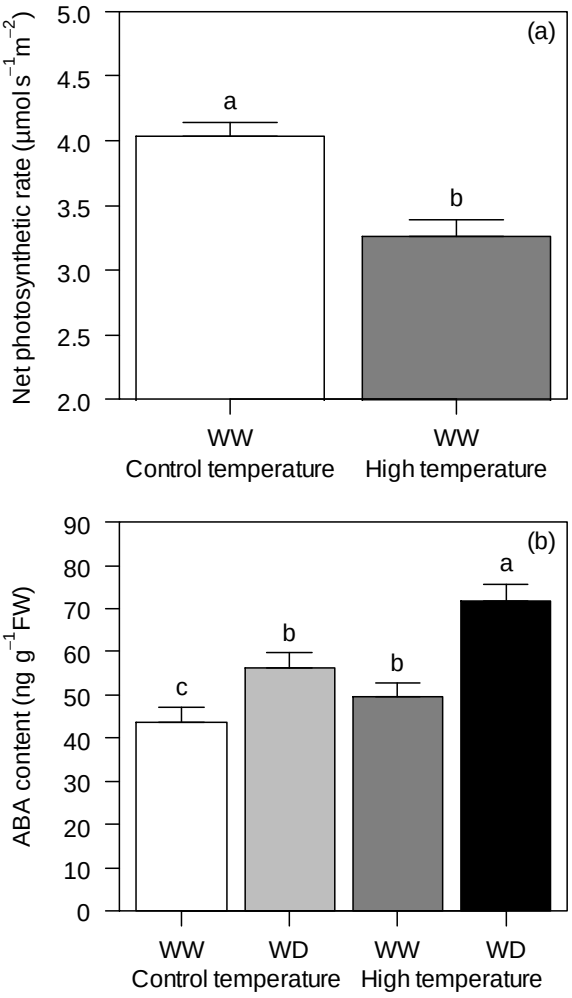

Figure 6. Net photosynthetic rate (a) and ABA content (b) under control (CT, 20/17 °C day/night) and high temperature (HT, 30/25 °C day/night), and in well-watered (WW, 0.35 g H_20 g^{-1} dry soil) and water deficit (WD, 0.20 g H_20 g^{-1} dry soil) conditions. Bars represent means + SE of nine accessions. Different letters indicate significant differences following Kruskal-Wallis test (P < 0.05). Net photosynthetic rate was not measured in WD conditions.

Biomass allocation to roots increases under water deficit and reproductive allocation increases at high temperature

Biomass allocation also changed at the whole plant and leaf levels in response to isolated and combined WD and HT (Table 2; Fig. 3). Interestingly, at the whole-plant level, WD and HT had different effects on allocation to roots and to reproductive structures. WD resulted in a significant increase in biomass allocation to roots, but reproductive allocation did not change significantly (Fig. 4a). The reverse was found under HT where no changes were detected in the biomass allocation to roots whereas a significant positive effect was observed on reproductive allocation.

Water deficit and high temperature have different effects on leaf structure

Leaves produced at HT tended to be thinner and had a higher specific leaf area (SLA), while in WD leaf dry matter content (LDMC) was increased (Fig. 4b-d; Supporting Information Fig. S2g-i). More precisely, SLA was much affected by HT in well-watered conditions and was significantly higher in all genotypes with little variation observed in WD, while LDMC tended to increase in response to WD, particularly at HT, and decrease under HT in well-watered conditions.

High temperature but not water deficit induces leaf hyponasty

In all accessions, HT induced a highly significant increase in leaf insertion angle, i.e. hyponasty, associated with a significant reduction in the proportion of blade compared to petiole length (Fig. 4e,f; Table 2). WD had no significant effect on hyponasty either at control or high temperature. By contrast, a significant increase in blade ratio was found in response to WD, resulting in significant water by temperature interaction in the ANOVA for this trait (Table 2).

Water deficit and high temperature have opposite but additive effects on leaf epidermis anatomy

WD and HT had opposite effects on the cellular anatomy of leaf epidermis but there was no water by temperature interaction as shown in the ANOVA (Table 2) indicating that the effects were globally additive. Across genotypes, cell and stomata densities increased in response to WD both at control and high temperature, whereas these traits tended to decrease in response to HT (Fig. 5). Stomatal index exhibited much less variation, but genotype and treatment effects were detected (Table 2; Supporting Information Fig. S2l-n). HT resulted in lower stomatal index (Fig. 5c). On the contrary, stomatal index tended to increase in response to WD but the effect of this treatment was not detectable in several genotypes.

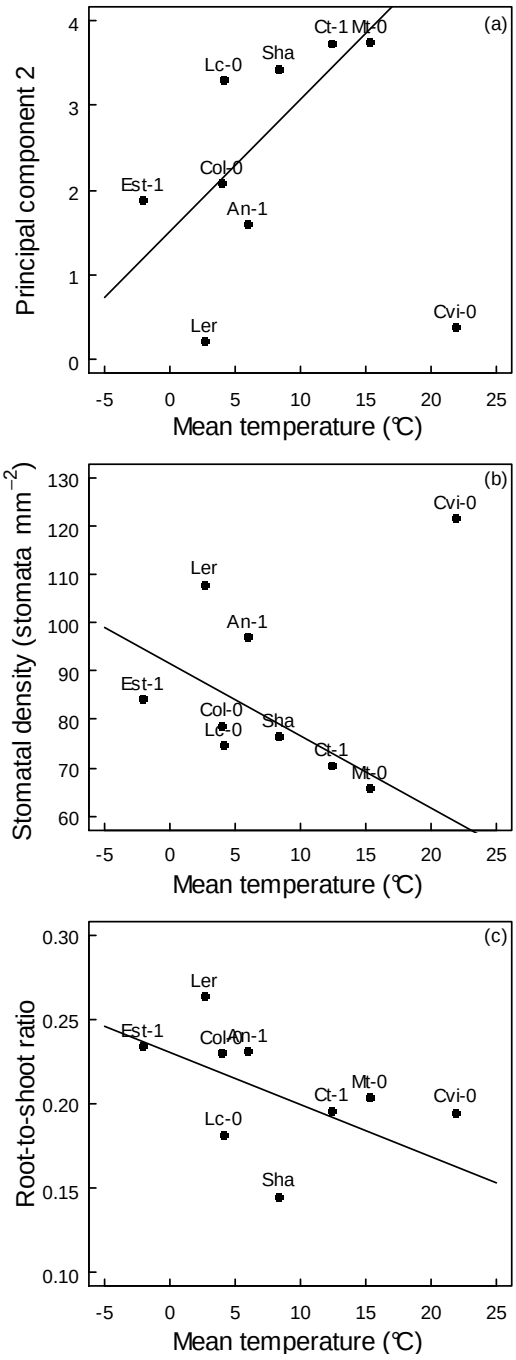

Figure 7. Relationships between mean temperature at the collection sites of nine *Arabidopsis* accessions and (a) PC2 coordinates (Fig. 1), (b) stomatal density, and (c) root-to-shoot ratio under high temperature (30 °C) but well-watered (0.35 g H_20 g^{-1} dry soil) conditions.

Photosynthesis is reduced at high temperature and ABA content increases under water deficit and high temperature

In well-watered conditions, net photosynthetic rate was significantly reduced by HT from 3.95 ± 0.73 at 20 °C to 3.30 ± 0.56 µmol CO_2 s^{-1} m^{-2} at 30 °C (Fig. 6a; Table 2). No significant genotype by temperature interaction was detected (P = 0.29; Table 2). Across all genotypes, leaf ABA content was significantly increased under WD and HT, and it was even more increased in response to the combination of the two stresses WD and HT (Fig. 6b).

Do responses to high temperature and water deficit relate to accessions climatic origin?

Beyond mean responses to single or combined treatments, the accessions studied herein displayed a range of sensitivities for their different traits. We explored whether any part of the responses of the accessions was related to the climatic conditions at geographical origin of the populations in which they were collected. The data from the PCA was used in order to reduce the number of comparisons and therefore the risk of type I error.

For each treatment, no trend was observed between accessions coordinates on PC1 from the PCA on trait values and mean monthly temperature at geographical origin of the populations. However, for plants grown under HT in well-watered conditions, a positive trend was found between coordinates on PC2 and temperature of origin (Fig. 7a). Inspection of Fig. 7 revealed that the accession from Cape Verde Island (Cvi-0) had a contrasted response compared to the other accessions. When excluding Cvi-0 from the analysis, the correlation was high and significant (r = 0.80; P < 0.01; Fig. 7a). The collection site of this accession presents the higher temperature although it was reported that Cvi-0 has been collected at 1200 m asl (Tonsor et al. 2008b), thus possibly encountering lower temperatures. As seen earlier, PC2 was negatively correlated to stomatal and cell density and biomass allocation to roots. Therefore the accessions that originate from sites with higher temperature tend to have less stomata per unit leaf surface and to allocate less biomass to the roots than accessions from colder sites when cultivated under high temperature (Fig. 7b,c).

Positive trends were also found between the coordinates on PC2 from the PCA on trait values and mean monthly precipitation from September to May in all treatments (r = 0.40 to 0.73). While not statistically significant, this corresponded to a stronger reduction in stomatal density under WD, HT or both for accessions originating from sites with high precipitations (r = –0.36, –0.51 and –0.56, respectively).

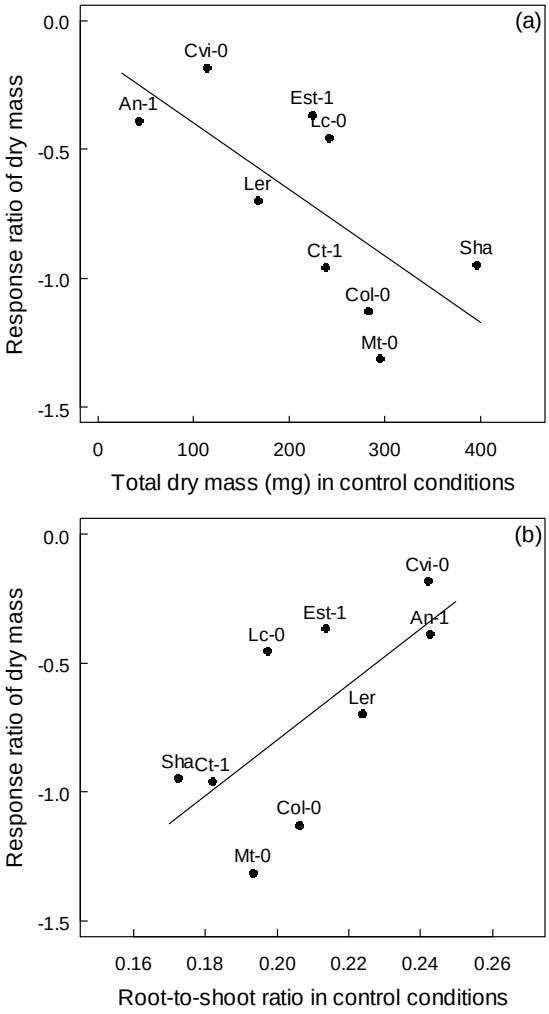

Figure 8. Relationships between the response ratio of total dry mass to water deficit (0.20 g H_20 g^{-1} dry soil/20 °C soil water content/air temperature) of nine *Arabidopsis* accessions and (a) the total dry mass and (b) root-to-shoot ratio in control conditions (0.35 g H_20 g^{-1} dry soil /20 °C).

Relationships between plant traits and tolerance to high temperature and water deficit

We explored the relationships between plant traits as measured in controlled conditions and accessions response to HT and WD. A negative correlation was found between absolute plant size in controlled conditions and the response ratio of plant size to the treatments. This trend was significant in response to WD (r = –0.73; P = 0.03; Fig. 8a) but not to HT (r = –0.27; P = 0.48) or the combination of HT and WD (r = –0.50; P = 0.17). Thus, stunted accessions (e.g. An-1) tend to be more tolerant to WD. Furthermore, the root-to-shoot ratio in controlled conditions was positively correlated with the response ratio of plant size to WD (r = 0.68; P = 0.04; Fig. 8b) and with the response ratio of leaf production rate under combined HTxWD (r = 0.72; P = 0.04). Thus, accessions with bigger root compartment relative to shoot tended to better maintain growth under WD and to keep producing leaves at the same rate as control under combined stresses.

Discussion

Water deficit and high temperature: independent or interacting responses?

Complex interactive responses can occur in plants experiencing multiple environmental stresses (Mittler 2006). Here we report the single or combined effects of soil water deficit and high temperature on a large set of plant traits from the cellular to the whole-plant levels in a collection of accessions of the model plant *A. thaliana*. Plant growth was significantly reduced under HT and WD and their combination was more detrimental to plant performance as also described in previous studies (Xu and Zhou 2006, Prasad et al. 2008). Interestingly, single trait as well as multiple traits analyses revealed that the combined effects of these two stresses were globally additive. This held true for traits responding in the same (e.g. plant mass) or reverse (e.g. stomatal density) directions to the two stresses and suggests a certain degree of independency between the mechanisms involved in the responses to WD and HT applied herein. Some traits were specific of the response to either WD or HT. This was the case for biomass allocation to roots which increased in response to WD, and conversely for reproductive allocation, leaf insertion angle and specific leaf area which significantly increased in response to HT (Xu and Zhou 2006). However, among the large number of traits investigated no single trait was affected only by the combination of HT and WD. The impact of the combined stresses has been rarely studied. In wheat and sorghum, Machado & Paulsen (2001) found that plant water status in response to HT were highly dependent on soil water availability. The work by Rizhsky and collaborators showed that some molecular responses

were specific to the combination of heat and drought compared to either stress alone (Rizhsky et al. 2002, Rizhsky et al. 2004). Yet our study is to our knowledge the first addressing this issue in different ecotypes and using a broad range of growth, developmental and physiological traits and the lack of HTxWD interaction is the rule for most of them, at least for the moderate levels of stresses applied during the whole plant cycle.

As generally found, plant growth dynamics (leaf production and leaf expansion) were significantly impaired in response to HT (Loveys et al. 2002) and WD (Granier et al. 2006, Hummel et al. 2010), leading to reduced plant size at reproductive stage and therefore reduced seed production (Aarssen and Clauss 1992). However, the two stresses had contrasting effects onto the timing of reproduction. As commonly found in natural and crop species (McMaster et al. 2009), WD delayed reproduction but contrasted effects on final leaf number were found across accessions. By contrast, under HT fewer leaves were produced when early reproduction occurred. Early reproduction following a moderate increase in temperature has been previously reported in *A. thaliana* (Balasubramanian et al. 2006) and other species (Barnabas et al. 2008). However, very sparse data are available on the combined effects of HT and WD on reproductive phenology in natural species (but see Barnabas et al. 2008 for a review in cereals). Here we found that the effects were globally additive in such a way that WD also delayed flowering under HT.

Although the majority of plants reached the flowering stage and a significant increase in biomass allocation to the reproductive stem was found under HT, flower abortions were clearly visible on later reproductive stages and very few pods reached maturity (not shown). The fecundity of the plants was particularly impaired under combined stresses. This was not surprising since reproductive structures are particularly sensitive to heat stress (Zinn et al. 2010) and even more to combinations of heat and drought (Barnabas et al. 2008). Notably, high temperatures (31-33 °C) very close to that experienced here (30 °C) have been shown to be sufficient to impair anthers development in non-acclimated plants of *A. thaliana* (Sakata et al. 2010). Apparently, vegetative acclimation to long-lasting treatments as experienced here did not change this response.

Is genetic variability of responses related to the climate of origin?

In our study, except the young seedling stage (before the emergence of the firsts true leaves), plants developed entirely under HT, WD or both. This may have led to acclimation processes possibly reinforcing plant tolerance to these stresses. Applying steady-state contrasted temperatures would also have produced different responses than those identified in the case of acute increase of temperature applied at a particular developmental stage as it is

largely found in the literature. Nevertheless, a high genotypic variability in traits values was observed in the different growing conditions and a significant genotype by environment interaction was found. This is not surprising given that the chosen accessions originated from a wide range of environments with varying temperature and drought constraints. A high variability of traits related to growth and phenology has been identified in natural populations of *A. thaliana* (Montesinos-Navarro et al. 2011). And genotypic variability among natural accessions has previously been identified for traits related to adaptation to water deficit (McKay et al. 2003) and temperature (Tonsor et al. 2008a). Here, we applied a HT-level within the physiological range of *A. thaliana* and close to the basal thermotolerance of the accession Col-0 (Ludwig-Muller et al. 2000b). Unfortunately, as far as we know basal thermotolerance has not been consistently evaluated for other accession than Col-0. Therefore, we cannot exclude that the variability of responses to HT observed here between the accessions was related to contrasted basal thermotolerance, which could also depend on the environment encountered in their habitat of origin. Few relationships between plant tolerance to HT and the climatic environment at the collection site of the accessions were found in this study. This is in accordance with Loveys et al. (2002) who found no relationship between thermal origin of the accessions and the production of dry matter in response to increasing temperature at the interspecific level. However, a lack of association could arise from the small number of accessions considered in our study. In a more geographically restricted study but including a large set of *Arabidopsis* natural populations, Montesinos-Navarro et al. (2011) showed that the variation of traits exhibited in controlled conditions was consistent with the temperature and water constraints encountered at the collection sites along an altitudinal gradient, pointing towards a likely adaptive differentiation of the populations to the environmental conditions. Here, we found that accessions that originate from sites with higher mean temperature during the vegetative growth tend to have less stomata per unit leaf surface and to allocate less biomass to the roots than accessions from colder sites when grown under high temperature.

Stomatal density and plant response to high temperature and water deficit

Despite the prevailing opinion that stomatal density would increase in response to HT (Wahid et al. 2007) data from literature are not unanimous see Luomala et al. (2005). Indeed, it is most likely that stomatal density depends on tight interactions between plant water balance (water status and transpiration) and the environmental conditions, particularly relative humidity and vapour pressure deficit (VPD_{air}) encountered by the plant during leaf growth (Lake and Woodward 2008). Assuming that conditions favouring expansion dilute stomata at

the leaf surface, increases in humidity in the vicinity of the plant are expected to reduce stomatal density. In this study, the possible effects of VPD_{air} on stomatal density at HT were excluded since VPD_{air} was maintained equal between the control (20 °C) and the HT (30 °C) treatment. In order to fulfil this condition of constant VPD_{air} relative air humidity was maintained higher under HT (85%) than under control (65%) conditions, possibly favouring the development of leaves with lower stomatal density at HT compared to control temperature. This was observed despite the significantly higher transpiration rate under HT compared to control temperature (Supporting Information Fig. S4). In addition, our results unequivocally show that soil water deficit led to increases in stomatal densities either at control or high temperature, thus counteracting the effects of HT. The same trend of decreasing and increasing stomatal density in response to HT and WD, respectively, was found in almost all genotypes. Despite the fact that VPD_{air} was maintained equal between the two temperature treatments, accelerated depletion of soil water or lower leaf water potential may have interfered with plant responses at HT due to higher rates of transpiration (Machado and Paulsen 2001; Supporting Information Fig. S4). Interestingly, relationships were found between stomatal density and meteorological conditions at the collection sites. Stomatal density was lower in accessions collected in warmer sites and/or sites with higher amount of precipitations, particularly when considering the responses to HT and WD.

Contrary to what was suggested by Lake & Woodward (2008), we found no relationship between ABA content in the rosette leaves and stomatal density. We cannot exclude a differential response of abaxial versus adaxial leaf epidermis in our experiments (see Luomala et al. (2005)); however, we observed that stomatal densities of both sides of the leaves are correlated either under well-watered or WD conditions (Vile & Pervent unpublished).

Similarities between responses to high temperature and low light

It is noteworthy that some of the specific responses to HT were also characteristic of responses to low light intensity. For instance, it is well known that specific leaf area increases and leaf thickness decreases in response to low light (Poorter et al. 2009) and that shade leaves have higher specific leaf area and are thinner than leaves exposed to direct sun light (McMillen and McClendon 1983). Chabot & Chabot (1977) reported that decreasing light and moderately elevated temperature had similar effects on thickness. In *Arabidopsis*, a clear similarity between the responses to light and high temperature resides also in hyponastic growth, i.e. the increase in leaf insertion angle (Van Zanten et al. 2009). These authors reported very similar trends of variation in leaf angle in response to HT and low light, and we have recently shown that the hyponastic response to HT can be reversed by increasing light

intensity (Vasseur et al. 2011 = Manuscript #3). Taken together, these results suggest that part of the responses to a moderate heat stress could be associated to a defect in carbon acquisition through photosynthesis, which is impaired under HT, and/or an increased competition for carbon use due to enhanced physico-chemical processes and increased protection mechanisms (notably heat shock proteins; Heckathorn et al. 1996). Accordingly, tolerance to warm temperatures is increased at high CO_2 concentration in C3 plants (Huxman et al. 1998, Taub et al. 2000) and decreased at low nitrogen supply due to a limited production of nitrogen-costly heat shock proteins (Heckathorn et al. 1996). The interactive effects of high temperature and light on plant functioning were analysed here under lower light than encountered in natural conditions. To test whether our results would hold under higher light conditions as found in the nature, especially at high temperature, experiments should be performed at higher light intensities. Interactions between WD, HT and light also remain to be investigated (Vasseur et al. 2011 = Manuscript #3).

Inherent trait variation and plant tolerance to high temperature and water deficit

Ecological research has engaged major efforts to identify plant traits, as measured in controlled or natural conditions, that could be good predictors of plant responses to changes in their environment (Grime 2001, Vile et al. 2006, Violle et al. 2007). Here, we found a trade-off between plant size in control conditions and tolerance to WD. A similar negative relationship between plant size and plant tolerance to WD was found in an analysis of 20 accessions capturing much of the genetic variation of *A. thaliana* worldwide (Clark et al. 2007) and a new collection of 88 accessions from Europe and Asia (Bouteillé et al. unpublished; $r = –0.54$ and $–0.25$; $P = 0.013$ and 0.022, respectively). A reanalysis of the data from Bouchabke et al. (2008) also showed a significant negative relationship between total leaf area in well-watered conditions and its response to a mild WD applied for 10 days ($r = –0.49$; $P = 0.014$). Interestingly, we found a similar ranking of responses to WD for the 6 common accessions (but Sha to a lesser extent) between Bouchabke et al. (2008) and our study. Such a trade-off between plant size and the response ratio to WD was also found in a reanalysis of the data of a recent study on stress-related specific mutants of *Arabidopsis* (Skirycz et al. 2011) although plant size variation between lines was weak ($r = –0.43$; $P = 0.014$). These authors report that growth reduction caused by stress was independent of plant size under control conditions but they used the relative response of mutants compared to the wild-type, not the response ratio for each line. A first explanation for this trade-off would reside in the fact that large plants consume more water and therefore experience greater water

shortage. However, the experimental procedure used in the present study as well as in Bouchabke et al. (2008) and in Skirycz et al. (2011), i.e. a daily irrigation to adjust the soil water content, is unlikely to have favoured small plants that consume less water. A trade-off between plant size and plant tolerance to WD is in accordance with the results of He et al. (2010) that populations of *Centaurea stoebe* with inherently bigger plant size are more susceptible to stressing (water and nutrient) conditions. In contrast to these authors, who did not observe any relationship with other traits than plant size, here we found a positive relationship between the root-to-shoot ratio and plant tolerance to WD which could give a proportionate advantage under inherent water shortage.

On the other hand, the negative trend between plant size and *Arabidopsis* tolerance to HT was weaker and not significant. No single trait was identified as a good predictor of plant response to HT. Some elements suggest that changes in leaf inclination could participate to thermotolerance adjustments by reducing intercepted light and hence tissue temperature (Salvucci and Crafts-Brandner 2004). Although leaf insertion angle increased in response to HT and this response varied between accessions, in our data hyponasty was not related to thermotolerance. Also, in contrast to the results of van Zanten et al. (2009), no relationship was observed between the change in leaf angle in response to HT and the diurnal temperature range at the geographical origin of the accessions. This discrepancy could in part be explained by the higher but shorter temperature treatment experienced in van Zanten et al. (38 °C during 7h) compared to our study (30 °C during *ca.* 15 d).

Finally, plant tolerance to WD under HT, in terms of plant size reduction, was also related to plant size in well-watered and control temperature conditions albeit the relationship was weaker than for WD under control temperature. Thus inherent plant size would participate to soil-water-plant relationships in a larger extent than to the response to increasing temperature.

Conclusion

Despite the likely interactive processes involved in plant response to high temperature and water deficit, here we showed that at least moderate levels of these two stresses have additive effects on a large set of plant traits related to growth and development in the model species *Arabidopsis thaliana*. This would have important consequences for modelling plant growth under combined stresses. Some traits were affected only by one or the other stress, highlighting the specific sensitivity of some processes such as reproduction in response to high temperature and resources allocation for a better water acquisition in response to water

deprivation. In natural environments, variation in temperature and water availability can act together or independently on covarying traits and on the distribution of plant species. It was therefore not surprising to find a significant natural variation in *Arabidopsis* tolerance to high temperature and water deficit applied separately or in combination. Genetic variability in the responses of several traits to the different stresses accompanied this natural range of tolerances and was in good correspondence with some characteristics of the climatic origin of the natural populations. This opens several avenues to explore the underlying physiological processes shaping the distribution of this and other species.

Acknowledgements

We thank J.-J. Thioux, M. Dauzat, A. Bédiée and G. Rolland for the technical support during the experiments. We thank A. Skirycz for providing data, and two anonymous referees for improvements to the manuscript.

References

Aarssen, L. W. and M. J. Clauss. 1992. Genotypic variation in fecundity allocation in *Arabidopsis thaliana*. Journal of Ecology **80**:109-114.

Aguirrezabal, L., S. Bouchier-Combaud, A. Radziejwoski, M. Dauzat, S. J. Cookson, and C. Granier. 2006. Plasticity to soil water deficit in *Arabidopsis thaliana*: dissection of leaf development into underlying growth dynamic and cellular variables reveals invisible phenotypes. Plant Cell and Environment **29**:2216-2227.

Aubert, Y., D. Vile, M. Pervent, D. Aldon, B. Ranty, T. Simonneau, A. Vavasseur, and J. P. Galaud. 2010. RD20, a stress-inducible caleosin, participates in stomatal control, transpiration and drought tolerance in *Arabidopsis thaliana*. Plant and Cell Physiology **51**:1975-1987.

Balasubramanian, S., S. Sureshkumar, J. Lempe, and D. Weigel. 2006. Potent induction of *Arabidopsis thaliana* flowering by elevated growth temperature. Plos Genetics **2**:980-989.

Barnabas, B., K. Jäger, and A. Fehér. 2008. The effects of drought and heat stress on reproductive processes in cereals. Plant Cell and Environment **31**:11-38.

Barrieu, P. and T. Simonneau. 2000. The monoclonal antibody MAC252 does not react with the (-) enantiomer of abscisic acid. Journal of Experimental Botany **51**:305-307.

Boese, S. R. and N. P. A. Huner. 1990. Effect of growth temperature and temperature shifts on spinach leaf morphology and photosynthesis. Plant Physiology **94**:1830-1836.

Bouchabke, O., F. Chang, M. Simon, R. Voisin, G. Pelletier, and M. Durand-Tardif. 2008. Natural variation in *Arabidopsis thaliana* as a tool for highlighting differential drought responses. Plos One **3**:e1705.

Boyer, J. S. 1982. Plant productivity and environment. Science **218**:443-448.

Boyer, J. S. 1985. Water transport. Annual Review of Plant Physiology and Plant Molecular Biology **36**:473-516.

Boyes, D. C., A. M. Zayed, R. Ascenzi, A. J. McCaskill, N. E. Hoffman, K. R. Davis, and J. Görlach. 2001. Growth stage-based phenotypic analysis of Arabidopsis: a model for high throughput functional genomics in plants. The Plant Cell **13**:1499-1510.

Chabot, B. F. and J. F. Chabot. 1977. Effects of light and temperature on leaf anatomy and photosynthesis in *Fragaria vesca*. Oecologia **26**:363-377.

Chaves, M. M., J. S. Pereira, J. Maroco, M. L. Rodrigues, C. P. P. Ricardo, M. L. Osorio, I. Carvalho, T. Faria, and C. Pinheiro. 2002. How plants cope with water stress in the field. Photosynthesis and growth. Annals of Botany **89**:907-916.

Chessel, D., A.-B. Dufour, and J. Thioulouse. 2004. The ade4 package-I- One-table methods. R News **4**:5-10.

Ciais, P., M. Reichstein, N. Viovy, A. Granier, J. Ogee, V. Allard, M. Aubinet, N. Buchmann, C. Bernhofer, A. Carrara, F. Chevallier, N. De Noblet, A. D. Friend, P. Friedlingstein, T. Grunwald, B. Heinesch, P. Keronen, A. Knohl, G. Krinner, D. Loustau, G. Manca, G. Matteucci, F. Miglietta, J. M. Ourcival, D. Papale, K. Pilegaard, S. Rambal, G. Seufert, J. F. Soussana, M. J. Sanz, E. D. Schulze, T. Vesala, and R. Valentini. 2005. Europe-wide reduction in primary productivity caused by the heat and drought in 2003. Nature **437**:529-533.

Clark, R. M., G. Schweikert, C. Toomajian, S. Ossowski, G. Zeller, P. Shinn, N. Warthmann, T. T. Hu, G. Fu, D. A. Hinds, H. M. Chen, K. A. Frazer, D. H. Huson, B. Schoelkopf, M. Nordborg, G. Raetsch, J. R. Ecker, and D. Weigel. 2007. Common sequence polymorphisms shaping genetic diversity in *Arabidopsis thaliana*. Science **317**:338-342.

Cook, G. D., J. R. Dixon, and A. C. Leopold. 1964. Transpiration: its effects on plant leaf temperature. Science **144**:546-547.

Fu, Q. A. and J. R. Ehleringer. 1989. Heliotropic leaf movements in common beans controlled by air temperature. Plant Physiology **91**:1162-1167.

Granier, C., L. Aguirrezabal, K. Chenu, S. J. Cookson, M. Dauzat, P. Hamard, J. J. Thioux, G. Rolland, S. Bouchier-Combaud, A. Lebaudy, B. Muller, T. Simonneau, and F. Tardieu. 2006. PHENOPSIS, an automated platform for reproducible phenotyping of plant responses to soil water deficit in *Arabidopsis thaliana* permitted the identification of an accession with low sensitivity to soil water deficit. New Phytologist **169**:623-635.

Grime, J. P. 2001. Plant strategies, vegetation processes and ecosystem properties. Seconde edition. John Wiley and Sons, Chichester.

He, W. M., G. C. Thelen, W. M. Ridenour, and R. M. Callaway. 2010. Is there a risk to living large? Large size correlates with reduced growth when stressed for knapweed populations. Biological Invasions **12**:3591-3598.

Heckathorn, S. A., G. J. Poeller, J. S. Coleman, and R. L. Hallberg. 1996. Nitrogen availability alters patterns of accumulation of heat stress-induced proteins in plants. Oecologia **105**:413-418.

Hedges, L. V., J. Gurevitch, and P. S. Curtis. 1999. The meta-analysis of response ratios in experimental ecology. Ecology **80**:1150-1156.

Hoagland, D. R. and D. I. Arnon. 1950. The water-culture method for growing plants without soil. California Agricultural Experiment Station Circular **347**:1-32.

Hoffmann, M. H. 2002. Biogeography of *Arabidopsis thaliana* (L.) Heynh. (Brassicaceae). Journal of Biogeography **29**:125-134.

Hopkins, R., J. Schmitt, and J. R. Stinchcombe. 2008. A latitudinal cline and response to vernalization in leaf angle and morphology in *Arabidopsis thaliana* (Brassicaceae). New Phytologist **179**:155-164.

Hsaio, T. C. 1973. Plant responses to water stress. Annual Review of Plant Physiology **24**:519-570.

Hummel, I., F. Pantin, R. Sulpice, M. Piques, G. Rolland, M. Dauzat, A. Christophe, M. Pervent, M. Bouteillé, M. Stitt, Y. Gibon, and B. Muller. 2010. *Arabidopsis thaliana* plants acclimate to water deficit at low cost through changes of C usage; an integrated perspective using growth, metabolite, enzyme and gene expression analysis. Plant Physiology **154**:357-372.

Huxman, T. E., E. P. Hamerlynck, M. E. Loik, and S. D. Smith. 1998. Gas exchange and chlorophyll fluorescence responses of three south-western Yucca species to elevated CO_2 and high temperature. Plant Cell and Environment **21**:1275-1283.

IPCC. 2007. Climate Change 2007: The physical science basis. Contribution of Working Group I to the Fourth Assessment Report of the Intergovernmental Panel on Climate Change. Cambridge University Press, Cambridge, UK and New York, NY.

Jenks, M. A. and A. J. Wood, editors. 2010. Genes for plant abiotic stress. Wiley-Blackwell, Chichester.

Johnson, I. R. and J. H. M. Thornley. 1985. Temperature-dependence of plant and crop processes. Annals of Botany **55**:1-24.

Koini, M. A., L. Alvey, T. Allen, C. A. Tilley, N. P. Harberd, G. C. Whitelam, and K. A. Franklin. 2009. High temperature-mediated adaptations in plant architecture require the bHLH transcription factor PIF4. Current Biology **19**:408-413.

Körner, C. 2006. Significance of temperature in plant life. Pages 48-69 *in* J. I. L. Morison and M. D. Morecroft, editors. Plant growth and climate change. Blackwell Publishing Ltd, Oxford, UK.

Kuroyanagi, T. and G. M. Paulsen. 1988. Mediation of high-temperature Injury by roots and shoots during reproductive growth of wheat. Plant Cell and Environment **11**:517-523.

Lafta, A. M. and J. H. Lorenzen. 1995. Effect of high temperature on plant growth and carbohydrate metabolism in potato. Plant Physiology **109**:637-643.

Lake, J. A. and F. I. Woodward. 2008. Response of stomatal numbers to CO_2 and humidity: control by transpiration rate and abscisic acid. New Phytologist **179**:397-404.

Lecoeur, J., J. Wery, O. Turc, and F. Tardieu. 1995. Expansion of Pea leaves subjected to short water deficit: cell number and cell size are sensitive to stress at different periods of leaf development. Journal of Experimental Botany **46**:1093-1101.

Lobell, D. B. and G. P. Asner. 2003. Climate and management contributions to recent trends in US agricultural yields. Science **299**:1032.

Loveys, B. R., I. Scheurwater, T. L. Pons, A. H. Fitter, and O. K. Atkin. 2002. Growth temperature influences the underlying components of relative growth rate: an investigation using inherently fast- and slow-growing plant species. Plant Cell and Environment **25**:975-987.

Ludwig-Muller, J., P. Krishna, and C. Forreiter. 2000a. A glucosinolate mutant of Arabidopsis is thermosensitive and defective in cytosolic Hsp90 expression after heat stress. Plant Physiology **123**:949-958.

Ludwig-Muller, J., P. Krishna, and C. Forreiter. 2000b. A glucosinolate mutant of *Arabidopsis* is thermosensitive and defective in cytosolic Hsp90 expression after heat stress. Plant Physiology **123**:949-958.

Luomala, E. M., K. Laitinen, S. Sutinen, S. Kellomaki, and E. Vapaavuori. 2005. Stomatal density, anatomy and nutrient concentrations of Scots pine needles are affected by elevated CO_2 and temperature. Plant Cell and Environment **28**:733-749.

Machado, S. and G. M. Paulsen. 2001. Combined effects of drought and high temperature on water relations of wheat and sorghum. Plant and Soil **233**:179-187.

McKay, J. K., J. H. Richards, and T. Mitchell-Olds. 2003. Genetics of drought adaptation in *Arabidopsis thaliana*: I. Pleiotropy contributes to genetic correlations among ecological traits. Molecular Ecology **12**:1137-1151.

McMaster, G. S., J. W. White, A. Weiss, P. S. Baenziger, W. Wilhelm, J. W. Porter, and P. D. Jamieson. 2009. Simulating crop phenological responses to water deficits. Pages 277-300 *in* L. R. Ahuja, Reddy, V.R., Anapalli, S.A., and Yu, Q., editor. Modeling the response of crops to limited water: recent advances in understanding and modeling water stress effects on plant growth processes. ASA-SSA-CSSA, Madison, WI.

McMillen, G. G. and J. H. McClendon. 1983. Dependence of photosynthetic rates on leaf density thickness in deciduous woody plants grown in sun and shade. Plant Physiology **72**:674-678.

Mittler, R. 2006. Abiotic stress, the field environment and stress combination. Trends in Plant Science **11**:15-19.

Montesinos-Navarro, A., J. Wig, F. X. Pico, and S. J. Tonsor. 2011. *Arabidopsis thaliana* populations show clinal variation in a climatic gradient associated with altitude. New Phytologist **189**:282-294.

New, M., D. Lister, M. Hulme, and I. Makin. 2002. A high-resolution data set of surface climate over global land areas. Climate Research **21**:1-25.

Parent, B., O. Turc, Y. Gibon, M. Stitt, and F. Tardieu. 2010. Modelling temperature-compensated physiological rates, based on the co-ordination of responses to temperature of developmental processes. J Exp Bot **61**:2057-2069.

Passioura, J. B. 1996. Drought and drought tolerance. Plant Growth Regulation **20**:79-83.

Poorter, H., U. Niinemets, L. Poorter, I. J. Wright, and R. Villar. 2009. Causes and consequences of variation in leaf mass per area (LMA): a meta-analysis (vol 182, pg 565, 2009). New Phytologist **183**:1222-1222.

Porter, J. R. 2005. Rising temperatures are likely to reduce crop yield. Nature **436**:174.

Prasad, P. V. V., S. A. Staggenborg, and Z. Ristic. 2008. Impacts of drought and/or heat stress on physiological, developmental, growth and yield processes of crop plants. Pages 301-355 *in* L. R. Ahuja, V. R. Reddy, S. A. Saseendran, and Q. Yu, editors. Response of crops to limited

water: understanding and modeling water stress effects on plant growth processes. ASA, CSSA, SSSA, Madison, WI, USA.

Quarrie, S. A., P. N. Whitford, N. E. J. Appleford, T. L. Wang, S. K. Cook, I. E. Henson, and B. R. Loveys. 1988. A monoclonal antibody to (S)-abscisic acid - Its characterization and use in a radioimmunoassay for measuring abscisic acid in crude extracts of cereal and lupin leaves. Planta **173**:330-339.

R Development Core Team. 2009. R: a language and environment for statistical computing. R Foundation for Statistical Computing, Vienna, Austria.

Ritchie, J. T. and D. S. NeSmith. 1991. Temperature and crop development. Pages 6-29 *in* R. J. Hanks and J. T. Ritchie, editors. Modelling plant and soil systems. American Society of Agronomy, Madison, WI.

Rizhsky, L., H. Liang, J. Shuman, V. Shulaev, S. Davletova, and R. Mittler. 2004. When defense pathways collide. The response of Arabidopsis to a combination of drought and heat stress. Plant Physiology **134**:1683-1696.

Rizhsky, L., H. J. Liang, and R. Mittler. 2002. The combined effect of drought stress and heat shock on gene expression in tobacco. Plant Physiology **130**:1143-1151.

Sage, R. F. and D. S. Kubien. 2007. The temperature response of C_3 and C_4 photosynthesis. Plant Cell and Environment **30**:1086-1106.

Saidi, Y., A. Finka, and P. Goloubinoff. 2011. Heat perception and signalling in plants: a tortuous path to thermotolerance. New Phytologist **190**:556-565.

Sakata, T., T. Oshino, S. Miura, M. Tomabechi, Y. Tsunaga, N. Higashitani, Y. Miyazawa, H. Takahashi, M. Watanabe, and A. Higashitani. 2010. Auxins reverse plant male sterility caused by high temperatures. Proceedings of the National Academy of Sciences of the United States of America **107**:8569-8574.

Salvucci, M. E. and S. J. Crafts-Brandner. 2004. Relationship between the heat tolerance of photosynthesis and the thermal stability of rubisco activase in plants from contrasting thermal environments. Plant Physiology **134**:1460-1470.

Skirycz, A., K. Vandenbroucke, P. Clauw, K. Maleux, B. D. Meyer, S. Dhondt, A. Pucci, N. Gonzalez, F. Hoeberichts, V. B. Tognetti, M. Galbiati, C. Tonelli, Frank Van Breusegem, M. Vuylsteke, and D. Inzé. 2011. Survival and growth of Arabidopsis plants given limited water are not equal. Nature Biotechnology **29**:212-214.

Taub, D. R., J. R. Seemann, and J. S. Coleman. 2000. Growth in elevated CO_2 protects photosynthesis against high-temperature damage. Plant Cell and Environment **23**:649-656.

Thuiller, W., S. Lavorel, M. B. Araujo, M. T. Sykes, and I. C. Prentice. 2005. Climate change threats to plant diversity in Europe. Proceedings of the National Academy of Sciences of the United States of America **102**:8245-8250.

Tisné, S., I. Schmalenbach, M. Reymond, M. Dauzat, M. Pervent, D. Vile, and C. Granier. 2010. Keep on growing under drought: genetic and developmental bases of the response of rosette area using a recombinant inbred line population. Plant Cell and Environment **33**:1875-1887.

Tonsor, S. J., C. Scott, I. Boumaza, T. R. Liss, J. L. Brodsky, and E. Vierling. 2008a. Heat shock protein 101 effects in A. thaliana: genetic variation, fitness and pleiotropy in controlled temperature conditions. Molecular Ecology **17**:1614-1626.

Tonsor, S. J., C. Scott, I. Boumaza, T. R. Liss, J. L. Brodsky, and E. Vierling. 2008b. Heat shock protein 101 effects in *A. thaliana*: genetic variation, fitness and pleiotropy in controlled temperature conditions. Molecular Ecology **17**:1614-1626.

Van Zanten, M., L. A. Voesenek, A. J. Peeters, and F. F. Millenaar. 2009. Hormone- and light-mediated regulation of heat-induced differential petiole growth in *Arabidopsis thaliana*. Plant Physiology **151**:1446-1458.

Vasseur, F., F. Pantin, and D. Vile. 2011. Changes in light intensity reveal a major role for carbon balance in Arabidopsis responses to high temperature. Plant Cell and Environment.

Vile, D., B. Shipley, and E. Garnier. 2006. A structural equation model to integrate changes in functional strategies during old-field succession. Ecology **87**:504-517.

Violle, C., M. L. Navas, D. Vile, E. Kazakou, C. Fortunel, I. Hummel, and E. Garnier. 2007. Let the concept of trait be functional! Oikos **116**:882-892.

Wahid, A., S. Gelani, M. Ashraf, and M. R. Foolad. 2007. Heat tolerance in plants: an overview. Environmental and Experimental Botany **61**:199-223.

Xu, Z. Z. and G. S. Zhou. 2006. Combined effects of water stress and high temperature on photosynthesis, nitrogen metabolism and lipid peroxidation in a perenial grass *Leymus chinensis*. Planta **224**:1080-1090.

Zhang, X., B. Wollenweber, D. Jiang, F. Liu, and J. Zhao. 2008. Water deficits and heat shock effects on photosynthesis of a transgenic *Arabidopsis thaliana* constitutively expressing ABP9, a bZIP transcription factor. J Exp Bot **59**:839-848.

Zinn, K. E., M. Tunc-Ozdemir, and J. F. Harper. 2010. Temperature stress and plant sexual reproduction: uncovering the weakest links. Journal of Experimental Botany **61**:1959-1968.

Supporting Information

Table S1. Loadings of the variables included in the PCA on mean trait values per genotype and treatment. All variables have been log-transformed.

Trait	Factor 1	Factor 2	Factor 3
Leaf number at flowering (leaf)	-0.849	0.291	-0.249
Total dry mass (mg)	-0.836	0.405	0.017
Specific leaf area (cm^{-2} g^{-1})	0.806	0.413	0.232
Leaf dry matter content (mg DM g^{-1} FM)	-0.218	-0.516	-0.767
Leaf thickness (μm)	-0.684	-0.048	0.416
Reproductive allocation (%)	0.946	-0.058	-0.031
Root allocation (%)	-0.008	-0.743	-0.132
Leaf allocation (%)	-0.925	0.233	0.035
Root to shoot ratio	0.585	-0.661	0.017
Cell density (cells mm^{-2})	-0.019	-0.851	0.143
Stomatal density (st. mm^{-2})	-0.298	-0.854	0.204
Stomatal index (% st. cell $^{-1}$)	-0.686	-0.208	0.156
Maximum leaf production rate (R_{max}, leaf d^{-1})	-0.624	0.475	0.062
Duration of leaf production (d)	-0.737	-0.063	-0.482
Leaf insertion angle (°)	0.732	0.324	-0.283
Blade ratio	-0.628	-0.573	0.247

Table S2. Spearman's coefficients of rank correlation between genotypes coordinates on first (above diagonal) and second (below diagonal) principal components from the within-treatment. PCA performed on trait values under control (CT, 20/17 °C day/night) and high temperature (HT, 30/25 °C day/night), and in well-watered (WW, 0.35 g H_20 g^{-1} dry soil) and water deficit (WD, 0.20 g H_20 g^{-1} dry soil) conditions. Coefficients in bold typeface were significant at **P* < 0.05, ***P* < 0.01. *n* = 9.

CTxWW	**0.73***	**0.68***	**0.80***
0.92**	CTxWD	0.58	**0.65***
0.85**	**0.73***	HTxWW	0.58
0.77*	**0.63**	**0.73***	HTxWD

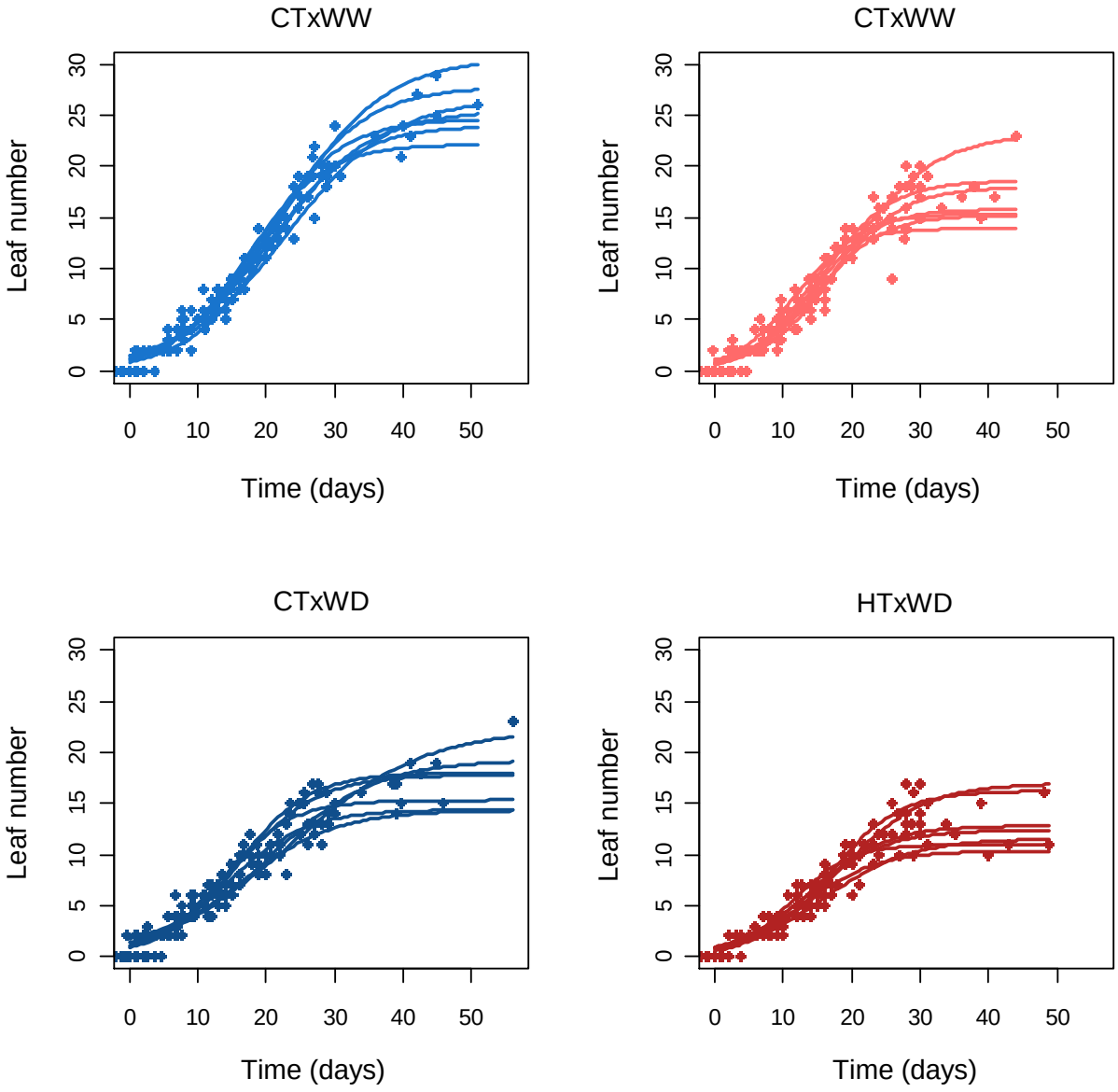

Figure S1. Production of leaves of *A. thaliana* Col-0 from cotyledonous stage to silique maturation. Each fitted curve represents one individual plant grown under control (CT, 20/17 °C day/night) and high temperature (HT, 30/25 °C day/night), and in well-watered (WW, 0.35 g H_20 g^{-1} dry soil) and water deficit (WD, 0.20 g H_20 g^{-1} dry soil) conditions. Curve fitting of leaf production over time (days from cotyledonous stage) was calculated according to Eq. 1.

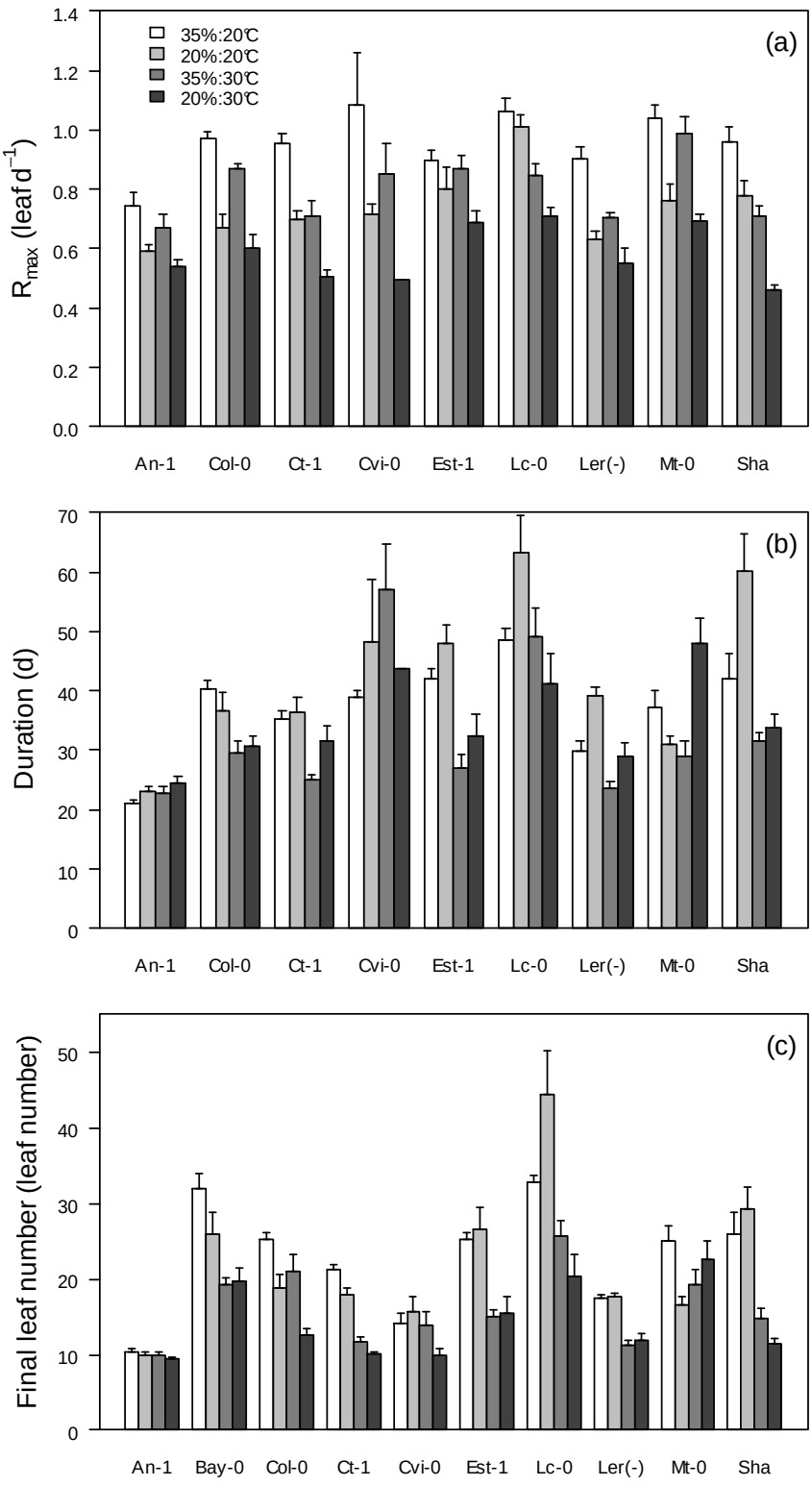

Figure S2. Mean trait values by genotypes under control (CT, 20/17 °C day/night) and high temperature (HT, 30/25 °C day/night), and in well-watered (WW, 0.35 g H_20 g^{-1} dry soil) and water deficit (WD, 0.20 g H_20 g^{-1} dry soil) conditions.

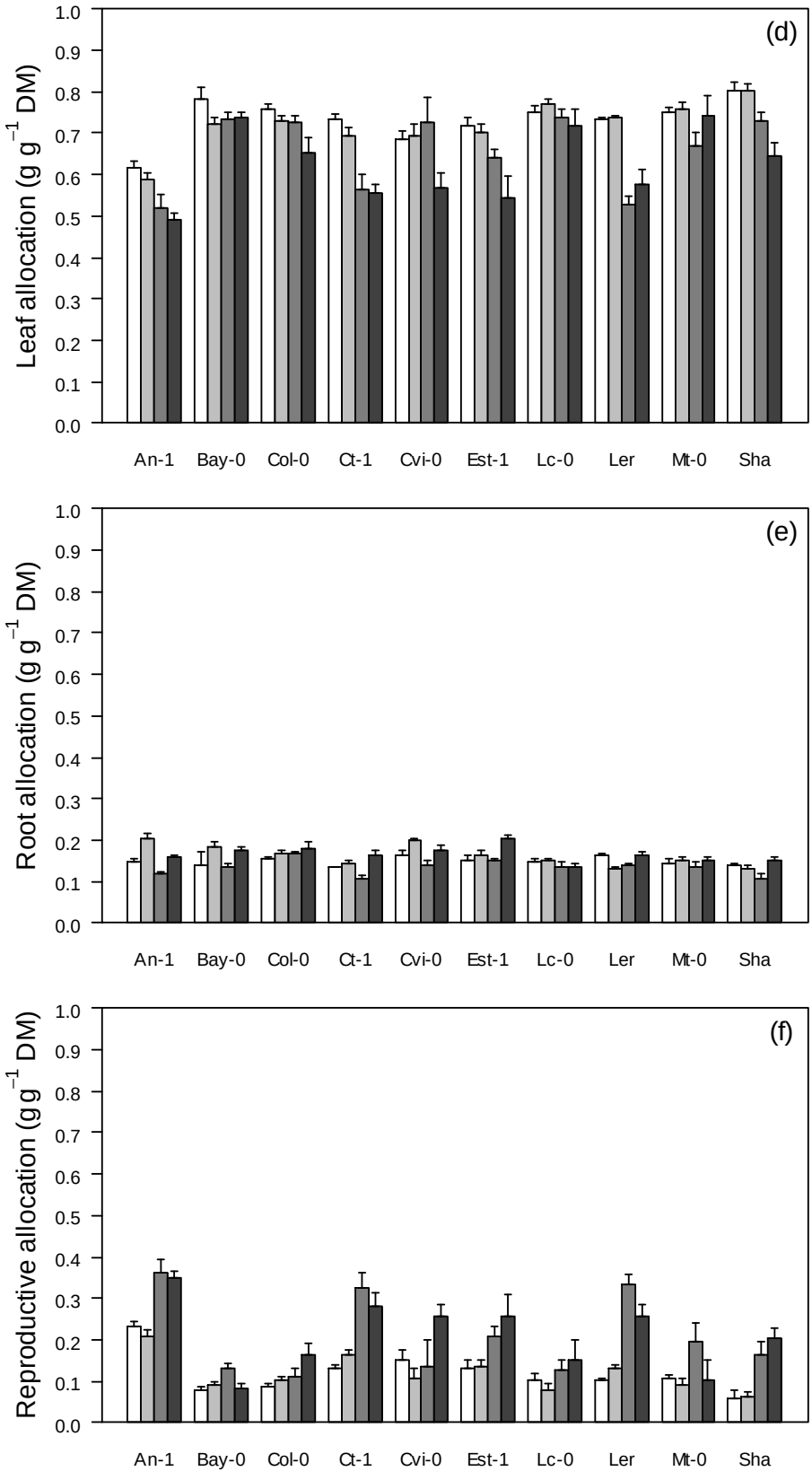
(d)
Leaf allocation (g g^{-1} DM)
1.0
0.9
0.8
0.7
0.6
0.5
0.4
0.3
0.2
0.1
0.0
An-1 Bay-0 Col-0 Ct-1 Cvi-0 Est-1 Lc-0 Ler Mt-0 Sha
(e)
Root allocation (g g^{-1} DM)
1.0
0.9
0.8
0.7
0.6
0.5
0.4
0.3
0.2
0.1
0.0
An-1 Bay-0 Col-0 Ct-1 Cvi-0 Est-1 Lc-0 Ler Mt-0 Sha
(f)
Reproductive allocation (g g^{-1} DM)
1.0
0.9
0.8
0.7
0.6
0.5
0.4
0.3
0.2
0.1
0.0
An-1 Bay-0 Col-0 Ct-1 Cvi-0 Est-1 Lc-0 Ler Mt-0 Sha

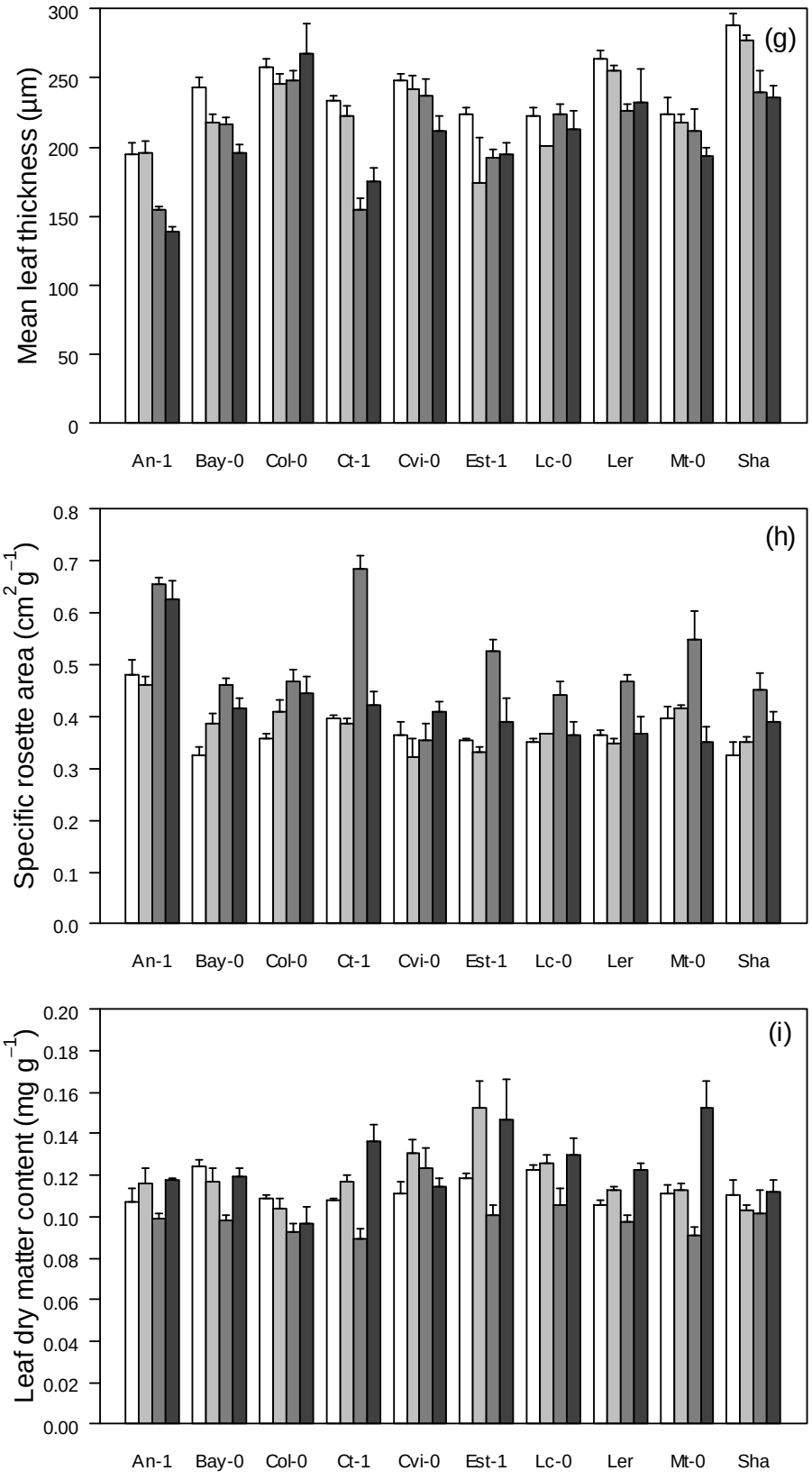

Figure S2. (suite)

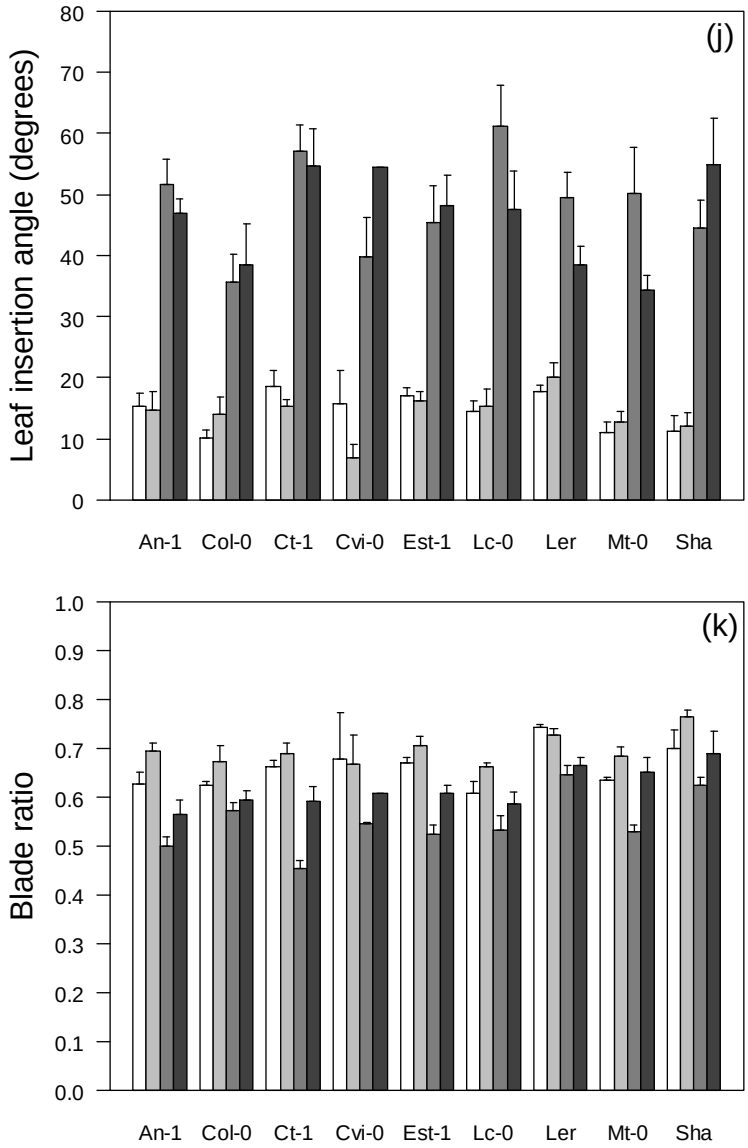

Figure S2. (suite)

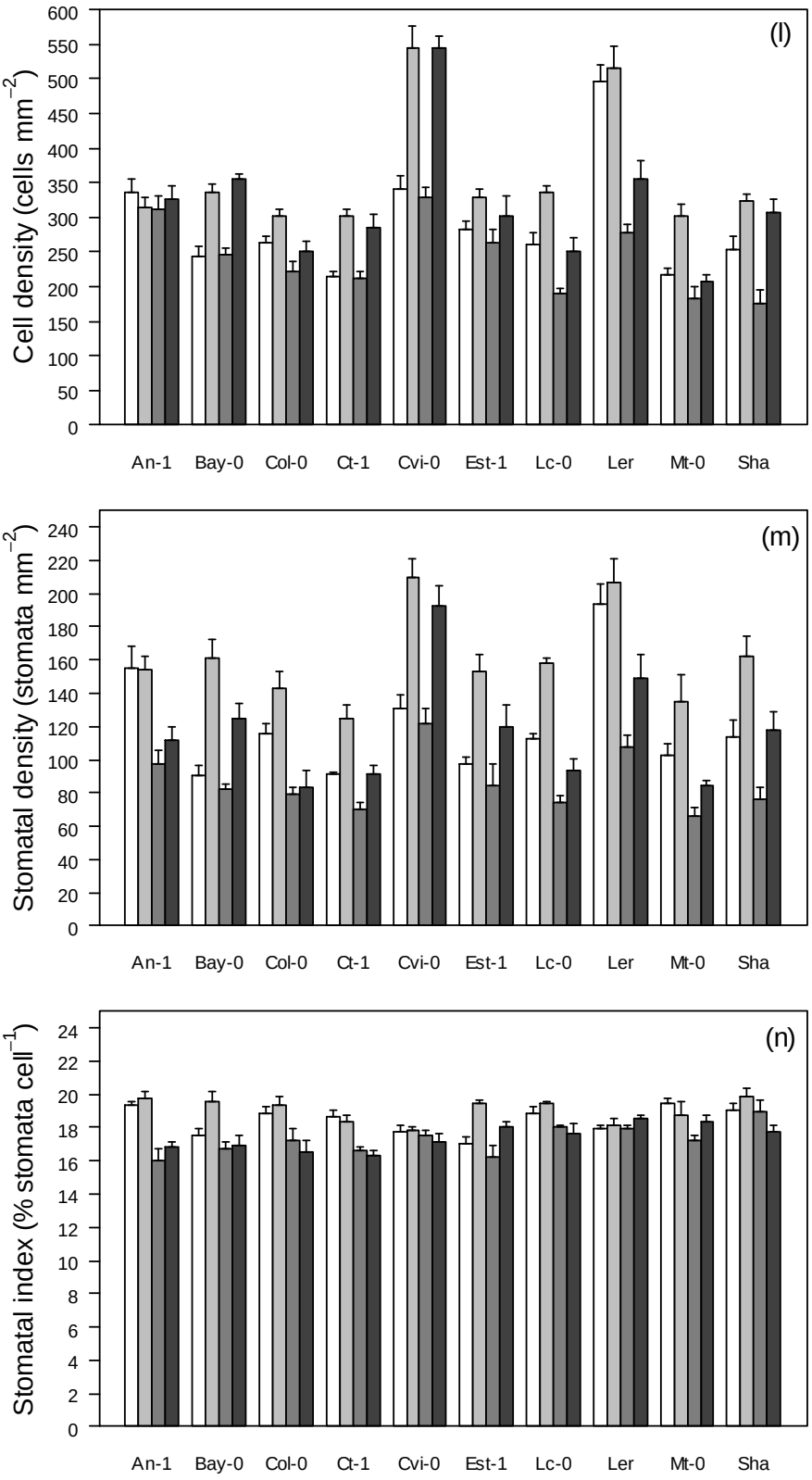

Figure S2. (suite)

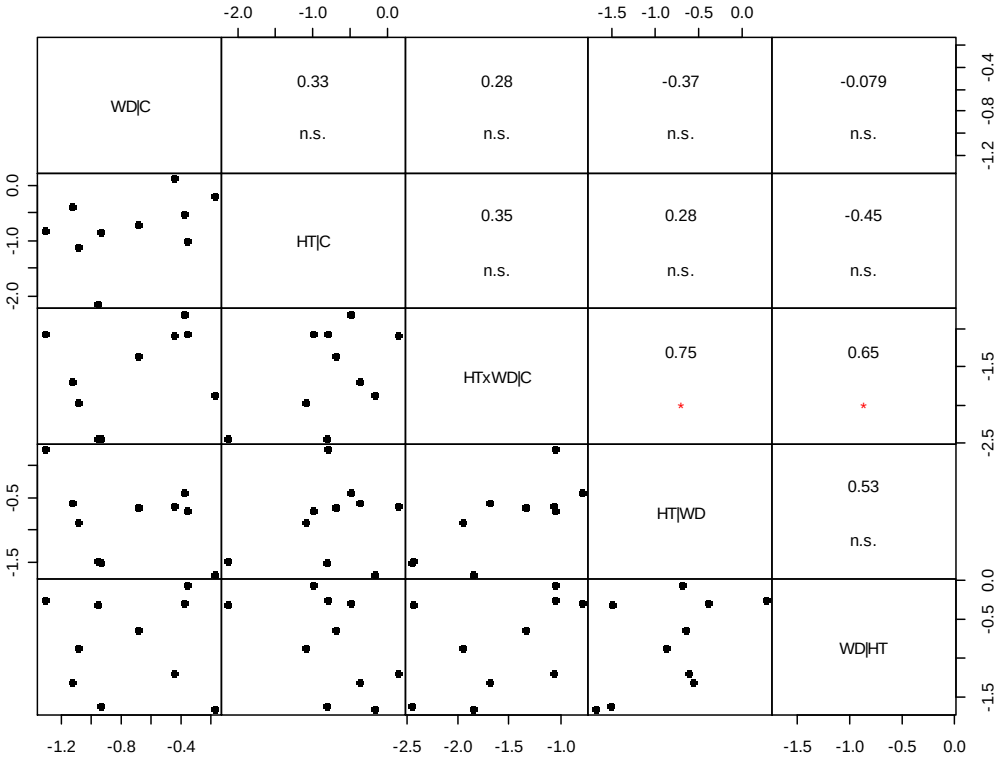

Figure S3. Correlation matrix of response ratios (log) for total dry mass.

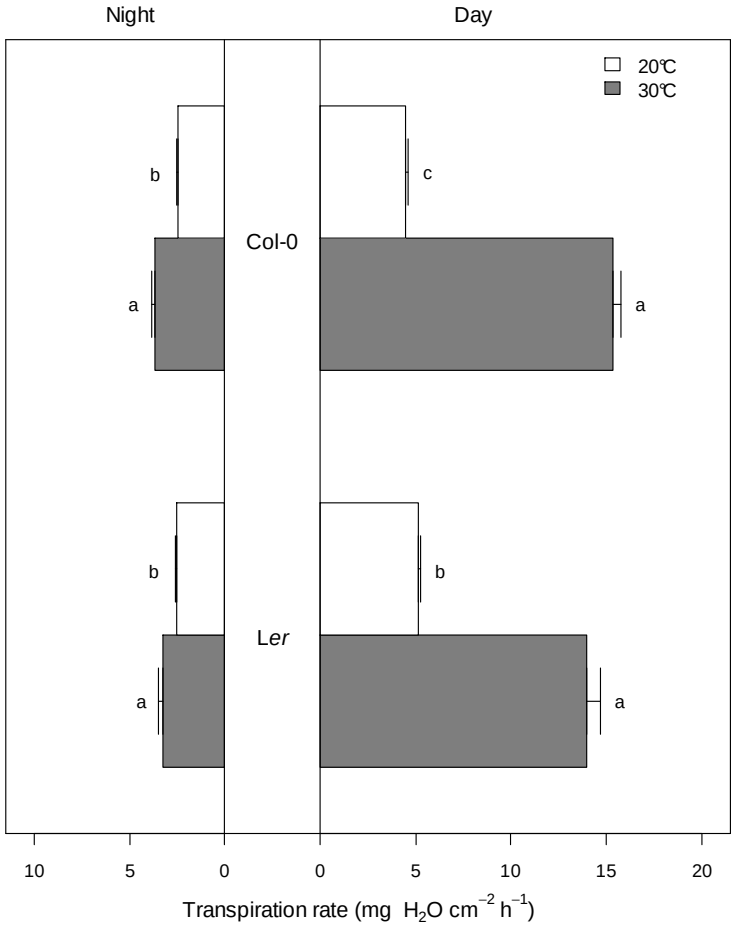

Figure S4. Night and day transpiration rates of Col-0 and L*er* accessions. Transpiration was determined gravimetrically in plants at bolting stage grown under control (20 °C, white) and high (30 °C, grey) temperature in well-watered conditions. Bars are means +/- SE (n = 5-10). Different letters indicate significant differences (P < 0.05) following Kruskal-Wallis nonparametric tests independently performed for night and day.

Manuscript #2

Genetic architecture of the Arabidopsis phenotypic space in response to water deficit and high temperature

François Vasseur[1], Christine Granier[1] and Denis Vile[1]

[1]Laboratoire d'Ecophysiologie des Plantes sous Stress Environnementaux (LEPSE), UMR 759, INRA-SUPAGRO, F-34060 Montpellier, France

Adapted from an article in preparation.

Abstract

The phenotypic covariations between plant traits illustrate the coordination of processes that allow plant growth and reproduction in diverse environmental conditions. Soil water availability and air temperature are major environmental constraints that interact together and that strongly affect phenotypic trait values and covariations. The genetic architecture that defines the structure and the plasticity of the phenotypic space is a key feature of the evolutionary adaptation of individual characters. Using a powerful phenotyping platform, we present a quantitative analysis of the pattern of covariations between traits related to life history, reproductive success, leaf morphology, growth, and carbon and water economics. We used a mapping population of *Arabidopsis thaliana* grown under prolonged exposures to isolated and combined soil water deficit and high temperature, and mapped the quantitative trait loci (QTL) involved in the variability of the multidimensional phenotypic space. The phenotypic space observed across 12 major plant traits exhibited strong plasticity in response to both stresses. Two hierarchical classes of pleiotropic QTL respectively induced changes in the direction and in the volume of the phenotypic space, depending on the environmental conditions. Our findings give new insight in the understanding of how pleiotropic loci generate and limit the variability in plant ecological strategies in interaction with environmental constraints.

Key-words: Trade-offs, genetic constraints, modular pleiotropy, phenotypic covariation, GxE interactions, QTL, reaction norms, life history, growth, net photosynthesis, transpiration

Introduction

The coordination of plant processes that ensure growth and reproduction under diverse environmental conditions is reflected through the network of interrelationships that exist between plant functional traits (Grime 1988, Stearns 1989, Westoby et al. 2002, Vile et al. 2006, Violle et al. 2007). The phenotype is often represented by a few discrete or continuous observable properties (traits) but could be best viewed as a multidimensional space that interacts with the environment (McGuigan et al. 2011, Wagner and Zhang 2011). The genetic architecture of integrated phenotypes in various environments is a key feature for understanding the evolution of complex organisms (Pigliucci and Preston 2004).

Covariations and trade-offs between traits reflect pleiotropic constraints restricting the range of reachable trait-trait combinations by limiting the genetic variability in one trait independently of the others (Wagner and Zhang 2011). Fisher (1930) was the first to model the pleiotropic structure of the phenotypic space by asserting that 'every gene affects every trait'. However, with the development of molecular biology and quantitative genetics, the Fisher's view of universal pleiotropy was revisited (e.g. Martin and Lenormand 2006, Pavlicev and Wagner 2012). It was notably posited that pleiotropy may be restricted to the strongest genetic covariations within functional modules, then called 'modular pleiotropy' (Wagner et al. 1996, Wagner et al. 2007). Evidences of modular pleiotropy were recently found in yeast, nematodes and mice (Wang et al. 2010). Strikingly, Wang and colleagues (2010) demonstrated that, instead of universal pleiotropy, "most genes affect a small fraction of traits whereas genes affecting more traits have larger per-trait effects". Thus, because univariate genetic effects – if they exist – are drastically smaller than multivariate genetic effects, the results of quantitative genetic analyses – specifically, the quantitative trait loci (QTL) analyses – would first identify loci with major pleiotropic effects. Consistent with this idea, many pleiotropic hotspots have been identified in plants, notably in *Arabidopsis thaliana* (Fu et al. 2009).

Water deficit (WD) and high temperature (HT) are among the major abiotic constraints impairing plant growth and productivity in natural and field conditions (Boyer 1982, Ciais et al. 2005). These two stresses often occur simultaneously but very few studies have investigated their combined phenotypic effects in an integrated approach ((Mittler 2006); but see (Vile et al. 2012 = Manuscript #1)). We recently showed that these two stresses affect many correlated traits such as whole-plant growth, leaf morphology and reproductive phenology of various accessions of *Arabidopsis thaliana*, sometimes in opposite directions

(Vile et al. 2012 = Mansucript #1). We also found significant genotype-by-environment (GxE) interactions. However, the restricted number of genotypes considered in this previous study impaired any investigation about the genetic architecture of the phenotypic space. Here we benefited from the recent advances in high throughput phenotypic screening under strictly controlled environmental conditions (Granier et al. 2006, Vasseur et al. 2012 = Manuscript #5) to perform a multidimensional genetic analysis of Arabidopsis response to water deficit and high temperature. We selected the L*er* x Cvi population of recombinant inbred lines because it carries segregating alleles with strong pleiotropic effects (Fu et al. 2009, Vasseur et al. 2012 = Manuscript #5). We investigated the variability of 12 traits related to life history, growth, reproduction, leaf morphology, carbon assimilation and water consumption. We combined multivariate and mixed-modeling approaches to dissect the structure of the phenotypic space across and within environments, and map QTL.

We show that pleiotropic QTL had different effects on the phenotypic space depending on the traits and the environment. Our findings illustrate that the genetic constraints on multiple correlated traits were hierarchically organized in response to WD and HT between loci that determine the direction of the phenotypic space by affecting every traits, and loci that determine the volume of the phenotypic space by affecting some traits independently of the others. Our findings show that the genetic variability in the plasticity of the traits related to carbon fixation was higher than that of the traits related to water loss, growth, life history and reproductive allocation. Overall, our results shed light on the different pleiotropic mechanisms that govern plant performance and evolvability.

Materials and methods

Plant material and growth conditions

We used a population of recombinant inbred lines (RILs) previously generated from a reciprocal cross between two parental *Arabidopsis thaliana* accessions: Landsberg *erecta* (L*er*) and Cape Verde Islands (Cvi) (Alonso-Blanco et al. 1998). This population was chosen because L*er* and Cvi were initially collected from divergent locations with contrasted climates (Northern Europe and tropical Cape Verde Island, respectively), and because L*er* and Cvi carry different alleles at strong pleiotropic QTL (Fu et al. 2009Vasseur, 2012 #84 = Manuscript #5). We performed four experiments under isolated and combined high temperature and water deficit. The experiments were performed using the PHENOPSIS facility (Granier et al. 2006) that maintains constant growing environment (air temperature, water vapor pressure deficit, incident light and soil water content) and allows for the

automated rosette area measurements of 504 potted plants. In each experiment, we phenotyped the parental accessions (L*er* and Cvi; *n* = 8 replicates) and 120 RILs (*n* = 4) selected from the 162 available lines.

Seeds of all lines were stored at 4 °C in the dark ensuring stratification. Five seeds from each genotype were directly sown at the soil surface in 225 mL culture pots filled with a mixture (1:1, v:v) of loamy soil and organic compost (Neuhaus N2). Pots were damped with sprayed deionized water three times a day and placed in the PHENOPSIS automaton growth chamber in darkness (20 °C, 85% air relative humidity) until germination. After germination, plants were cultivated at 20 °C with a daily cycle of 12 h light supplied from a bank of HQi lamps which provided 190 µmol m^{-2} s^{-1} photosynthetic photon flux density (PPFD) at plant height. Water vapor pressure deficit (VPD) was maintained constant at 0.5-0.6 kPa and soil moisture at 0.35 g H_20 g^{-1} dry soil.

Soil water deficit (WD) and high temperature (HT) treatments were applied after emergence of the first two true leaves, avoiding early-growth effects. Control air temperature (CT) was set to 20/17 °C day/night, while HT was set to 30/25 °C. VPD was maintained at 0.7-0.8 kPa both under CT and HT. Soil water content was controlled before sowing to estimate the amount of dry soil and water in each pot. Soil water content was maintained at 0.35 and 0.20 g H_20 g^{-1} dry soil with a modified one-tenth-strength Hoagland solution in the well-watered (WW) and WD treatments, respectively. Pot weight was automatically adjusted to reach the target soil water content by weighing and watering each individual pot once a day. Temperature and watering regimes were chosen on the basis of previous reports (Vile et al. 2012 = Manuscript #1). All detailed meteorological data, including daily soil water content, air temperature and VPD, are available in the PHENOPSIS database (Fabre et al. 2011).

Measurements of phenotypic traits

Phenology and reproductive traits

Age at reproduction was estimated as the number of days from sowing to first flower open (Table 1). At first flower open, each rosette was cut, reproductive stem was separated from the rosette and their fresh weights determined immediately ($FW_{rosette}$ and FW_{repro}, respectively, mg). The rosette was wrapped in moist paper and kept at 4 °C overnight in darkness. After complete rehydration, water-saturated weight of the rosette was determined ($SFW_{rosette}$, mg). Leaf blades were separated from the petioles and scanned for area measurements. In parallel, a transparent imprint of the adaxial epidermis of the sixth leaf was obtained by drying off a varnish coat spread on the surface of the leaf. Leaf blades, petioles

Table 1. List of the traits measured and estimated.

Variable name	Abbreviation	Unit	Measurements and calculus
Rosette fresh weight	$FW_{rosette}$	mg	measured at flowering
Reproductive fresh weight	FW_{repro}	mg	measured at flowering
Saturated rosette fresh weight	$SFW_{rosette}$	mg	measured at flowering
Petioles dry mass	$DM_{petioles}$	mg	measured at flowering
Blades dry mass	DM_{blades}	mg	measured at flowering
Rosette dry mass	$DM_{rosette}$	mg	$DM_{blades} + DM_{petioles}$
Reproductive dry mass	DM_{repro}	mg	measured at flowering
Total leaf area	$LA_{rosette}$	cm^2	measured at flowering
Leaf mass per area	LMA	$g\ m^{-2}$	$DM_{blades} / LA_{rosette}$
Relative water content	RWC	%	$(FW_{rosette} – DM_{rosette}) / (SFW_{rosette} – DM_{rosette})$
stomatal density	SD	stomata mm^{-2}	measured at flowering
maximum rate of leaf expension	R_{max}	$m^2\ d^{-1}$	sigmoid model fitted
Absolute growth rate	*G*	$g\ d^{-1}$	R_{max} x LMA
Relative growth rate	RGR	$mg\ d^{-1}\ mg^{-1}$	$dG / dDM_{rosette}$
Net photosynthesis	*A*	$nmol\ s^{-1}$	measured at flowering
Mass-based net photosynthetic rate	A_{mass}	$nmol\ g^{-1}\ s^{-1}$	A / DM_{blades}
Area-based net photosynthetic rate	A_{area}	$nmol\ g^{-1}\ cm^{-2}$	$A / LA_{rosette}$
Transpiration	*ET*	$mg\ H_2O\ d^{-1}$	measured at bolting
Mass-based transpiration rate	ET_{mass}	$mg\ H_2O\ d^{-1}\ mg^{-1}$	ET / DM_{blades}
Area-based transpiration rate	ET_{area}	$mg\ H_2O\ d^{-1}\ cm^{-2}$	$ET / LA_{rosette}$

and reproductive stem were then separately oven-dried at 65 °C for 96 h, and their dry masses were determined (mg). Vegetative dry mass at reproduction ($DM_{rosette}$) was calculated as the sum of dry masses of petioles ($DM_{petioles}$) and blades (DM_{blades}).

Leaf morphology and stomatal density

Total leaf area ($LA_{rosette}$, cm^2) was determined as the sum of individual leaf blade areas. Leaf dry mass per area (LMA, g m^{-2}) was calculated as the ratio of DM_{blades} and $LA_{rosette}$. Relative water content (RWC, %) was estimated as the proportion of water in the fresh rosette at harvesting compared to the maximum weight of water when water-saturated, such as: RWC = ($FW_{rosette}$ − $DM_{rosette}$) / ($SFW_{rosette}$ − $DM_{rosette}$). Mean stomatal density (stomata mm^{-2}) was determined in two 0.12 mm^2 zones located at the bottom and at the top of the leaf from the epidermal imprints of the 6th leaf placed under a microscope (Leitz DM RB, Leica, Wetzlar, Germany) and coupled to an image analyzer (imageJ).

Rosette-level relative growth rate, net photosynthesis and water fluxes

Dynamic measurement of growth was performed using daily zenithal images of the plants acquired by the PHENOPSIS automaton (Sony SSC-DC393P camera). The total projected leaf area of the rosette (RA, cm^2) was determined every 2 to 3 days (ImageJ). A sigmoid curve was fitted for each plant following:

$$RA = \frac{a}{1+e^{\left(\frac{(d-d_0)}{b}\right)}}$$

where d is the number of days after emergence of the first two true leaves, a is the maximum vegetative rosette area, d_0 is the time when $a/2$ leaf area has expanded and b is related to the maximum rate of leaf production. The maximum rate of leaf expansion (R_{max}, m^2 d^{-1}) was calculated from the first derivative of the logistic model at d_0 as $R_{max} = a/(4b)$. Assuming that LMA did not vary over time during the period of maximum expansion rate, we calculated maximum absolute growth rate (G, g dry mass d^{-1}) from R_{max} and LMA. Following Kolokotrones et al. (2010), we fitted a nonlinear quadratic model: $\log_{10}(G) = \log_{10}(b_0) + b_1\log_{10}(DM_{rosette}) + b_2(\log_{10}(DM_{rosette}))^2$, using the Generalized Estimation Equation (*gee* package in the statistical program R 2.12). Relative growth rate (RGR, mg d^{-1} mg^{-1}) was calculated as the derivative of the quadratic function linking absolute growth rate G to rosette dry mass ($RGR = dG/dDM_{rosette}$).

Photosynthesis was measured at flowering and under growing conditions using a whole-plant chamber prototype designed for Arabidopsis by M. Dauzat (INRA, Montpellier, France) and K.J. Parkinson (PP System, UK) and connected to an infrared gas analyzer system (CIRAS 2, PP systems, USA). To insure plant gas exchange was not corrupted by soil

Table 2. Mixed-models on the 12 phenotypic traits. Each phenotypic trait P is modeled as: P = W + T + WxT + G + GxW + GxT + GxWxT. HT and WD used as fixed effects. G used as random effects. Optimum condition (CTxWW) used as intercept. Confidence intervals (CI) estimated with a Markov Chain Monte Carlo algorithm following 1000 permutations.

	Fixed E-effects								Variance components			
Trait	**CTxWW**		**WD effect**		**HT effect**		**HTxWD effect**		**G**	**GxW**	**GxT**	**GxTxW**
Age at reproduction	1.59	[1.58;1.61]	0.08	[0.07;0.09]	-0.1	[-0.11;-0.09]	-0.01	[-0.02;0]	78.8	2.0	8.0	0.0
Vegetative dry mass	1.44	[1.39;1.49]	-0.20	[-0.23;-0.17]	-0.63	[-0.68;-0.59]	0.01	[-0.04;0.05]	87.7	0.0	4.2	1.3
Reproductive dry mass	1.01	[0.97;1.04]	-0.27	[-0.3;-0.24]	-0.58	[-0.61;-0.56]	0.03	[0;0.07]	59.3	3.5	3.1	4.1
Total leaf area	3.01	[2.97;3.06]	-0.33	[-0.36;-0.3]	-0.48	[-0.53;-0.45]	0.02	[-0.02;0.06]	86.3	0.1	4.4	2.1
LMA	1.36	[1.35;1.38]	0.13	[0.12;0.15]	-0.18	[-0.2;-0.17]	-0.03	[-0.05;-0.01]	63.5	2.3	7.9	1.6
RWC	1.87	[1.86;1.87]	-0.04	[-0.04;-0.04]	0.07	[0.07;0.08]	-0.03	[-0.04;-0.02]	0.0	9.0	10.6	4.0
Stomatal density	2.28	[2.26;2.3]	0.21	[0.2;0.22]	-0.01	[-0.03;0.01]	-0.05	[-0.07;-0.03]	34.3	0.0	19.6	7.4
A_{mass}	2.24	[2.2;2.28]	-0.27	[-0.3;-0.24]	-0.04	[-0.08;0.01]	-0.21	[-0.26;-0.16]	7.4	1.8	33.9	5.4
A_{area}	-0.39	[-0.42;-0.36]	-0.14	[-0.17;-0.11]	-0.23	[-0.27;-0.19]	-0.23	[-0.28;-0.18]	0.0	0.0	25.1	8.7
ET_{mass}	1.75	[1.71;1.79]	-0.35	[-0.38;-0.32]	0.58	[0.55;0.61]	0.19	[0.15;0.23]	71.5	2.2	5.6	0.0
ET_{area}	2.11	[2.08;2.14]	-0.22	[-0.25;-0.19]	0.4	[0.37;0.43]	0.16	[0.13;0.2]	56.4	2.4	7.7	0.0
RGR	0.77	[0.76;0.79]	0.01	[0;0.03]	0.1	[0.1;0.12]	-0.07	[-0.09;-0.06]	37.9	36.9	12.6	5.7

Table 3. Pairwise comparisons of the structure of the multidimensional phenotypic spaces between the four environments. The phenotypic variance-covariance matrix in each environment is compared to each other (CTxWW vs CTxWD vs HTxWW vs HTxWD) with the statistical approach developed by Jouan-Rimbaud and colleagues (1998). The three coefficients allow the comparison of three properties of the structure of multidimensional data sets: the direction of the data sets (P), the variance-covariance of the data sets (C), and the location of the data sets' centroids (R).

		CTxWW	**CTxWD**	**HTxWW**	**HTxWD**
Direction of loading patterns (P)	**CTxWW**	-			
	CTxWD	0.97	-		
	HTxWW	0.87	0.87	-	
	HTxWD	0.75	0.81	0.96	-
Variance-covariance matrix structure (C)	**CTxWW**	-			
	CTxWD	0.82	-		
	HTxWW	0.58	0.74	-	
	HTxWD	0.49	0.71	0.81	-
Centroids location (R)	**CTxWW**	-			
	CTxWD	0.00	-		
	HTxWW	0.00	0.00	-	
	HTxWD	0.00	0.00	0.00	-

respiration, we sealed the soil surface with four layers of plastic film. The flowering stem was detached from the rosette before measurement to record leaf gas exchange only. Whole-plant photosynthetic rate (A, nmol s^{-1}) was expressed on a blade dry mass basis (A_{mass}, nmol g^{-1} s^{-1}) and on a blade area basis (A_{area}, nmol g^{-1} cm^{-2}) using the ratio A / DM_{blades} and A / $LA_{rosette}$, respectively. Whole-plant water loss was measured at inflorescence emergence (bolting stage) by daily weighing of the pots over four consecutive days. Soil evaporation was prevented by sealing the soil surface with four layers of a plastic film. The absolute transpiration rate (ET, mg H_2O d^{-1}) was estimated as the slope of the linear regression between pot weight and time. Similarly, transpiration was expressed on a rosette area basis (ET_{area}, mg H_2O d^{-1} cm^{-2}) and on a blade dry mass basis (ET_{mass}, mg H_2O d^{-1} mg^{-1}), using the ratio ET / $LA_{rosette}$ and ET / DM_{blades}, respectively. A full list of variables is presented in Table 1.

Statistical analyses and quantitative genetics

Phenotypic and genetic correlations

The coefficient of phenotypic correlation was estimated as the Pearson's product moment between each trait, in each condition. In each environmental condition, the coefficient of genetic correlation between pairs of traits was estimated by dividing the covariance of the mean of each RIL by the product of the square roots of among-line variance components for each trait (Roff and Preziosi 1994). In the estimation of the genetic variability in reaction norms, differences in individual trait values depending on the allelic value at QTL were estimated with a post-hoc Tukey's test following two-way ANOVA within each environment. All statistical analyzes were performed using R 2.12.

Multidimensional analysis of the phenotypic space

Multidimensional phenotypic spaces across environments were statically compared using the procedure of Jouan-Rimbaud et al. (1998). This procedure uses dimensional reduction of multivariate datasets through eigen analysis. It computes three parameters that allow the pairwise comparison of the structure of multivariate datasets. The first parameter P tries to answer the following question: do the original variables have the same weight in the orientation of the two datasets? If P falls below 0.7 then the angle between the directions of each cloud is more than 45°. Such case illustrates that the original variables (i.e. the traits within each environment) do not have the same contribution to the latent variables (the traits across environments). The second coefficient, C, compares the variance–covariance matrices. C indicates whether two datasets (i.e. phenotypic spaces) have a similar volume, or envelope, both in magnitude and direction. C values close to 0 indicate that the volumes of the clouds of

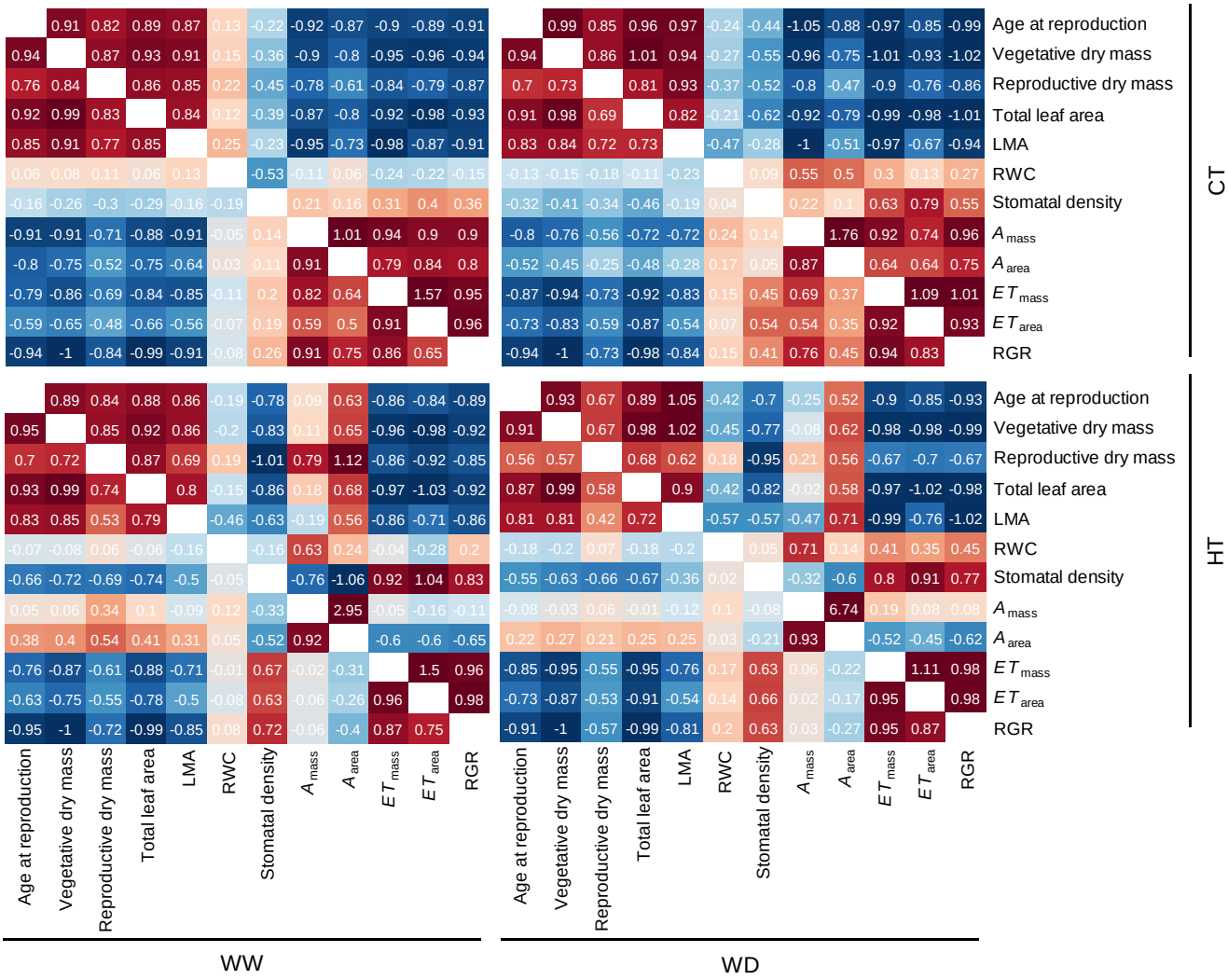

Figure 1. Genetic and phenotypic correlations between traits among environments. Heatmaps of the coefficients of genetic correlation (above-diagonal, estimated by dividing the covariance of the RIL means between two traits by the product of the square roots of among-line variance components) and phenotypic correlation (below-diagonal, Pearson's product moment) after $\log_{10}$-transformation of the data. Top-left panel: CTxWW, top-right panel: CTxWD, bottom-left panel: HTxWW, bottom-right panel: HTxWD. Age at reproduction (d), vegetative and reproductive dry masses (mg), total leaf area (cm^2), leaf dry mass per area (LMA, g m^{-2}), relative water content (RWC, %), stomatal density (mm^{-2}), mass-based net photosynthetic and transpiration rates (A_{mass}, nmol CO_2 s^{-1} g^{-1} and ET_{mass}, mg H_2O d^{-1} mg^{-1}, respectively), area-based net photosynthesis and transpiration rates (A_{area}, nmol CO_2 s^{-1} cm^{-2} and ET_{area}, mg H_2O d^{-1} cm^{-2}, respectively), and relative growth rate (RGR, mg d^{-1} mg^{-1}).

points are completely different, either because one is smaller than the other and/or because they have different directions. Finally, the third coefficient, R, uses the squared Mahalanobis distance to compare the position of the centroids of the phenotypic spaces. The closer *R* is to 1, the closer the positions of the centroids of each phenotypic space are. Analyses were performed with R/*represent* package.

To jointly analyze the phenotypic space *across* and *within* environment, we used a multiple factor analysis (MFA). In contrast to a classical principal component analysis (PCA), MFA takes into account the internal grouping structure among variables or among individuals. The core of MFA is a general factor analysis applied to all active sets of individuals. The contribution of a data point to the inertia of an axis is the quotient between the inertia of its projection and the inertia of the whole scatterplot's projection on this axis (see (Pages 2002)). Principal components (PCs) then represent major axes of covariation between sets of phenotypic traits. MFA was performed on all the trait values recorded in the four environments (*dual multiple factor analysis*, R/*FactoMineR* package).

We analyzed the genetic and environment effects on individual traits using a mixed-effect model (R/*lme4* package) fitted on individual trait values and on the individuals coordinates along the first three PCs of the MFA, respectively. The optimum condition, CTxWW, was used as intercept in the model (from which HT and WD have additive or interactive effects). The phenotypic variability, at both univariate and multivariate levels, is the result of (*i*) environmental effects due to air temperature (T) and water availability (W), separately or in interaction (all treated as fixed factors), (*ii*) genetic effects at the individual level (G, treated as a random factor), and (*iii*) random individual-level genotype-by-environment (GxE) interactions (i.e. GxW, GxT, GxWxT, all treated as random factors). The variance components (i.e. the proportion of phenotypic variance attributable to G and GxE effects) were extracted from each fitted model.

Quantitative genetics

We used 144 AFLP markers spanning all the *Arabidopsis thaliana* genome ($2n = 10$; (Alonso-Blanco et al. 1998)) to perform a QTL analysis of the best linearized unbiased predictors (BLUPs) extracted from the mixed-effect models fitted on the positions along each PC. We used the BLUPs of the G and GxE effects that accounted for at least 5% of the total variance in PC's loadings. We used composite interval mapping to map QTL (R/*qtl* package). The 5%-significance level threshold was calculated for QTL LOD scores following 1000 permutations ($2.53 < LOD_{threshold} < 2.78$). Percent of variability explained by each QTL and epistatic interactions between QTL were quantified with composite interval mapping, using

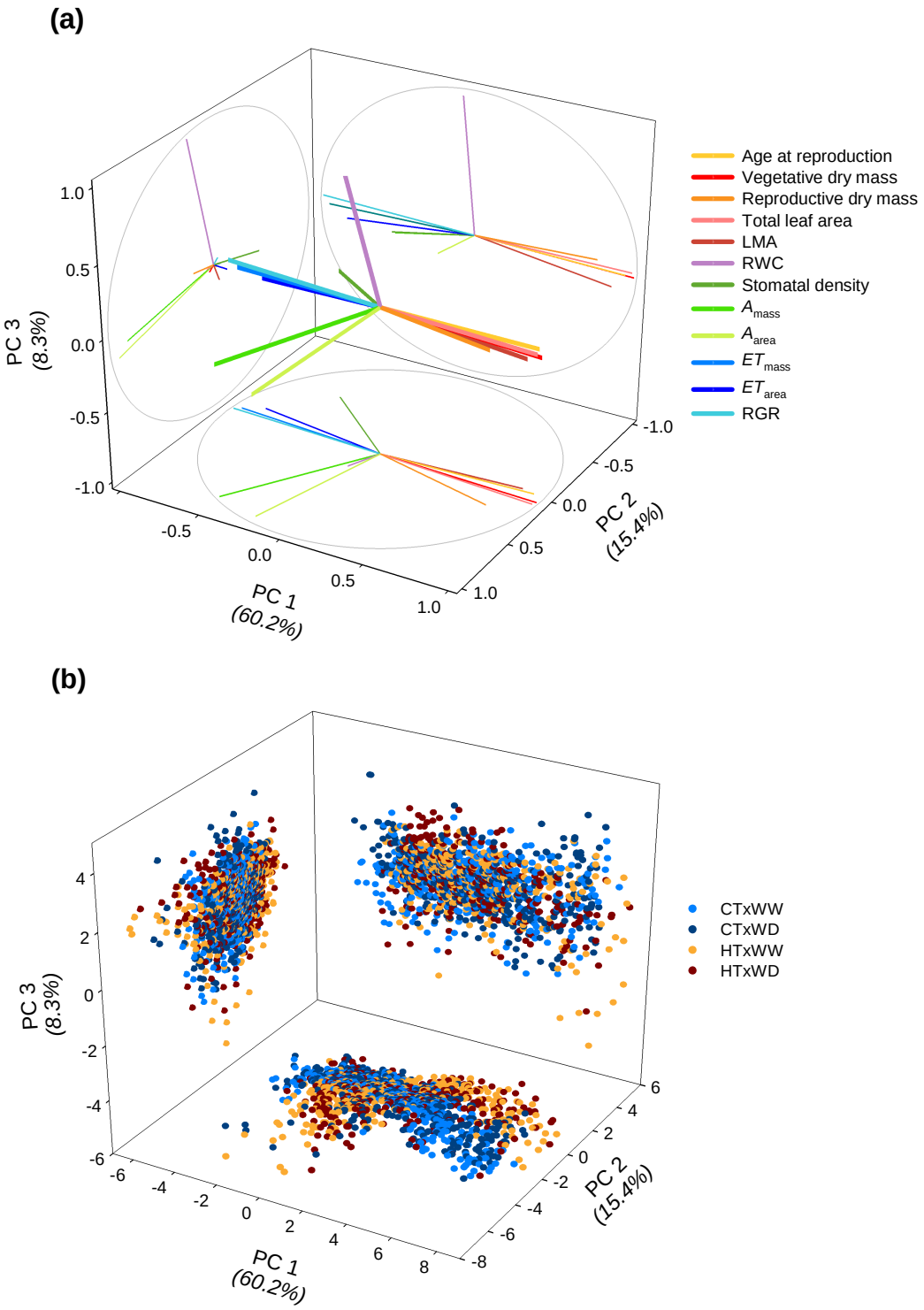

Figure 2. Multiple factor analysis (MFA): cross-environment structure. 3D-representation of the cross-environment covariations between traits in the phenotypic space generated by the first three PCs. (a) Variables projections: age at reproduction (d), vegetative and reproductive dry masses (mg), total leaf area (cm^2), leaf dry mass per area (LMA, g m^{-2}), relative water content (RWC, %), stomatal density (mm^{-2}), mass-based net photosynthetic and transpiration rates (A_{mass}, nmol CO_2 s^{-1} g^{-1} and ET_{mass}, mg H_2O d^{-1} mg^{-1}, respectively), area-based net photosynthesis and transpiration rates (A_{area}, nmol CO_2 s^{-1} cm^{-2} and ET_{area}, mg H_2O d^{-1} cm^{-2}, respectively), and relative growth rate (RGR, mg d^{-1} mg^{-1}). Variables are projected on the PCs planes (bottom panel: PC1 vs PC2; left panel: PC2 vs PC3; font panel: PC1 vs PC3). (b) Individuals projections (bottom panel: PC1 vs PC2; left panel: PC2 vs PC3; font panel: PC1 vs PC3). Light blue: CTxWW; dark blue: CTxWD; orange: HTxWW; and dark red: HTxWD.

the markers for which LOD > $LOD_{threshold}$ as cofactor. Confidence interval for each QTL location was estimated with maximum likelihood following an iterative scan (1000 bootstrap permutations). Throughout the manuscript, we report significant QTL effects and epistatic interactions at the 5%-significance level.

Results

Variability in individual traits to high temperature and water deficit

High temperature (HT) and water deficit (WD) had additive effects on size-related traits (age at reproduction, vegetative and reproductive dry masses, and total leaf area) and interactive effects on the other traits (Table 2, Figure S1). In average across population, under control air temperature (CT) and well-watered soil conditions (WW) plants accumulated 75 mg vegetative dry mass. In average, dry mass was significantly reduced by 44% by HT, and by 14% by WD. These negative effects on plant size were also reflected in the variation of total leaf area and reproductive dry mass, but not in the variation of age at reproduction, LMA and stomatal density that were significantly reduced under HT and increased under WD. Inversely, the relative growth rate (RGR) and the transpiration rates (per mass or area units) were increased by HT, but reduced by WD. Finally, the net photosynthetic rate was significantly reduced by both HT and WD and more strongly by their combination, although the effects differed slightly depending on net photosynthetic rate per unit leaf mass (A_{mass}) or per unit leaf area (A_{area}).

Within each environment, the component of phenotypic variation that was attributable to genetic effects independently of the environment (G) varied strongly depending on the trait (Table 2). Indeed, G effects represented between 34% and 88% of the variability in all traits but net photosynthetic rates and RWC (for which G effects represented < 7.5% of the variability). In addition, there were important variance components attributable to genotype-by-environment interactions (Table 1), specifically for the net photosynthetic rates for which GxT > 30% and GxTxW > 10%. The QTL analysis of all traits within each environment revealed that only a few loci with strong pleiotropic effects explained the phenotypic variability in the 12 traits observed whatever the environment (Figure S2).

Structure of the multidimensional phenotypic space across and within environments

We performed a multivariate factor analysis (MFA) to explore the multidimensional phenotypic space under both isolated and combined HT and WD. While similar in their approaches, the principal advantage of MFA compared to PCA is that MFA allows comparing

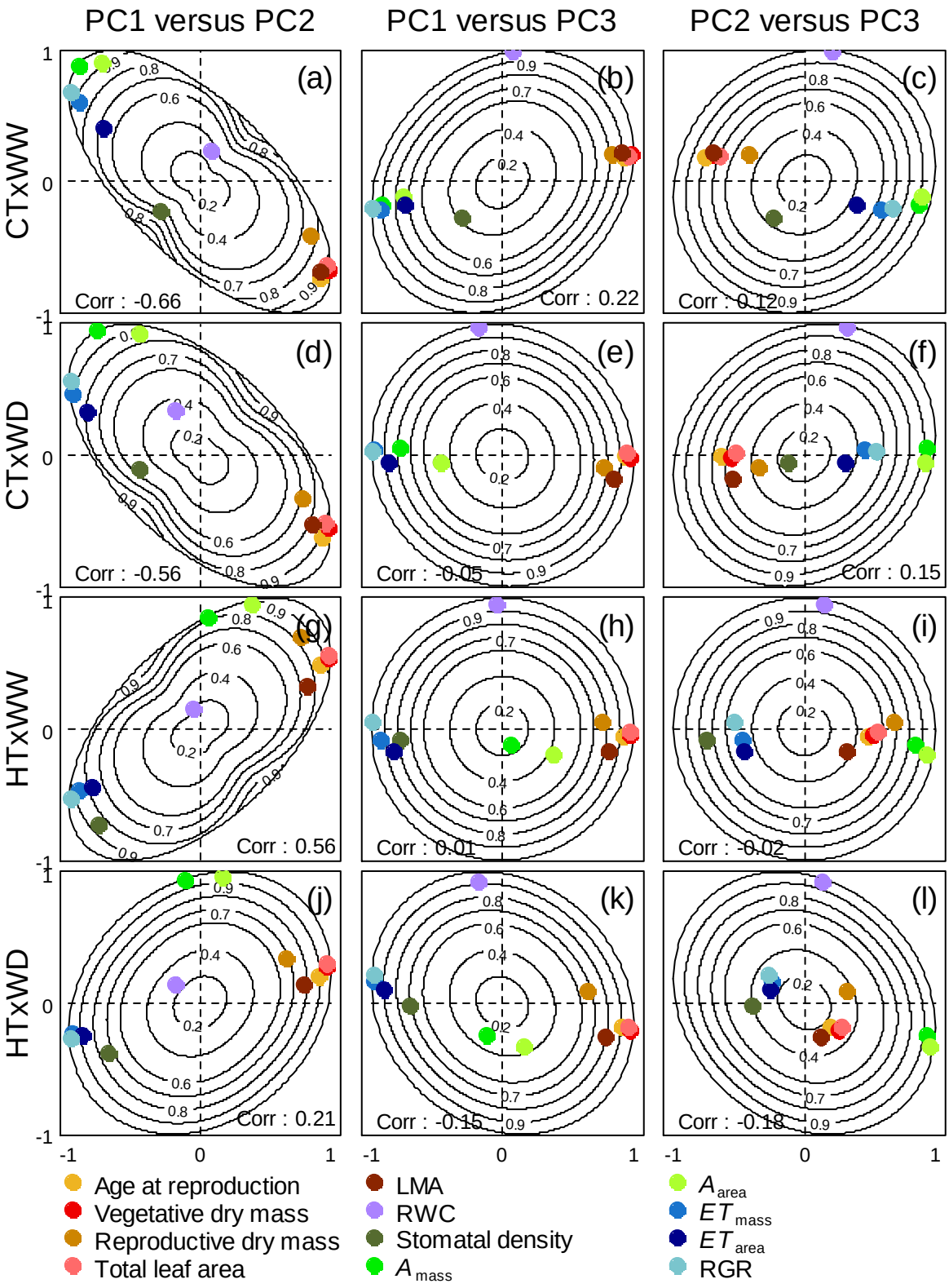

Figure 3. Multiple factor analysis (MFA): within-environment structure. Colored points display the covariation between phenotypic traits and PCs within each environment. Ellipses represent the quality of the variable projection on the PCs plane. Age at reproduction (d), vegetative and reproductive dry masses (mg), total leaf area (cm^2), leaf dry mass per area (LMA, g m^{-2}), relative water content (RWC, %), stomatal density (mm^{-2}), mass-based net photosynthetic and transpiration rates (A_{mass}, nmol CO_2 s^{-1} g^{-1} and ET_{mass}, mg H_2O d^{-1} mg^{-1}, respectively), area-based net photosynthesis and transpiration rates (A_{area}, nmol CO_2 s^{-1} cm^{-2} and ET_{area}, mg H_2O d^{-1} cm^{-2}, respectively), and relative growth rate (RGR, mg d^{-1} mg^{-1}). 'Corr' is the coefficient of correlation between PCs. (a-c) Structure of the phenotypic space in CTxWW. (d-f) Structure of the phenotypic space in CTxWD. (g-i) Structure of the phenotypic space in HTxWW. (j-l) Structure of the phenotypic space in HTxWD.

the general pattern of trait covariations *across* environment to the patterns of trait covariations *within* each environment (for details see (Pages 2002)). Across treatments, the first three principal components (PCs) together explained 84% of the total variance in the phenotypic data (PC1, PC2 and PC3 explained 60.2%, 15.4% and 8.3%, respectively; Figure 1; Figure 2; See Supporting Tables 1 and 2 for correlations of variables with PCs and variable contributions to each PC). Two sets of negatively correlated traits contributed most to PC1. The first set is composed of age and size (vegetative and reproductive dry mass, total leaf area) at reproduction, leaf dry mass per area (LMA), which were all positively correlated to each other. The second set of traits that contributed to PC1 included ET_{mass} and ET_{area}, RGR and to a lesser extent stomatal density. A_{mass} and A_{area} were positively correlated to PC2, as well as stomatal density but to a lesser extent. RWC contributed most to the variability along PC3. The projections of the individuals in the PC1-PC2 plane (Figure 2b) revealed a difference in the distribution of the individuals depending on growth temperature. The environment effects were less visible on the two other planes (PC1-PC3 and PC2-PC3). The rates of photosynthesis per unit of mass and area (A_{mass} and A_{area}, respectively) were strongly correlated with each other (Figure 1; Figure 2a), as well as the transpiration rates per unit of mass and area with each other (ET_{mass} and ET_{area}). For convenience, we will refer to net photosynthetic rate whatever the unit hereafter (same for the transpiration rate).

The *within*-group MFA show the internal structure of trait covariations within each environment (Figure 3). Analysis revealed that the traits were inversely correlated between CT and HT in the PC1-PC2 plane (Figure 3a,d,g,j). The net photosynthetic rate contributed negatively to PC1 and positively to PC2 under CT, but contributed only to PC2 under HT. This result indicated that the net photosynthetic rate was strongly correlated with transpiration and RGR under CT whereas these correlations were weaker under HT (Figure 1). In contrast to photosynthesis, stomatal density was well represented in the PC1-PC2 plane under HT but not under CT. This resulted from a poor correlation between stomatal density and both transpiration and RGR under CT, and a stronger correlation with these traits under HT. The analysis also revealed that photosynthetic rate and stomatal density were respectively strongly and weakly correlated to plant life history, leaf morphology and reproductive allocation under CT, but conversely weakly and strongly correlated to the same traits under HT, respectively. RWC did not contribute to the changes in correlation patterns between environments. It also displayed only very weak correlations with any other trait, whatever the environment (Figure 1).

Table 4. Mixed-effects model of the individual coordinates within multidimensional phenotypic space. Using the coordinates of the individual position along the PCs of the MFA, a mixed-effect model was performed as: P = W + T + WxT + G + GxW + GxT + GxWxT; where the position along each axis (P) is the result of (*i*) fixed environmental effects (W, T and WxT for water availability, temperature and their interaction, respectively), (*ii*) random genetic effects (G, independent of environment), and (*iii*) random genotype-by-environment interactions (GxE = GxW + GxT + GxWxT). Optimal condition (CTxWW) used as intercept. Confidence intervals (CI) were estimated with Markov Chain Monte Carlo bootstrap permutations.

		PC					
		1		2		3	
Fixed effects	intercept	-0.29	[-0.50;-0.02]	-0.02	[-0.16;+0.16]	-0.02	[-0.13;+0.10]
	WD	0.24	[+0.04;+0.40]	0.01	[-0.16;+0.17]	-0.02	[-0.13;+0.15]
	HT	0.63	[+0.31;+0.77]	0.03	[-0.21;+0.24]	-0.01	[-0.14;+0.15]
	HTxWD	-0.41	[-0.61;-0.10]	-0.10	[-0.33;+0.15]	0.02	[-0.19;+0.20]
Variance components	G	87.4		0.0		0.7	
	GxW	0.0		1.2		10.4	
	GxT	3.1		33.7		14.2	
	GxWxT	1.4		11.1		0.4	

We used the analytical method developed by Jouan-Rimbaud and colleagues (1998) to assess the differences in the structure of the phenotypic space between each environment. The computation of three parameters allows the pairwise comparison of (*i*) the direction of phenotypic spaces (parameter P), (*ii*) the volume, both in magnitude and direction, of variance–covariance matrices between the traits (parameter C), and (*iii*) the location of the centroids of the phenotypic spaces (parameter R). As indicated by the values of the parameter P (Table 3), the direction of the phenotypic spaces was very similar between WW and WD conditions whatever the air temperature (P = 0.97 and 0.96 under CT and HT, respectively). However, the orientation of the phenotypic space was more affected by temperature (*i.e.* lower P) whatever the watering regime. P was the lowest (P = 0.75) when comparing the optimal condition (CTxWW) to the most stressful condition (HTxWD). The same trends were observed for the volume of the phenotypic spaces (C). The parameter C was higher when comparing the phenotypic spaces in the same thermal environment – i.e. the phenotypic spaces have closer volume, or envelop – while C strongly decreased in response to HT. Finally, the parameter R was null for each comparison, indicating strong differences in the location of centroids of the phenotypic spaces in each environment. Overall, this analysis revealed strong effects of temperature on the covariance structure of the phenotypic space and weaker effects of soil water availability.

Mixed-effects models revealed hierarchical genetic variability in phenotypic plasticity

We extracted the individual coordinates along the first three PCs from the MFA to investigate the genetic determinisms of the phenotypic space in response to HT and WD. Using a mixed-effect modeling approach, we found significant fixed effects (i.e. average effect at the population level) of HT, WD and HTxWD along PC1, but not along PC2 or PC3 (Table 4). Along PC1, a large part of the phenotypic variability was attributable to genetic effects independently of the environment (G > 87%), whereas only a small part was attributable to genotype-by-environment interactions (all GxE < 4%). At the opposite, G had a low contribution to variance on PC2 and PC3 (G < 1%), and higher part of the variance was attributable to GxE effects (GxT = 14% and 34% for PC2 and PC3, respectively; GxTxW = 0% and 11% for PC2 and PC3, respectively).

Next, we extracted the best linearized unbiased predictors (BLUPs) from the mixed-effect models for the G and GxE effects that represented > 5% of variance components. This allowed mapping the QTL associated with integrated variability (G) and integrated plasticity to temperature (GxT), water availability (GxW), and their interaction (GxTxW). The analysis

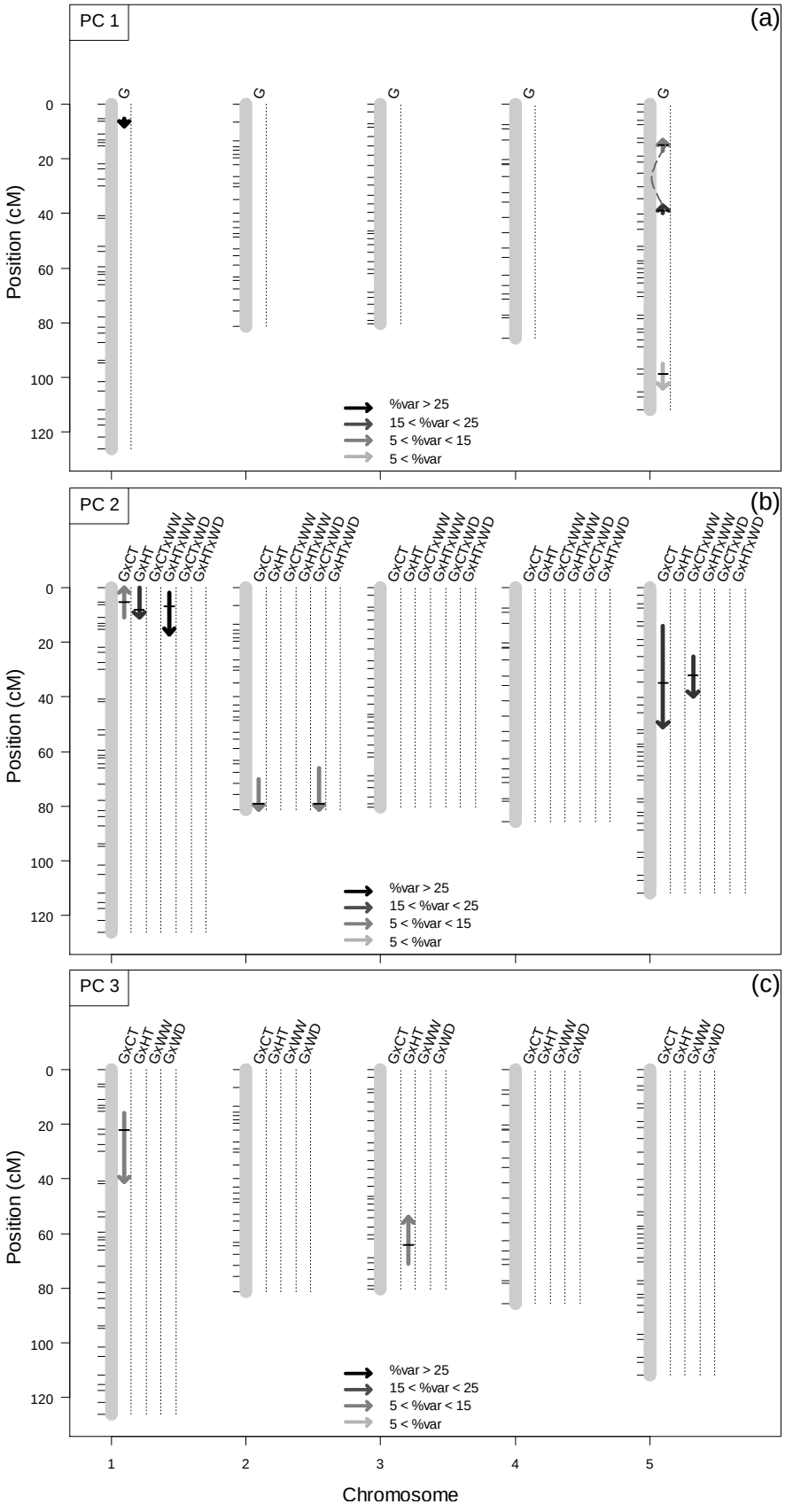

Figure 4. QTL for G and GxE effects on plant integrated phenotypes. (a) QTL mapped for G effects on the individuals position along PC1 ($P < 0.05$). (b) QTL mapped for GxCT, GxHT, GxCTxWW, GxHTxWW, GxCTxWD and GxHTxWD effects on the individuals position along PC2 ($P < 0.05$). (c) QTL mapped for GxCT, GxHT, GxWW, and GxWD effects on the individuals position along PC3 ($P < 0.05$). Arrows length represents confidence interval and arrows color represents the percent of variability explained by each QTL (< 5% to > 25%: lighter grey to black, respectively). Arrows pointed up represent positive effect of Cvi allele compared to L*er* allele, arrows pointed down represent negative effect of Cvi allele compared to L*er* allele. Dashed lines represent significant epistatic interactions between QTL ($P < 0.05$).

revealed four QTL for the G effects along PC1 (all $P < 0.01$; Figure 4a and Supporting Table S3). Among these, three had major effects: one at the top of chromosome 1 (CRY2) explained 32% of the variance, and two epistatic QTL closely located on chromosome 5 (BH.180C and GH.473C) explained together more than 35% of the variance (including epistatic effects; $P < 0.001$). Along PC2, we found strong additional effects of CRY2 and GH.473C, but their effects depended on the environmental conditions (Figure 4b and Supporting Table S3). At CRY2, the Cvi allele had a positive effect on the position along PC2 under CT but a negative effect under HT, specifically when plants were well-watered. At GH.473C, the Cvi allele has a negative effect on the position along PC2 under CT, specifically under CTxWW. A QTL at the end of chromosome 2 (MSAT2.22) explained more than 24% of the variability along PC2 depending on the environment. At this locus, the Cvi allele had a negative effect on the position along PC2, but only under CT and specifically under CTxWD. Concerning the phenotypic variability along PC3, we found two QTL that had a negative effect under CT (EC.66C; 13.5% of variability explained) , and a positive effect under HT, FD.98C (12.1% of variability explained) respectively.

The genotype and genotype-by-environment QTL of the multidimensional phenotype (Figure 4, Supporting Table S3) were consistent with their effects on individual traits (Table 2). Some of these effects are depicted on Figure 5. For instance, the large genotypic effect of CRY2 along PC1 is consistent with its effects on age at reproduction, vegetative and reproductive dry mass, LMA, and ET_{mass} (Figure 5; $P < 0.001$). Similarly, the effects of CRY2 on A_{mass}, a PC2-related trait, depended on the combination of soil water availability and temperature (Figure 5j). Consistent with the analysis of PC3 coordinates, we found no effect of CRY2 on RWC whatever the environment. MSAT2.22 had significant but weak effects on age and size at reproduction, and no significant effect on ET_{mass}, whatever the environment. However, consistent with the genetic analysis of PC2, MSAT2.22 had significant effects on the slope of the reaction norms of photosynthesis in response to soil water availability and air temperature. Finally, FD.98C had no effect on age and size at reproduction, transpiration and photosynthetic rates whatever the environment, but this QTL had significant effects on RWC depending on the environment.

Discussion

We observed strong phenotypic correlations along PC1 between LMA, traits related to plant life history (age and size at reproduction), transpiration rate and RGR. PC1-traits exhibited significant HT and WD effects at the population level. For instance, we observed an

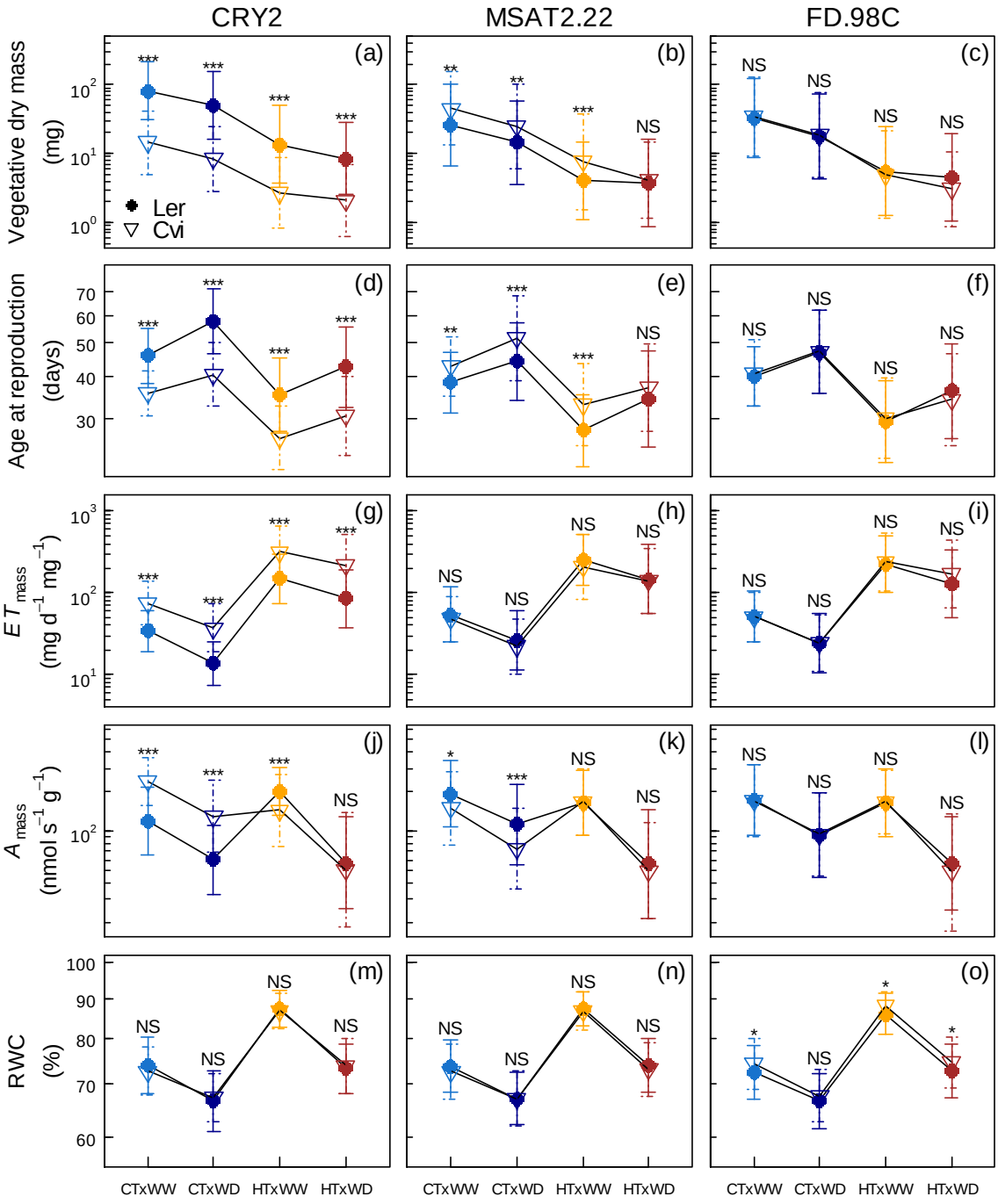

Figure 5. Genetic variability in reactions norms. Each point is the mean value of RILs depending on the environment and on the allele (L*er* or Cvi) at CRY2 (first column), MSAT2.22 (second column) and FD.98C (third column). Light blue: CTxWW; dark blue: CTxWD; orange: HTxWW; and dark red: HTxWD. Significance levels of post-hoc Tukey's test following two-ways ANOVA: *** = P < 0.001; ** = P < 0.01; * = P < 0.05; ° = P < 0.1.

increase in transpiration rate in response to HT, associated with a decrease in LMA and age at reproduction. Nonetheless, we observed no GxE interactions at the individual level, which resulted in a lack of plasticity for the trait covariation. The lack of interaction between HT and WD on PC1-traits at the population level supports the additive effects of the same treatments on the traits related to life history, biomass allocation and growth recently observed in (Vile et al. 2012 = Manuscript #1) on a set of natural accessions. The plasticity of the individual PC1-traits was also in accordance with those reported in Vile et al. (2012 = Manuscript #1), and the reader is invited to report to this previous study for a detailed discussion about this plasticity. Evolutionary biology is grounded upon the assumption that trait evolution is constrained by trait covariation and trade-offs (Roff 2007). Annual plants are notably constrained by growing 'as bigger as possible' and 'as faster as possible' (Metcalf and Mitchell-Olds 2009). This evolutionary trade-off relies on two functional assumptions: (*i*) bigger plants have higher reproductive success and (*ii*) long lifespan is detrimental for survival and performance. Independently of the environment, the positive correlation between vegetative and reproductive biomasses is in accordance with the first assumption, whereas the decrease in RGR with age at reproduction supports the second one. Therefore, our results highlight the role of these fundamental trade-offs in plant functioning whatever the environmental constraints.

Plant performance is also governed by global patterns of phenotypic covariations that illustrate the strategies for the utilization and conservation of resources (e.g. Reich et al. 1997, Bonser et al. 2010, Vasseur et al. 2012 = Manuscript #5). For instance, water use and carbon acquisition are tightly linked in the processes of transpiration and photosynthesis, which are also related to the structure and lifespan of photosynthetic organs (Wright et al. 2004, Mommer and Weemstra 2012). The variability in LMA can be interpreted as the necessity to build denser and thicker leaves to support higher leaf area and resist mechanical damages when plant age and size at reproduction increase (Blonder et al. 2011). Within each environment, big plants with high LMA exhibited lower transpiration rate compared to small plants with low LMA, although stomatal density and RWC did not correlate with those traits, at least in CT. It is difficult to postulate about the causality of the relationship between transpiration rate and PC1. We could hypothesize that a decrease in LMA reduced capillarity forces within the mesophyll, leading to an increase in transpiration rate. Besides, the increase in leaf size induced a decrease in the boundary layer conductance, which could participate to the decrease in transpiration rate (Pantin et al. 2012). Furthermore, the changes in plant architecture associated with changes in plant size, such as leaf overlapping, could also

contribute to the covariation observed between transpiration rate and PC1-traits. The same processes, such as stomata aperture, are involved in the regulation of gas exchanges and water fluxes (Pantin et al. 2012), which is assumed to result in a limited variability in water use efficiency (i.e. in the rate of carbon assimilated per unit of water loss). Surprisingly, stomatal density did not covary neither with photosynthesis or transpiration in CT. This suggests that water and gas fluxes are mainly driven by mesophyll thickness and/or stomatal closure in non-stressing thermal conditions, whatever the watering regime (Flexas et al. 2012). Net photosynthetic rate and PC1-traits negatively covary in CT (both WW and WD), which could be interpreted as (*i*) the consequence of the negative effect of LMA on CO_2 permeability and light interception (Shipley et al. 2006, Flexas et al. 2012), or (*ii*) the consequence of the changes in plant architecture that arose because of the changes in plant size. Strikingly, net photosynthesis did not covary with size-related traits and transpiration in HT (both WW and WD). 30 °C was identified as supra-optimal temperature for *A. thaliana* (Parent and Tardieu 2012). Hence, the saturation of the photosynthetic machinery in HT could explain the decoupling between leaf structure and carbon fixation capacities, leading to detrimental effect of HT on the trade-off between carbon gain, water use and lifespan. Moreover, the changes in leaf orientation (i.e. hyponastic movements) could also contribute to the lack of covariation between net photosynthetic rate and PC1-traits in HT (Vasseur et al. 2011 = Manuscript #3). The positive correlation between stomatal density and transpiration rate in HT could be a consequence of the around-the-clock stomatal aperture to satisfy cooling demand when temperature rises (Pantin et al. 2012). Contrary to the covariation of life history traits, our results illustrated how the trade-off between carbon fixation and water conservation interacts with air temperature and soil water availability.

The L*er* x Cvi population has been previously described as carrying pleiotropic 'hotspots' (Keurentjes et al. 2006, Fu et al. 2009, Vasseur et al. 2012 = Manuscript #5). Here we found that the QTL related to the variability along PC1 (CRY2, BH.180C and GH.473C) in each environment belong to these hotspots. As an example, CRY2 affected the 'height' of the reaction norms of PC1-traits, but not the slope. However, pleiotropic QTL that generated variability along PC1 had also opposite effects on PC2-traits depending on the temperature. CRY2, by affecting the slope of the reaction norms of PC2-traits, was responsible of the plasticity of the covariation of net photosynthesis with the PC1-traits. This temperature-dependent trait covariation was associated with a change in the direction of the phenotypic space. In addition to the effects of the major pleiotropic QTL that affected PC1-traits

independently of the environment and PC2-traits dependently of the environment, we identified QTL that affected only PC2-traits dependently of the environment. Hence, MSAT2.22 affected the plasticity of net photosynthesis to water deficit independently of size, transpiration and other PC1-traits. This result supports previous studies that identified MSAT2.22 as involved in the plasticity of water use efficiency using a measurement of carbon isotopic discrimination (McKay et al. 2003, Hausmann et al. 2005). Because it affected net photosynthesis independently of the other traits, this QTL was associated with variations that are perpendicular to the main axis of covariations.

Our findings demonstrated a modular organization of pleiotropic effects depending on the environment. Major pleiotropic QTL, such as CRY2, induced a change in the direction of the phenotypic space by affecting in opposite direction different functional modules in response to a change in temperature. In response to water deficit, the second type of pleiotropic QTL, such as MSAT2.22, induced a change in the volume of the phenotypic space by affecting only one functional module. The causal loci at MSAT2.22 could be a key genetic regulator of the plasticity of water use efficiency to water depletion, which offers valuable prospects for natural and breeder's selection.

Conclusion

The genetic structure of the plasticity of integrated phenotypes and its consequence for local adaptation is at the core of fascinating debates in the field of quantitative genetics, ecology and evolution for many decades (Bradshaw 1965, Gould and Lewontin 1979, Chapin 1991, Roff 1996, Wagner et al. 1996, Pigliucci and Preston 2004, McGuigan et al. 2011, Wagner and Zhang 2011). Our findings support the Chapin's hypothesis (1991) that major 'genetic hubs' would induce systemic phenotypic responses to abiotic stresses. They also demonstrate that such genetic hubs are organized into a hierarchical structure depending on their effects on the multidimensional phenotypic space. Further investigations, including reciprocal transplants in the field and fitness estimates, are needed to elucidate the role of these QTL specifically, and of pleiotropy in general, for the mechanisms of plant adaptation in response to major abiotic factors.

Acknowledgements

We thank M. Dauzat, A. Bédié, F. Bouvery, H. Durufle, J. Pasquet-Kok, J. Bresson, C. Balsera and G. Rolland for technical assistance with the PHENOPSIS platform and their help

during experiments. F.V. was funded by a CIFRE grant (ANRT, French Ministry of Research) supported by BAYER Crop Science (contract 0398/2009 - 09 42 008).

References

Alonso-Blanco, C., A. J. M. Peeters, M. Koornneef, C. Lister, C. Dean, N. van den Bosch, J. Pot, and M. T. R. Kuiper. 1998. Development of an AFLP based linkage map of L*er*, Col and Cvi *Arabidopsis thaliana* ecotypes and construction of a L*er*/Cvi recombinant inbred line population. Plant Journal **14**:259-271.

Blonder, B., C. Violle, L. P. Bentley, and B. J. Enquist. 2011. Venation networks and the origin of the leaf economics spectrum. Ecology Letters **14**:91-100.

Bonser, S. P., B. Ladd, K. Monro, M. D. Hall, and M. A. Forster. 2010. The adaptive value of functional and life-history traits across fertility treatments in an annual plant. Ann Bot **106**:979-988.

Boyer, J. S. 1982. Plant productivity and environment. Science **218**:443-448.

Bradshaw, A. D. 1965. Evolutionary significance of phenotypic plasticity in plants. Pages 115-155 *in* E. W. Caspari and J. M. Thoday, editors. Advances in Genetics. Academic Press.

Chapin, F. S. 1991. Integrated Responses of Plants to Stress. Bioscience **41**:29-36.

Ciais, P., M. Reichstein, N. Viovy, A. Granier, J. Ogee, V. Allard, M. Aubinet, N. Buchmann, C. Bernhofer, A. Carrara, F. Chevallier, N. De Noblet, A. D. Friend, P. Friedlingstein, T. Grunwald, B. Heinesch, P. Keronen, A. Knohl, G. Krinner, D. Loustau, G. Manca, G. Matteucci, F. Miglietta, J. M. Ourcival, D. Papale, K. Pilegaard, S. Rambal, G. Seufert, J. F. Soussana, M. J. Sanz, E. D. Schulze, T. Vesala, and R. Valentini. 2005. Europe-wide reduction in primary productivity caused by the heat and drought in 2003. Nature **437**:529-533.

Fabre, J., M. Dauzat, V. Negre, N. Wuyts, A. Tireau, E. Gennari, P. Neveu, S. Tisne, C. Massonnet, I. Hummel, and C. Granier. 2011. PHENOPSIS DB: an information system for *Arabidopsis thaliana* phenotypic data in an environmental context. BMC Plant Biol **11**:77.

Fisher, R. A. 1930. The genetical theory of natural selection. Clarendon Press, Oxford, England.

Flexas, J., M. M. Barbour, O. Brendel, H. M. Cabrera, M. Carriquí, A. Díaz-Espejo, C. Douthe, E. Dreyer, J. P. Ferrio, J. Gago, A. Gallé, J. Galmés, N. Kodama, H. Medrano, Ü. Niinemets, J. J. Peguero-Pina, A. Pou, M. Ribas-Carbó, M. Tomás, T. Tosens, and C. R. Warren. 2012. Mesophyll diffusion conductance to CO_2: An unappreciated central player in photosynthesis. Plant Science **193–194**:70-84.

Fu, J., J. J. Keurentjes, H. Bouwmeester, T. America, F. W. Verstappen, J. L. Ward, M. H. Beale, R. C. de Vos, M. Dijkstra, R. A. Scheltema, F. Johannes, M. Koornneef, D. Vreugdenhil, R. Breitling, and R. C. Jansen. 2009. System-wide molecular evidence for phenotypic buffering in Arabidopsis. Nature Genetics **41**:166-167.

Gould, S. J. and R. C. Lewontin. 1979. The spandrels of San Marco and the Panglossian paradigm: a critique of the adaptationist programme. Proc R Soc Lond B Biol Sci **205**:581-598.

Granier, C., L. Aguirrezabal, K. Chenu, S. J. Cookson, M. Dauzat, P. Hamard, J. J. Thioux, G. Rolland, S. Bouchier-Combaud, A. Lebaudy, B. Muller, T. Simonneau, and F. Tardieu. 2006. PHENOPSIS, an automated platform for reproducible phenotyping of plant responses to soil water deficit in *Arabidopsis thaliana* permitted the identification of an accession with low sensitivity to soil water deficit. New Phytologist **169**:623-635.

Grime, J. P. 1988. Plant strategies and the dynamics and structure of plant-communities. Nature **336**:630-630.

Hausmann, N. J., T. E. Juenger, S. Sen, K. A. Stowe, T. E. Dawson, and E. L. Simms. 2005. Quantitative trait loci affecting delta13C and response to differential water availibility in *Arabidopsis thaliana*. Evolution **59**:81-96.

Jouan-Rimbaud, D., D. L. Massart, C. A. Saby, and C. Puel. 1998. Determination of the representativity between two multidimensional data sets by a comparison of their structure. Chemometrics and Intelligent Laboratory Systems **40**:129-144.

Keurentjes, J. J. B., J. Y. Fu, C. H. R. de Vos, A. Lommen, R. D. Hall, R. J. Bino, L. H. W. van der Plas, R. C. Jansen, D. Vreugdenhil, and M. Koornneef. 2006. The genetics of plant metabolism. Nature Genetics **38**:842-849.

Kolokotrones, T., V. Savage, E. J. Deeds, and W. Fontana. 2010. Curvature in metabolic scaling. Nature **464**:753-756.

Martin, G. and T. Lenormand. 2006. A general multivariate extension of Fisher's geometrical model and the distribution of mutation fitness effects across species. Evolution **60**:893-907.

McGuigan, K., L. Rowe, and M. W. Blows. 2011. Pleiotropy, apparent stabilizing selection and uncovering fitness optima. Trends in Ecology & Evolution **26**:22-29.

McKay, J. K., J. H. Richards, and T. Mitchell-Olds. 2003. Genetics of drought adaptation in *Arabidopsis thaliana*: I. Pleiotropy contributes to genetic correlations among ecological traits. Molecular Ecology **12**:1137-1151.

Metcalf, C. J. and T. Mitchell-Olds. 2009. Life history in a model system: opening the black box with *Arabidopsis thaliana*. Ecology Letters **12**:593-600.

Mittler, R. 2006. Abiotic stress, the field environment and stress combination. Trends Plant Sci **11**:15-19.

Mommer, L. and M. Weemstra. 2012. The role of roots in the resource economics spectrum. New Phytologist **195**:725-727.

Pages, J. 2002. Structural universals and formal relations. Synthese **131**:215-221.

Pantin, F., T. Simonneau, and B. Muller. 2012. Coming of leaf age: control of growth by hydraulics and metabolics during leaf ontogeny. New Phytologist **196**:349-366.

Parent, B. and F. Tardieu. 2012. Temperature responses of developmental processes have not been affected by breeding in different ecological areas for 17 crop species. New Phytologist **194**:760-774.

Pavlicev, M. and G. P. Wagner. 2012. A model of developmental evolution: selection, pleiotropy and compensation. Trends in Ecology & Evolution **27**:316-322.

Pigliucci, M. and K. Preston. 2004. Phenotypic Integration: Studying the ecology and evolution of complex phenotypes. Oxford University Press.

Reich, P. B., M. B. Walters, and D. S. Ellsworth. 1997. From tropics to tundra: global convergence in plant functioning. Proceedings of the National Academy of Sciences of the United States of America **94**:13730-13734.

Roff, D. A. 1996. The evolution of genetic correlations: an analysis of patterns. Evolution **50**:1392-1403.

Roff, D. A. 2007. Contributions of genomics to life-history theory. Nat Rev Genet **8**:116-125.

Roff, D. A. and R. Preziosi. 1994. The estimation of the genetic correlation: the use of the jackknife. Heredity **73**:544-548.

Shipley, B., M. J. Lechowicz, I. Wright, and P. B. Reich. 2006. Fundamental trade-offs generating the worldwide leaf economics spectrum. Ecology **87**:535-541.

Stearns, S. C. 1989. Trade-Offs in Life-History Evolution. Functional Ecology **3**:259-268.

Vasseur, F., F. Pantin, and D. Vile. 2011. Changes in light intensity reveal a major role for carbon balance in Arabidopsis responses to high temperature. Plant Cell and Environment.

Vasseur, F., C. Violle, B. J. Enquist, C. Granier, and D. Vile. 2012. A common genetic basis to the origin of the leaf economics spectrum and metabolic scaling allometry. Ecology Letters **15**:1149-1157.

Vile, D., M. Pervent, M. Belluau, F. Vasseur, J. Bresson, B. Muller, C. Granier, and T. Simonneau. 2012. Arabidopsis growth under prolonged high temperature and water deficit: independent or interactive effects? Plant Cell and Environment **35**:702-718.

Vile, D., B. Shipley, and E. Garnier. 2006. A structural equation model to integrate changes in functional strategies during old-field succession. Ecology **87**:504-517.

Violle, C., M. L. Navas, D. Vile, E. Kazakou, C. Fortunel, I. Hummel, and E. Garnier. 2007. Let the concept of trait be functional! Oikos **116**:882-892.

Wagner, G. P., Altenberg, and L. 1996. Perspective: complex adaptations and the evolution of evolvability. Wiley, Hoboken, NJ, ETATS-UNIS.

Wagner, G. P., M. Pavlicev, and J. M. Cheverud. 2007. The road to modularity. Nature Reviews Genetics **8**:921-931.

Wagner, G. P. and J. Z. Zhang. 2011. The pleiotropic structure of the genotype-phenotype map: the evolvability of complex organisms. Nature Reviews Genetics **12**:204-213.

Wang, Z., B. Y. Liao, and J. Zhang. 2010. Genomic patterns of pleiotropy and the evolution of complexity. Proc Natl Acad Sci U S A **107**:18034-18039.

Westoby, M., D. S. Falster, A. T. Moles, P. A. Vesk, and I. J. Wright. 2002. Plant ecological strategies: some leading dimensions of variation between species. Annual Review of Ecology and Systematics **33**:125-159.

Wright, I. J., P. B. Reich, M. Westoby, D. D. Ackerly, Z. Baruch, F. Bongers, J. Cavender-Bares, T. Chapin, J. H. C. Cornelissen, M. Diemer, J. Flexas, E. Garnier, P. K. Groom, J. Gulias, K. Hikosaka, B. B. Lamont, T. Lee, W. Lee, C. Lusk, J. J. Midgley, M. L. Navas, U. Niinemets, J. Oleksyn, N. Osada, H. Poorter, P. Poot, L. Prior, V. I. Pyankov, C. Roumet, S. C. Thomas, M. G. Tjoelker, E. J. Veneklaas, and R. Villar. 2004. The worldwide leaf economics spectrum. Nature **428**:821-827.

Supporting Information

Table S1. Correlations of phenotypic traits along each PC of the MFA: comparison across- versus within-environments. Age at reproduction (d), vegetative and reproductive dry masses (mg), total leaf area (cm^2), leaf dry mass per area (LMA, g m^{-2}), relative water content (RWC, %), stomatal density (mm^{-2}), mass-based net photosynthetic and transpiration rates (A_{mass}, nmol CO_2 s^{-1} g^{-1} and ET_{mass}, mg H_2O d^{-1} mg^{-1}, respectively), area-based net photosynthesis and transpiration rates (A_{area}, nmol CO_2 s^{-1} cm^{-2} and ET_{area}, mg H_2O d^{-1} cm^{-2}, respectively), and relative growth rate (RGR, mg d^{-1} mg^{-1}).

		PC1	PC2	PC3
all environments	Age at reproduction	0.9305	-0.0314	-0.0298
	Vegetative dry mass	0.9837	0.0441	-0.0333
	Total leaf area	0.9702	0.0699	-0.0029
	Reproductive dry mass	0.7605	0.1992	0.033
	Stomatal density	-0.532	-0.4615	-0.118
	RWC	-0.0867	0.2061	0.9495
	LMA	0.8521	-0.0519	-0.1322
	A_{mass}	-0.5097	0.8313	-0.1174
	A_{area}	-0.2335	0.9122	-0.195
	ET_{mass}	-0.9438	-0.0705	-0.0206
	ET_{area}	-0.8256	-0.1331	-0.095
	RGR	-0.9837	-0.0441	0.0333
CTxWW	Age at reproduction	0.9314	-0.6953	0.2322
	Vegetative dry mass	0.9856	-0.6098	0.2493
	Total leaf area	0.9718	-0.5823	0.2411
	Reproductive dry mass	0.8395	-0.3492	0.2298
	Stomatal density	-0.3029	-0.2767	-0.3268
	RWC	0.0898	0.2126	0.9611
	LMA	0.9112	-0.5989	0.2454
	A_{mass}	-0.9214	0.8282	-0.2479
	A_{area}	-0.7588	0.903	-0.2039
	ET_{mass}	-0.9201	0.5049	-0.2818
	ET_{area}	-0.7407	0.3315	-0.2524
	RGR	-0.9856	0.6098	-0.2493
CTxWD	Age at reproduction	0.9407	-0.3968	0.018
	Vegetative dry mass	0.9868	-0.295	3.00E-04
	Total leaf area	0.9662	-0.2691	0.0584
	Reproductive dry mass	0.7826	-0.1143	-0.0783
	Stomatal density	-0.4626	-0.315	-0.1189
	RWC	-0.1768	0.297	0.9463
	LMA	0.8475	-0.3016	-0.1891
	A_{mass}	-0.7892	0.8082	0.0185
	A_{area}	-0.4849	0.9037	-0.1103
	ET_{mass}	-0.9668	0.1958	0.0088
	ET_{area}	-0.8566	0.0828	-0.119
	RGR	-0.9868	0.295	-3.00E-04
HTxWW	Age at reproduction	0.9306	0.4604	-0.172
	Vegetative dry mass	0.9841	0.5025	-0.1663
	Total leaf area	0.9783	0.534	-0.1384
	Reproductive dry mass	0.7391	0.6676	-0.0515
	Stomatal density	-0.7371	-0.6996	0.0127
	RWC	-0.0611	0.1797	0.952
	LMA	0.8401	0.3058	-0.2753
	A_{mass}	-0.0074	0.87	-0.1146
	A_{area}	0.3324	0.9529	-0.2204
	ET_{mass}	-0.9213	-0.4514	0.0162
	ET_{area}	-0.8184	-0.4408	-0.0834
	RGR	-0.9841	-0.5025	0.1663
HTxWD	Age at reproduction	0.9156	0.337	-0.2241
	Vegetative dry mass	0.979	0.419	-0.2409
	Total leaf area	0.9685	0.4373	-0.2047
	Reproductive dry mass	0.6552	0.4499	0.075
	Stomatal density	-0.6874	-0.5145	-0.0383
	RWC	-0.1835	0.1334	0.9395
	LMA	0.8044	0.2482	-0.3021
	A_{mass}	-0.1371	0.8587	-0.173
	A_{area}	0.1573	0.9282	-0.2783
	ET_{mass}	-0.9644	-0.3915	0.1847
	ET_{area}	-0.889	-0.3971	0.1019
	RGR	-0.979	-0.419	0.2409

Table S2. Contribution of phenotypic traits to each PC of the MFA. The contribution of a data point to the inertia of an axis is the quotient between the inertia of its projection and the inertia of the whole scatterplot's projection on this axis. Age at reproduction (d), vegetative and reproductive dry masses (mg), total leaf area (cm^2), leaf dry mass per area (LMA, g m^{-2}), relative water content (RWC, %), stomatal density (mm^{-2}), mass-based net photosynthetic and transpiration rates (A_{mass}, nmol CO_2 s^{-1} g^{-1} and ET_{mass}, mg H_2O d^{-1} mg^{-1}, respectively), area-based net photosynthesis and transpiration rates (A_{area}, nmol CO_2 s^{-1} cm^{-2} and ET_{area}, mg H_2O d^{-1} cm^{-2}, respectively), and relative growth rate (RGR, mg d^{-1} mg^{-1}).

	PC1	PC2	PC3
Age at reproduction	11.9855	0.0532	0.0891
Vegetative dry mass	13.395	0.105	0.1113
Total leaf area	13.0294	0.2636	9.00E-04
Reproductive dry mass	8.0064	2.141	0.109
Stomatal density	3.9185	11.4915	1.3949
RWC	0.1041	2.2912	90.2982
LMA	10.05	0.1452	1.7503
A_{mass}	3.5963	37.288	1.3809
A_{area}	0.7548	44.8929	3.8068
ET_{mass}	12.3304	0.2682	0.0427
ET_{area}	9.4347	0.9552	0.9045
RGR	13.395	0.105	0.1113

Table S3. QTL for G and GxE effects on the dimensions of plant phenotypic space. QTL mapping was performed on the BLUPs of genetic effects (G) and genotypic-by-environment (GxE) effects (i.e. GxT, GxW, and GxTxW for the genotypic interactions with air temperature, water availability, and their interactions, respectively). BLUPs estimated from mixed-effects models (that explain > 5% of variance). Position and confidence interval were estimated with maximum likelihood following an iterative scan (1000 bootstrap permutations), and percent of variability was estimated with two-ways ANOVA in composite interval mapping. All QTL presented are significant ($P > 0.05$). 'QTL id' is the name of the closest AFLP marker to the LOD score peak.

PC	BLUPs	Marker	Chr	Position (cM)	% var
1	G	CRY2	1	6 [5.3-8]	31.9
		BH.180C	5	15 [13-17]	12.9
		GH.473C	5	39 [37-40]	21.2
		BF.168L	5	99 [95-104]	3.2
2	GxCT	CRY2	1	5.3 [0-10.8]	11.1
		MSAT2.22	2	79 [70-81]	11.4
		GH.473C	5	35 [14-51]	16.5
	GxHT	CRY2	1	8 [0-11]	17.0
	GxCTxWW	GH.473C	5	32 [25-40]	21.2
	GxHTxWW	CRY2	1	7 [2-17]	25.5
	GxCTxWD	MSAT2.22	2	79 [66-81]	13.3
3	GxCT	EC.66C	1	22 [16-41]	13.5
	GxHT	FD.98C	3	64 [54-71]	12.1

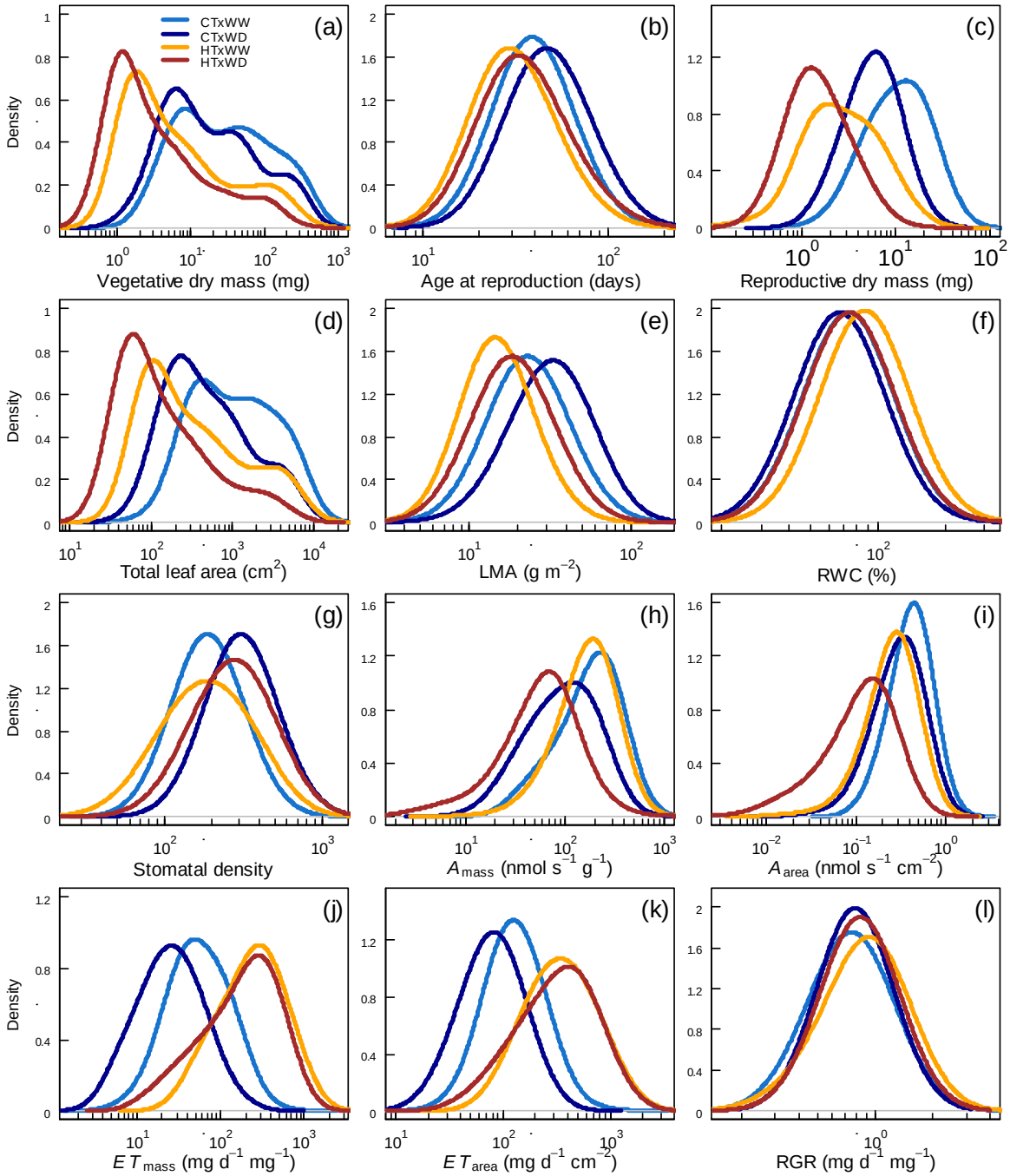

Figure S1. Distribution of the 12 phenotypic traits depending on the environment. Curves represent the density of the distribution for the 12 phenotypic traits. Light blue: CTxWW; dark blue: CTxWD; orange: HTxWW; and dark red: HTxWD. Age at reproduction (d), vegetative and reproductive dry masses (mg), total leaf area (cm^2), leaf dry mass per area (LMA, g m^{-2}), relative water content (RWC, %), stomatal density (mm^{-2}), mass-based net photosynthetic and transpiration rates (A_{mass}, nmol CO_2 s^{-1} g^{-1} and ET_{mass}, mg H_2O d^{-1} mg^{-1}, respectively), area-based net photosynthesis and transpiration rates (A_{area}, nmol CO_2 s^{-1} cm^{-2} and ET_{area}, mg H_2O d^{-1} cm^{-2}, respectively), and relative growth rate (RGR, mg d^{-1} mg^{-1}).

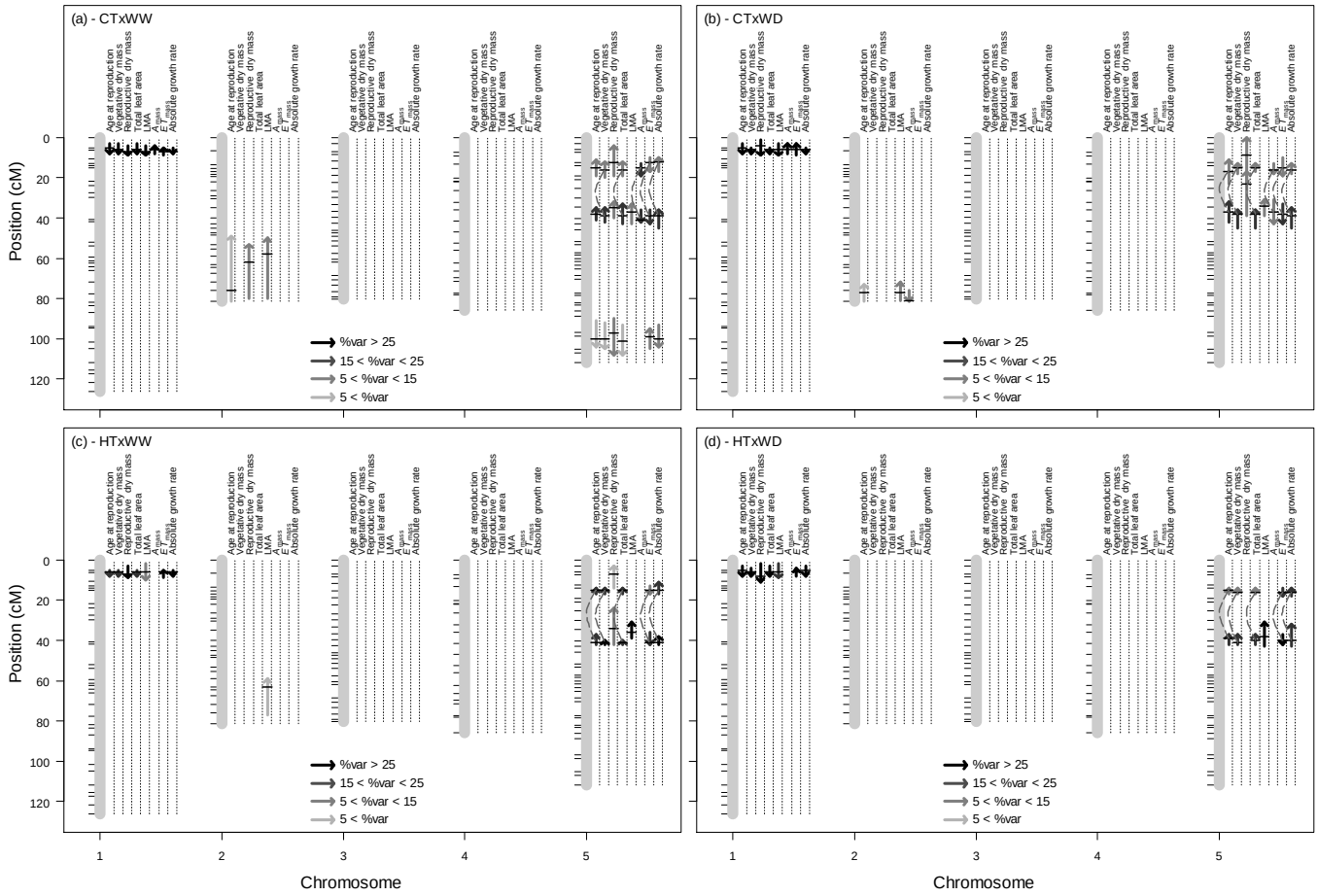

Figure S2. QTL analysis of 8 phenotypic traits within the four environments. (a), (b), (c) and (d): CTxWW, CTxWD, HTxWW, and HTxWD, respectively. From column 1 to 8: age at reproduction (days), vegetative dry mass (mg), reproductive dry mass (mg), total leaf area (cm^2), leaf mass per area (LMA, g m^{-2}), mass-based net photosynthetic rate (A_{mass}, nmol s^{-1} g^{-1}), mass-based transpiration rate (ET_{mass}, mg d^{-1} g^{-1}), and absolute growth rate (mg d^{-1}). Arrows length represents confidence interval and arrows color represents the percent of variability explained by each QTL (< 5% to > 25%: lighter grey to black, respectively). Arrows direction represents the effect of Cvi allele against L*er* allele. Dashed lines represent significant epistatic interactions between QTL ($P < 0.05$).

Chapter 2

Do similar plant responses to different abiotic factors arise from the same cause?

"When a thing ceases to be a subject of controversy, it ceases to be a subject of interest. »
William Hazlitt

Chapter objectives:

In this second chapter, we investigated adaptive hypotheses that may explain the origin of the phenotypic plasticity to high temperature. Specifically we asked:

- Why do the integrated responses to high temperature resemble those encountered in low light intensity?
- Why does plant have erected leaves under high temperature: to cool or to thrive?

Our results give new insights into the evolutionary constraints on the trade-off between maximizing carbon gain and minimizing water loss. In a breeding perspective, we argue that manipulating leaf cooling and carbon metabolism through the engineering of plant architecture offers valuable prospects to improve the efficiency of water use in a warming world.

Manuscript #3

Changes in light intensity reveal a major role for carbon balance in Arabidopsis responses to high temperature

François Vasseur[1], Florent Pantin[1] and Denis Vile[1]

[1]Laboratoire d'Ecophysiologie des Plantes sous Stress Environnementaux (LEPSE), UMR 759, INRA-SUPAGRO, F-34060 Montpellier, France

Article first published online: 28 June 2011 in *Plant, Cell and Environment*
Volume 34, Issue 9, Pages 1563–1576, DOI: 10.1111/j.1365-3040.2011.02353.x
url: http://onlinelibrary.wiley.com/doi/10.1111/j.1365-3040.2011.02353.x/pdf

Abstract

High temperature (HT) is a major limiting factor for plant productivity. Since some responses to HT, notably hyponasty, resemble those encountered in low light, we hypothesized that plant responses to HT are under the control of carbon balance. We analyzed the interactive effects of HT and irradiance level on hyponasty and a set of traits related to plant growth in natural accessions of *Arabidopsis thaliana* and mutants affected in heat dissipation through transpiration (*NCED6*-OE, *ost2*) and starch metabolism (*pgm*). HT induced hyponasty, reduced plant growth, and modified leaf structure. Low light worsened the effects of HT, whilst increasing light restored trait values close to levels observed at control temperature. Leaf temperature *per se* did not play a major role in the observed responses. By contrast, a major role of carbon balance was supported by hyponastic growth of *pgm* as well as morphological, physiological (photosynthesis, sugar and starch contents) and transcriptional data. Carbon balance could be a common sensor of HT and low light, leading to responses specific of the shade-avoidance syndrome. Hyponasty and associated changes in plant traits could be key traits conditioning plant performance under competition for light, particularly in warm environments.

Key-words: Arabidopsis thaliana, carbon status, growth, hyponasty, high temperature, light.

Introduction

High temperature (HT) is among the most damaging factors for plant productivity (Jones 1992). For most plant species, even a moderate increase in temperature leads to significant changes in leaf structure and morphology (Poorter et al. 2009). HT affects central processes such as photosynthesis, leaf expansion, germination, buds and flower abortion or cell division (Berry and Björkman 1980, Penfield 2008). Indeed, the rates of numerous plant processes increase with temperature up to an optimum above which dramatic physiological and developmental changes occur, leading to a rapid decrease of these rates (Ong 1983, Gillooly et al. 2001, Granier et al. 2002).

HT could affect plant carbon balance because carbohydrate demand increases while its supply decreases: rates of physiological processes increase whilst photosynthetic yield decreases (Berry and Björkman 1980, Kobza and Edwards 1987). Accordingly, tolerance to warm temperatures is increased at high CO_2 concentration in C3 plants (Huxman et al. 1998, Taub et al. 2000). Furthermore, the allocation of carbohydrates into costly processes such as the biosynthesis of protection proteins (notably heat shock proteins; Heckathorn et al. 1996) raises with increasing temperature. In line with this, Heckathorn et al. reported that plant tolerance to heat stress is decreased at low nitrogen supply due to a limited production of nitrogen-costly heat shock proteins. Since photosynthesis is a major driver of plant carbon balance light availability should also be taken into account to investigate plant responses to HT.

Because leaf orientation directly determines light interception, it has been proposed that leaf phototropism could be part of plant responses to temperature. For instance, in several species changes in leaf angle avoid blade over-heating when light intensity is maximal (Fu and Ehleringer 1989, King 1997, Falster and Westoby 2003). In *Arabidopsis thaliana* as well as in other species, hyponasty, i.e. upward leaf movements (Kang 1979), is one of the first morphological responses to HT (Koini et al. 2009). Hyponastic response varies widely among natural accessions of Arabidopsis and is related to the daily temperature variation encountered in the collection sites, suggesting an adaptive role for this trait (Van Zanten et al. 2009). Recently, Franklin (2010) also reported that Arabidopsis rosettes displaying hyponastic growth have a higher transpiration rate. HT-induced hyponasty could therefore contribute to optimize leaf cooling by increasing transpiration (possibly through an increase of boundary layer conductance), reducing the stress due to excess irradiance, or by repositioning the photosynthesizing tissues away from the heated soil (Gray et al. 1998).

Hyponasty is also a typical response to low light intensity and to decreased red to far-red ratio (Hangarter 1997, Maliakal et al. 1999, Smith 2000), occurring under the control of the phytochrome and cryptochrome pathways (Smalle et al. 1997, Vandenbussche et al. 2003, Kozuka et al. 2005, Millenaar et al. 2009). Hyponasty has therefore been proposed to be a morphological response typical of the shade-avoidance syndrome, allowing plants to reach more light and maximize carbon gain as in the case of competition for light under a canopy (Pierik et al. 2004, Mullen et al. 2006, van Zanten et al. 2010a). Van Zanten et al. (2009) showed that HT-induced and low light-induced hyponasty display very similar responses in terms of kinetics and amplitude. Interestingly, low light-induced hyponasty was also observed in multiple loss-of-function photoreceptor mutants (Millenaar et al. 2009). Taken together, these results suggest a tight link between hyponasty and carbon balance.

Here, we aimed at deciphering the role of carbon balance into plant responses to HT. To this end, we investigated to what extent Arabidopsis responses to HT are driven by light intensity. Specifically, we tested whether hyponasty induced by HT prevents elevation of leaf temperature or is an anticipated response against carbon depletion. For this purpose, the responses of *Arabidopsis thaliana* accessions and mutants affected in carbon balance and regulation of leaf temperature via transpiration were studied at three light intensities under prolonged elevated temperature. We chose the physiologically relevant HT of 30 °C which is known to affect growth and hyponasty in Arabidopsis (Van Zanten et al. 2009). This temperature was unlikely to cause mortality since it has been described as the temperature of basal thermotolerance of the Col-0 reference accession (Ludwig-Muller et al. 2000). In parallel with leaf temperature, leaf carbon status was investigated through sugars and starch contents, CO_2 exchanges, chlorophyll fluorescence, and a transcriptional analysis of targeted genes. Finally, using a multi-level analysis of plant traits, we highlighted that changes in growth and development induced by HT are tightly related to changes in carbon status.

Materials and methods

Plant material

Four *Arabidopsis thaliana* (L.) Heynh accessions (NASC numbers in brackets) were chosen for their variability in the phenotypic responses to growth conditions (Millenaar et al. 2005, Tonsor et al. 2008): Col-0 (N1092); An-1 (N944); Cvi-0 (N902) and L*er* (NW20). L*er* carries a mutation at *ERECTA* which affects multiple plant traits also affected by HT and light (Masle et al. 2005, Tisné et al. 2010). This gene is also involved in the control of ethylene-induced hyponasty (van Zanten et al. 2010a). Therefore, L*ER*, a complemented accession

homozygous for Col-0 allele at *ERECTA* was included in our analysis (Torii et al. 1996). A starch synthesis deficient mutant *pgm* (Caspar et al. 1985), and two mutants affected in stomata opening: an 'open stomata', *ost2* (Merlot et al. 2002) and a 'closed stomata', *NCED6*-OE (Lefebvre et al. 2006), all in Col-0 background, completed this selection.

Growth conditions and treatments

Five seeds of each genotype were sown in 225 mL pots filled with a damped mixture (1:1, v/v) of loamy soil and organic compost (Neuhaus N2), and placed at 4°C in the dark for 48 h. After germination, plants were grown in a chamber at 20 °C air temperature and 12/12 h photoperiod under a photosynthetic active radiation (PAR) of 175 µmol m^{-2} s^{-1} supplied from a bank of HQi lamps until the emergence of the two first leaves (stage 1.02 in Boyes et al. 2001) (Table S1). Pots were moved daily to avoid boundary effects. From stage 1.02 onwards, air temperature was set to 20 °C/17 °C day/night in a first growth chamber and to 30 °C/25 °C in three others. PAR was maintained at 175 µmol m^{-2} s^{-1} until 6th leaf emergence (stage 1.06). Then, HT-treated plants were grown under low (LL, 70 µmol m^{-2} s^{-1}), moderate (ML, 175 µmol m^{-2} s^{-1}), and high (HL, 330 µmol m^{-2} s^{-1}) light. In each chamber, vapor pressure deficit (VPD) was maintained at 0.6/0.4 kPa during day/night. Each pot was weighed daily and watered with a one-tenth-strength Hoagland's solution (Hoagland and Arnon 1950) to maintain soil water content at a well-watered level of 0.35 g H_20 g^{-1} dry soil equivalent to a predawn water potential of -0.3 MPa (Granier et al. 2006, Hummel et al. 2010). Six to eight plants were harvested at first silique emergence (stage 6.02)

Measurement of plant traits

Whole plant and leaf traits

Total length, blade length, and tip height of the youngest fully-expanded leaf were determined three times per week in all genotypes during the two weeks following lights treatments. Measurements were performed at different times of the day on randomly selected plants to avoid effects of weak changes occurring along the day due to the endogenous rhythms (Mullen et al. 2006), and during the vegetative stage to avoid effects of drastic changes in carbon status due to floral transition (Christophe et al. 2008). Blade ratio was calculated as blade length to total leaf length. Leaf insertion angle (degree) was calculated as θ = arcsine(leaf tip height/leaf length)×180/π. Mean values of leaf angle and blade ratio were calculated for the two weeks period and used in further analyses.

Plants were harvested shortly after flowering when the first silique emerged (stage 6.01; from 35 to 100 days after sowing). Rosettes were cut and immediately weighed (FW, mg)

Table 1. Results of univariate analyses of variance (ANOVAs). Numbers are mean squares (type III) from the partitioning of phenotypic variation among five genotypes (G) including four accessions (An-1, Col-0, Cvi-0, L*er*) and the complemented L*ER* line grown at 20 °C under moderate light intensity (175 µmol m^{-2} s^{-1}), and at high temperature (30 °C) under low (70 µmol m^{-2} s^{-1}), moderate (175 µmol m^{-2} s^{-1}), and high light intensity (330 µmol m^{-2} s^{-1}). Hypothesis testing was based on F-ratios from type III mean squares for all ANOVAs. Mean squares in bold typeface followed by a symbol were significant at ¤, P < 0.10; *, *P* < 0.05; **, *P* < 0.01; ***, *P* < 0.001. Mean squares reported are those from the full model including all interactions. All nonsignificant terms (normal typeface) are reported, but were removed from the final model. [a] ln-transformed variable.

	Moderate light intensity (temperature effect)				High temperature (light effect)				Light and temperature treatments merged			
Trait	G	T	GxT	R^2	G	L	GxL	R^2	G	E	GxE	R^2
Leaf insertion angle	**1287*** **	**13517*** **	**172.0*** **	**0.95*** **	**1202*** **	**6217*** **	**159.8*** **	**0.79*** **	**1843*** **	**12132*** **	**142.5*** **	**0.90*** **
Leaf blade ratio	**323.7*** **	**363.8*** **	**43.99*** **	**0.72*** **	**495.8*** **	**1469*** **	**62.96*** **	**0.85*** **	**705.2*** **	**1398*** **	**58.18*** **	**0.84*** **
Vegetative duration	**1134*** **	82.36	87.67¤	**0.59*** **	**2304*** **	**1448*** **	**196.3*** **	**0.71*** **	**2398*** **	**1247*** **	**166.2*** **	**0.73*** **
Leaf number at flowering	**674.0*** **	**211.2*** **	**68.74*** **	**0.67*** **	**475.7*** **	**255.3*** **	**37.69** **	**0.63*** **	**785.1*** **	**322.5*** **	**44.31*** **	**0.69*** **
Total fresh mass[a]	**3.532*** **	**1.759*** **	**0.148** **	**0.78*** **	**3.884*** **	**2.648*** **	**0.196*** **	**0.78*** **	**4.839*** **	**3.039*** **	**0.159*** **	**0.81*** **
Specific leaf area	**3630*** **	**5665*** **	**736*** **	**0.70*** **	**6434*** **	**41516*** **	193.0	**0.82*** **	**6698*** **	**33360*** **	**462*** **	**0.84*** **
Leaf dry matter content	**2.751*** **	**4.061*** **	**1.023***	**0.35*** **	**3.177*** **	**26.45*** **	0.292	**0.56*** **	**3.550*** **	**19.43*** **	0.536	**0.56*** **
Leaf thickness	**25176*** **	**43302*** **	**28190*** **	**0.57*** **	**23064*** **	**42647*** **	**3170** **	**0.58*** **	**27.52*** **	**59676*** **	**4265*** **	**0.64*** **
Cell density[a]	**1.307*** **	**0.320** **	**0.496*** **	**0.59*** **	**1.496*** **	**1.435*** **	0.084¤	**0.65*** **	**1.528*** **	**1.008*** **	**0.225*** **	**0.66*** **
Stomatal density[a]	**1.471*** **	**3.739*** **	**0.589*** **	**0.72*** **	**2.483*** **	**0.430*** **	**0.123***	**0.67*** **	**2.255*** **	**1.286*** **	**0.298*** **	**0.70*** **
Stomatal index	**4.220*** **	**131.1*** **	**9.476** **	**0.42*** **	**17.44*** **	**38.68*** **	**4.127**	**0.37*** **	**15.05*** **	**106.6*** **	**6.026** **	**0.57*** **

after removal of inflorescences. Rosettes were wrapped in moist paper and placed into Petri dishes at 4 °C in darkness overnight to achieve complete rehydration. Water-saturated fresh weight (SW) was then determined. Total leaf number (LN) was determined and leaf blades were separated from their petiole and scanned for area measurements before being oven-dried at 65 °C for 48 h to determine their dry weight (DW). Rosette area (RA, cm^2) was determined as the sum of individual leaf blade areas measured with an image analyzer (Bioscan-Optimas 4.10, Edmond, WA, USA). Relative water content (RWC = (FW – DW)/(SW – DW), %), leaf dry matter content (DW/FW, mg g^{-1}) and specific leaf area (RA/DW, cm^2 g^{-1}) were calculated at the rosette level. Mean leaf thickness (µm) was estimated as SW_{blade} / RA (Vile et al. 2005). Epidermal imprints of 6th leaf were placed under a microscope (Leitz DM RB, Leica, Wetzlar, Germany) coupled to an image analyzer. Mean cell density and stomatal density were determined in two 0.12 mm^2 zones. Stomatal index was calculated as 100 × stomatal number / (stomatal number + stomatal number × 2 + cell number).

Transpiration and leaf temperature

Transpirational water loss was determined on five to eight plants of Col-0, L*er*, *NCED6*-OE and *ost2* at bolting by successive weighing of the pots over 3 days and nights. Soil evaporation was prevented by sealing soil surface with four layers of a plastic film. Whole-plant transpiration rate (mg H_2O h^{-1}) was estimated as the slope of the linear relationship between weight and time, and then expressed per dissected rosette area (mg H_2O h^{-1} cm^{-2}). Leaf temperature (°C) was determined at two points of 4-6 rosettes by infrared imaging (ThermaCAM B20HSV, FLIR Systems, Wilsonville, OR, USA).

Net photosynthesis, respiration and dark-adapted chlorophyll fluorescence

Rate of CO_2 assimilation was measured on four Col-0 and L*er* plants at bolting (between stages 3.90 and 5.01 of Boyes et al. (2001); *ca* 15 days after the beginning of light treatments) using a single leaf chamber designed for Arabidopsis connected to an infrared gas analyzer system (CIRAS 2, PP systems, Amesbury, MA, USA). Dark respiration and chlorophyll fluorescence were measured using a fluorescence module supplied by the manufacturer on plants dark-adapted for at least 20 min and submitted to a saturating light flash to estimate photosystem II (PSII) yield capacity as Fv/Fm, where Fv is the difference between the maximum (Fm) and the minimum fluorescence signals (Maxwell and Johnson 2000). Carbon fluxes were determined at steady-state (approximately 15 min after light was switched on or off) under 390 ppm CO_2.

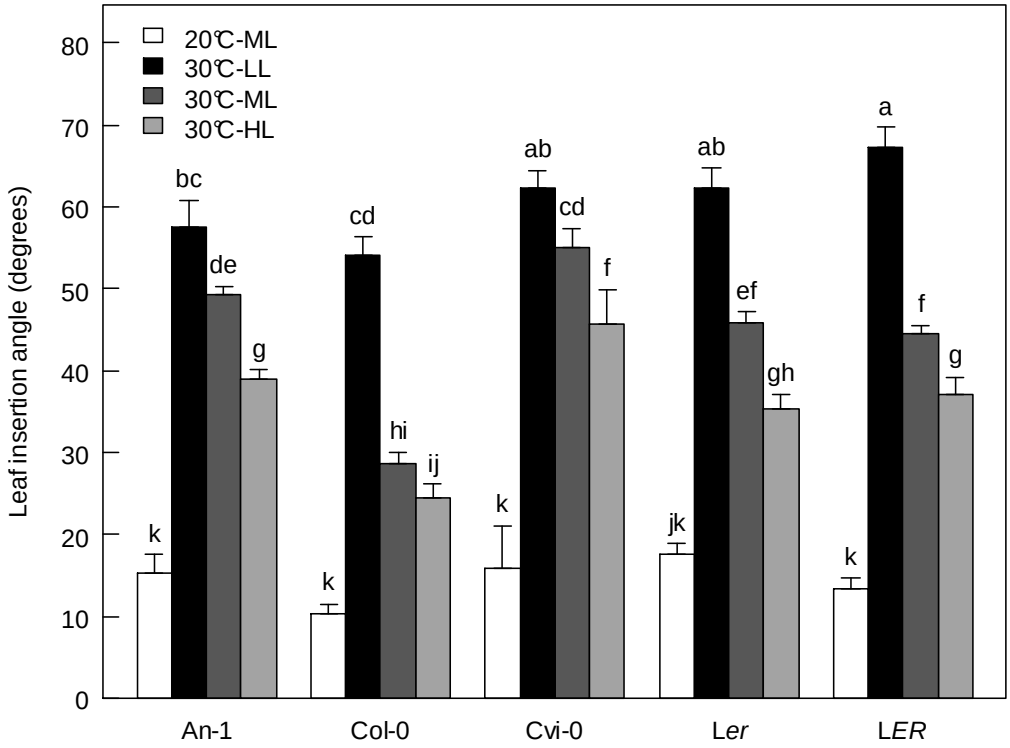

Figure 1. Hyponastic growth response to high temperature and light intensity of four Arabidopsis accessions and the complemented line at *ERECTA* (L*ER*). Leaf angle is the average of six values measured within two weeks after the beginning of light treatments on plants grown at 20 °C under moderate light intensity (ML, 175 µmol m^{-2} s^{-1}; white bars), and at high temperature (30 °C) under low (LL, 70 µmol m^{-2} s^{-1}; black bars), moderate (ML, 175 µmol m^{-2} s^{-1}; dark grey bars), and high light intensity (HL, 330 µmol m^{-2} s^{-1}; light grey bars). Bars are means ± SE (n = 6-10). Letters indicate significant differences following Kruskal-Wallis nonparametric test ($P < 0.05$).

Sugars and starch contents

Four samples containing two to four rosettes of Col-0, L*er* or *pgm* were harvested three days after the beginning of light treatments at the end of the day or night, and immediately frozen in liquid nitrogen. Starch and soluble sugars (as the sum of glucose, fructose, and sucrose) contents were analyzed by enzymatic assay as in Hummel et al. (2010).

Genes expression

Three hyponastically expanding leaves of Col-0 and L*er* grown at HT were harvested on four plants (stage 1.06) and immediately frozen in liquid nitrogen. A first harvest was performed in the middle of the morning, before any light treatment (t_0). Two subsequent harvests were performed 1 h (t_1) and 24 h (t_{24}) after light treatments. Another harvest was performed three days later at the end of the daytime or nighttime. RNA was isolated using NucleoSpin® RNA Plant (Macherey-Nagel, Düren, Germany). Reverse transcription and amplification of cDNA were performed as described in Table S4. Real-time quantification of target cDNA was performed in a LightCycler 480® (Roche, Penzberg, Germany) using specific primers (Table S4). Cycle threshold (Ct) values were determined by the fit point method. PCR efficiency (E) was deduced from a standard dilution series as E = -1/slope. Relative quantification was determined using the Delta Delta Ct method with E correction. Two reference genes (*CIPK23*, At1g30270; *TUB4*, At5g44340.1) were selected for normalization on the basis of their expression stability. Finally, all expression values at t_1 and t_{24} were normalized by the gene expression at t_0 (before any light treatment).

Statistical analyses

Genotype, temperature and light effects on traits were analyzed in ANOVAs and Kruskall-Wallis tests for multiple comparisons. Gene expression was analyzed in a hierarchical clustering analysis using Euclidean distances after log-transformation and plotted as a heatmap. A principal component analysis (PCA) was performed to study the relationships between traits, genotypes and environments. All statistical tests were performed using R 2.10 (R Development Core Team 2009).

Results

High temperature-induced hyponasty is modulated by light intensity

A strong HT-induced hyponasty, i.e. an increase in leaf insertion angle, was observed in all accessions and the complemented line L*ER* (Fig. 1). At the same light level (175 µmol m^{-2} s^{-1}), leaf angle was more than doubled at 30 °C compared to 20 °C, and varied significantly

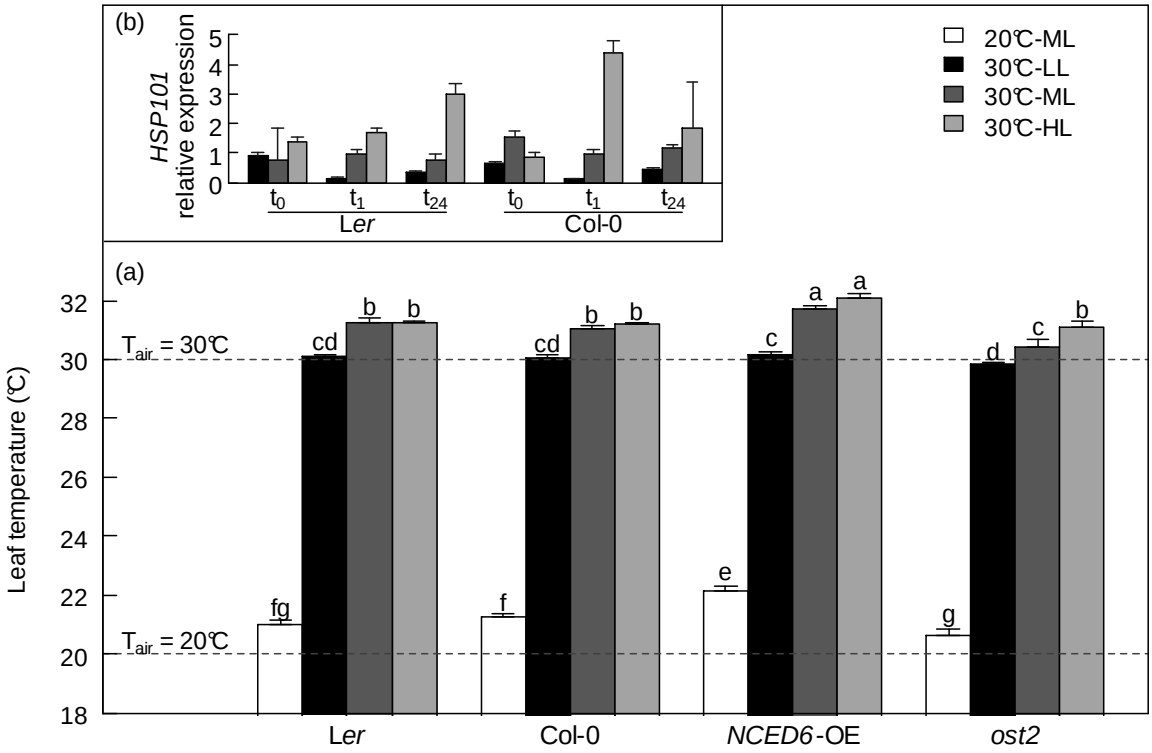

Figure 2. Leaf temperature sensing in response to temperature and light. (a) Surface temperature of hyponastic leaves measured by infra-red imaging in Col-0 and L*er* accessions, and two mutants impaired in stomata opening (*NCED6*-OE) and closing (*ost2*). Plants were grown at 20 °C under moderate light intensity (ML, 175 µmol m^{-2} s^{-1}; white bars), and at high temperature (30 °C) under low (LL, 70 µmol m^{-2} s^{-1}; black bars), moderate (ML, 175 µmol m^{-2} s^{-1}; dark grey bars), and high light intensity (HL, 330 µmol m^{-2} s^{-1}; light grey bars). Bars are means ± SE (n = 5-16). Letters indicate significant differences following Kruskal-Wallis nonparametric test (P < 0.05). (b) Expression of *HSP101* at HT at 0 h, 1 h and 24 h after light treatment. Plants were grown until emergence of leaf 6 at high temperature (30 °C) under ML and then transferred under LL, HL, or left under ML. Hyponastic leaves were harvested 1 h (t_1) and 24 h (t_{24}) after light treatment. Each expression was normalized according to t_0, *i.e.* before transfer under LL or HL.

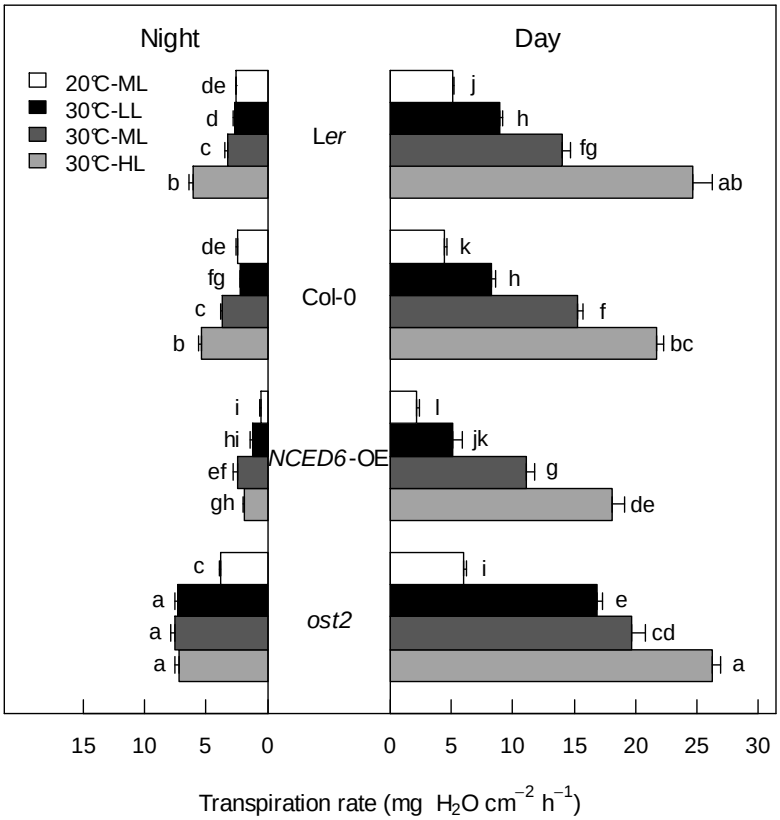

Figure 3. Night and day transpiration rates of Col-0 and L*er* accessions and of two mutants impaired in stomata opening (*NCED6*-OE) and closing (*ost2*). Transpiration was determined gravimetrically in plants at bolting stage grown at 20 °C under moderate light intensity (ML, 175 µmol m^{-2} s^{-1}; white bars), and at high temperature (30 °C) under low (LL, 70 µmol m^{-2} s^{-1}; black bars), moderate (ML, 175 µmol m^{-2} s^{-1}; dark grey bars), and high light intensity (HL, 330 µmol m^{-2} s^{-1}; light grey bars). Bars are means ± SE (n = 5-10). Letters indicate significant differences (P < 0.05) following Kruskal-Wallis nonparametric tests independently performed for night and day.

between genotypes (P < 0.001, Table 1) from 2.9-fold in Col-0 to 3.5-fold in Cvi-0. Remarkably, the HT-induced hyponasty was significantly increased under low light (LL, 70 µmol m^{-2} s^{-1}) in all genotypes, with Col-0 showing the highest response. Conversely, a significant decrease in HT-induced hyponasty was found under high light (HL, 330 µmol m^{-2} s^{-1}). On the other hand, the blade ratio tended to decrease in response to HT, particularly at LL (Table 1, Supporting Information Fig. S1f). These results clearly show that HT-induced hyponastic growth and the proportion of leaf blade are modulated by light levels.

Hyponasty does not coincide with leaf temperature

At HT, leaf temperature of Col-0 and L*er* was higher under HL and lower under LL compared to ML (Fig. 2a). Accordingly, after 1 h exposure to HL or LL, a strong transcriptional induction or repression, respectively, of the heat stress marker gene *Heat Shock Protein 101* (*HSP101*) was found in both accessions (Fig. 2b). This response was maintained after 24 h exposure to the light treatments. Therefore, exposure to HL induced a higher leaf temperature that superimposed with that of elevated air temperature but did not coincide with higher leaf angle.

To further rule out the hypothesis that leaf temperature solely determines the hyponastic response, we analyzed two mutants impaired in stomata opening and closing. As expected, the open (*ost2*) and closed (*NCED6*-OE) stomata mutants were respectively cooler and warmer compared to the wild-type Col-0 in the control irradiance level (Fig. 2a). Those differences were related to differences in transpiration rates significantly higher in *ost2* and lower in *NCED6*-OE (Fig. 3). In all genotypes, HT and HL induced a higher transpiration compared to control temperature (Fig. 3). Interestingly, in Col-0 and L*er*, this trend held true during day and night, despite the absence of heat gain from irradiance. However, this increase in latent heat dissipation through transpiration under HL was yet not sufficient to counterbalance the conjugated effects on leaf temperature of lower leaf angle and higher heat gain due to irradiance. Finally, leaf temperature did not positively correlate with leaf angle, neither within a given environment nor within a given genotype. Indeed, we observed that the hyponastic response of *NCED6*-OE and *ost2* did not differ significantly from Col-0 (P > 0.54, Fig. 4).

Hyponasty interplays with starch metabolism

Since leaf temperature was not the primary determinant of hyponasty and that LL worsened hyponasty, we investigated the involvement of carbon balance using a genetic manipulation. The *pgm* mutant, strongly impaired in starch synthesis (Caspar et al. 1985) showed a very different response compared to the wild-type Col-0. This mutant not only

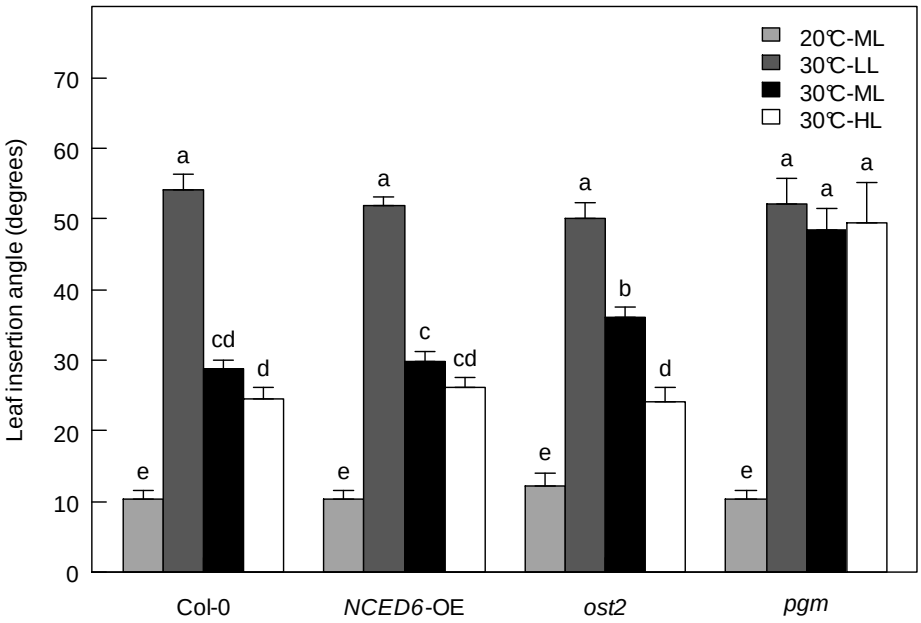

Figure 4. Leaf insertion angle of the wild-type Col-0 and mutants impaired in stomata opening (*NCED6*-OE) and closing (*ost2*), and in starch synthesis (*pgm*). Leaf angle is the average of six values measured within two weeks after the beginning of light treatments on plants grown at 20 °C under moderate light intensity (ML, 175 µmol m^{-2} s^{-1}; white bars), and at high temperature (30 °C) under low (LL, 70 µmol m^{-2} s^{-1}; black bars), moderate (ML, 175 µmol m^{-2} s^{-1}; dark grey bars), and high light intensity (HL, 330 µmol m^{-2} s^{-1}; light grey bars). Bars are means ±SE (n = 6-10). Letters indicate significant differences following Kruskal-Wallis nonparametric test ($P < 0.05$).

displayed a significantly steeper leaf angle than Col-0 under HT (Fig. 4; Table 1) but light level had also no significant effect on its HT-induced hyponastic response. Consistent with previous studies (Gibon et al. 2004a), the starchless (Fig. 5c,d) *pgm* mutant displayed a significantly higher sugar concentration at the end of the day compared to Col-0 whatever the growth condition (Fig. 5a). Sugar contents at the end of the night were similarly low between *pgm* and Col-0, though significantly different under ML (Fig. 5b). The tight link between carbon metabolism and HT-induced hyponasty evidenced by the *pgm* mutant prompted us to further investigate the involvement of carbon balance in plant responses to HT.

Light modulates the deleterious effects of high temperature on carbon status

Since increasing incident light intensity reverted HT-induced hyponasty and *pgm* mutant had altered responses, we hypothesized that leaf carbon status could be a good candidate to unify both LL- and HT-induced responses. Changes in carbon assimilation and status induced by variations in temperature and light were thus investigated. Overall, plants under HT accumulated less carbohydrates during the day and were more carbon-depleted at the end of night, while HL restored the contents encountered at the control temperature (Fig. 5). Although LL did not affect significantly sugar concentration under HT, starch content was significantly lower.

Net photosynthetic rate was significantly reduced by HT in Col-0 but not in L*er* (Fig. 6a), while dark respiration was not significantly affected by HT in both accessions. Not surprisingly, net photosynthesis increased with light intensity in both accessions. PSII yield capacity, as evaluated by chlorophyll fluorescence (Fv/Fm), was reduced at HT in both accessions, whereas increasing light intensity led to a recovery of Fv/Fm levels close to those encountered in control conditions in Col-0 (Fig. 6b). Although increasing light caused a slight increase in leaf temperature, a shift from 70 to 330 µmol m^{-2} s^{-1} PAR was sufficient to balance and even abolish the negative effects of HT on net carbon assimilation and PSII quantum efficiency.

The carbon status of the plants under HT was also investigated through the expression of specific marker genes (Blasing et al. 2005). *DIN10* and *DIN6* (Fujiki et al. 2001) and *TPS8* (Hummel et al. 2010) were selected as markers of carbon limitation, whilst *CPN60A* and *CPN60B* (Hummel et al. 2010) were used as markers of high carbon supply. Dynamics of relative transcript abundance of each gene were compared to the levels encountered at the end of the day or night. These latter stages have been well-described as bringing the rosette to a high and low sugar status, respectively (Gibon et al. 2004b).

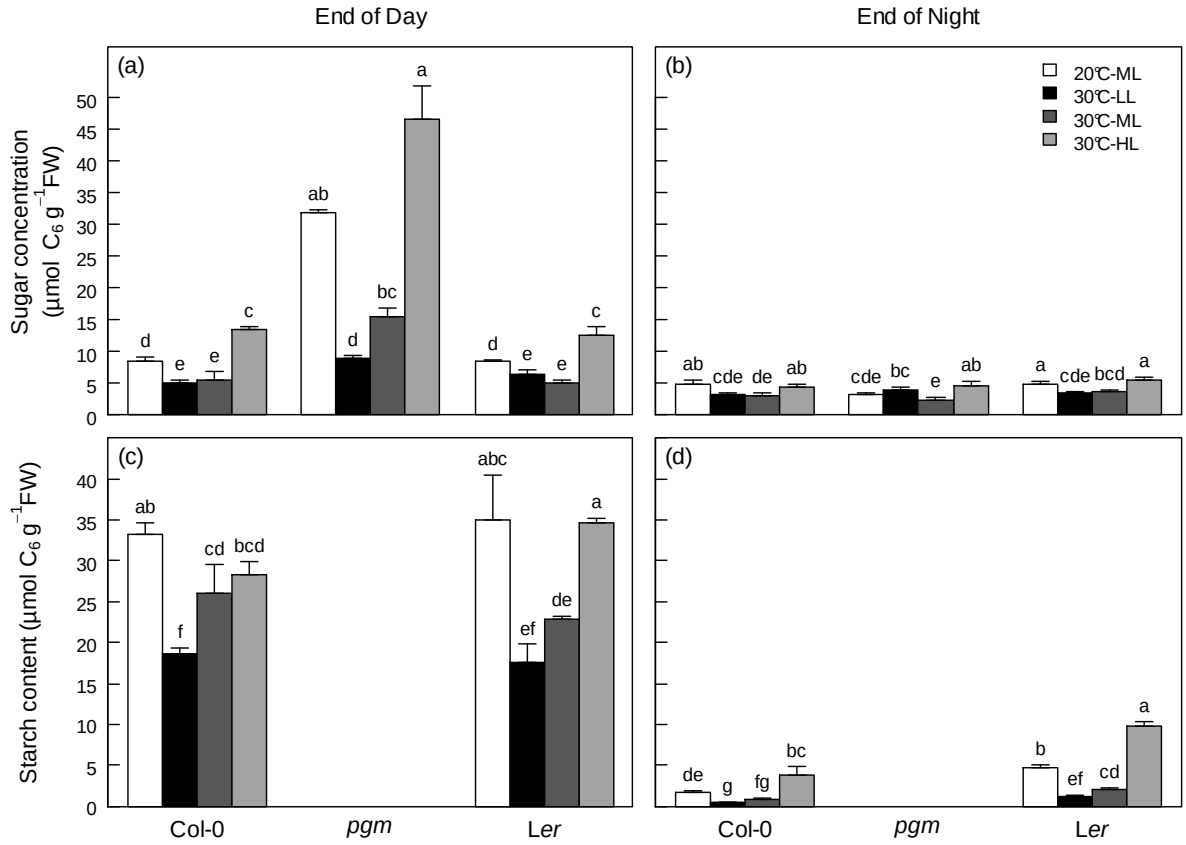

Figure 5. Sugar and starch contents of the Col-0 and L*er* accessions, and the starch deficient mutant *pgm* in response to temperature and light. Plants were grown at 20 °C under moderate light intensity (ML, 175 µmol m^{-2} s^{-1}; white bars), and at high temperature (30 °C) under low (LL, 70 µmol m^{-2} s^{-1}; black bars), moderate (ML, 175 µmol m^{-2} s^{-1}; dark grey bars), and high light intensity (HL, 330 µmol m^{-2} s^{-1}; light grey bars). Sugar concentration (a, b) and starch content (c, d) were determined 3 days after the beginning of light treatments, at the end of the day and at the end of the night, respectively. Sugar concentration is the sum of sucrose, glucose and fructose. Sugar and starch contents are expressed in C_6 equivalents. Bars are means ± SE (n = 4). Letters indicate significant differences following Kruskal-Wallis nonparametric test ($P < 0.05$). No detectible levels of starch were found in *pgm*.

As indicated by the proximity of Col-0 and L*er* in the clustering, the genotypic effect on the expression of all genes was negligible under all environmental conditions (Fig. 7). As expected, *DIN10*, *DIN6* and *TPS8* were enhanced and CPN60A and CPN60B were repressed at the end of the night when carbon is limiting, whilst the opposite trend was true at the end of the day (Fig. 7). Therefore, these genes can reasonably be used as indicators of leaf carbon status. Within 1 h following changes in light conditions, the expression of genes indicative of high carbon supply was clearly repressed under LL and enhanced under HL. On the other hand, the expression of genes indicative of carbon limitation was strongly enhanced 1 h after exposure to LL and after 24 h, yet to a lesser extent. The reverse was true under HL. Overall, transcript levels under LL mimicked those encountered at the end of the night whereas under HL these levels resembled those encountered at the end of the day.

In summary, results at the metabolic, photosynthetic, and transcriptional levels converge to indicate that carbon status is significantly impaired under HT but can be improved by increasing light intensity, whilst reducing light intensity leads to a worsened carbon balance.

Interaction between high temperature and light on growth: a multi-scale analysis of plant traits

Our data clearly indicated that HT and light interact in the regulation of leaf hyponasty and carbon status. We therefore extended our analysis to other growth-related traits. A PCA was performed on morphological and anatomical traits from the cellular to the leaf and whole-plant levels measured in the four accessions Col-0, Cvi-0, An-1, L*er* and the complemented line L*ER* (Table 1, Fig. 8 and Supporting Information Fig. S1). The complemented line L*ER* was included in the analysis since no detectible effect of *ERECTA* was found to modify the interpretation of the results. For instance, no significant difference in the hyponastic response to both temperature and light was found between L*er* and L*ER* (Fig. 1a; Table S2; Supporting Information Fig. S1f). However, L*er* was characterized by high epidermal cell density which was significantly decreased in L*ER* (Supporting Information Fig. S1g), as expected (Masle et al. 2005, Tisné et al. 2010). L*ER* also exhibited a marginally significant weaker leaf angle than L*er* at 20 °C, and a lower leaf blade ratio whatever the environmental condition (Table S2 and Supporting Information Fig. S1f).

The first and second principal components (PC) explained 53% and 17% of the total variance, respectively. PC1 was positively correlated with leaf angle and specific leaf area, and negatively correlated with total fresh weight, leaf number, leaf thickness, leaf dry matter content, stomatal index and blade ratio (Fig. 8a; Table S2 for loadings). PC2 was mainly

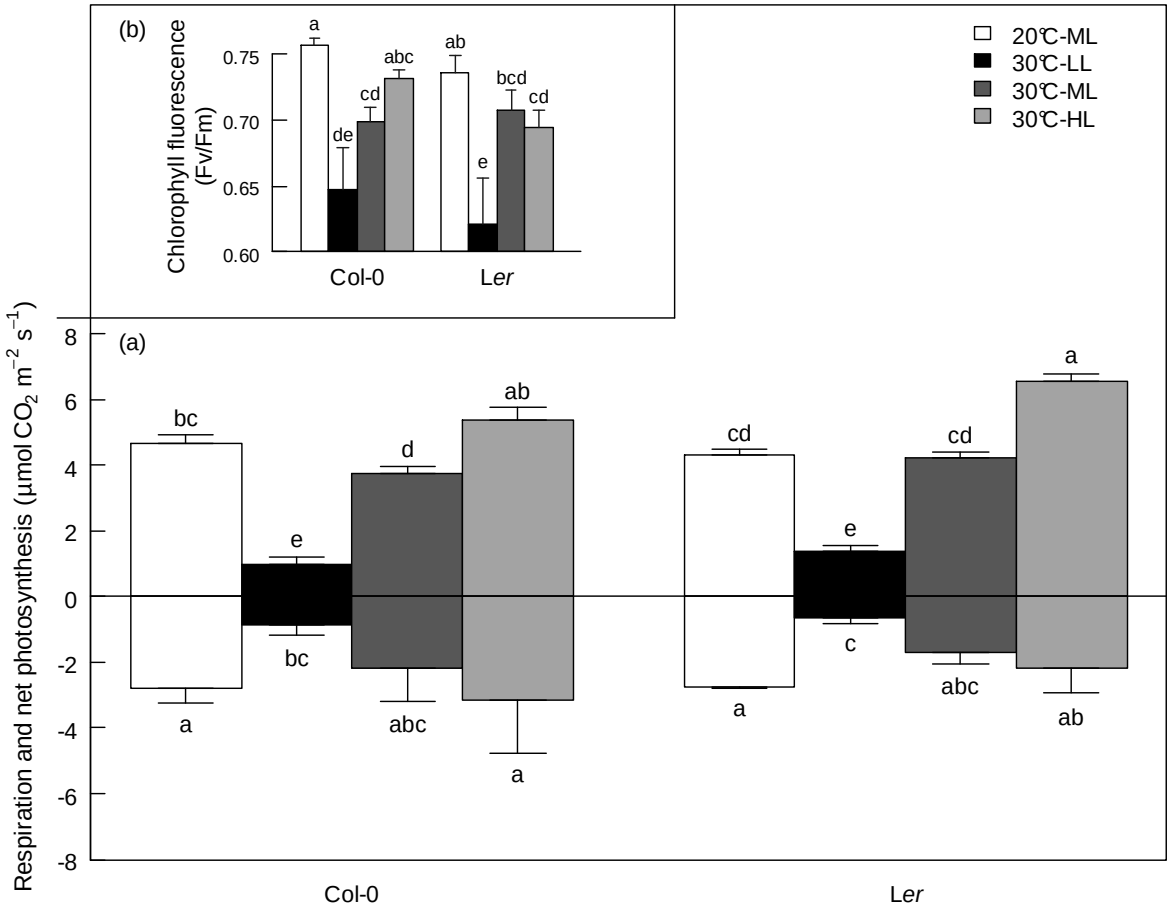

Figure 6. Photosynthetic performance of Col-0 and L*er* accessions acclimated to contrasted temperature and light conditions. (a) Net photosynthetic rate and dark respiration. (b) PSII yield capacity estimated by chlorophyll fluorescence. CO_2 fluxes and chlorophyll fluorescence after dark adaptation were measured in ambient conditions at 20 °C under moderate light intensity (ML, 175 µmol m^{-2} s^{-1}; white bars), and at high temperature (30 °C) under low (LL, 70 µmol m^{-2} s^{-1}; black bars), moderate (ML, 175 µmol m^{-2} s^{-1}; dark grey bars), and high light intensity (HL, 330 µmol m^{-2} s^{-1}; light grey bars). Bars are means ±SE (n = 7-11 for CO_2 flues, n = 3-5 for fluorescence). Letters indicate significant differences following Kruskal-Wallis nonparametric test ($P < 0.05$).

explained by vegetative stage duration. Epidermal cell density was poorly represented on the first two PCs but explained the main proportion of PC3.

Projection of individuals revealed significant effects of temperature and light ($P < 0.001$, ANOVA on PC coordinates; Fig. 8b). More interestingly, PC1 discriminated the individuals in a consistent way according to the environment, with a strong effect of HT under LL and a progressive recovery with increasing light intensity (Fig. 8b). Not only this gradient was represented by the hyponastic response as previously characterized, but it was also explained by an increase in specific leaf area and a decrease in plant fresh mass, leaf thickness, leaf dry matter content, and stomatal index. HT caused the production of thinner leaves, but increasing light intensity allowed plants to re-allocate assimilates into thicker and denser leaves. By contrast, reducing light intensity amplified the effects of HT observed on leaf structure. HT significantly reduced plant size, but increasing light intensity resulted in larger plants (Supporting Information Fig. S1). The same trend held true for the other traits on PC1. Within the groups discriminated by the temperature and light treatments, individuals were mainly separated by vegetative stage duration on PC2 and a composite axis represented by rosette fresh weight and cell density but to a lesser extent. This discrimination was driven by a significant genotype effect (Table 1). For instance, An-1 had significantly smaller rosette and shorter vegetative duration than Col-0 or Cvi-0. Despite some differences in plant size, very similar responses to the treatments were found in the 'open' (*ost2*) and the 'closed stomata' (*NCED6*-OE) mutants compared to the wild-type Col-0. In addition to its contrasted hyponastic response, *pgm* was significantly smaller than Col-0 and displayed a clear delay in flowering.

Overall, our results show that increasing light intensity under HT not only restores leaf angle close to levels encountered under control temperature, but also restores many others traits related to leaf structure, plant growth and development.

Discussion

High temperature and low light-induced hyponasty: does the same consequence arise from the same cause?

A high temperature (HT) of 30 °C induced hyponastic growth in all Arabidopsis accessions we investigated here. This response was significantly increased under low light (LL, 70 µmol m^{-2} s^{-1}), which is consistent with previous findings at 38 °C and light intensity < 20 µmol m^{-2} s^{-1} (Millenaar et al. 2005, Van Zanten et al. 2009). Remarkably, we found that

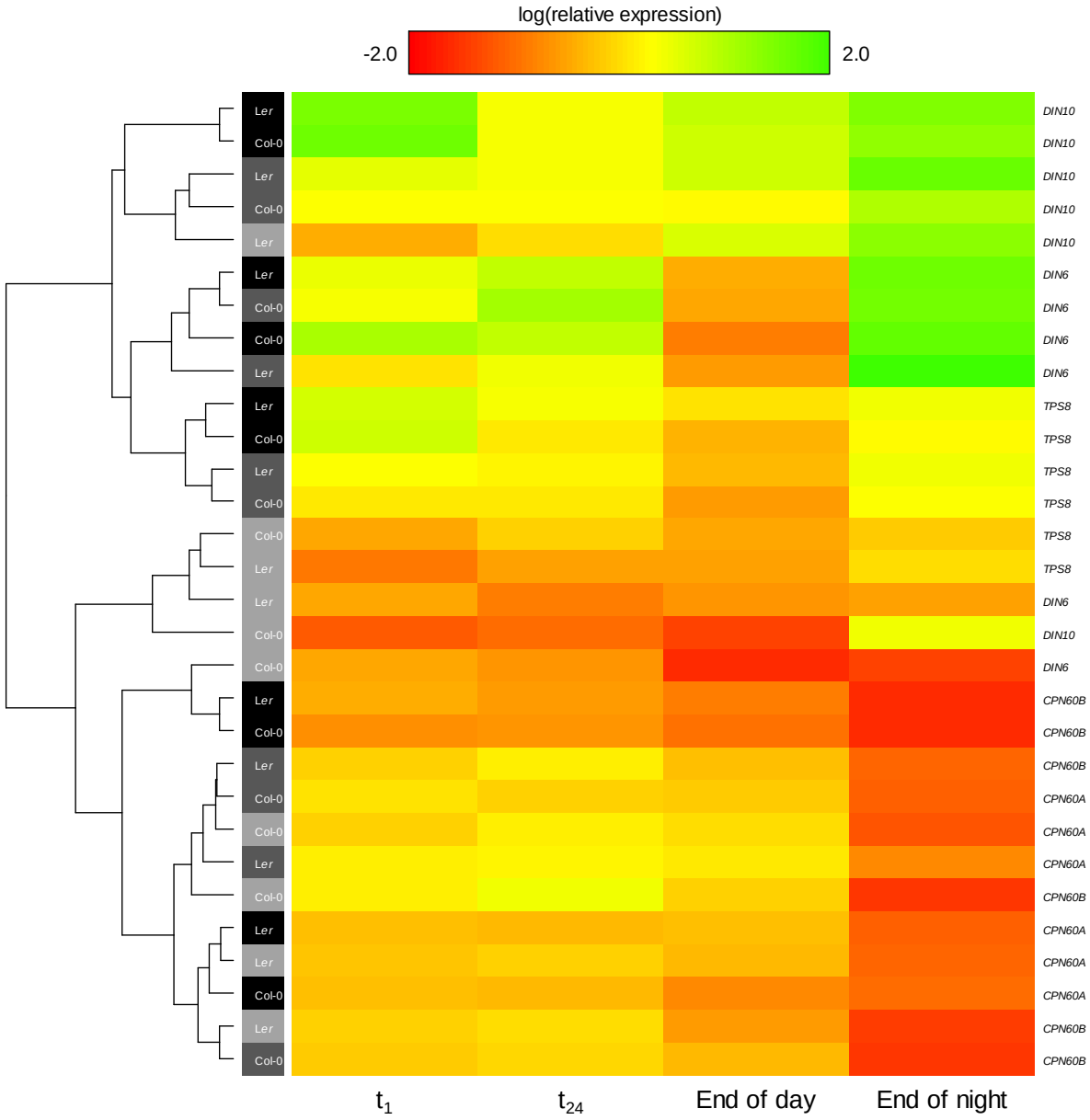

Figure 7. Expression of marker genes of carbon starvation of Col-0 and Ler accessions grown at high temperature under contrasting light intensities. Overlay heat map showing expression levels of genes induced (*DIN6*, *DIN10*, *TPS8*) or repressed (*CPN60A*, *CPN60B*) by carbon starvation in plants grown until emergence of leaf 6 at high temperature (30 °C) under moderate light intensity (ML, 175 µmol m^{-2} s^{-1}) and then transferred under low light intensity (LL, 70 µmol m^{-2} s^{-1}; black boxes of the left side bar), high light intensity (HL, 330 µmol m^{-2} s^{-1}; light grey boxes of the left side bar), or kept under ML (dark grey boxes of the left side bar). Hyponastic leaves were harvested 1 h (t_1) and 24 h (t_{24}) after light treatment. Two days after beginning of light treatments, plants were harvested at the end of the day and night. Each box represents the effect of change in light intensity on relative expression level of each marker gene identified on the right side. Level values are log-transformed values. The dendrogram represents the proximity between each gene expression pattern, as calculated from a hierarchical clustering analysis using Euclidean distances after log-transformation**.**

high light (HL) reversed the effects of HT on hyponasty, leading to leaf angle values similar to those encountered under control temperature (20 °C).

Different hypotheses may explain the interacting effects of HT and light on leaf angle. HT-induced hyponasty could be triggered by leaf temperature itself, contributing to leaf cooling by (*i*) decreasing incoming radiant heat (Fu and Ehleringer 1991, Falster and Westoby 2003), (*ii*) decreasing conductive and radiative heat transfer by moving the leaf away from the heated soil as suggested by Gray et al. (1998) for hypocotyl elongation, and (iii) increasing transpiration through an increased boundary layer conductance. Here, the HT-induced hyponastic responses of two mutants impaired in stomata closure (*ost2*) and opening (*NCED6*-OE) were not different from that of the wild-type, although these mutants had respectively cooler and warmer leaves due to differential transpiration (Merlot et al. 2002, Lefebvre et al. 2006). Furthermore, under HL leaves were warmed by 1.1 °C despite a higher transpiration rate and lower insertion angles than leaves under low and moderate irradiance. Leaf warming was confirmed by the induction of *HSP101* which acts as a virtual thermometer (Young et al. 2001). If leaf temperature was the only trigger of HT-induced hyponasty, increasing light would have led to increased hyponasty. Our results clearly rule out this assumption pointing towards other possible roles of light in hyponasty.

Several studies reported a role for photoreceptors in hyponasty under LL- (Somers et al. 1991, Robson et al. 1993, Morelli and Ruberti 2002, Vandenbussche et al. 2005, Mullen et al. 2006, Millenaar et al. 2009) and HT (Koini et al. 2009, Van Zanten et al. 2009). However, while hyponasty is delayed in photoreceptor mutants during the first hours following HT or LL treatments, a response similar to the wild-type was observed afterward (Van Zanten et al. 2009). Millenaar *et al.* (2009) also found that a prolonged exposure to LL led to hyponastic growth induction even in multiple loss-of-function photoreceptor mutants. Here, leaf angles were measured during two weeks after the beginning of light treatments, i.e. after the recovery period of hyponasty in the photoreceptor mutants described in Van Zanten et al. (2009), therefore excluding a major role for photoreceptors in the patterns observed.

Sugars act both as signal and carbon supply for several plant processes, including differential petiole-to-blade leaf growth (Kozuka et al. 2005). Previous studies have also shown that regulators of starch metabolism or derived signals are integrators of plant metabolism and growth (Sulpice et al. 2009). Here, we found that changes in leaf inclination following changes in light level fitted in a consistent way with leaf carbon status, as measured by sugar and starch contents. Specifically, starch content and leaf angle were negatively correlated along the environmental conditions (Supporting Information Fig. S3). Moreover,

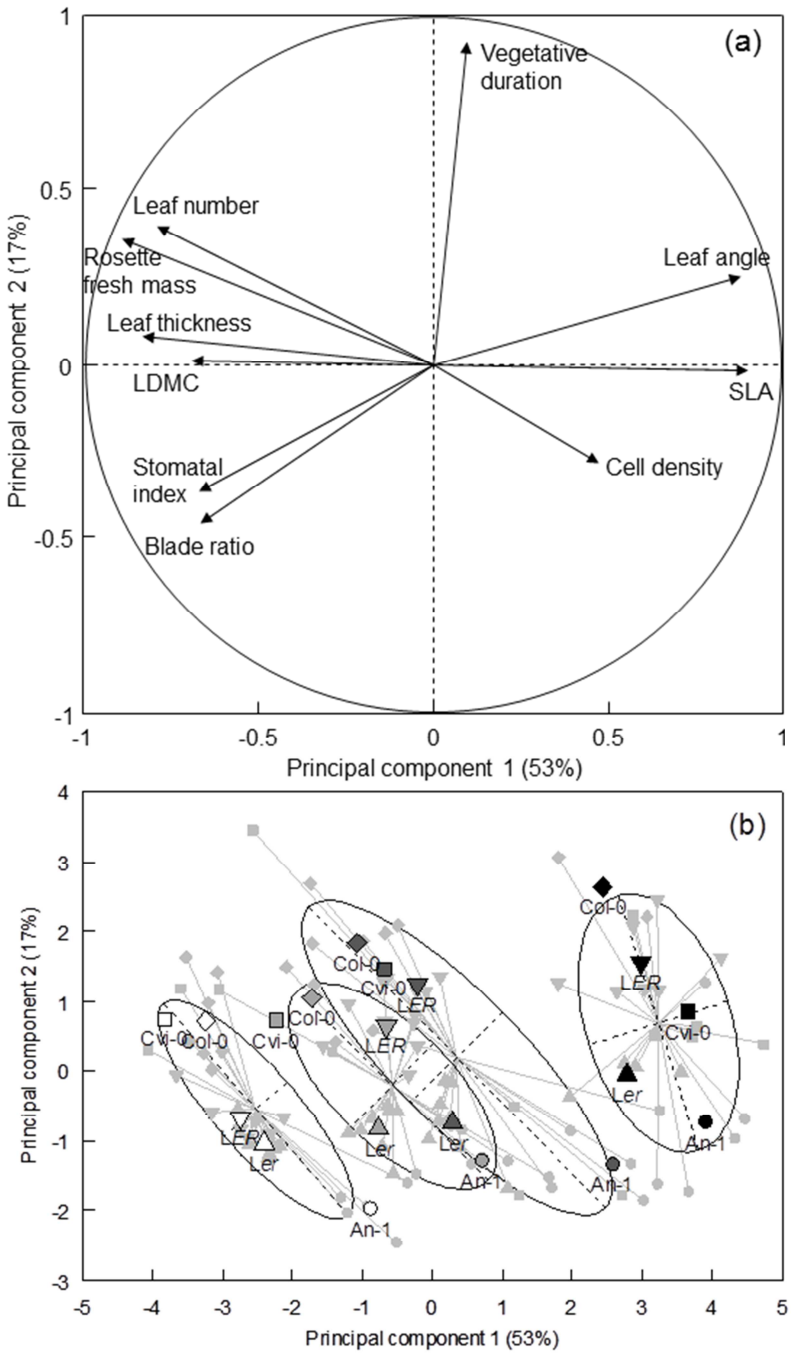

Figure 8. Principal component analysis on multiple plant traits measured on Arabidopsis accessions in contrasted temperature and light treatments. The first two axes are shown which account for 70% of the total inertia. (a) Projection of the variables. (b) Projection of individual plants (grey symbols) and centers of gravity for each treatment and each accession (An-1, circles; Col-0, diamonds; Cvi-0, squares; L*er*, triangles; L*ER*, upside-down triangles). Plants were grown at 20 °C under moderate light intensity (ML, 175 µmol m^{-2} s^{-1}; white symbols), and at high temperature (30 °C) under low (LL, 70 µmol m^{-2} s^{-1}; black symbols), moderate (ML, 175 µmol m^{-2} s^{-1}; dark grey symbols), and high light intensity (HL, 330 µmol m^{-2} s^{-1}; light grey symbols). LDMC: leaf dry matter content; SLA: specific leaf area.

constitutive HT-induced hyponasty was found in *pgm*, a starch deficient mutant whose diurnal physiological state resembles that of a wild-type plant exposed to an extended night (Gibon et al. 2004a). Provided that HT and LL induce carbon starvation, this could explain why a prolonged exposure of the wild-type to these environments led to a similar response than that of *pgm*. Millenaar et al. (2009) also reported that a pharmacological inhibition of the photosynthetic electron transport chain induced hyponasty under non-inducing light intensity and control temperature. Expression patterns of genes related to carbon status were in agreement with a possible role of carbon status on hyponasty. They also revealed that plants sense a carbon limiting environment largely before they really experience carbon depletion. In Arabidopsis, diurnal changes in leaf angle are negligible regarding to the changes in leaf angle (Mullen et al. 2006) due to the environment, but they follow the diurnal pattern of carbohydrate availability and starch content which are tightly linked to the circadian clock (Blasing et al. 2005, Graf et al. 2010). Indeed, leaf inclination is enhanced at night, when carbon supply relies on starch, and reduced at dawn when photosynthesis resumes. Overall, changes in carbon metabolism could be a common signal of both LL- and HT-induced hyponasty, with sugars or starch degradation products acting either as a primary signal or in a parallel pathway following exposure to unfavorable growth conditions.

The possible role of carbon status in hyponasty does not preclude a molecular crosstalk with hormonal and photocontrol regulation. Here, no significant changes in transcript levels of genes related to ethylene biosynthesis or signaling were found (data not shown), in agreement with Millenaar et al. (2009) under LL and Van Zanten et al. (2009) at HT. In these alternative pathways, ETHYLENE-INSENSITIVE 3 (EIN3), could be the receptor of ethylene signaling linking ethylene-induced hyponasty and sugars, given that EIN3 is degraded in presence of glucose in interaction with light (Yanagisawa et al. 2003, Lee et al. 2006) and cooperates with the PHYTOCHROME INTERACTING FACTOR 1 (PIF1) to prevent photo-oxidation and promote greening (Zhong et al. 2009). PIF4, function of which is important in both LL- (Cole et al. 2011) and HT-induced hyponasty (Koini et al. 2009), appears also as a candidate in the crosstalk between carbon status and phytochrome pathways.

Our results support the view that the primary cause of leaf hyponasty under moderately HT is related to the shade-avoidance syndrome and suggest that leaf temperature and transpiration *per se* have a minor role in this response. HT-induced hyponasty is therefore likely part of plant response selected to counteract carbon starvation rather than leaf warming itself.

Plant responses to high temperature mimic a carbon starvation

In addition to the effects of HT on hyponasty, our results show that its deleterious effects on plant growth are partially abolished with increasing light intensity. As shown for hyponasty, we hypothesized that HT-induced responses reflect an altered plant carbon status that may be counteracted by light intensity, at least for a moderately increased temperature.

There are several reasons why plants under elevated temperature would be carbon-limited. For instance Morison and Lawlor (1999) showed that assimilate demand could be increased while photosynthetic capacity becomes limited in warm conditions. Kinetics of numerous plant processes are known to increase with temperature until an optimum above which rates strongly decrease before lethality (Jacobs and Pearson 1999, Gillooly et al. 2001, Parent et al. 2010). Accordingly, this study provides evidences that leaf heating is associated to an unbalanced carbon supply/demand. As indicated by sugar and starch contents, plant carbon status under HT was significantly impaired. Furthermore, the induction of heat response genes such as *HSP101* and associated downstream metabolic pathways suggests that higher carbon allocation to maintenance was required under HT. This net carbon loss translated into reduced structural growth as indicated by lower leaf dry matter content and thickness and higher specific leaf area at HT (Chabot and Chabot 1977, Atkin et al. 2006; Fig. 8). Hence, it is not surprising that plant tolerance to HT was increased at higher CO_2 concentration (Huxman et al. 1998, Albert et al. 2011).

Here, we demonstrated that plant carbon status under HT was also significantly improved with increasing irradiance. This was indicated by an increase in sugar and starch contents, and the expression of specific marker genes. High light counterbalanced the deleterious effects of HT on net photosynthesis and PSII quantum efficiency, although higher light intensity induced higher leaf temperature, higher *HSP101* expression and a slight increase in respiration rate. A global recovery of HT damages was found with increasing light intensity whereas they were worsened under LL. As a result, plants grown at 30 °C under high light were bigger and morphologically more similar to plants grown at 20 °C but under moderate light intensity.

Furthermore, changes in many plant traits observed in response to HT were similar to changes associated with the shade-avoidance syndrome. For instance, hyponastic leaf growth and blade ratio decreases are typical responses to HT and LL (Gray et al. 1998, Tsukaya et al. 2002, Franklin and Whitelam 2005, Koini et al. 2009, Van Zanten et al. 2009, Heydarian et al. 2010, Van Zanten et al. 2010b). Several other changes in leaf and whole-plant traits are related to shading. Leaf structure is strongly altered by light intensity and leaves developed in

LL are thinner and tender, which can result in a better light harvesting (Chabot and Chabot 1977, Yano and Terashima 2001, Kim et al. 2005). These changes are well represented by the variations in specific leaf area (Witkowski and Lamont 1991, Poorter et al. 2009) which further increased under LL. Interestingly, increasing light at HT restored specific leaf area values close to the control values (Supporting Information Fig. S1). By increasing density of photosynthetic tissues (Hassiotou et al. 2010) together with lower leaf angle (i.e. higher light interception), side effects of HL could act synergistically to enhance net carbon gain under HT. Consistently, Foreman et al. (2011) have shown that light receptor action is critical for maintaining plant biomass at warm temperatures.

Flowering was delayed at HT and LL, in association with a decrease in leaf production rate (see also Mendez-Vigo et al. 2010). This contrasts with studies reporting that shade-avoidance and HT accelerate flowering in Arabidopsis (Devlin et al. 1999, Sparks et al. 2000, Botto and Smith 2002), but no data are available on their interactive effect. Our results are however in accordance with the negative effects of LL on Arabidopsis developmental rate under control temperature (Chenu et al. 2005), and could be interpreted as a symptom of decreased carbon availability under LL, since flowering is a major carbon sink (Christophe et al. 2008). In agreement, flowering time was clearly delayed in the starch deficient mutant *pgm* (Supporting Information Fig. S2), irrespectively of the light conditions; in line with a disturbed carbon balance (Corbesier et al. 1998).

Natural variability and ecological consequences of temperature and light interactions

Plants have to manage a trade-off between improvement of photosynthesis with a higher light interception and limitation of radiant heat gain. This trade-off is a typical issue that a plant could encounter under a shaded, warm canopy – an environment highly competitive for carbon fixation. Indeed, phenotypic plasticity to light and temperature is an important trait for plants to achieve carbon assimilation and growth (Kim et al. 2005, Atkin et al. 2006), while plasticity in response to light can be considered as an adaptive response determining competitive ability in a plant canopy (Dorn and Mitchellolds 1991, Schmitt 1997). In Arabidopsis, Van Zanten et al. (2009) suggested that HT-induced hyponasty is an adaptive response since it is negatively correlated to diurnal temperature range at the accession collection site. Here, variation between accessions was large enough to highlight the possibility for natural selection to act on the syndrome of traits described in this study.

Incident light levels used in this study were relatively low compared to those encountered in natural conditions, or to those that induce profound changes in the

photosynthetic machinery (Bailey et al. 2001). Here, increasing PAR from 175 to 330 µmol m^{-2} s^{-1} appeared sufficient to counterbalance the negative effects of a 10 °C elevation of air temperature. The results found here should stand up to light levels that induce photosystem breakdown or until damages due to heat gain from radiation become predominant over the improvement of photosynthesis. Whether HT-induced hyponasty would be observed in such conditions is still an open question. Further, as also suggested by Morison and Lawlor (1999), the results presented here warn us that the low levels of light used in many laboratory experiments testing the effects of HT may have altered the genuine response induced by HT. Nonetheless, hyponasty and subsequent changes in plant growth and development could be key traits conditioning plant performance under competition for light, particularly in a warming world.

Conclusion

Deleterious effects of HT on plants have been extensively studied but few reports have taken into account the interacting effect of light intensity to interpret the observed responses. Here, we demonstrated that light strongly interacts with plant responses to HT by modulating its carbon balance. Temperature elevation induce a decrease in carbon assimilation and an increase in assimilate demand due to the over-activation of certain molecular and physiological processes. These energetically costly pathways would modify the carbon balance which is respectively worsened under low light and restored with increasing light intensity. Because the dose-response to combined light and temperature varies between genotypes and between species, it is likely to play a key role in plant strategies and community dynamics.

Acknowledgements

We thank Christine Granier, Bertrand Muller and Matthew Hannah for comments on the manuscript; Myriam Dauzat, Alexis Bediee, Crispulo Balsera, Phillippe Clair and Gaëlle Rolland for help during the experiments. FV was funded by a CIFRE grant (ANRT, French Ministry of Research) supported by BAYER Crop Science (contract 0398/2009 - 09 42 008). FP was funded by French Ministry of Research.

References

Albert, K. R., H. Ro-Poulsen, T. N. Mikkelsen, A. Michelsen, L. van der Linden, and C. Beier. 2011. Effects of elevated CO_2, warming and drought episodes on plant carbon uptake in a temperate heath ecosystem are controlled by soil water status. Plant, Cell and Environment **34**:1207-1222.

Atkin, O. K., B. R. Loveys, L. J. Atkinson, and T. L. Pons. 2006. Phenotypic plasticity and growth temperature: understanding interspecific variability. Journal of Experimental Botany **57**:267-281.

Bailey, S., R. G. Walters, S. Jansson, and P. Horton. 2001. Acclimation of *Arabidopsis thaliana* to the light environment: the existence of separate low light and high light responses. Planta **213**:794-801.

Berry, J. and O. Björkman. 1980. Photosynthetic response and adaptation to temperature in higher plants. Annual Review of Plant Physiology **31**:491-543.

Blasing, O. E., Y. Gibon, M. Gunther, M. Hohne, R. Morcuende, D. Osuna, O. Thimm, B. Usadel, W.-R. Scheible, and M. Stitt. 2005. Sugars and circadian regulation make major contributions to the global regulation of diurnal gene expression in Arabidopsis. The Plant Cell **17**:3257-3281.

Botto, J. F. and H. Smith. 2002. Differential genetic variation in adaptive strategies to a common environmental signal in Arabidopsis accessions: phytochrome-mediated shade avoidance. Plant Cell and Environment **25**:53-63.

Boyes, D. C., A. M. Zayed, R. Ascenzi, A. J. McCaskill, N. E. Hoffman, K. R. Davis, and J. Görlach. 2001. Growth stage-based phenotypic analysis of Arabidopsis: a model for high throughput functional genomics in plants. The Plant Cell **13**:1499-1510.

Caspar, T., S. C. Huber, and C. Somerville. 1985. Alterations in growth, photosynthesis, and respiration in a starchless mutant of *Arabidopsis thaliana* (L.) deficient in chloroplast phosphoglucomutase activity. Plant Physiology **79**:11-17.

Chabot, B. F. and J. F. Chabot. 1977. Effects of light and temperature on leaf anatomy and photosynthesis in *Fragaria vesca*. Oecologia **26**:363-377.

Chenu, K., N. Franck, J. Dauzat, J. Barczi, H. Rey, and J. Lecoeur. 2005. Integrated responses of rosette organogenesis, morphogenesis and architecture to reduced incident light in *Arabidopsis thaliana* results in higher efficiency of light interception. Functional Plant Biology **32**:1123-1134.

Christophe, A., V. Letort, I. Hummel, P. Cournède, P. de Reffye, and J. Lecœur. 2008. A model-based analysis of the dynamics of carbon balance at the whole-plant level in *Arabidopsis thaliana*. Functional Plant Biology **35**:1147-1162.

Cole, B., S. A. Kay, and J. Chory. 2011. Automated analysis of hypocotyl growth dynamics during shade avoidance in Arabidopsis. The Plant Journal **65**:991-1000.

Corbesier, L., P. Lejeune, and G. Bernier. 1998. The role of carbohydrates in the induction of flowering in *Arabidopsis thaliana*: comparison between the wild type and a starchless mutant. Planta **206**:131-137.

Devlin, P. F., P. R. H. Robson, S. R. Patel, L. Goosey, R. A. Sharrock, and G. C. Whitelam. 1999. Phytochrome D acts in the shade-avoidance syndrome in Arabidopsis by controlling elongation growth and flowering time. Plant Physiology **119**:909-916.

Dorn, L. A. and T. Mitchellolds. 1991. Genetics of *Brassica-Campestris* .1. Genetic constraints on evolution of life-history characters. Evolution **45**:371-379.

Falster, D. S. and M. Westoby. 2003. Leaf size and angle vary widely across species: what consequences for light interception? New Phytologist **158**:509-525.

Foreman, J., H. Johansson, P. Hornitschek, E.-M. Josse, C. Fankhauser, and K. J. Halliday. 2011. Light receptor action is critical for maintaining plant biomass at warm ambient temperatures. The Plant Journal **65**:441-452.

Franklin, K. A. 2010. Light and temperature signal crosstalk in plant development. XVIII Congress of the Federation of European Societies of Plant Biology (FESPB).

Franklin, K. A. and G. C. Whitelam. 2005. Phytochromes and shade-avoidance responses in plants. Annals of Botany **96**:169-175.

Fu, Q. A. and J. R. Ehleringer. 1989. Heliotropic leaf movements in common beans controlled by air temperature. Plant Physiology **91**:1162-1167.

Fu, Q. A. and J. R. Ehleringer. 1991. Modification of paraheliotropic leaf movement in *Phaseolus vulgaris* by photon flux density. Plant Cell and Environment **14**:339-343.

Fujiki, Y., Y. Yoshikawa, T. Sato, N. Inada, M. Ito, I. Nishida, and A. Watanabe. 2001. Dark-inducible genes from *Arabidopsis thaliana* are associated with leaf senescence and repressed by sugars. Physiologia Plantarum **111**:345-352.

Gibon, Y., O. E. Blaesing, J. Hannemann, P. Carillo, M. Höhne, J. H. M. Hendriks, N. Palacios, J. Cross, J. Selbig, and M. Stitt. 2004a. A robot-based platform to measure multiple enzyme activities in Arabidopsis using a set of cycling assays: comparison of changes of enzyme activities and transcript levels during diurnal cycles and in prolonged darkness. The Plant Cell **16**:3304-3325.

Gibon, Y., O. E. Blasing, N. Palacios-Rojas, D. Pankovic, J. H. M. Hendriks, J. Fisahn, M. Hohne, M. Gunther, and M. Stitt. 2004b. Adjustment of diurnal starch turnover to short days: depletion of sugar during the night leads to a temporary inhibition of carbohydrate utilization, accumulation of sugars and post-translational activation of ADP-glucose pyrophosphorylase in the following light period. The Plant Journal **39**:847-862.

Gillooly, J. F., J. H. Brown, G. B. West, V. M. Savage, and E. L. Charnov. 2001. Effects of size and temperature on metabolic rate. Science **293**:2248-2251.

Graf, A., A. Schlereth, M. Stitt, and A. M. Smith. 2010. Circadian control of carbohydrate availability for growth in Arabidopsis plants at night. Procedings of the National Academy of Science USA **107**:9458-9463.

Granier, C., L. Aguirrezabal, K. Chenu, S. J. Cookson, M. Dauzat, P. Hamard, J. J. Thioux, G. Rolland, S. Bouchier-Combaud, A. Lebaudy, B. Muller, T. Simonneau, and F. Tardieu. 2006. PHENOPSIS, an automated platform for reproducible phenotyping of plant responses to soil water deficit in *Arabidopsis thaliana* permitted the identification of an accession with low sensitivity to soil water deficit. New Phytologist **169**:623-635.

Granier, C., C. Massonnet, O. Turc, B. Muller, K. Chenu, and F. Tardieu. 2002. Individual leaf development in *Arabidopsis thaliana*: a stable thermal-time-based programme. Annals of Botany **89**:595-604.

Gray, W. M., A. Ostin, G. Sandberg, C. P. Romano, and M. Estelle. 1998. High temperature promotes auxin-mediated hypocotyl elongation in Arabidopsis. Procedings of the National Academy of Science, USA **95**:7197-7202.

Hangarter, R. P. 1997. Gravity, light and plant form. Plant, Cell and Environment **20**:796-800.

Hassiotou, F., M. Renton, M. Ludwig, J. R. Evans, and E. J. Veneklaas. 2010. Photosynthesis at an extreme end of the leaf trait spectrum: how does it relate to high leaf dry mass per area and associated structural parameters? Journal of Experimental Botany **61**:3015-3028.

Heckathorn, S. A., G. J. Poeller, J. S. Coleman, and R. L. Hallberg. 1996. Nitrogen availability alters patterns of accumulation of heat stress-induced proteins in plants. Oecologia **105**:413-418.

Heydarian, Z., R. Sasidharan, M. C. H. Cox, R. Pierik, L. A. C. J. Voesenek, and A. J. M. Peeters. 2010. A kinetic analysis of hyponastic growth and petiole elongation upon ethylene exposure in *Rumex palustris*. Annals of Botany **106**:429-429.

Hoagland, D. R. and D. I. Arnon. 1950. The water-culture method for growing plants without soil. California Agricultural Experiment Station Circular **347**:1-32.

Hummel, I., F. Pantin, R. Sulpice, M. Piques, G. Rolland, M. Dauzat, A. Christophe, M. Pervent, M. Bouteillé, M. Stitt, Y. Gibon, and B. Muller. 2010. *Arabidopsis thaliana* plants acclimate to water deficit at low cost through changes of C usage; an integrated perspective using growth, metabolite, enzyme and gene expression analysis. Plant Physiology **154**:357-372.

Huxman, T. E., E. P. Hamerlynck, M. E. Loik, and S. D. Smith. 1998. Gas exchange and chlorophyll fluorescence responses of three south-western Yucca species to elevated CO_2 and high temperature. Plant Cell and Environment **21**:1275-1283.

Jacobs, B. C. and C. J. Pearson. 1999. Growth, development and yield of Rice in response to cold temperature. Journal of Agronomy and Crop Science **182**:79-88.

Jones, H. G. 1992. Plants and microclimate: a quantitative approach to environmental plant physiology. Cambridge University Press, New York, USA.

Kang, B. G. 1979. Epinasty. Springer-Verlag, Berlin.

Kim, G. T., S. Yano, T. Kozuka, and H. Tsukaya. 2005. Photomorphogenesis of leaves: shade-avoidance and differentiation of sun and shade leaves. Photochemical and Photobiological Sciences **4**:770-774.

King, D. A. 1997. The functional significance of leaf angle in Eucalyptus. Australian Journal of Botany **45**:619-639.

Kobza, J. and G. E. Edwards. 1987. Influences of leaf temperature on photosynthetic carbon metabolism in Wheat. Plant Physiology **83**:69-74.

Koini, M. A., L. Alvey, T. Allen, C. A. Tilley, N. P. Harberd, G. C. Whitelam, and K. A. Franklin. 2009. High temperature-mediated adaptations in plant architecture require the bHLH transcription factor PIF4. Current Biology **19**:408-413.

Kozuka, T., G. Horiguchi, G. T. Kim, and H. Tsukaya. 2005. Regulation of petiole elongation during shade-avoidance response is highly dependent on ROT3 and DOC1. Plant and Cell Physiology **46**:213-223.

Lee, J.-H., X. W. Deng, and W. T. Kim. 2006. Possible role of light in the maintenance of EIN3/EIL1 stability in Arabidopsis seedlings. Biochemical and Biophysical Research Communications **350**:484-491.

Lefebvre, V., H. North, A. Frey, B. Sotta, M. Seo, M. Okamoto, E. Nambara, and A. Marion-Poll. 2006. Functional analysis of Arabidopsis *NCED6* and *NCED9* genes indicates that ABA synthesized in the endosperm is involved in the induction of seed dormancy. Plant Journal **45**:309-319.

Ludwig-Muller, J., P. Krishna, and C. Forreiter. 2000. A glucosinolate mutant of Arabidopsis is thermosensitive and defective in cytosolic Hsp90 expression after heat stress. Plant Physiology **123**:949-958.

Maliakal, S. K., K. McDonnell, S. A. Dudley, and J. Schmitt. 1999. Effects of red to far-red ratio and plant density on biomass allocation and gas exchange in *Impatiens capensis*. International Journal of Plant Sciences **160**:723-733.

Masle, J., S. R. Gilmore, and G. D. Farquhar. 2005. The *ERECTA* gene regulates plant transpiration efficiency in Arabidopsis. Nature **436**:866-870.

Maxwell, K. and G. N. Johnson. 2000. Chlorophyll fluorescence - a practical guide. Journal of Experimental Botany **51**:659-668.

Mendez-Vigo, B., M. Andres, M. Ramiro, J. M. Martinez-Zapater, and C. Alonso-Blanco. 2010. Temporal analysis of natural variation for the rate of leaf production and its relationship with flowering initiation in *Arabidopsis thaliana*. Journal of Experimental Botany:1611-1623.

Merlot, S., A. C. Mustilli, B. Genty, H. North, V. Lefebvre, B. Sotta, A. Vavasseur, and J. Giraudat. 2002. Use of infrared thermal imaging to isolate Arabidopsis mutants defective in stomatal regulation. The Plant Journal **30**:601-609.

Millenaar, F. F., M. C. Cox, Y. E. van Berkel, R. A. Welschen, R. Pierik, L. A. Voesenek, and A. J. Peeters. 2005. Ethylene-induced differential growth of petioles in Arabidopsis. Analyzing natural variation, response kinetics, and regulation. Plant Physiology **137**:998-1008.

Millenaar, F. F., M. van Zanten, M. C. Cox, R. Pierik, L. A. Voesenek, and A. J. Peeters. 2009. Differential petiole growth in *Arabidopsis thaliana*: photocontrol and hormonal regulation. New Phytologist **184**:141-152.

Morelli, G. and I. Ruberti. 2002. Light and shade in the photocontrol of Arabidopsis growth. Trends in Plant Science **7**:399-404.

Morison, J. I. L. and D. W. Lawlor. 1999. Interactions between increasing CO_2 concentration and temperature on plant growth. Plant Cell and Environment **22**:659-682.

Mullen, J. L., C. Weinig, and R. P. Hangarter. 2006. Shade avoidance and the regulation of leaf inclination in Arabidopsis. Plant Cell and Environment **29**:1099-1106.

Ong, C. K. 1983. Response to temperature in a stand of Pearl-Millet (*Pennisetum typhoides* S. and H.). 4. Extension of individual leaves. Journal of Experimental Botany **34**:1731-1739.

Parent, B., O. Turc, Y. Gibon, M. Stitt, and F. Tardieu. 2010. Modelling temperature-compensated physiological rates, based on the co-ordination of responses to temperature of developmental processes. Journal of Experimental Botany **61**:2057-2069.

Penfield, S. 2008. Temperature perception and signal transduction in plants. New Phytologist **179**:615-628.

Pierik, R., M. L. C. Cuppens, L. A. C. J. Voesenek, and E. J. W. Visser. 2004. Interactions between ethylene and gibberellins in phytochrome-mediated shade avoidance responses in Tobacco. Plant Physiology **136**:2928-2936.

Poorter, H., U. Niinemets, L. Poorter, I. J. Wright, and R. Villar. 2009. Causes and consequences of variation in leaf mass per area (LMA): a meta-analysis. New Phytologist **183**:1222-1222.

R Development Core Team. 2009. R: a language and environment for statistical computing. R Foundation for Statistical Computing, Vienna, Austria.

Robson, P. R. H., G. C. Whitelam, and H. Smith. 1993. Selected components of the shade-avoidance syndrome are displayed in a normal manner in mutants of *Arabidopsis thaliana* and *Brassica rapa* deficient in phytochrome-B. Plant Physiology **102**:1179-1184.

Schmitt, J. 1997. Is photomorphogenic shade avoidance adaptive? Perspectives from population biology. Plant Cell and Environment **20**:826-830.

Smalle, J., M. Haegman, J. Kurepa, M. Van Montagu, and D. V. D. Straeten. 1997. Ethylene can stimulate Arabidopsis hypocotyl elongation in the light. Proceedings of the National Academy of Sciences, USA **94**:2756-2761.

Smith, H. 2000. Phytochromes and light signal perception by plants: an emerging synthesis. Nature **407**:585-591.

Somers, D. E., R. A. Sharrock, J. M. Tepperman, and P. H. Quail. 1991. The *HY3* long hypocotyl mutant of Arabidopsis is deficient in phytochrome-B. The Plant Cell **3**:1263-1274.

Sparks, T. H., E. P. Jeffree, and C. E. Jeffree. 2000. An examination of the relationship between flowering times and temperature at the national scale using long-term phenological records from the UK. International Journal of Biometeorology **44**:82-87.

Sulpice, R., E.-T. Pyl, H. Ishihara, S. Trenkamp, M. Steinfath, H. Witucka-Wall, Y. Gibon, B. Usadel, F. Poree, M. C. Piques, M. Von Korff, M. C. Steinhauser, J. J. B. Keurentjes, M. Guenther, M. Hoehne, J. Selbig, A. R. Fernie, T. Altmann, and M. Stitt. 2009. Starch as a major integrator in the regulation of plant growth. Proceedings of the National Academy of Sciences, USA **106**:10348-10353.

Taub, D. R., J. R. Seemann, and J. S. Coleman. 2000. Growth in elevated CO_2 protects photosynthesis against high-temperature damage. Plant Cell and Environment **23**:649-656.

Tisné, S., I. Schmalenbach, M. Reymond, M. Dauzat, M. Pervent, D. Vile, and C. Granier. 2010. Keep on growing under drought: genetic and developmental bases of the response of rosette area using a recombinant inbred line population. Plant Cell and Environment **33**:1875-1887.

Tonsor, S. J., C. Scott, I. Boumaza, T. R. Liss, J. L. Brodsky, and E. Vierling. 2008. Heat shock protein 101 effects in *A. thaliana*: genetic variation, fitness and pleiotropy in controlled temperature conditions. Molecular Ecology **17**:1614-1626.

Torii, K. U., N. Mitsukawa, T. Oosumi, Y. Matsuura, R. Yokoyama, R. F. Whittier, and Y. Komeda. 1996. The arabidopsis *ERECTA* gene encodes a putative receptor protein kinase with extracellular leucine-rich repeats. The Plant Cell **8**:735-746.

Tsukaya, H., T. Kozuka, and G. T. Kim. 2002. Genetic control of petiole length in *Arabidopsis thaliana*. Plant Cell and Physiology **43**:1221-1228.

van Zanten, M., L. Basten Snoek, E. van Eck-Stouten, M. C. Proveniers, K. U. Torii, L. A. Voesenek, A. J. Peeters, and F. F. Millenaar. 2010a. Ethylene-induced hyponastic growth in Arabidopsis thaliana is controlled by *ERECTA*. Plant Journal **61**:83-95.

Van Zanten, M., L. B. Snoek, E. van Eck-Stouten, M. C. G. Proveniers, K. U. Torii, L. A. Voesenek, A. J. Peeters, and F. F. Millenaar. 2010b. Ethylene-induced hypotnastic growth in *Arabidopsis thaliana* is controlled by *ERECTA*. The Plant Journal **61**:83-95.

Van Zanten, M., L. A. Voesenek, A. J. Peeters, and F. F. Millenaar. 2009. Hormone- and light-mediated regulation of heat-induced differential petiole growth in *Arabidopsis thaliana*. Plant Physiology **151**:1446-1458.

Vandenbussche, F., R. Pierik, F. F. Millenaar, L. A. C. J. Voesenek, and D. Van Der Straeten. 2005. Reaching out of the shade. Current Opinion in Plant Biology **8**:462-468.

Vandenbussche, F., W. H. Vriezen, J. Smalle, L. J. J. Laarhoven, F. J. M. Harren, and D. Van Der Straeten. 2003. Ethylene and auxin control decreased light intensity. Plant Physiology **133**:517-527.

Vile, D., E. Garnier, B. Shipley, G. Laurent, M. L. Navas, C. Roumet, S. Lavorel, S. Diaz, J. G. Hodgson, F. Lloret, G. F. Midgley, H. Poorter, M. Rutherford, P. J. Wilson, and I. J. Wright. 2005. Specific leaf area and dry matter content estimate thickness in laminar leaves. Annals of Botany **96**:1129-1136.

Witkowski, E. T. F. and B. B. Lamont. 1991. Leaf specific mass confounds leaf density and thickness. Oecologia **88**:486-493.

Yanagisawa, S., S. D. Yoo, and J. Sheen. 2003. Differential regulation of *EIN3* stability by glucose and ethylene signalling in plants. Nature **425**:521-525.

Yano, S. and I. Terashima. 2001. Separate localization of light signal perception for sun or shade type chloroplast and palisade tissue differentiation in *Chenopodium album*. Plant and Cell Physiology **42**:1303-1310.

Young, T. E., J. Ling, C. J. Geisler-Lee, R. L. Tanguay, C. Caldwell, and D. R. Gallie. 2001. Developmental and thermal regulation of the Maize heat shock protein, HSP101. Plant Physiology **127**:777-791.

Zhong, S., M. Zhao, T. Shi, H. Shi, F. An, Q. Zhao, and H. Guo. 2009. *EIN3*/*EIL1* cooperate with *PIF1* to prevent photo-oxidation and to promote greening of Arabidopsis seedlings. Proceedings of the National Academy of Sciences, USA **106**:21431-21436.

Supporting Information

Supplemental Table S1. **Results of univariate analyses of variance (ANOVAs).** Mean squares (type III) from the partitioning of phenotypic variation among L*er* and the complemented line L*ER* grown at 20 °C under moderate light intensity (175 µmol m^{-2} s^{-1}), and at high temperature (30 °C) under low (70 µmol m^{-2} s^{-1}), moderate (175 µmol m^{-2} s^{-1}), and high light intensity (330 µmol m^{-2} s^{-1}). Hypothesis testing was based on F-ratios from type III mean squares for all ANOVAs. Mean squares in bold typeface followed by asterisk were significant at *$P < 0.05$, **$P < 0.01$, ***$P < 0.001$. Mean squares followed by a dot were significant at $P < 0.10$. Mean squares reported are those from the full model including all interactions. All nonsignificant terms (normal typeface) are reported, but were removed from the final model.

Trait	Genotype (G) and temperature (T) effects at moderate light intensity				Genotype (G) and light (L) effects at high temperature				Genotype (G) and ligh and temperature treatments merged (E) effect			
	G	T	GxT	R^2	G	L	GxL	R^2	G	E	GxE	R^2
Leaf insertion angle (degrees)	**170.9*** **	**6090*** **	13.40	**0.96*** **	55.60	**3376*** **	37.10	**0.85*** **	0.500	**6249*** **	58.00.	**0.93*** **
Leaf blade ratio (%)	**412.8*** **	**295.5*** **	1.840	**0.92*** **	**789.3*** **	**484.0*** **	4.670	**0.85*** **	**960.0*** **	**609*** **	3.270	**0.88*** **
Vegetative duration (days)	6.478	0.723	54.66	0.05	**416.4*** **	**651.1*** **	**103.6***	**0.57*** **	**262.4** **	**514*** **	**121.2*** **	**0.59*** **
Leaf number at flowering (leaf)	4.803	**173.5*** **	**20.31***	**0.57*** **	**33.40** **	**68.76*** **	8.385.	**0.48*** **	8.278	**132.4*** **	**13.90*** **	**0.63*** **
Total fresh mass (mg)[a]	**0.216** **	**1.398*** **	0.021	**0.61*** **	**0.311*** **	**1.291*** **	0.013	**0.66*** **	**0.206** **	**1.708*** **	0.018	**0.76*** **
Specific leaf area (cm^2 g^{-1})	47.30	**3347*** **	8.400	**0.64*** **	39.10	**20190*** **	17.80	**0.90*** **	67.2	**16883*** **	12.8	**0.91*** **
Leaf dry matter content (mg DM g^{-1} FM)	0.016	**1.492*** **	0.112	**0.30*** **	**0.438***	**11.01*** **	0.204.	**0.84*** **	0.124	**8.141*** **	**0.265***	**0.81*** **
Leaf thickness (µm)	1614	**53980*** **	**4493***	**0.54*** **	**2264***	**16126*** **	585	**0.56*** **	720	**39885*** **	**2852***	**0.68*** **
Cell density (cells mm^{-2})[a]	**3.435*** **	**1.381*** **	0.016	**0.73*** **	**1.300*** **	**1.024*** **	**0.157***	**0.64*** **	**2.713*** **	**0.857*** **	**0.155** **	**0.71*** **
Stomatal density (st. mm^{-2})[a]	**3.595*** **	**3.701*** **	0.052	**0.86*** **	**2.961*** **	**0.318** **	**0.194***	**0.63*** **	**4.562*** **	**1.258*** **	**0.130***	**0.76*** **
Stomatal index (% st. $Cell^{-1}$)	0.152	**39.16*** **	**8.537***	**0.36*** **	**25.05** **	**21.74*** **	3.673	**0.39*** **	**18.06** **	**47.47*** **	**6.737***	**0.58*** **

[a]: ln-transformed variables.

Table S2. Loadings of the variables on the three firsts principal components of the principal component analysis (PCA).

Variable	PC1 (53%)	PC2 (17%)	PC3 (9%)
Vegetative duration (days)	0.097	0.926	-0.227
Leaf number at flowering (leaf)	-0.791	0.401	0.049
Rosette fresh mass (mg, log)	-0.892	0.363	0.054
Leaf insertion angle (degrees)	0.880	0.254	-0.193
Leaf blade ratio (%)	-0.668	-0.459	-0.097
Specific leaf area ($cm^2\ g^{-1}$)	0.902	-0.014	0.243
Leaf dry matter content (mg DM g^{-1} FM)	-0.692	0.015	-0.421
Leaf thickness (µm)	-0.834	0.082	-0.105
Cell density (cells mm^{-2})[§]	0.475	-0.282	-0.747
Stomatal index (% st. $Cell^{-1}$)	-0.673	-0.366	0.045

Table S4. Real-time reverse transcription-polymerase chain reaction procedure and list of primers used. Reverse transcription was performed with 1 µg of total RNAs incubated at 70 °C with 2.85 ml of 90 µM pd(N)6 random hexamer, adjusted to 20 µl with milliQ water and then cooled for 5 min. 1 µl Reverse Transcriptase (Promega, Madison, USA) was then added to each sample after 5 min of incubation with 8 µl reaction mix (4 µl buffer 5X, 2 µl dNTPs at 10 mM, 0.5 µl RNasine et 40 U μl^{1} and 1.5 µl milliQ water). Amplification of total cDNAs was performed under the following conditions: 10 min at 25 °C, followed by 1 h at 42 °C, and finally 5 min at 95 °C. cDNAs were diluted twice before any further reaction. The absence of contaminating gDNA in the cDNA template was checked by loading PCR product of *GAPDH* gene amplification on agarose 2% gel (At1g12900; 5'-CACAGCTTTAGCTGCTCCTG-3' and 5'-CTGTCTTGCTCCCTTTGTCA-3'). The two primers allowed different size amplifications from cDNA (184 bp) and gDNA (269 bp). Real-time quantification of target cDNA was performed in a LightCycler 480® (Roche, Penzberg, Germany) and a specific primers set (Table S2). Pairs of primers for gene-specific amplification were designed using PRIMER3 software (http://biotools.umassmed.edu/bioapps/primer3_www.cgi). Each reaction was performed using 0.33 µM of each primer with LightCycler 480 Syber Green Master I X1 (Roche) and 25 ng of cDNA template under the following conditions: 5 min at 95 °C, followed by 45 cycles with 10 s at 95 °C, 10 s at 60 °C, 10 s at 72°C and temperature transitions of 4.8 °C s^{-1}. Finally, a melting curve (consisting of 5 s 95 °C, 1 min at 65 °C, and heating at 97 °C at a rate of 0.11 °C s^{-1}) was determined to ensure amplification specificity. Data were analyzed using the Roche LightCycler software 1.5.0 (Roche). Cycle threshold (Ct) values were determined by the fit point method from exponential phase of each amplification. For each gene of interest, PCR efficiency (E) was deduced from a standard dilution series, by the relation E = -1/slope. Relative quantification was determined using the Delta Delta Ct method with E correction. For normalization, two reference genes (*CIPK23*, At1g30270; *TUB4*, At5g44340.1) were selected on the basis of their expression stability in leaves under HT and light treatments. Finally, all the expression values of each gene at t_1 and t_{24} were normalized by the average of the gene expression values before any light treatment (t_0).

Gene	TAIR reference	Forward	Reverse
CIPK23 (control)	At1g30270.1	5'-GGGACTTAAGGACATTGTTTGG-3'	5'-AGTACCACCACCATCGGTTC-3'
TUB4 (control)	At5g44340.1	5'-GTGATCTGCGACGAACACGGCA-3'	5'-AGAACAGCGCGAGGAACGTACT-3'
DIN6	At3g47340.1	5'-TTGGCCGGTACTAAGGCGGC-3'	5'-CGTGGTGCACCGTCCCCAAA-3'
DIN10	At5g20250.1	5'-GGCGGAGTTAGACCCGGGGA-3'	5'-GTCCACGCCAGCATCAGCCA-3'
CPN60A	At2g28000.1	5'-TATCGAGGAAGGCATAGTTCCAGGTGGTGG-3'	5'-CGGGAATAACAGTGGAGAGATGCACCAAAG-3'
CPN60B	At1g55490.1	5'-GGTGCTGGCTAACGATAATGTGAAATTTG	5'-CATGTTCTAAGCAACATCTCACAACCTTTG-3'
TPS8	At1g70290.1	5'-CATGTTTGAGAGCATATTAAGCACAGTGAC-3'	5'-GCTTCATCGTCCAAGAAGTATTTAGCTTTG-3'
HSP101	At1g74310.1	5'-CGCCTCATTGGGGCACCACC-3'	5'-CGACTGTCCTGCCTTGCCCG-3'

Table S3. Mean meteorological conditions in the experiments. CT: control temperature (20°C); HT: high temperature (30°C); ML: moderate light intensity; LL: low light; HL: high light. PAR: photosynthetically active radiation; VPD: vapor pressure deficit.

Temperature and light treatments		PAR (µmol m^{-2} s^{-1})	Air humidity (%)		VPD (kPa)		Temperature (℃)	
		Day	Day	Night	Day	Night	Day	Night
From germination to stage 1.02								
CT	ML	175	80.55	86.61	0.43	0.32	21.55	21.11
HT	LL	175	81.25	85.22	0.49	0.37	21.84	21.03
	ML	175	83.50	88.01	0.43	0.30	21.76	21.16
	HL	175	82.57	86.53	0.45	0.33	21.78	20.92
From stage 1.02 to 1.06								
CT	ML	175	80.55	86.61	0.43	0.32	21.55	21.11
HT	LL	175	87.12	88.09	0.54	0.37	29.74	24.77
	ML	175	88.43	88.58	0.48	0.36	29.82	24.82
	HL	175	87.24	87.95	0.53	0.38	29.68	24.81
From stage 1.06 to 6.02								
CT	ML	175	80.55	86.61	0.43	0.32	21.55	21.11
HT	LL	70	85.09	87.34	0.61	0.39	29.55	24.68
	ML	175	84.22	88.29	0.65	0.36	29.61	24.53
	HL	333	84.57	87.57	0.64	0.39	29.60	24.72

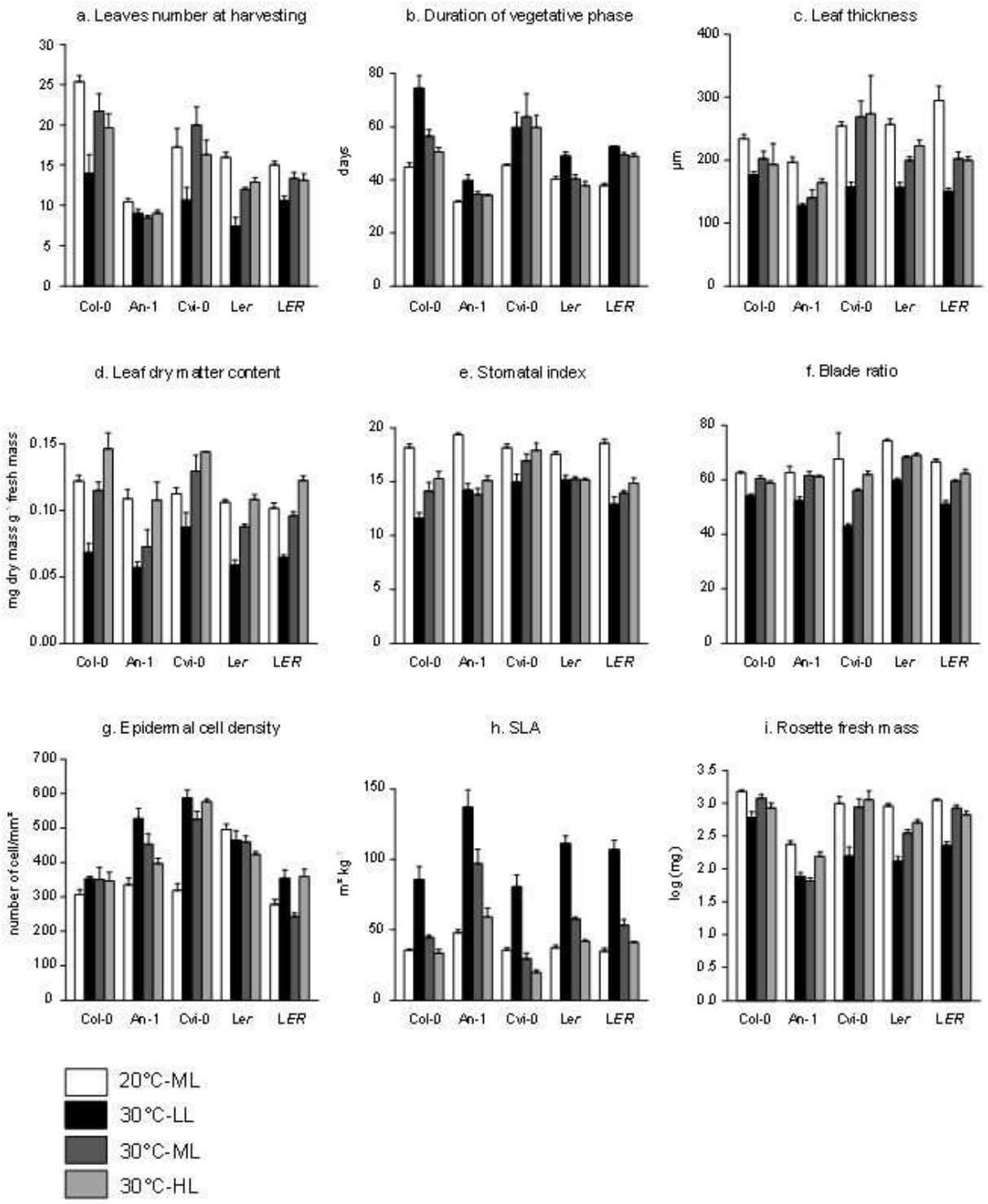

Figure S1. Barplot of each variable represented on the PCA (Fig. 8) for the 4 accessions and the L*ER* complemented line. Plants were grown at 20 °C under moderate light intensity (ML, 175 µmol m^{-2} s^{-1}; white bars), and at high temperature (30 °C) under low (LL, 70 µmol m^{-2} s^{-1}; black bars), moderate (ML, 175 µmol m^{-2} s^{-1}; dark grey bars), and high light intensity (HL, 330 µmol m^{-2} s^{-1}; light grey bars).

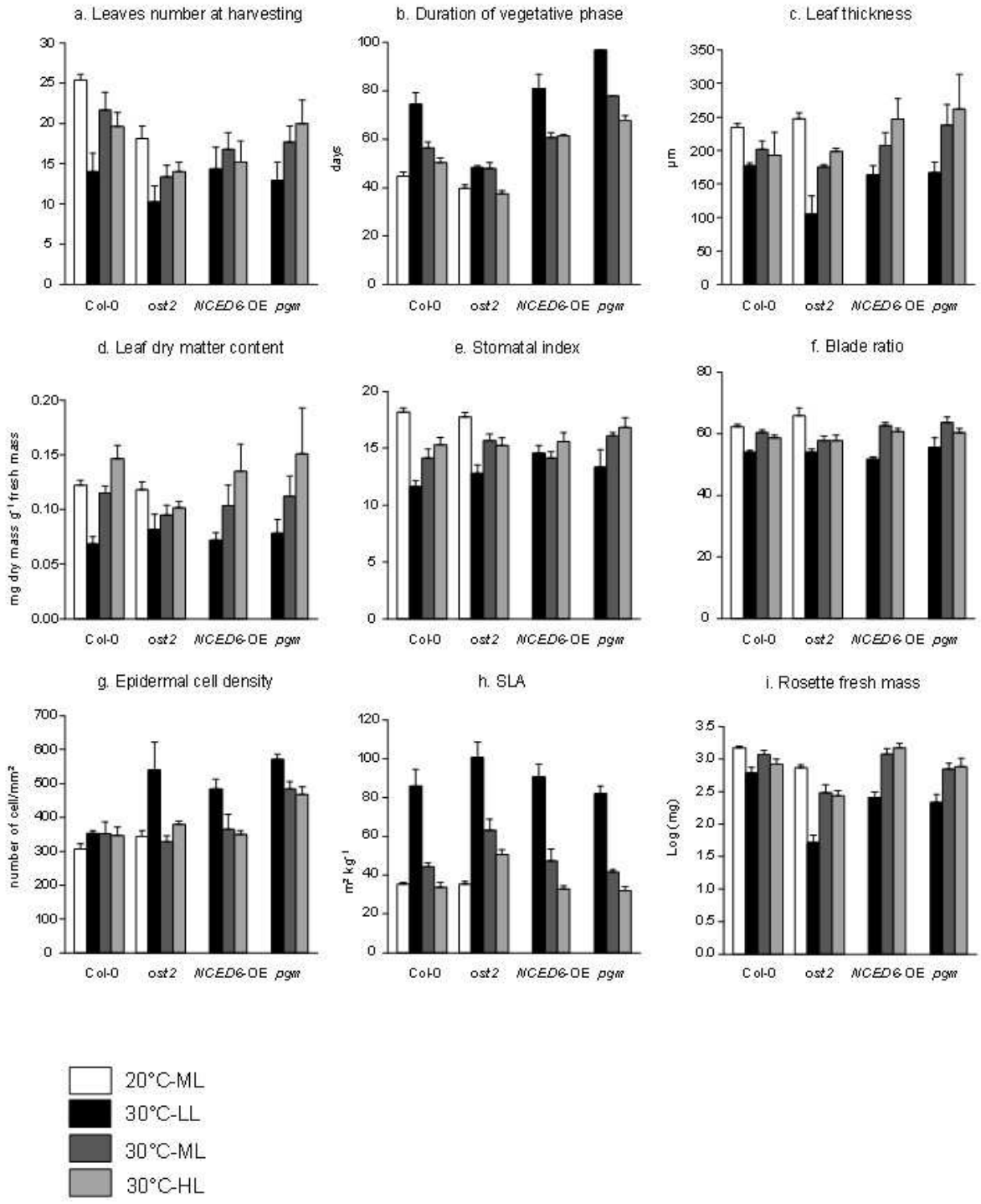

Figure S2. Barplot of each variable represented on the PCA (Fig. 8) for Col-0 and the 3 mutants *pgm*, *NCED6*-OE and *ost2*. Plants were grown at 20°C under moderate light intensity (ML, 175 µmol m^{-2} s^{-1}; white bars), and at high temperature (30°C) under low (LL, 70 µmol m^{-2} s^{-1}; black bars), moderate (ML, 175 µmol m^{-2} s^{-1}; dark grey bars), and high light intensity (HL, 330 µmol m^{-2} s^{-1}; light grey bars).

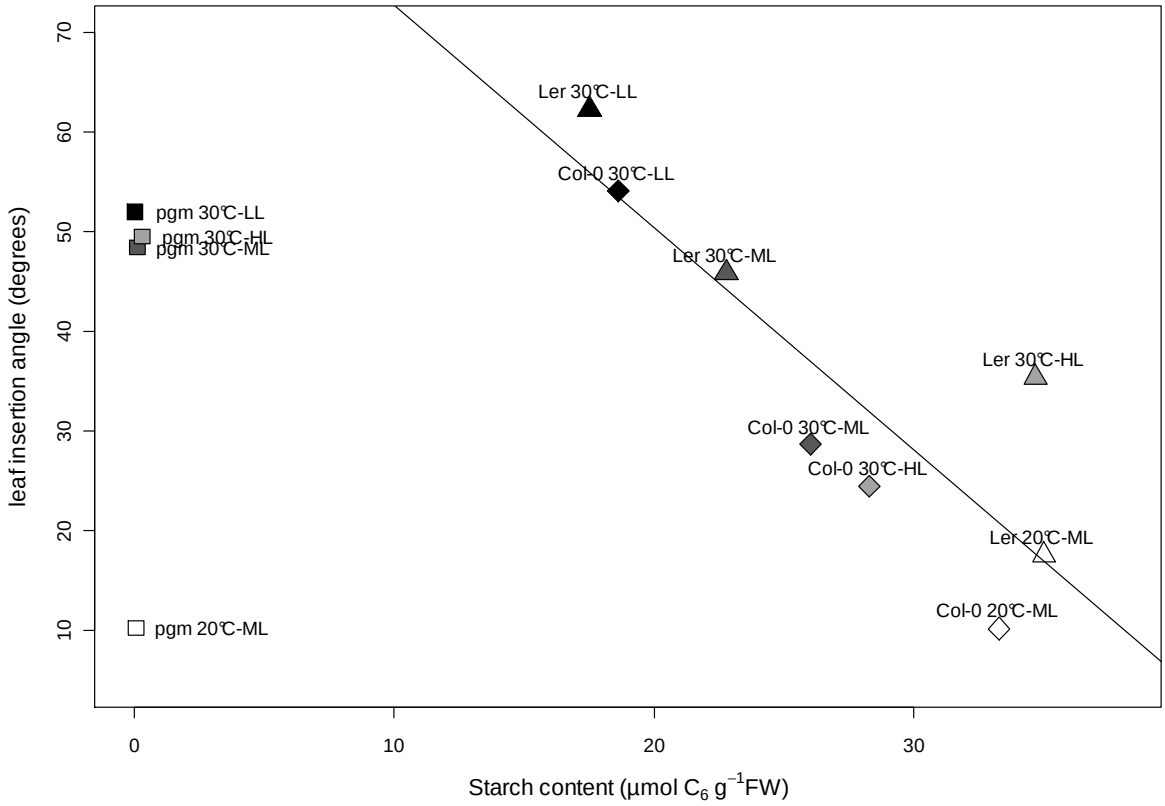

Figure S3. Correlation between starch concentration and leaf angle in Col-0, L*er* and the mutant *pgm*. Plants were grown at 20 °C under moderate light intensity (ML, 175 µmol m^{-2} s^{-1}; white symbols), and at high temperature (30 °C) under low (LL, 70 µmol m^{-2} s^{-1}; black symbols), moderate (ML, 175 µmol m^{-2} s^{-1}; dark grey symbols), and high light intensity (HL, 330 µmol m^{-2} s^{-1}; light grey symbols). r = -0.86, $P < 0.05$.

Manuscript #4

Erected leaves as an adaptation to high temperature: beyond cooling, carbon matters

Florent Pantin[1,2], François Vasseur[1], Ravi Valluru[1], Bertrand Muller[1], Thierry Simonneau[1] and Denis Vile[1]

[1] Laboratoire d'Ecophysiologie des Plantes sous Stress Environnementaux (LEPSE), UMR 759, INRA-SUPAGRO, F-34060 Montpellier, France

[2] Department of Cell and Developmental Biology, John Innes Centre, Norwich Research Park, Colney, Norwich, NR4 7UH, United Kingdom

Letter submitted to *New Phytologist*.

Introduction

Excessive temperature impairs plant performance in a large range of natural and agricultural conditions (Battisti and Naylor 2009). To protect their tissues against damaging temperatures, plants have evolved different mechanisms, an efficient one being leaf cooling induced by transpiration. The higher the transpiration, the more energy is withdrawn from the leaf as latent heat to fuel the process of water evaporation. The diffusion of water vapour is facilitated by stomata, these minute pores at the leaf surface controlled by a pair of guard cells. Stomatal conductance quantifies the extent to which the guard cells let water vapour flows through the stomatal pore they control. Stomatal conductance superimposes with the boundary layer conductance, namely the unstirred air layer at the vicinity of the leaf surface. The higher is the boundary layer conductance (the thinner is the boundary layer), the faster is heat dissipated from the leaves. Hence, plants can achieve leaf cooling by an increase in stomatal conductance – through stomatal opening – or an increase in boundary layer conductance – through architectural modifications that increase the exposure of the leaf to the surrounding air. Being the result of changes in stomatal aperture or shoot architecture, leaf cooling has most often been considered as the most important target in plant adaptation to high temperature. Genotypes with higher transpiration rates are therefore expected as better adapted to high temperature conditions which has proved to be the case under non limiting water (Lu et al. 1998). However, high temperature results in high evaporative demand and most often coexists with limited soil water reserve. Plant adaptation to high temperature is then viewed as a trade-off between the benefit in terms of leaf cooling and the cost in terms of water loss. However, high temperature also triggers dramatic changes in the plant carbon balance: carbohydrate demand increases with the acceleration of many physiological processes, while carbohydrate supply decreases with photosynthesis drawdown (Morison and Lawlor 1999, Gent and Seginer 2012).

Because water and carbon balances are major determinants of leaf growth (Pantin et al. 2012), it is important to understand the way how environmental stresses affect water and carbon relations of the plant. Here, we argue that carbon metabolism is a major component of plant response to high temperature, which may override the trade-off between leaf cooling and water conservation. Specifically, we argue that leaf cooling arising from changes in architecture in response to high temperature in Arabidopsis is a side-effect of an evolutionary selection for maximising carbon assimilation.

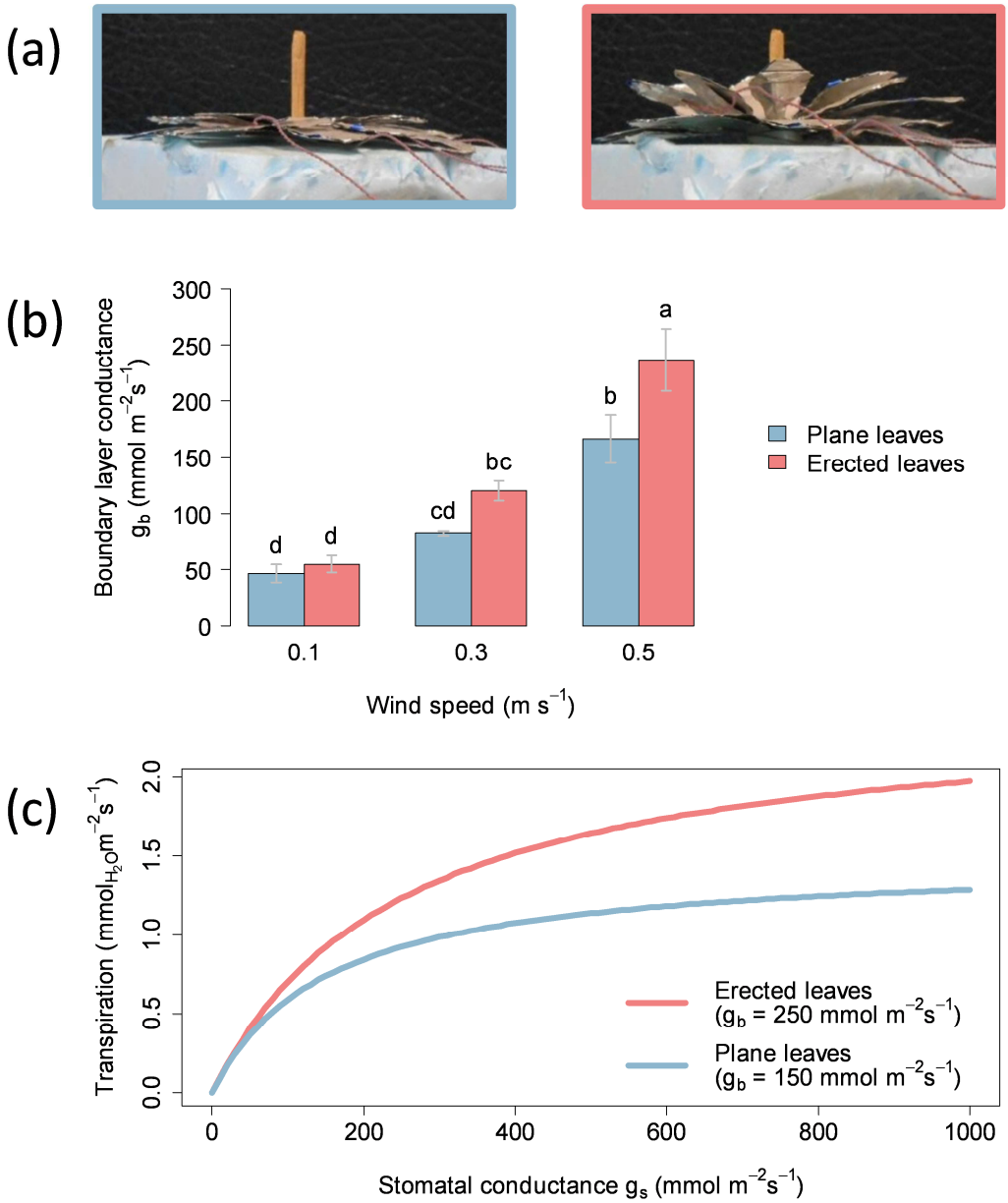

Figure 1. Rosette architecture affects boundary layer conductance and transpiration. (a) Two aluminium models were built to mimic the shape of Arabidopsis rosettes with plane (left) or erected (right) leaves fitted with thermocouples. (b) These models were exposed to different wind speeds and surface temperature was monitored. This allowed the quantification of the boundary layer conductance to heat of the rosette models and its conversion into boundary layer conductance for water vapour g_b (Appendix 8 in Jones, 1992). Letters indicate significant differences between treatments after a LSD test at the 95% confidence level. Note that leaves erected with an angle of about 20 ° confer a higher g_b than in plane leaves, especially at high wind speed. (c) The effect of the architecture-induced increase in g_b on transpiration was simulated as a function of stomatal conductance to water vapour g_s according to the laws ruling water transfer (Eqn. 5.17 in Jones, 1992), assuming a temperature of 20 °C and a vapour pressure deficit of 1 kPa. Note that the erected leaves induce a higher transpiration than the plane leaves when g_s is at least in the same order of magnitude as g_b.

The cooling hypothesis: changes in shoot architecture as an adaptive process to decrease leaf temperature

In Arabidopsis, moderately high temperatures (28-32 °C) induce changes in plant architecture and organ morphology. Notably, upward leaf movement is triggered by differential growth in the petiole, a process known as hyponasty (Koini et al. 2009). This is accompanied by long-term modifications of leaf shape, with an elongated petiole as well as a smaller and thinner blade (Vile et al. 2012 = Manuscript #1). All these responses contribute to decrease leaf temperature and thus counteract heat stress. By changing leaf angle, hyponasty reduces the exposure of the shoot to radiant heat from the incoming light (Fu and Ehleringer 1989, Falster and Westoby 2003), and to convective heat from the soil surface (as suggested by Gray et al. 1998, for high temperature-induced hypocotyl elongation). Furthermore, both hyponasty and the decrease in leaf dimensions may increase evaporative cooling through an increase in boundary layer conductance. Firstly, heat transfer theory and experiments have shown that a decrease in area of a flat surface such as a leaf decreases the boundary layer thickness (Parkhurst 1970, Givnish 1978, Jones 1992). Moreover, hyponasty is thought to increase leaf exposure to the air flow. To test this hypothesis, we built two aluminium models similar in shape to Arabidopsis rosettes with plane or erected leaves (Figure 1a), which we exposed to different wind speeds and monitored for surface temperature with thermocouples. By avoiding confusing effects due to stomatal conductance, this approach allowed us to determine the boundary layer conductance to heat of the rosette models, which was converted into boundary layer conductance for water vapour g_b (Appendix 8 in Jones 1992). At very low wind speed, no significant difference in g_b could be found between the plane and the erected leaf models (Figure 1b). When wind speed was increased gradually, an increasing difference arose between the two rosettes, with erected leaves conferring a higher g_b than the plane leaves. We then simulated the effect on transpiration of an increase in g_b similar as observed for erected leaves at a wind speed of 0.5 m s^{-1} as a function of stomatal conductance g_s (Eqn. 5.17 in Jones 1992). At low g_s, the difference in g_b does not drive any difference in transpiration, because the resistance to water flow imposed by the boundary layer is negligible compared to the one imposed by the stomata (Figure 1c). However, when the order magnitude of g_s is close to that of g_b, the increase in g_b due to leaf hyponasty has a strong effect on transpiration – and thus leaf cooling. Thus, all the morphological changes triggered in response to high temperature converge to decrease leaf temperature in Arabidopsis. This is consistent with the recent findings of Crawford et al. (2012), showing that well-watered plants

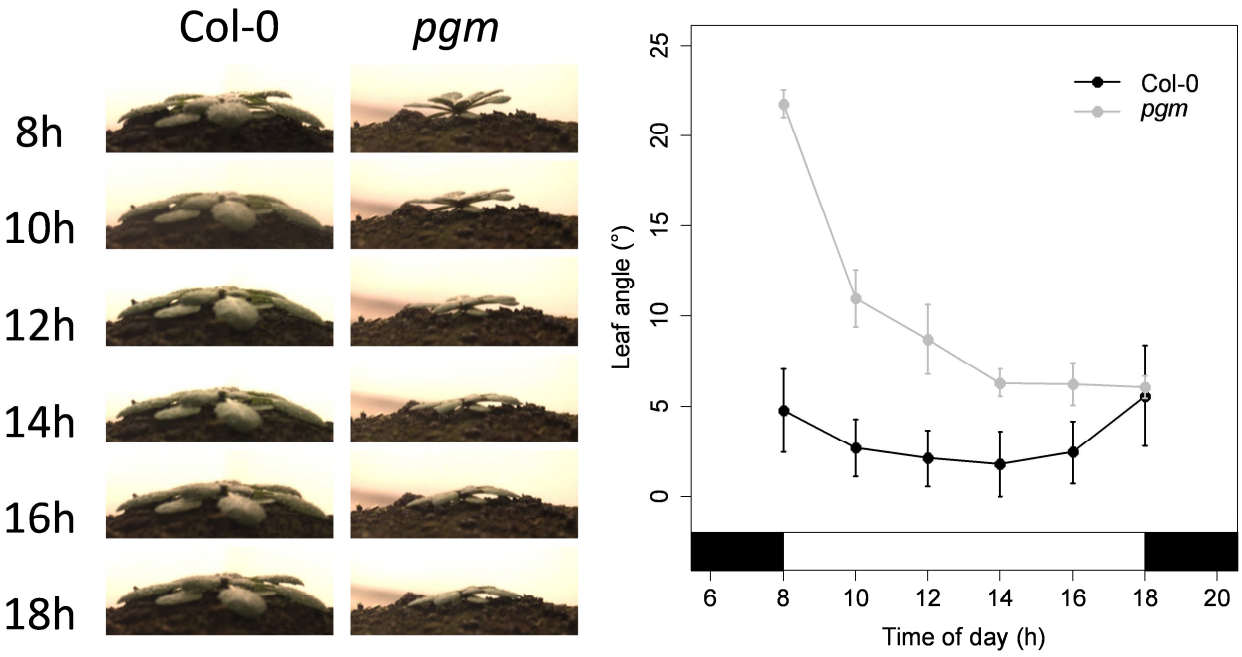

Figure 2. Starch metabolism affects hyponastic movements of the leaves. The angle of growing leaves was monitored during a 10 h photoperiod for the wild-type Col-0 and the starch-deficient mutant *pgm*. A time-series of representative pictures is also provided for both genotypes. Plants were grown as in Pantin et al. (2011). Note that contrary to Col-0, leaf angle in *pgm* decreases throughout the day.

grown at 28 °C are cooler than plants grown at 22 °C when assayed at 28 °C, due to a higher transpiration which results from long-term changes in plant architecture that override minor changes in stomatal density. It is thus tempting to suggest that plasticity in leaf architecture has been selected during evolution to favour leaf cooling against water conservation in Arabidopsis. It must be stressed, however, that both the increase in boundary layer conductance and the decrease in leaf thickness make leaf temperature to track more closely the fluctuations in air temperature (Eqn. 9.11 in Jones 1992).

The metabolic hypothesis: shoot responses to high temperature mimic the shade-avoidance syndrome

It is also worth noting that in Arabidopsis, the changes in leaf morphology and architecture triggered by high temperature are very similar to those triggered by low light, gathered under the term 'shade-avoidance syndrome' (Franklin 2008). Notably, in Arabidopsis plants subjected to low irradiance hyponasty is viewed as response mechanism to competition for light against putative neighbouring leaves, as in other rosette species (Pierik et al. 2005, Mullen et al. 2006). The dynamics of this response is very similar to the one induced by high temperature (Van Zanten et al. 2009). Interestingly, the leaf movements in the starch-deficient mutant *pgm* (Caspar et al. 1985), in which the central metabolism mimics this of a wild-type subjected to severe carbon starvation (Gibon et al. 2004), are very different from that of the wild-type Col-0 observed during a 10-h photoperiod (Figure 2). In the wild-type, growing leaves are slightly erected at the end of the night-period, when the reserve in carbohydrates is at lowest; leaf angle then decreases before it gradually recovers the values observed in the early morning (see also Mullen et al. 2006). By contrast, leaves are much more erected in *pgm* at the end of the night-period, when the mutant experiences the most severe starvation; leaf angle then decreases sharply and do not recover at the end of day-period, when sugars are in dramatic excess due to the lack of starch synthesis in this mutant (Caspar et al. 1985). This suggests that carbon status negatively influences these hyponastic movements. Because high temperature negatively affects carbon balance (Morison and Lawlor 1999), this raises the hypothesis that the changes in rosette architecture observed under high temperature mimic the shade-avoidance syndrome to favour carbon assimilation against water conservation.

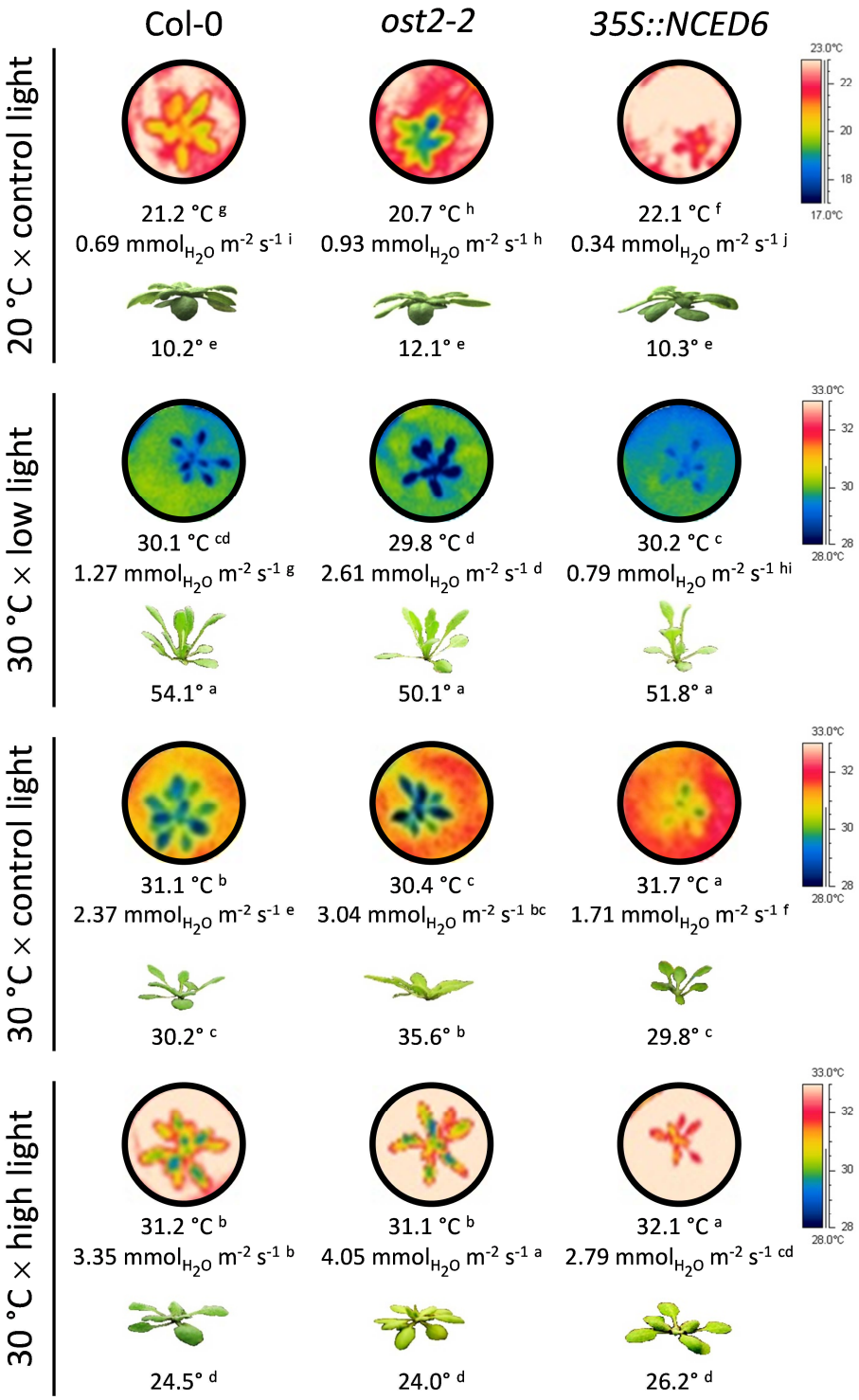

Figure 3. Changes in rosette architecture are uncoupled from changes in leaf temperature and transpiration. The *ost2-2* mutant (stomata constitutively open compared to Col-0) and the *35S::NCED6* transformant (stomata constitutively closed compared to Col-0) were subjected to high temperature and three levels of irradiance at 12 h photoperiod, and compared to control temperature at control irradiance. Circular pictures are false-colour infrared images of plants indicating surface temperature. Note the different colour scale between the control temperature (20 °C) and the high temperature (30 °C). The mean temperature of the genotype in its experimental condition is indicated below each image, together with an independent measurement of whole rosette transpiration. A representative picture of the rosette is also provided, with a mean of the leaf angle observed in each treatment. Experimental procedures are described in Vasseur et al. (2011). For each variable, letters in exponent indicate significant differences between treatments after a Kruskal-Wallis test at the 95% confidence level. Note that the changes in temperature and transpiration induced by the mutations and the environmental conditions are not consistent with the cooling hypothesis, according to which the changes in rosette architecture are triggered to decrease leaf temperature *per se*.

Testing both hypotheses

To distinguish between the cooling hypothesis and the metabolic hypothesis, we subjected two mutants differentially affected in their regulation of transpiration to high temperature and three levels of irradiance at 12 h photoperiod (Vasseur et al. 2011 = Manuscript #3). In the *ost2-2* mutant, the constitutive activation of the plasma membrane H^+-ATPase AHA1 prevents stomatal closure (Merlot et al. 2007). In the *35S::NCED6* transformant, the overexpression of a key enzyme in the biosynthesis pathway of abscisic acid leads to overproduction of this drought hormone and thus to stomatal closure (Lefebvre et al. 2006). Assuming the cooling hypothesis, we would expect that the changes in leaf temperature induced (*i*) by the stomatal transpiration make hyponasty to decrease in *ost2-2* and to increase in *35S::NCED6*, and (*ii*) by the irradiance make hyponasty to decrease in low light and to increase in high light. Contrary to this hypothesis, leaf insertion angle of plants grown at 30 °C was not significantly different between the wild-type Col-0 and *35S::NCED6*, while it increased significantly in *ost2-2*, although leaf temperature and transpiration varied as expected from the mutations in stomatal regulation (Figure 3). Furthermore, leaf insertion angle at high temperature increased significantly in all genotypes under low light (70 µmol m^{-2} s^{-1}) while it decreased significantly under moderately high light (330 µmol m^{-2} s^{-1}) compared to control light intensity (175 µmol m^{-2} s^{-1}), although leaf temperature and transpiration varied as expected from the changes in radiant heat (Figure 3). That increasing irradiance at high temperature partially restores the phenotype observed at control temperature was in favour of the metabolic hypothesis, according to which the architectural changes induced by high temperature are linked to the plant carbon status. To evaluate this alternative hypothesis, we exposed the starchless mutant *pgm* to the same environmental treatments. Hyponasty under high temperature not only was higher in *pgm* than in Col-0, but also was unaffected by the light regime, suggesting an extreme carbon starvation induced by high temperature in this mutant (Figure 4). Accordingly, the reserve of carbohydrates at the end of the night, a critical threshold for carbon metabolism and thus a marker of carbon starvation (Sulpice et al. 2009), was very low in *pgm* under each experimental condition. By contrast, in Col-0 at high temperature this safety margin was increased when grown under high light. In line with the metabolic hypothesis, an integrative analysis combining morphological, physiological, and transcriptional measurements on several Arabidopsis accessions, concluded that moderately high light restores several leaf

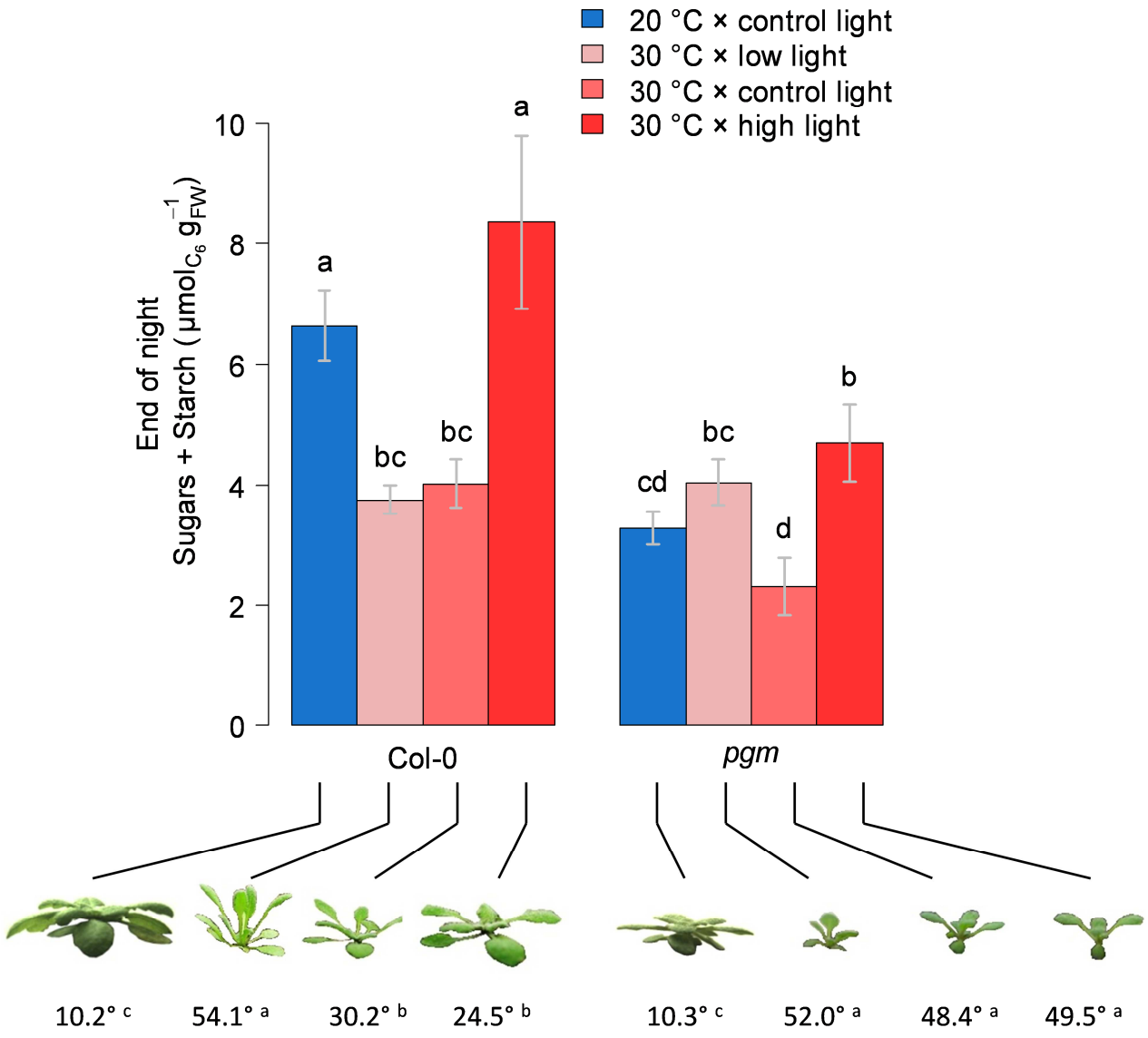

Figure 4. Interaction between carbon metabolism and rosette architecture. The starch-deficient mutant *pgm* was subjected to high temperature and three levels of irradiance at 12 h photoperiod, and compared to control temperature at control irradiance. The carbohydrates (starch, sucrose, glucose, fructose) were determined at the end of the night-period as a marker of carbon starvation. A representative picture of the rosette is also provided, with a mean of the leaf angle observed in each treatment during the day-period. Experimental procedures are described in Vasseur et al. (2011 = Manuscript #3). For each variable, letters indicate significant differences between treatments after a Kruskal-Wallis test at the 95% confidence level. Note that hyponasty in *pgm* under high temperature was very high and unaffected by the light regime, consistent with *pgm*'s very low safety margin for carbon metabolism in each condition, contrary to the wild-type Col-0.

traits and carbon status markers close the ones observed at control temperature, while low light worsens the effects of high temperature (Vasseur et al. 2011 = Manuscript #3).

Conclusion

As a conclusion, we defend the view that the architectural changes induced by high temperature in Arabidopsis under well-watered conditions are at least partly the functional consequence of an altered carbon balance. The convergence points in the signalling pathways of shade-avoidance and high temperature sensing (Koini et al. 2009, Stavang et al. 2009, Foreman et al. 2011, Franklin et al. 2011, Kumar et al. 2012) further suggest that key regulatory components have been recruited from the same network to achieve the same evolutionary function: carbon satiation. In this perspective, leaf cooling appears as a side-benefit of the shade-avoidance syndrome triggered under high temperature. Through a selection for higher stomatal conductance, breeders have already selected cool genotypes inadvertently (Radin et al. 1994). Our study suggests that manipulating both leaf cooling and carbon metabolism through the engineering of plant architecture also offers valuable prospects to improve water use efficiency in a warming world.

Acknowledgments

We thank Yann Boursiac and Philippe Hamard for assistance during the experiments. F.P. was supported by a fellowship of the French Ministry of Research during his PhD. F.V. was funded by a CIFRE grant (ANRT, French Ministry of Research) supported by BAYER Crop Science (contract 0398/2009 – 09 42 008) for his PhD. R.V. was funded by a postdoctoral grant supported by INRA (Department Environment and Agronomy).

References

Battisti, D. S. and R. L. Naylor. 2009. Historical warnings of future food insecurity with unprecedented seasonal heat. Science **323**:240-244.

Caspar, T., S. C. Huber, and C. Somerville. 1985. Alterations in growth, photosynthesis, and respiration in a starchless mutant of *Arabidopsis thaliana* (L.) deficient in chloroplast phosphoglucomutase activity. Plant Physiology **79**:11-17.

Crawford, A. J., D. H. McLachlan, A. M. Hetherington, and K. A. Franklin. 2012. High temperature exposure increases plant cooling capacity. Current Biology **22**:R396-397.

Falster, D. S. and M. Westoby. 2003. Leaf size and angle vary widely across species: what consequences for light interception? New Phytologist **158**:509-525.

Foreman, J., H. Johansson, P. Hornitschek, E.-M. Josse, C. Fankhauser, and K. J. Halliday. 2011. Light receptor action is critical for maintaining plant biomass at warm ambient temperatures. The Plant Journal **65**:441-452.

Franklin, K. A. 2008. Shade avoidance. New Phytologist **179**:930-944.

Franklin, K. A., S. H. Lee, D. Patel, S. V. Kumar, A. K. Spartz, C. Gu, S. Ye, P. Yu, G. Breen, J. D. Cohen, P. A. Wigge, and W. M. Gray. 2011. Phytochrome-interacting factor 4 (PIF4) regulates auxin biosynthesis at high temperature. Proc Natl Acad Sci U S A **108**:20231-20235.

Fu, Q. A. and J. R. Ehleringer. 1989. Heliotropic leaf movements in common beans controlled by air temperature. Plant Physiology **91**:1162-1167.

Gent, M. P. and I. Seginer. 2012. A carbohydrate supply and demand model of vegetative growth: response to temperature and light. Plant Cell and Environment **35**:1274-1286.

Gibon, Y., O. E. Blaesing, J. Hannemann, P. Carillo, M. Höhne, J. H. M. Hendriks, N. Palacios, J. Cross, J. Selbig, and M. Stitt. 2004. A Robot-based platform to measure multiple enzyme activities in Arabidopsis using a set of cycling assays: comparison of changes of enzyme activities and transcript levels during diurnal cycles and in prolonged darkness. The Plant Cell **16**:3304-3325.

Givnish, T. J. 1978. Ecological aspects of plant morphology: leaf form in relation to environment. Acta Biotheoretica **27**:83-142.

Gray, W. M., A. Ostin, G. Sandberg, C. P. Romano, and M. Estelle. 1998. High temperature promotes auxin-mediated hypocotyl elongation in Arabidopsis. Procedings of the National Academy of Science, USA **95**:7197-7202.

Jones, H. G. 1992. Plants and microclimate: a quantitative approach to environmental plant physiology. Cambridge University Press, New York, USA.

Koini, M. A., L. Alvey, T. Allen, C. A. Tilley, N. P. Harberd, G. C. Whitelam, and K. A. Franklin. 2009. High temperature-mediated adaptations in plant architecture require the bHLH transcription factor PIF4. Current Biology **19**:408-413.

Kumar, S. V., D. Lucyshyn, K. E. Jaeger, E. Alos, E. Alvey, N. P. Harberd, and P. A. Wigge. 2012. Transcription factor PIF4 controls the thermosensory activation of flowering. Nature **484**:242-245.

Lefebvre, V., H. North, A. Frey, B. Sotta, M. Seo, M. Okamoto, E. Nambara, and A. Marion-Poll. 2006. Functional analysis of Arabidopsis *NCED6* and *NCED9* genes indicates that ABA synthesized in the endosperm is involved in the induction of seed dormancy. Plant Journal **45**:309-319.

Lu, Z. M., R. G. Percy, C. O. Qualset, and E. Zeiger. 1998. Stomatal conductance predicts yields in irrigated Pima cotton and bread wheat grown at high temperatures. Journal of Experimental Botany **49**:453-460.

Merlot, S., N. Leonhardt, F. Fenzi, C. Valon, M. Costa, L. Piette, A. Vavasseur, B. Genty, K. Boivin, A. Muller, J. Giraudat, and J. Leung. 2007. Constitutive activation of a plasma membrane H(+)-ATPase prevents abscisic acid-mediated stomatal closure. EMBO Journal **26**:3216-3226.

Morison, J. I. L. and D. W. Lawlor. 1999. Interactions between increasing CO_2 concentration and temperature on plant growth. Plant Cell and Environment **22**:659-682.

Mullen, J. L., C. Weinig, and R. P. Hangarter. 2006. Shade avoidance and the regulation of leaf inclination in Arabidopsis. Plant Cell and Environment **29**:1099-1106.

Pantin, F., T. Simonneau, and B. Muller. 2012. Coming of leaf age: control of growth by hydraulics and metabolics during leaf ontogeny. New Phytologist **196**:349-366.

Parkhurst, D. F. 1970. Optimal leaf size in relation to environment.

Pierik, R., F. F. Millenaar, A. J. Peeters, and L. A. Voesenek. 2005. New perspectives in flooding research: the use of shade avoidance and *Arabidopsis thaliana*. Ann Bot **96**:533-540.

Radin, J. W., Z. Lu, R. G. Percy, and E. Zeiger. 1994. Genetic variability for stomatal conductance in Pima cotton and its relation to improvements of heat adaptation. Proc Natl Acad Sci U S A **91**:7217-7221.

Stavang, J. A., J. Gallego-Bartolome, M. D. Gomez, S. Yoshida, T. Asami, J. E. Olsen, J. L. Garcia-Martinez, D. Alabadi, and M. A. Blazquez. 2009. Hormonal regulation of temperature-induced growth in Arabidopsis. Plant Journal **60**:589-601.

Sulpice, R., E.-T. Pyl, H. Ishihara, S. Trenkamp, M. Steinfath, H. Witucka-Wall, Y. Gibon, B. Usadel, F. Poree, M. C. Piques, M. Von Korff, M. C. Steinhauser, J. J. B. Keurentjes, M. Guenther, M. Hoehne, J. Selbig, A. R. Fernie, T. Altmann, and M. Stitt. 2009. Starch as a major integrator in the regulation of plant growth. Proceedings of the National Academy of Sciences, USA **106**:10348-10353.

Van Zanten, M., L. A. Voesenek, A. J. Peeters, and F. F. Millenaar. 2009. Hormone- and light-mediated regulation of heat-induced differential petiole growth in *Arabidopsis thaliana*. Plant Physiology **151**:1446-1458.

Vasseur, F., F. Pantin, and D. Vile. 2011. Changes in light intensity reveal a major role for carbon balance in Arabidopsis responses to high temperature. Plant Cell and Environment.

Vile, D., M. Pervent, M. Belluau, F. Vasseur, J. Bresson, B. Muller, C. Granier, and T. Simonneau. 2012. Arabidopsis growth under prolonged high temperature and water deficit: independent or interactive effects? Plant Cell and Environment **35**:702-718.

Chapter 3

Plant integrated phenotypes: ecological and evolutionary perspectives

"Ecology is rather like sex – every new generation likes to think they were the first to discover it »
Michael Allaby

Chapter objectives:

In this third chapter, we examined the constraints on the evolution of individual characters within complex phenotypes. Specifically the genetic variability and the plasticity of trait covariation to water deficit and high temperature were examined. We asked the two following questions:

- How does genetic variability govern the plant functional strategies within a homogeneous environment?
- How does trait covariation vary in response to combined water deficit and high temperature?

We described the coordinated changes in plant size, metabolism, physiology and morphology in response to changes in the environmental conditions. The results identified QTL with strong effect on plant performance and reproductive success. The study of allometric relationships allowed inferring strong hypotheses about how complex organisms as *Arabidopsis thaliana* may evolve in natural conditions.

Manuscript #5

A Common Genetic Basis to the Origin of the Leaf Economics Spectrum and Metabolic Scaling Allometry

François Vasseur[1], Cyrille Violle[2,3], Brian J. Enquist[2,4], Christine Granier[1] and Denis Vile[1]

[1]INRA, Montpellier SupAgro, UMR759 Laboratoire d'Ecophysiologie des Plantes sous Stress Environnementaux (LEPSE), F-34060 Montpellier, France
[2]Departement of Ecology and Evolutionary Biology, University of Arizona, 1041 E Lowell St., Tucson, Arizona, 85721, USA
[3]CNRS, UMR5175, Centre d'Ecologie Fonctionnelle et Evolutive, F-34000 Montpellier, France
[4]The Santa Fe Institute, 1399 Hyde Park Road, Santa Fe, New Mexico 87501, USA

Article first published online: 31 Jul 2012 in *Ecology Letters*
Volume 15, Issue 10, Pages 1149-1157, DOI: 10.1111/j.1461-0248.2012.01839.xurl: http://onlinelibrary.wiley.com/doi/10.1111/j.1461-0248.2012.01839.x/pdf

Abstract

Many facets of plant form and function are reflected in general cross-taxa scaling relationships. Metabolic scaling theory (MST) and the leaf economics spectrum (LES) have each proposed unifying frameworks and organizational principles to understand the origin of botanical diversity. Here we test the evolutionary assumptions of MST and the LES using a cross of two genetic variants of *Arabidopsis thaliana*. We show that there is enough genetic variation to generate a large fraction of variation in the LES and MST scaling functions. The progeny sharing the parental, naturally occurring, allelic combinations at two pleiotropic genes exhibited the theorized optimum ¾ allometric scaling of growth rate and intermediate leaf economics. Our findings: (*i*) imply that a few pleiotropic genes underlie many plant functional traits and life histories; (*ii*) unify MST and LES within a common genetic framework; and (*iii*) suggest that observed intermediate size and longevity in natural populations originates from stabilizing selection to optimize physiological trade-offs.

Key-words: Leaf economics spectrum; metabolic scaling theory; plant allometry; quantitative trait loci; *Arabidopsis thaliana*; functional trait; net photosynthetic rate; growth rate; flowering time; life history.

Introduction

Since Julian Huxley (1932) showed that traits covaried with each other according to simple mathematical relationships, understanding covariation of traits within integrated phenotypes has been a central focus of comparative biology (Gould 1966, Coleman et al. 1994). Organismal size is a central trait in biology and influences how numerous traits and ecological processes, and dynamics covary (Niklas 1994). The dependence of a given biological trait, *Y*, on organismal mass, *M*, is known as allometry (Huxley 1932). Allometric relationships are characterized by 'power laws' where traits vary or scale with *M* as:

$$Y = Y_0 M^{\theta} \quad (1)$$

where θ is the scaling exponent and Y_0 is a normalization constant that may be characteristic of a given genotype or taxon. A sampling of *intra*- and *inter*-specific data reveals that the central tendency of θ often approximates quarter-powers (Niklas 1994; e.g., 1/4, 3/4, 3/8, etc.), although for any given relationship considerable variation may exist (Glazier 2005, Price et al. 2010) and the 'canonical' value of θ is still debated (Riisgard 1998, Kolokotrones et al. 2010), notably within vascular plants (Reich et al. 2006, Enquist et al. 2007b, Mori et al. 2010).

In addition to allometric scaling, other scaling relationships between traits have also been reported. For example, the trade-offs that govern the carbon and nutrient economy of plants appear to generate trait covariation functions that are also approximate power-laws (Reich et al. 1997, Westoby et al. 2002). Indeed, the nexus of trait correlations that makes up the leaf economics spectrum (LES) reflects the fundamental trade-off between the rate of acquisition of resources and lifespan (Charnov 1993, Reich et al. 1997, Wright et al. 2004, Shipley et al. 2006, Blonder et al. 2011). The LES describes how multiple physiological and morphological leaf traits, including net photosynthetic rate, dry mass per area (LMA), longevity, and nitrogen (N) concentration, covary across vascular plant taxa. This spectrum of covariations reflects the fact that leaves with long lifespan require more structural investment (associated with high LMA, reduced CO_2 permeability and light intensity inside the leaf), and a low mass-based photosynthetic and respiration rate (Kikuzawa 1991, Reich et al. 1997, Wright et al. 2004, Blonder et al. 2011). Conversely, high rates of photosynthesis are characterized by low LMA values. Further, low LMA leaves are more vulnerable to herbivory and physical damages (Kikuzawa 1991, Westoby et al. 2002). The LES appears to be universal across biomes and has been applied to understand functional variation in scaling

relationships at whole-plant (Baraloto et al. 2010) and community (Kikuzawa and Lechowicz 2006) levels.

Metabolic scaling theory (MST) posits that various scaling exponents in biology – most notably, the scaling of whole plant metabolism (*B*) and growth rate (*dM/dt*) with *M* – are the result of natural selection on the scaling of whole-plant resource use. In particular, MST hypothesizes that for volume-filling vascular networks, natural selection will act to maximize the scaling of whole-organism resource uptake but simultaneously minimize the scaling of vascular transport resistance (West et al. 1999). As a result, values of θ will tend to cluster around 'quarter-powers' so that $dM/dt \propto B \propto M^{3/4}$. However, in making this assumption, MST implicitly assumes that there is potential variation in θ and that this variation is heritable (Enquist and Bentley 2012). Indeed, elaborations of MST openly state that selection is expected to act on θ (Price et al. 2007, Olson et al. 2009) but we know of no examples showing a clear genetic basis to the scaling exponents highlighted by MST.

Similarly to MST, explanations for the LES are framed in the context of how selection optimizes the trade-off between investment for organ longevity and return on investment in carbon and nitrogen (Kikuzawa 1991, Westoby et al. 2000). Because of the physiological linkages between the traits that govern leaf economics, the global variation of many of the LES traits have been hypothesized to be under the control of a common genetic mechanism (Chapin et al. 1993). Consistent with this hypothesis, several pleiotropic genes underlying many continuous traits related to plant development, physiology and growth have been identified in Arabidopsis (e.g. McKay et al. 2003, Masle et al. 2005, Fu et al. 2009, Mendez-Vigo et al. 2010) and other species (e.g. Poorter et al. 2005, Edwards et al. 2011). The evolutionary importance of pleiotropic genes in explaining observed coordinated changes in covarying traits has been intensively debated (e.g. Pavlicev and Wagner 2012). Because of the difficulty of measuring traits related to carbon fixation (but see Edwards et al. 2011, Flood et al. 2011), the genetic bases underlying plant life histories and the LES remained to be elucidated. Thus, the role of pleiotropic genes and genetic constraints in shaping the evolutionary dynamics of plant functional diversity is unclear (Donovan et al. 2011).

Arguments for the origin of the scaling relationships described by the LES and MST have not been tested. In particular, they make two implicit evolutionary assumptions. First, they assume that there is variation in the subsidiary traits underpinning scaling relationships. Secondly, they assume that subsequent Darwinian selection on scaling relationships occurs at the *intra*-specific level. However, studies that have assessed the predictions and generality of the LES and MST have mainly been conducted at the *inter*-specific level. Here, we test the

evolutionary assumptions of botanical scaling theory. We characterized the scaling of carbon and nutrient economics and the allometric scaling of growth rate across numerous Arabidopsis genotypes spanning 3 orders of magnitude in size.

We utilized a powerful high-throughput phenotyping platform (Granier et al. 2006) to grow a population of recombinant inbred lines or RILs under strictly controlled environmental conditions. Two pleiotropic quantitative trait loci (QTL) with major effects (*EDI* and *FLG*) have been identified through the analysis of plant development and life history in these RILs (Alonso-Blanco et al. 1998, El-Assal et al. 2001, Doyle et al. 2005, Fu et al. 2009). Allelic variability in these genes leads to a corresponding diversity in the timing of flowering, the rate of leaf production and the general pattern of vegetative growth (Mendez-Vigo et al. 2010). We hypothesize that variation in life history, in particular the time to reach reproductive maturity, has important consequences for the lifetime carbon and nutrient budget at the leaf and whole-plant levels. As a result, selection should act on the scaling of carbon and nutrient budgets via the traits that underlie their physiological rates and life histories.

Materials and methods

Plant material

We analyzed genetic variability in leaf economics and the scaling of plant growth across the RILs previously generated from a cross between Landsberg *erecta* (L*er*) and Cape Verde Islands (Cvi) (Alonso-Blanco et al. 1998), two accessions that derived from contrasted locations. We also selected near isogenic lines (NILs) and targeted mutants to confirm the quantitative trait loci (QTL) identified from the genetic analysis and test candidate genes, respectively. NILs were chosen from the population previously developed by introgressing genomic regions Cvi into L*er* (Keurentjes et al. 2007). The NIL LCN 1-2.5 (NASC code N717045; Cvi-EDI_{Ler}) carries a Cvi fragment at the top of chromosome I and was selected to confirm the *EDI* locus. LCN 5-7 (N717123; Cvi-FLG_{Ler}) carries a Cvi fragment in the middle of chromosome V and was selected to confirm the *FLG* locus. Genetic and molecular studies have identified two candidate genes of the regulatory pathway of circadian clock as major contributors of *EDI* and *FLG* effects: *CRY2*, a gene coding a blue-light receptor (El-Assal et al. 2001), and *HUA2*, a gene coding a transcription factor of the AGAMOUS pathway (Doyle et al. 2005), respectively. We selected two knock-out mutants to investigate the candidate gene *CRY2*: one in Col-4 background (N3732; $cry2_{Col}$) and one in L*er* background (N108; $cry2_{Ler}$). To investigate the candidate gene *HUA2*, we selected a knock-out mutant of *HUA2*

in Col-0 (N656341; *hua2*$_{Col}$). The choice of Col background was motivated by the collection of mutants available in stock centers.

Growth conditions

We performed two experiments utilizing the PHENOPSIS automated growth chamber (Granier et al. 2006). The PHENOPSIS facility maintains constant growing environment and allows for the precise temporal monitoring and automated measurements of 504 potted plants. In Experiment 1, we phenotyped the parental accessions (L*er* and Cvi; n = 8 replicates) and 120 RILs (n = 4) selected from the 162 available lines (See Appendix S1 in Supporting Information). Plants were grown in four randomized blocks. In Experiment 2, we phenotyped the two parental accessions (n = 8), 16 RILs (n = 6) spanning the range of trait variability observed in Experiment 1, the NILs (n = 7), and the mutants and associated wild-types (both n = 10). All detailed growing and meteorological conditions are given in Appendix S1 and Table S1 therein, in Supporting Information.

Measurements of plant traits

The total projected leaf area of the rosette (RA, cm^2) was determined every 2 to 3 days from zenithal images of the plants. A sigmoid curve was fitted for each plant following:

$$RA = \frac{a}{1+e^{\left(\frac{(d-d_0)}{b}\right)}} \quad (1)$$

where d is the number of days after emergence of the firsts two true leaves, a is the maximum vegetative rosette area, d_0 is the time when a/2 leaf area has expanded and b is related to the maximum rate of leaf production. The maximum rate of leaf expansion (R_{max}, m^2 d^{-1}) was calculated from the first derivative of the logistic model at d_0 as $R_{max} = a/(4b)$.

Photosynthesis was measured at flowering and under growing conditions using a whole-plant chamber prototype designed for Arabidopsis by M. Dauzat (INRA, Montpellier, France) and K.J. Parkinson (PP System, UK) and connected to an infrared gas analyzer system (CIRAS 2, PP systems, USA). To insure plant gas exchange was not corrupted by soil respiration, we sealed the soil surface with four layers of plastic film. The flowering stem was detached from the rosette before measurement to record leaf gas exchange only. Whole-plant photosynthetic rate was expressed on a dry mass basis (nmol g^{-1} s^{-1}).

All plants were harvested after photosynthetic measurements. Each rosette was cut, wrapped in moist paper and kept at 4 °C overnight in darkness to achieve complete rehydration. Leaf blades were then separated from their petiole and scanned for area measurements. Next, both were oven-dried at 65 °C for 72 h and their dry weight was

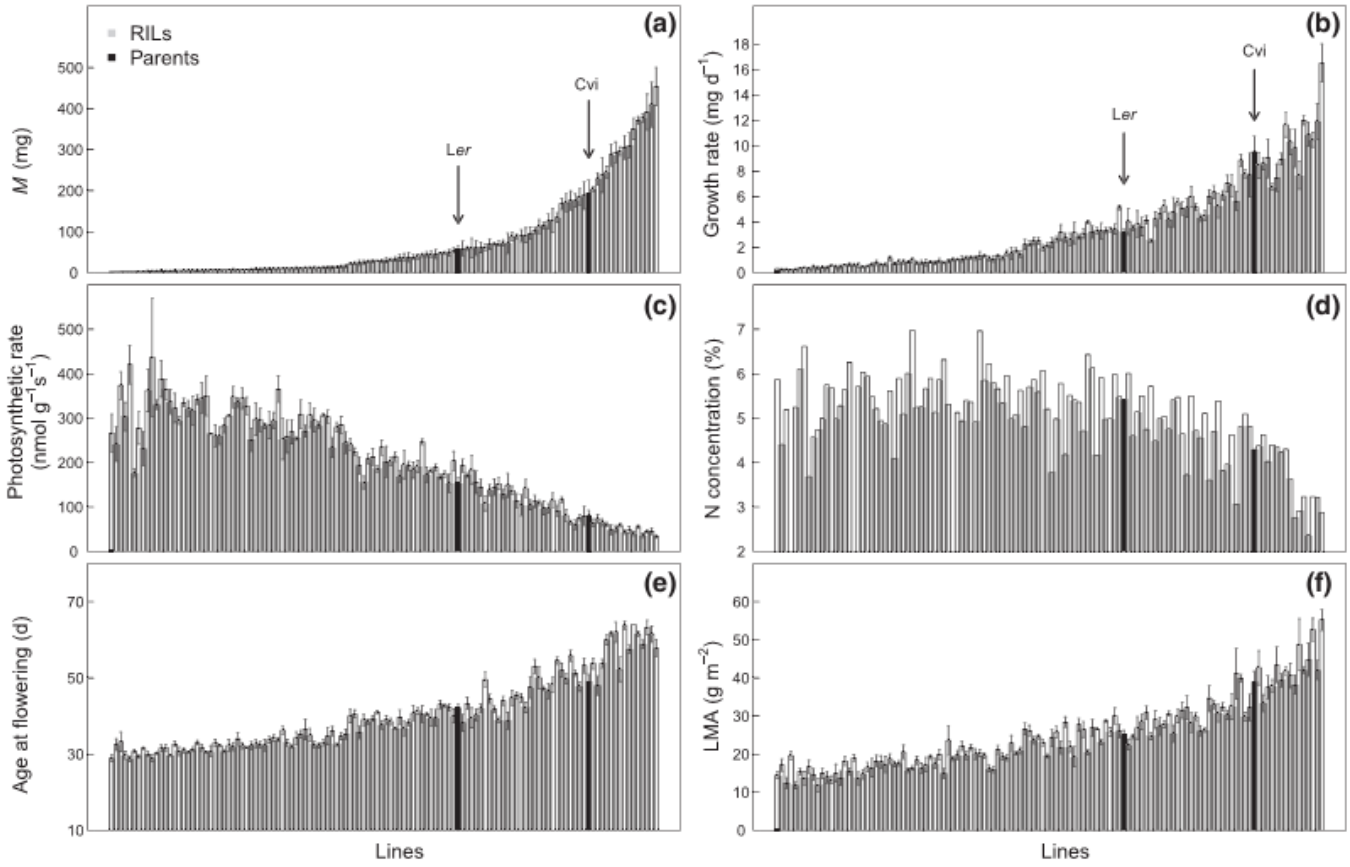

Figure 1. Variation of physiological and growth-related traits in the *A. thaliana* L*er* × Cvi RILs population. (a) plant dry mass (*M*); (b), growth rate; (c), mass-based photosynthetic rate; (d), N concentration; (e) age at flowering and (f) leaf dry mass per area (LMA). Bars are means ± *se* for each RIL (*n* = 4 except for N concentration *n* = 1) and for the parents (L*er* and Cvi; arrows; *n* = 8 except for N concentration *n* = 1). Data from Experiment 1. Lines ordered by increasing plant dry mass.

determined. Aboveground plant dry mass (*M*, mg) was determined as the sum of dry mass of petioles and blades. Total leaf area (cm^2) was determined as the sum of individual leaf blade areas. Leaf dry mass per area (LMA, g m^{-2}) was calculated as the ratio of dry mass and total leaf area. Assuming that LMA did not vary over time during the period of maximum expansion rate, we calculated maximum absolute growth rate (*G*, g dry mass d^{-1}) from R_{max} and LMA. In order to obtain sufficient dried material for chemical analyses, leaf blades and petioles were ground together to determine N concentration by mass spectrometry (EA2000, Eurovec, Isoprime, Elementar). Leaf lifespan was estimated from the oldest active leaf that showed some signs of senescence at harvest from the daily pictures of the 16 RILs in Experiment 2. This estimation was used to test the relationship between age at flowering and leaf lifespan (See Appendix S2). Traits were measured on each individual, except N concentration which was measured on a single replicate in Experiment 1 and on three replicates in Experiment 2. Phenotypic data are stored in the PHENOPSIS database (see Appendix S1).

Statistical analyses

We first assessed the allometric relationship between aboveground dry mass (*M*) and maximum absolute growth rate (*G*) across all RILs by fitting a linear model: $\log_{10}(G) = \log_{10}(b_0) + b_1\log_{10}(M)$. Inspection of the residuals from this model revealed a significant departure from linearity (Figs S1 and S2). Next, following Kolokotrones et al. (2010), we fit a nonlinear quadratic model: $\log_{10}(G) = \log_{10}(b_0) + b_1\log_{10}(M) + b_2(\log_{10}(M))^2$, using the Generalized Estimation Equation (*gee* package in the statistical program R 2.12). The slope θ_q of the quadratic at any given *M* value was calculated as the derivative of the quadratic function $\theta_q = b_1 + 2b_2\log_{10}(M)$.

Broad-sense heritability (H^2) of each trait was estimated as the ratio of (among – within) lines (RILs) to total (among + within) variance components with replicate plant within RIL treated as random effect (R/*nlme* package).

We used 144 AFLP markers spanning all the genome to perform a QTL analysis of all traits by composite interval mapping (R/*qtl* package). For each trait, 5%-level significance threshold for QTL LOD scores were calculated following 1000 permutations. Here, this threshold did not exceed 2.9. Relationship QTL (rQTL) were detected by testing the allelic effect on the major axis slope of the allometric relationship at each locus (Tisne et al. 2008; Fig. S3, Pavlicev and Wagner 2012).

Table 1. Correlations between traits, heritabilities and percentage of variation explained by the loci *EDI* and *FLG* in the recombinant inbred lines. Pearson's correlations (lower matrix). Broad-sense heritabilities (H^2). Plant dry mass (M); allometric exponent (θ_q); leaf dry mass per area (LMA). No epistatic interactions were found between *EDI* and *FLG* ($P > 0.05$) except for N concentration (see Supporting Information). Data from Experiment 1.

	M	Growth rate	θ_q	Age at flowering	Photosynthetic rate	LMA	H^2 (%)	EDI (%)	FLG (%)
M							0.89	23.8	21.4
Growth rate	0.98						0.84	25.8	19.5
θ_q	-0.98	-0.96					0.90	33.8	21.9
Age at flowering	0.96	0.91	-0.97				0.82	26.8	23.1
Photosynthetic rate	-0.92	-0.86	0.94	-0.95			0.80	29.3	19.1
LMA	0.94	0.93	-0.94	0.93	-0.93		0.68	25.2	21.3
N concentration	-0.60	-0.53	0.66	-0.67	0.72	-0.66	-	19.1	16.4

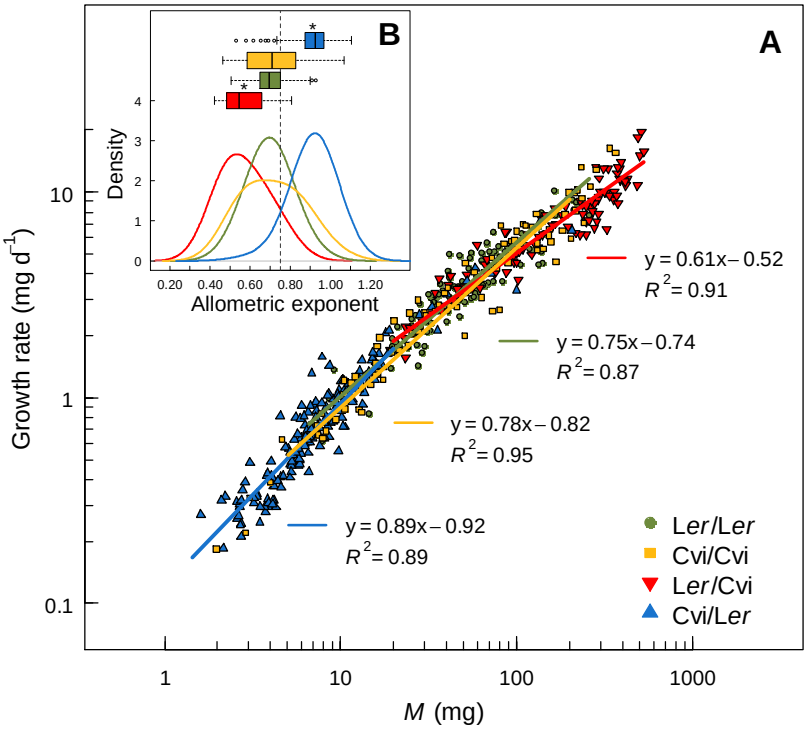

Figure 2. *EDI* and *FLG* effects on the allometric scaling of plant growth. (A) Regression lines and equations (standardized major axis) of the relationships between aboveground plant dry mass (M) and growth rate shown across individuals for the four sub-populations defined by the two loci *EDI* and *FLG*. Parental types Cvi/Cvi (yellow squares) and L*er*/L*er* (green circles), and recombinant types Cvi/L*er* (blue upward triangles) and L*er*/Cvi (red downward triangles) at the two loci *EDI*/*FLG*, respectively. (B) Density distributions and box-and-whisker plots of the local allometric exponent θ_q according to the allelic combination at the two QTL (same colors used). Vertical dotted line: expected θ value (0.75) of allometric exponent following MST predictions. Asterisks represent significant differences from 0.75 ($P < 0.001$). Data from Experiment 1.

Results

Across the RILs, we observed a considerable amount of trait variation. All of the morphological, physiological and growth-related traits showed significant between-line variance ($P < 0.001$) despite the weak differences between the parental accessions L*er* and Cvi (Fig. 1 and Table S2). Interestingly, the range of variation in these traits was often a considerable fraction of the global variation in these traits (see Fig. S4). Broad sense heritabilities ranged from 0.68 (LMA) to 0.89 (plant dry mass) (Table 1). Such high heritability values reflect the important role of genetics in determining the observed trait variation, and also point to the low environmental variability within the PHENOPSIS automaton (e.g. lack of significant block effect for all traits (all $P > 0.10$)).

Our results show that, in accordance with MST predictions, the maximum absolute plant growth rate (G), across all RILs, scaled to the ¾-power of plant dry mass (M) (Fig. 2; $G = 6.32M^{0.76}$; $R^2 = 0.96$). However, a quadratic model better fitted to the allometric relationship so that as plant mass increases, there is a progressive shallowing of the allometric exponent, θ (Figs S1 and S2). However, as we show below, this curvilinearity was generated by a shift in scaling exponent across RILs.

Next, we determined if there was a genetic basis to the observed variation in allometric scaling. We performed a QTL detection for the allometric growth exponent, θ_q, estimated for each RIL by fitting the quadratic model, and a rQTL analysis of the relationship scaling. These two analyses identified two loci that control variation in the allometric exponent (LOD score > 2.9; Figs 3A and S3) and exhibit additive effects. These loci were: *EDI*, located at the top of chromosome 1 (CI = [5; 11] cM), and *FLG* in the middle of chromosome 5 (CI = [37; 45] cM). Their additive effect explained 68% of the total variability in θ_q (Table 1; Fig 3A and Fig. S5). As previously found through the dissection of Arabidopsis' life history (Alonso-Blanco et al. 1998, Mendez-Vigo et al. 2010), these two QTL were also the major determinants of age at flowering (Fig. 3B), indicating that variation in θ_q is also associated with life history variation. We found that the subsets of RILs carrying the parental combinations at *EDI* /*FLG* loci (parental types; i.e. L*er*/L*er* and Cvi/Cvi) shared a *common* allometric slope ($P = 0.34$) that did not differ significantly from ¾ ($\theta = 0.77$; CI = [0.74; 0.80]; Fig. 2). However, the recombinant types at *EDI* /*FLG* loci displayed either significantly higher (Cvi/L*er*; $\theta = 0.89$; CI = [0.85; 0.94]) or significantly lower (L*er*/Cvi; $\theta = 0.61$; CI = [0.58; 0.65]) scaling exponents (both $P < 0.001$; Fig. 2). Our analysis revealed no epistatic interactions between *EDI* and *FLG* ($P > 0.05$ except for N concentration, see Fig. S5).

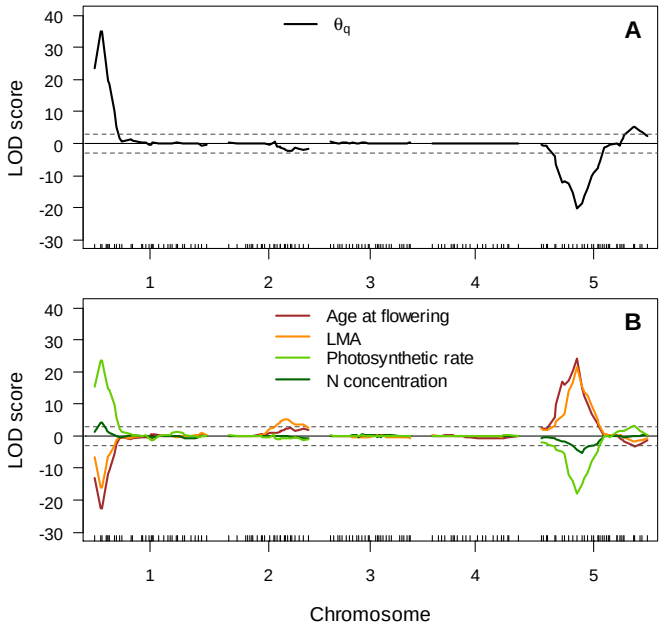

Figure 3. QTL analysis of the allometric exponent of plant growth and of the traits underlying the leaf economics. Likehood value of a QTL presence at the specified position along the five chromosomes (LOD score) for (A) the allometric exponent of plant growth (θ_q), and (B) the traits underlying the leaf economics. LMA: leaf dry mass per area. Dotted lines: maximum significance threshold across traits (2.9). Data from Experiment 1.

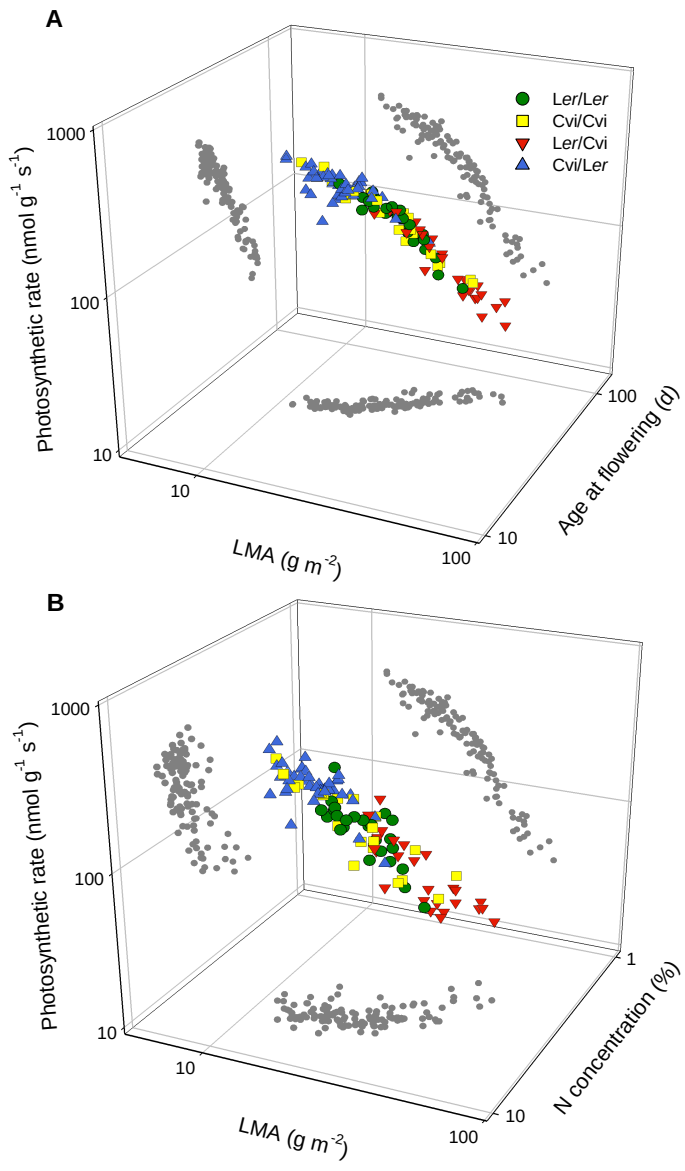

Figure 4. *EDI* and *FLG* effects on the patterns of correlation between the traits underlying the leaf economics in the *A. thaliana* Ler × Cvi RILs population. Each point is the mean value of four replicates per RIL (except for N concentration, n = 1). Parental types Cvi/Cvi (yellow squares) and L*er*/L*er* (green circles), and recombinant types Cvi/L*er* (blue upward triangles) and L*er*/Cvi (red downward triangles) at the two loci *EDI*/*FLG*, respectively. LMA: leaf dry mass per area. Bivariate relationships are shown on 2D plans (grey dotted symbols). See Table 1 for correlation statistics. Data from Experiment 1.

A strong pattern of covariation was found across RILs between the physiological and morphological traits involved in the leaf economics spectrum, LES. We found that mass-based net photosynthetic rate and N concentration were positively correlated, whereas they were negatively correlated with age at flowering and LMA (Table 1; Fig. 4). Our genetic analysis revealed that *EDI* and *FLG* are also major pleiotropic QTL with additive effects that explained 63%, 56%, 60% and 35% of the variability in age at flowering, LMA, mass-based photosynthetic rate and N concentration, respectively (Table 1; Figs 3B and S5). As a result, we observed strong correlations between these traits and the allometric exponent, θ_q (Table 1). Values of θ_q were positively correlated with variation in traits related to carbon fixation (photosynthetic rate and N concentration) and negatively correlated with the traits related to organ longevity (age at flowering and LMA). Together these results demonstrate that differing allelic combinations at the *EDI* and *FLG* loci result in plants displaying significant differences in leaf economics (Figs 4 and S6) with concomitantly significant changes in metabolic exponent (Figs 2 and 4). Nonetheless, each of the parental types did not exhibit significant changes in θ_q and each was characterized by the predicted 'optimal' ¾-power allometric scaling of growth rate and intermediate LES strategies. In contrast, recombinant types showed extreme LES and MST phenotypes characterized by either strongly hastened or delayed flowering life histories. These extremes in life history are characterized by either increased or decreased LES traits and steeper or shallower allometric exponents, respectively (Fig. 2).

The role of *EDI* and *FLG* in controlling the allometric scaling of plant growth and the traits that underlie leaf economics was confirmed in Experiment 2. A high reproducibility of the phenotypes was observed among the 16 RILs grown in both experiments (correlations between trait values $r_{Spearman} > 0.93$ and $P < 0.001$). Across these 16 RILs, we observed significant differences in LES traits (Fig. S7) and allometric slopes (Fig. S8) according to the allelic combination at *EDI* and *FLG* loci. Although the values of the exponent θ_q varied from 1.33 to 0.57, the values of the parental types were again not significantly different from 0.75 ($P > 0.35$ in both parental types; Fig. S8), as observed in Experiment 1. Moreover, the introgressions of the Cvi chromosomal region carrying *EDI* or *FLG* into L*er* significantly hastened (Cvi-EDI_{Ler}) or delayed flowering (Cvi-FLG_{Ler}), respectively (Fig. 5 and Table S2), with an associated decreased or increased plant size, growth rate, LMA, photosynthetic rate and *N* concentration in a coordinated way (Fig. 5 and Table S2). For the 16 RILs grown in Experiment 2, we found a highly significant relationship between the lifespan of the oldest senescing leaf and age at flowering ($R^2 = 0.86$; $P < 0.001$; Fig. S9) indicating that at least in this population, age at flowering is a reasonable proxy for mean lifespan of the first leaves.

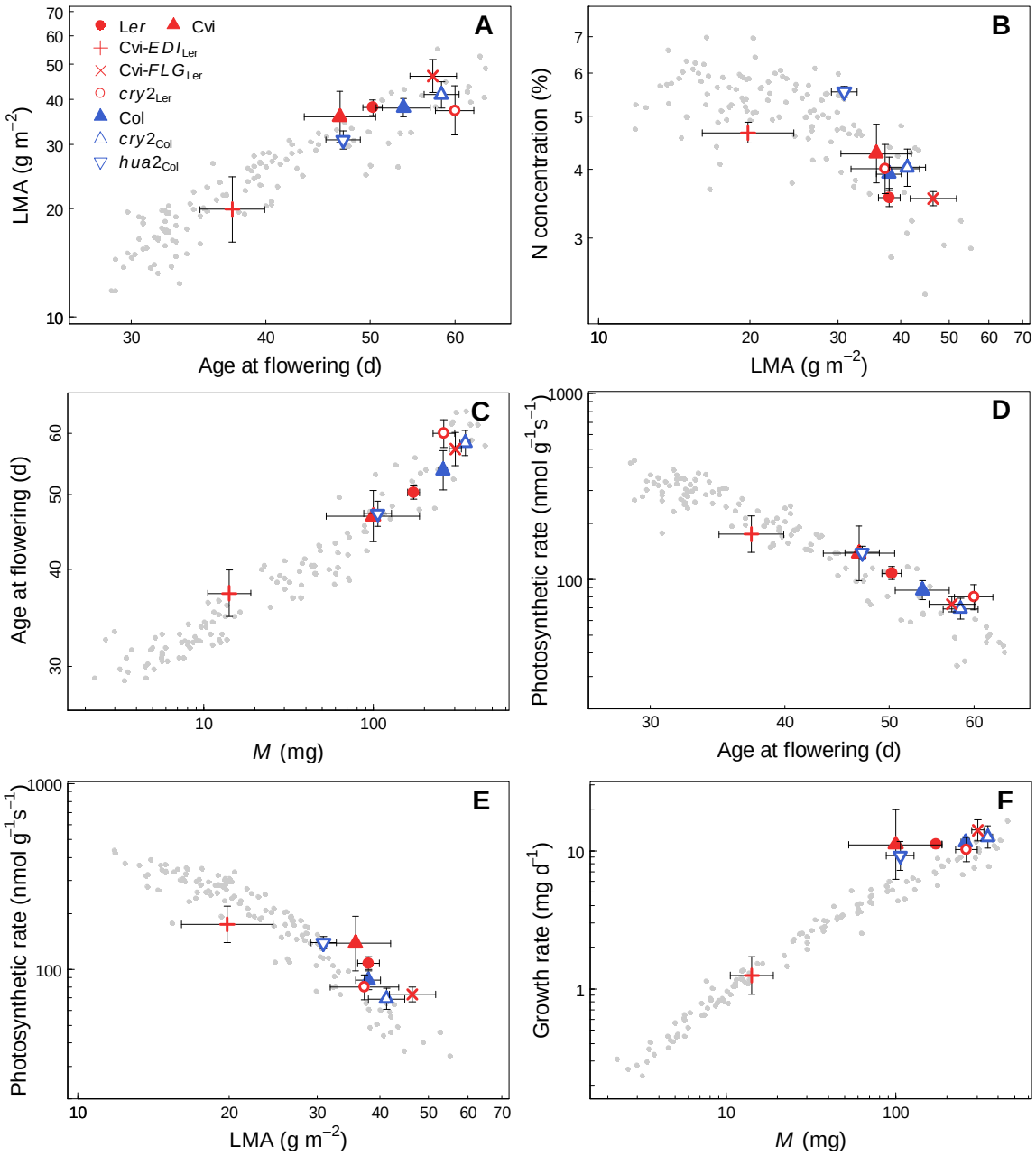

Figure 5. QTL confirmation and validation of *CRY2* and *HUA2* as major contributors of the variation in leaf economics and scaling allometry of plant growth in Arabidopsis. Projections of mean ± sd (n = 3-10) trait values of NILs, KO-mutants and wild-types (Experiment 2) in the patterns of leaf economics (A-E) and allometric scaling relationships (F) observed across RILs (Experiment 1, grey points). NILs are Cvi fragments introgressed into L*er* at the top of chromosome I (Cvi-EDI_{Ler}; red plus sign) and in the middle of chromosome V (Cvi-FLG_{Ler}; red cross). $cry2_{Ler}$ (red circle) and $cry2_{Col}$ (blue point up triangle) are KO-mutants of *CRY2* in L*er* (red filled circle) and Col (blue filled triangle) genetic backgrounds, respectively. $hua2_{Col}$ (blue point down triangle) is a KO-mutant of *HUA2* in Col background. Cvi (red point up triangle). Leaf dry mass per area (LMA); plant dry mass (M).

Lastly, we investigated the candidate genes, *CRY2* and *HUA2* as major contributors of *EDI* and *FLG* effects, respectively. The $hua2_{Col}$ KO-mutant displayed significant changes in leaf economics ($P < 0.05$ for all traits; Table S2 and Fig. 5), whereas the *CRY2* ($cry2_{Ler}$ and $cry2_{Col}$) KO-mutants displayed strong differences in age at flowering and less difference in photosynthetic rate, LMA and N concentration (Table S2 and Fig. 5). We found no difference in the phenotypes of $cry2_{Ler}$ and $cry2_{Col}$, suggesting that the genetic background did not influence our results. Finally, the effects of *CRY2* and *HUA2* on growth strategy were confirmed since NILs and mutants displayed significant changes in plant mass but no changes in growth rate, indicating a departure from the allometric relationship.

Discussion

In this paper we assessed several of the implicit assumptions of MST and the LES. We demonstrated that a few genes can generate a large fraction of variation in MST exponents and LES traits. Within Arabidopsis, these genes appear to be responsible for constraining the covariation of the leaf economics and the allometric scaling of plant growth. Based on our findings we propose a novel conceptual framework that links the principles of MST to the LES.

Our findings support two central evolutionary assumptions of MST. First, MST implicitly assumes that selection can act on metabolic scaling exponents. In other words, there is genetic variation in metabolic scaling that selection can act upon. Interestingly, as previously observed for *inter*-specific metabolic allometric scaling of mammals (Kolokotrones et al. 2010) and plants (Enquist et al. 2007a, Mori et al. 2010) the relationship between whole-plant growth rate and plant biomass across RILs was curvilinear and not a pure power-law. This decrease in allometric exponent within increased size is also consistent with the decline in relative growth rate or RGR with size observed in other species (Poorter et al. 2005; although these RGR studies have not typically controlled for allometric effects on RGR). Importantly, our results also show that the observed allometric curvilinearity was primarily due to a mixing of different exponents across genotypes. In other words, genetic variation for the metabolic growth exponent resulted in a curvilinear 'inter-RIL' scaling allometry. Second, the subsets of inbred lines carrying the parental (naturally occurring) allelic combinations at two specific QTL shared a *common* allometric exponent centered on ¾, whereas the recombinant types displayed higher and lower scaling exponents than the canonical '¾' hypothesized by MST (Fig. 2). These findings are consistent with a core MST

assumption that 'quarter-power' scaling is the outcome of stabilizing selection on metabolic allometries (Enquist et al. 2007a). Interestingly, recombinant types were characterized by strongly hastened or delayed flowering, as well as increased or decreased photosynthetic rates, LMA, and N concentration, respectively (Fig. 4 and Fig. S5). Together, these findings suggest a tight coupling between life history, LES traits, and MST.

As stated by Wright et al. (2004), "*leaf lifespan describes the average duration of the revenue stream from each leaf constructed*". However, whole-plant growth rates and competitive ability depend not only on the photosynthetic rate of individual leaves, but also on the geometry and dynamics of a plant's canopy, and the pattern of energy allocation among all organs (Givnish 1988). We argue that, at least for annual plants in which all the leaves die almost simultaneously during the final stage of reproduction, whole-plant functioning should be tightly coupled to the lifespan of the plant (Charnov 1993). Indeed, a strong correlation between plant age at flowering and leaf longevity was found in this study and in the literature (Appendix S2 and Fig. S9). Although the comparison with the interspecific GLOPNET data (Wright et al. 2004) is limited due to the differences in the levels of measurement – leaf versus whole-plant level in this study –, the ratio of interquartile range for photosynthesis and LMA showed that our data span 70% and 55% of the variation in these traits, respectively (Fig. S4). In addition, the observed variation in the scaling exponents of growth rate within the RILs captures most of the variation in allometric exponents observed worldwide (Price et al. 2007). Measurements of plant growth and photosynthetic rate at the canopy level integrate the changes in architectural constrains associated with size, such as leaf shape and leaf overlapping. Hence, these measurements reflect the physiological trade-offs and the variation in leaf morphology such as LMA, occurring at the whole-plant level. In this view, we argue that the changes in rosette architecture are likely also associated with the nexus of traits and allometric covariation that we observed. In particular, departure from space-filling branching for light interception, is likely the reason why we observe departure from the 'allometrically ideal' MST ¾-power scaling of plant growth (Price et al. 2007).

The effects of the QTL responsible for the variation in the scaling relationships were confirmed in the targeted NILs for which a coordinated change in the traits related to the leaf economics was observed (Fig. 5 and Table S2). In most relationships we find that the parental accession L*er* was closer to the parental accession Cvi (intermediate positions) than to the NILs (extreme positions). This is probably due to the opposite and counterbalancing effects of *EDI* (e.g. Cvi allele decreases size and age at flowering whereas it increases photosynthetic

rate and N concentration) and *FLG* (e.g. Cvi allele increases size and age at flowering whereas it decreases photosynthetic rate and N concentration). Two genes, *CRY2* and *HUA2* have been shown to be the major contributors of *EDI* and *FLG* pleiotropic effects, respectively (Fu et al. 2009). Our results show that a single amino acid Val-to-Met replacement in the Cvi allele of *CRY2* and a premature codon stop in the L*er* allele of *HUA2* cause a cascade of large changes across numerous leaf physiological traits, and in the scaling of plant metabolism. This shift in metabolic scaling associated with the effects of *HUA2* is consistent with the change in the rate of leaf production reported by Mendez-Vigo et al. (2010). The Cvi ecotype carries a rare allele of *CRY2*, unique over more than 100 sequenced ecotypes (El-Assal et al. 2001), whereas the L*er* allele of *HUA2* is identified as common only in ecotypes from UK and Central Europe (Doyle et al. 2005, Wang et al. 2007). Moreover, Cvi is an unusual accession from the Cape Verde Islands which exhibit peculiar climatic conditions. Although contrasted phenotypes could be expected in the Cvi accession, we observed 'allometric ideal' ¾ exponent, intermediate timing of flowering and intermediate leaf economics in both parental types, despite the climatic differences in the parental sites of origin. We argue that these findings are in accordance with Metcalf and Mitchell-Olds (2009) who hypothesized that selection to optimize the size at reproduction without sacrificing leaf and whole-plant functioning has likely resulted in an intermediate timing of reproduction. This explanation does not necessarily imply that flowering time is the target of natural selection but rather that there are integrated physiological trade-offs linking life history, leaf economics and plant allometry.

Our results also appear consistent with predictions from the 'Selection, Pleiotropy and Compensation' (SPC) model of Pavlicev and Wagner (2012). Specifically, this Dobzhansky-Muller view of evolutionary dynamics states that within isolated or semi-isolated populations differing allelic associations of pleiotropic genes with major effects on life history and physiology underlie trait covariation patterns and are possibly responsible for deleterious changes in metabolic scaling. In artificially-generated RILs, the allelic association of a few genes with major effects often leads to remarkably extreme phenotypes. However, these extreme phenotypes likely would not be successful in nature compared to naturally occurring genotypes due to hybrid breakdown (Bomblies et al. 2007). Specifically, the observed ¾ scaling exponent could be then maintained by selection because crosses between populations create hybrid breakdown. Nonetheless, despite the strong genetic effect depicted by the high heritabilities observed here, we strongly suggest that future tests of the evolutionary role of pleiotropy in maintaining allometric scaling and life history trade-offs utilize transplant

experiments in the field. The massive collection of Arabidopsis accessions that are currently genotyped or sequenced (e.g. Hancock et al. 2011) offer a promising tool to further explore the genetic diversity, and elucidate the evolutionary and ecological links between variation in climate and the traits that define leaf economics and metabolic allometry.

Genetic constraints, which occur when the genes controlling many correlated traits have antagonist effects, have also been proposed to shape the LES by restricting the genetic variation for each trait combination (Reich et al. 1999, Donovan et al. 2011). Using a mutant approach we show clear evidence that silencing the pleiotropic genes underlying the LES did not result in aberrant (i.e. out of the RILs pattern) or non-viable phenotypes but instead resulted in a coordinated adjustment of all physiological leaf traits. This result suggests that the LES is 'hardwired' into the genome. Specifically, due to direct pleiotropic effects or indirect physiological linkages, *CRY2* and *HUA2* constrain the space of possible trait values so as to avoid a change in one trait without a change in other correlated traits. Differences between phenotypes of NILs and mutants (such as between Cvi-FLG_{Ler} and $hua2_{Col}$) can be explained by (*i*) the effect of the genetic background, (*ii*) the contrasted effects of silencing one gene in KO-mutants versus carrying a natural variant of this gene in NILs, or (*iii)* the effects of other genes in the introgressed regions. As suggested by the differences in the phenotypes of $cry2_{Ler}$ and Cvi-EDI_{Ler}, unknown genes, linked to *CRY2* and *HUA2* in *EDI* and *FLG* respectively, could contribute to the QTL effects. For instance, *HUA2* has been shown to be mediated by the effect of a co-locating QTL, *FLC*, that acts as a positive regulator of *HUA2* effects (Mendez-Vigo et al. 2010). Together these findings suggest that genetic constraints limit the range of leaf trade-offs to a spectrum of covariations, but selection on major pleiotropic genes could arise inside the spectrum for a plant to take advantage of, depending on the environment, different optimal combinations of leaf economics.

We propose that, in general, across environmental gradients selection will act on leaf economics traits to select for genotypes that maintain an approximate ¾-power scaling of growth, but yet different LES trait values and thus result in the local adaptation of populations (Mitchell-Olds and Schmitt 2006, Alonso-Blanco et al. 2009). This does not necessarily imply that selection, in certain environments, could result in different values of the allometric exponent (Price et al. 2007) but rather is consistent with the general argument made by both LES and MST that, ultimately, botanical scaling relationships are the outcome of natural selection (West et al. 1999, Enquist et al. 2007b). If the same pleiotropic mechanism is general across Embryophytes then multiple *intra*- and *inter*-specific scaling relationships at the leaf and whole-plant levels could be tightly linked to genetic variability in few genes.

Conclusion

MST has been criticized on empirical, statistical, and theoretical grounds (e.g. Riisgard 1998, Glazier 2005, Reich et al. 2006) in part because of the difficulty in testing its basic assumptions (Enquist and Bentley 2012). Our study, for the first time, tests several of the fundamental evolutionary assumptions that underlie MST. Similarly, by translating the trade-offs between structural investment for longevity and return on investment in carbon and nitrogen, the LES has been hypothesized to be the outcome of natural selection to optimize leaf carbon balance within a given environment (Reich et al. 1999, Blonder et al. 2011, Donovan et al. 2011). Our results show that leaf economics and variation in metabolic allometries, at least in Arabidopsis, are intimately linked through the effects of key genes. Together, these findings support Chapin's (1993) hypothesis that variation in leaf and other plant metabolic traits have a common genetic underpinning and that evolutionary filtering of a small number of antagonistic pleiotropic genes could be at the origin of many botanical scaling relationships.

Acknowledgements

We thank M. Dauzat, A. Bédié, F. Bouvery, C. Balsera, J. Bresson and G. Rolland for technical assistance; M. Dauzat and K.J. Parkinson for designing the *Arabidopsis* whole-plant gas exchange chamber for CIRAS II. We thank N. Whiteman, M. Koornneef, S. Tisné, M. Reymond and B. Shipley for helpful comments, and J. Keurentjes for discussions on RILs and data supply. The authors are grateful to three anonymous reviewers for constructive comments and manuscript improvement. FV was funded by a CIFRE grant (ANRT, French Ministry of Research) supported by BAYER Crop Science (contract 0398/2009 - 09 42 008). CV was supported by a Marie Curie International Outgoing Fellowship within the 7th European Community Framework Program (DiversiTraits project, no. 221060). BJE was supported by an NSF ATB award.

References

Alonso-Blanco, C., M. G. M. Aarts, L. Bentsink, J. J. B. Keurentjes, M. Reymond, D. Vreugdenhil, and M. Koornneef. 2009. What has natural variation taught us about plant development, physiology, and adaptation? Plant Cell **21**:1877-1896.

Alonso-Blanco, C., A. J. M. Peeters, M. Koornneef, C. Lister, C. Dean, N. van den Bosch, J. Pot, and M. T. R. Kuiper. 1998. Development of an AFLP based linkage map of L*er*, Col and Cvi *Arabidopsis thaliana* ecotypes and construction of a L*er*/Cvi recombinant inbred line population. Plant Journal **14**:259-271.

Baraloto, C., C. E. T. Paine, L. Poorter, J. Beauchene, D. Bonal, A. M. Domenach, B. Herault, S. Patino, J. C. Roggy, and J. Chave. 2010. Decoupled leaf and stem economics in rain forest trees. Ecology Letters **13**:1338-1347.

Blonder, B., C. Violle, L. P. Bentley, and B. J. Enquist. 2011. Venation networks and the origin of the leaf economics spectrum. Ecology Letters **14**:91-100.

Bomblies, K., J. Lempe, P. Epple, N. Warthmann, C. Lanz, J. L. Dangl, and D. Weigel. 2007. Autoimmune response as a mechanism for a Dobzhansky-Muller-type incompatibility syndrome in plants. Plos Biology **5**:1962-1972.

Chapin, F. S., K. Autumn, and F. Pugnaire. 1993. Evolution of suites of traits in response to environmental stress. Am. Nat. **142**:S78-S92.

Charnov, E. L. 1993. Life history invariants : some explorations of symmetry in evolutionary ecology. Oxford University Press, Oxford England ; New York.

Coleman, J. S., K. D. McConnaughay, and D. D. Ackerly. 1994. Interpreting phenotypic variation in plants. Trends in Ecology & Evolution **9**:187-191.

Donovan, L. A., H. Maherali, C. M. Caruso, H. Huber, and H. de Kroon. 2011. The evolution of the worldwide leaf economics spectrum. Trends in Ecology & Evolution **26**:88-95.

Doyle, M. R., C. M. Bizzell, M. R. Keller, S. D. Michaels, J. D. Song, Y. S. Noh, and R. M. Amasino. 2005. HUA2 is required for the expression of floral repressors in *Arabidopsis thaliana*. Plant Journal **41**:376-385.

Edwards, C. E., B. E. Ewers, D. G. Williams, Q. G. Xie, P. Lou, X. D. Xu, C. R. McClung, and C. Weinig. 2011. The genetic architecture of ecophysiological and circadian traits in *Brassica rapa*. Genetics **189**:375-U1107.

El-Assal, S. E. D., C. Alonso-Blanco, A. J. M. Peeters, V. Raz, and M. Koornneef. 2001. A QTL for flowering time in Arabidopsis reveals a novel allele of *CRY2*. Nature Genetics **29**:435-440.

Enquist, B. J., A. P. Allen, J. H. Brown, J. F. Gillooly, A. J. Kerkhoff, K. J. Niklas, C. A. Price, and G. B. West. 2007a. Does the exception prove the rule? Nature **445**:E9-E10.

Enquist, B. J. and L. P. Bentley. 2012. Land Plants: New Theoretical Directions and Empirical Prospects. Pages 164-187 Metabolic Ecology. John Wiley & Sons, Ltd.

Enquist, B. J., B. H. Tiffney, and K. J. Niklas. 2007b. Metabolic scaling and the evolutionary dynamics of plant size, form, and diversity: toward a synthesis of ecology, evolution, and paleontology. International Journal of Plant Sciences **168**:729-749.

Fabre, J., M. Dauzat, V. Negre, N. Wuyts, A. Tireau, E. Gennari, P. Neveu, S. Tisne, C. Massonnet, I. Hummel, and C. Granier. 2011. PHENOPSIS DB: an information system for *Arabidopsis thaliana* phenotypic data in an environmental context. BMC Plant Biol **11**:77.

Flood, P. J., J. Harbinson, and M. G. Aarts. 2011. Natural genetic variation in plant photosynthesis. Trends in Plant Science **16**:327-335.

Fu, J., J. J. Keurentjes, H. Bouwmeester, T. America, F. W. Verstappen, J. L. Ward, M. H. Beale, R. C. de Vos, M. Dijkstra, R. A. Scheltema, F. Johannes, M. Koornneef, D. Vreugdenhil, R. Breitling, and R. C. Jansen. 2009. System-wide molecular evidence for phenotypic buffering in Arabidopsis. Nature Genetics **41**:166-167.

Givnish, T. J. 1988. Adaptation to sun and shade - a whole-plant perspective. Australian Journal of Plant Physiology **15**:63-92.

Glazier, D. S. 2005. Beyond the '3/4-power law': variation in the intra- and interspecific scaling of metabolic rate in animals. Biol. Rev. **80**:611-662.

Gould, S. J. 1966. Allometry and size in ontogeny and phylogeny. Biological Reviews **41**:587-640.

Granier, C., L. Aguirrezabal, K. Chenu, S. J. Cookson, M. Dauzat, P. Hamard, J. J. Thioux, G. Rolland, S. Bouchier-Combaud, A. Lebaudy, B. Muller, T. Simonneau, and F. Tardieu. 2006. PHENOPSIS, an automated platform for reproducible phenotyping of plant responses to soil water deficit in *Arabidopsis thaliana* permitted the identification of an accession with low sensitivity to soil water deficit. New Phytologist **169**:623-635.

Hancock, A. M., B. Brachi, N. Faure, M. W. Horton, L. B. Jarymowycz, F. G. Sperone, C. Toomajian, F. Roux, and J. Bergelson. 2011. Adaptation to climate across the *Arabidopsis thaliana* genome. Science **334**:83-86.

Huxley, J. S. 1932. Problems of relative growth. Methuen & co. LTD, London.

Keurentjes, J. J., L. Bentsink, C. Alonso-Blanco, C. J. Hanhart, H. Blankestijn-De Vries, S. Effgen, D. Vreugdenhil, and M. Koornneef. 2007. Development of a near-isogenic line population of *Arabidopsis thaliana* and comparison of mapping power with a recombinant inbred line population. Genetics **175**:891-905.

Kikuzawa, K. 1991. A cost-benefit-analysis of leaf habit and leaf longevity of trees and their geographical pattern. American Naturalist **138**:1250-1263.

Kikuzawa, K. and M. J. Lechowicz. 2006. Toward synthesis of relationships among leaf longevity, instantaneous photosynthetic rate, lifetime leaf carbon gain, and the gross primary production of forests. American Naturalist **168**:373-383.

Kolokotrones, T., V. Savage, E. J. Deeds, and W. Fontana. 2010. Curvature in metabolic scaling. Nature **464**:753-756.

Masle, J., S. R. Gilmore, and G. D. Farquhar. 2005. The *ERECTA* gene regulates plant transpiration efficiency in Arabidopsis. Nature **436**:866-870.

McKay, J. K., J. H. Richards, and T. Mitchell-Olds. 2003. Genetics of drought adaptation in *Arabidopsis thaliana*: I. Pleiotropy contributes to genetic correlations among ecological traits. Molecular Ecology **12**:1137-1151.

Mendez-Vigo, B., M. Andres, M. Ramiro, J. M. Martinez-Zapater, and C. Alonso-Blanco. 2010. Temporal analysis of natural variation for the rate of leaf production and its relationship with flowering initiation in *Arabidopsis thaliana*. Journal of Experimental Botany:1611-1623.

Metcalf, C. J. and T. Mitchell-Olds. 2009. Life history in a model system: opening the black box with *Arabidopsis thaliana*. Ecology Letters **12**:593-600.

Mitchell-Olds, T. and J. Schmitt. 2006. Genetic mechanisms and evolutionary significance of natural variation in *Arabidopsis*. Nature **441**:947-952.

Mori, S., K. Yamaji, A. Ishida, S. G. Prokushkin, O. V. Masyagina, A. Hagihara, A. T. M. R. Hoque, R. Suwa, A. Osawa, T. Nishizono, T. Ueda, M. Kinjo, T. Miyagi, T. Kajimoto, T. Koike, Y. Matsuura, T. Toma, O. A. Zyryanova, A. P. Abaimov, Y. Awaya, M. G. Araki, T. Kawasaki, Y. Chiba, and M. Umari. 2010. Mixed-power scaling of whole-plant respiration from seedlings to giant trees. Proceedings of the National Academy of Sciences of the United States of America **107**:1447-1451.

Niklas, K. J. 1994. Plant allometry - The scalling of form and process. First edition. The University of Chicago Press, Chicago.

Olson, M. E., R. Aguirre-Hernandez, and J. A. Rosell. 2009. Universal foliage-stem scaling across environments and species in dicot trees: plasticity, biomechanics and Corner's Rules. Ecology Letters **12**:210-219.

Pavlicev, M. and G. P. Wagner. 2012. A model of developmental evolution: selection, pleiotropy and compensation. Trends in Ecology & Evolution **27**:316-322.

Poorter, H., C. P. E. van Rijn, T. K. Vanhala, K. J. F. Verhoeven, Y. E. M. de Jong, P. Stam, and H. Lambers. 2005. A genetic analysis of relative growth rate and underlying components in *Hordeum spontaneum*. Oecologia **142**:360-377.

Price, C. A., B. J. Enquist, and V. M. Savage. 2007. A general model for allometric covariation in botanical form and function. Proc Natl Acad Sci U S A **104**:13204-13209.

Price, C. A., J. F. Gilooly, A. P. Allen, J. S. Weitz, and K. J. Niklas. 2010. The metabolic theory of ecology: prospects and challenges for plant biology. New Phytologist **188**:696-710.

Reich, P. B., D. S. Ellsworth, M. B. Walters, J. M. Vose, C. Gresham, J. C. Vollin, and W. D. Bowman. 1999. Generality of leaf trait relationships: a test across six biomes. Ecology **80**:1955-1969.

Reich, P. B., M. G. Tjoelker, J. L. Machado, and J. Oleksyn. 2006. Universal scaling of respiratory metabolism, size and nitrogen in plants. Nature **439**:457-461.

Reich, P. B., M. B. Walters, and D. S. Ellsworth. 1997. From tropics to tundra: global convergence in plant functioning. Proceedings of the National Academy of Sciences of the United States of America **94**:13730-13734.

Riisgard, H. U. 1998. No foundation of a "3/4 power scaling law" for respiration in biology. Ecology Letters **1**:71-73.

Shipley, B., M. J. Lechowicz, I. Wright, and P. B. Reich. 2006. Fundamental trade-offs generating the worldwide leaf economics spectrum. Ecology **87**:535-541.

Tisne, S., M. Reymond, D. Vile, J. Fabre, M. Dauzat, M. Koornneef, and C. Granier. 2008. Combined genetic and modeling approaches reveal that epidermal cell area and number in leaves are controlled by leaf and plant developmental processes in Arabidopsis. Plant Physiology **148**:1117-1127.

Wang, Q., U. Sajja, S. Rosloski, T. Humphrey, M. C. Kim, K. Bomblies, D. Weigel, and V. Grbic. 2007. HUA2 caused natural variation in shoot morphology of *A. thaliana*. Current Biology **17**:1513-1519.

West, G. B., J. H. Brown, and B. J. Enquist. 1999. A general model for the structure and allometry of plant vascular systems. Nature **400**:664-667.

Westoby, M., D. S. Falster, A. T. Moles, P. A. Vesk, and I. J. Wright. 2002. Plant ecological strategies: some leading dimensions of variation between species. Annual Review of Ecology and Systematics **33**:125-159.

Westoby, M., D. Warton, and P. B. Reich. 2000. The time value of leaf area. Am Nat **155**:649-656.

Wright, I. J., P. B. Reich, M. Westoby, D. D. Ackerly, Z. Baruch, F. Bongers, J. Cavender-Bares, T. Chapin, J. H. C. Cornelissen, M. Diemer, J. Flexas, E. Garnier, P. K. Groom, J. Gulias, K. Hikosaka, B. B. Lamont, T. Lee, W. Lee, C. Lusk, J. J. Midgley, M. L. Navas, U. Niinemets, J. Oleksyn, N. Osada, H. Poorter, P. Poot, L. Prior, P. VI, C. Roumet, S. C. Thomas, M. G. Tjoelker, E. J. Veneklaas, and R. Villar. 2004. The worldwide leaf economics spectrum. Nature **428**:821-827.

Supporting Information

Appendix S1. Supporting materials and methods

The selection of the 120 RILs was done on the basis of missing genotype data (99.9% genotyped) avoiding unbalanced parental-allele sampling (L*er*: 54.8%; Cvi: 45.2% against 55.6% and 44.4% in the original population).

Growing conditions

Five seeds from each genotype were sown at the soil surface in 225 mL pots filled with a mixture (1:1, v:v) of loamy soil and organic compost (Neuhaus N2). Pots were damped with sprayed deionized water three times a day and placed in the PHENOPSIS automaton in darkness (20 °C, 65% air relative humidity) until germination. After germination, plants were thinned out to one plant per pot and cultivated with a daily cycle of 12 h light supplied from a bank of HQi lamps which provided 190 µmol m^{-2} s^{-1} photosynthetic photon flux density at plant height. Water vapour pressure deficit was maintained at 0.6-0.7 kPa. Meteorological conditions were similar between experiments (see Table S1 below).

Soil water content was controlled before sowing to estimate the amount of dry soil and water in each pot. Soil water content was maintained at an optimal level (Granier et al. 2006) of 0.35 g H_20 g^{-1} dry soil with a modified one-tenth-strength Hoagland solution. Pot weight was automatically adjusted to reach the target soil water content by weighing and watering each individual pot every day.

All detailed meteorological data (recorded every 15 min) are available online at http://bioweb.supagro.inra.fr/phenopsis/ (Fabre et al. 2011).

Appendix S2. The relationship between timing of reproduction and lifespan.

In the main text, we argue that, at least for annual plants in which all the leaves die almost simultaneously during the final stage of reproduction, the whole-plant functioning should be in agreement with the lifespan of the plant. Consistent with this assumption, we found a high correlation between plant age at flowering and leaf longevity (see Fig. S8). In agreement with these results, Levey and Wingler (2005) found a tight link between the start of rosette senescence and the timing of the transition from vegetative to reproductive development (bolting) in a set of natural accessions of *Arabidopsis*, including L*er* and Cvi. This indicates that genotypes that flower later maintain a vegetatively active habit during a longer time period than early flowering ones. In agreement with the LES, this can be related to the variation in LMA observed in our study. In the same population of RILs Luquez et al. (2006) found a negative relationship between time to flowering and post-bolting rosette longevity under high nutrient growth conditions. This may obscure the analysis of resource allocation strategies at the whole-plant level. However, their results do not invalidate our claim since a reanalysis of their data showed a highly significant relationship between bolting and total longevity of the plant (r = 0.92 and 0.95 under low and high nutrient, respectively; both $P < 0.001$). Note that a significant positive relationship was found between bolting time as determined by Luquez et al. (2006) and flowering time as determined in our study (r = 0.85; $P < 0.001$). However, we acknowledge the need for further investigation across natural accessions and within local populations, and also in other species. In their genome-wide association study of 107 phenotypes, although no trait directly related to the LES was measured, Atwell et al. (2010) reported a highly significant correlation between flowering time and lifespan (r = 0.93; re-analysis of published data). In a recent study of RILs of the annual crop *Brassica rapa*, Edwards et al. (2011) found a positive relationship between LMA (measured at the whole-plant level) and days to flowering although it seems to depend on growth temperature and photoperiod. These authors also reported significant relationships between LMA, nitrogen content and photosynthesis (measured at the leaf level).

Supporting References

Atwell S., *et al.* (2010). Genome-wide association study of 107 phenotypes in *Arabidopsis thaliana* inbred lines. Nature, **465**:627-631.

Edwards C.E., *et al.* (2011). The genetic architecture of ecophysiological and circadian traits in *Brassica rapa*. Genetics, **189**:375-U1107.

Levey S. & Wingler A. (2005). Natural variation in the regulation of leaf senescence and relation to other traits in Arabidopsis. Plant Cell and Environ., **28**:223-231.

Luquez V.M., Sasal Y., Medrano M., Martin M.I., Mujica M. & Guiamet J.J. (2006). Quantitative trait loci analysis of leaf and plant longevity in *Arabidopsis thaliana*. Journal of Experimental Botany, **57**:1363-72.

Table S1. Meteorological data in the two experiments. Mean value ± sd of day and night air temperature (°C), air vapor pressure deficit (VPD, kPa) and light intensity (PPFD, µmol m^{-2} s^{-1}).

		Air temperature (℃)	VPD (kPa)	PPFD (µmol m^{-2} s^{-1})
day	exp1	20.06 ±0.08	0.74 ±0.12	188.84 ±10.9
	exp2	20.12 ±0.25	0.69 ±0.11	180.39 ±10.4
night	exp1	19.65 ±0.24	0.62 ±0.14	0.08 ±0.16
	exp2	16.95 ±0.29	0.45 ±0.09	1.66 ±1.44

Table S2. Effects of Cvi introgressions in L*er* (NILs) and mutations in *CRY2* and *HUA2* on functional traits. Values are the ratio of mean phenotypic values (data from Experiment 2). Each NIL introgressed at *EDI* (Cvi-EDI_{Ler}) and *FLG* (Cvi-FLG_{Ler}) was compared to the parental lines (L*er* and Cvi). Parents were also compared for all traits. Each mutant at *CRY2* ($cry2_{Col}$ in Col-4 background and $cry2_{Ler}$ in L*er*-0 background), and at *HUA2* ($hua2_{Col}$ in Col-0 background), was compared to its respective wild-type (background). Since we observed no difference between Col-4 and Col-0 on traits measured, we only represented Col-0 in Figure 5, although $cry2_{Col}$ was in Col-4 background. Genotypes were compared with a post-hoc Tukey test following ANOVA ($7 < n < 10$), except for N concentration for which a non-parametric Kruskal-Wallis test was used due to a limited number of observations ($n = 3$). Significance codes: *** $P < 0.001$; ** $P < 0.01$; * $P < 0.05$; . $P < 0.1$.

	Compared to	Age at flowering		LMA		Photosynthetic rate		N concentration		Growth rate		Plant mass	
L*er*	Cvi	0.93	NS	0.95	NS	1.34	**	1.21	*	1.11	NS	0.69	*
Cvi-EDI_{Ler}	L*er*	0.74	***	0.53	***	1.65	***	1.31	*	0.12	***	0.08	***
Cvi-FLG_{Ler}	L*er*	1.14	***	1.23	**	0.68	*	1.00	NS	1.28	NS	1.76	***
Cvi-EDI_{Ler}	Cvi	0.79	***	0.56	***	1.23	*	1.09	NS	0.11	***	0.12	***
Cvi-FLG_{Ler}	Cvi	1.22	***	1.29	***	0.51	***	0.82	*	1.15	NS	2.56	***
$cry2_{Col}$	Col-4	1.14	***	1.08	NS	0.84	NS	NA		1.13	NS	1.36	***
$cry2_{Ler}$	L*er*	1.19	***	0.99	NS	0.74	NS	1.13	NS	0.93	NS	1.51	**
$hua2_{Col}$	Col-0	0.88	***	0.81	*	1.59	***	1.41	*	0.82	NS	0.42	***
Col-0	Col-4	0.95	NS	1.00	NS	0.95	NS	NA		0.98	NS	1.00	NS

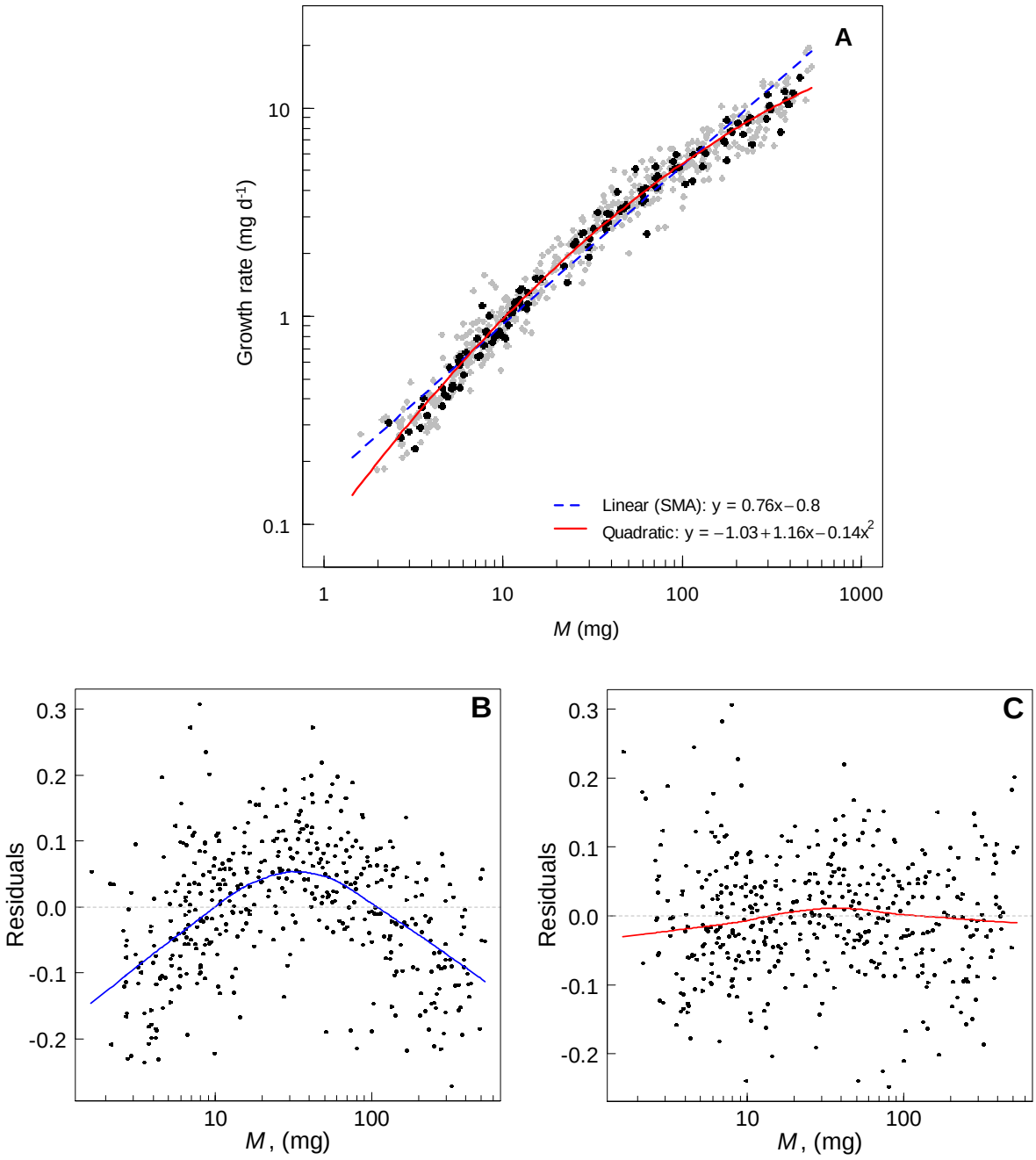

Figure S1. Curvature in the allometric scaling of plant growth. (**A**) Log_{10}-transformed relationship between growth rate and plant dry mass. Linear regression (SMA, blue line) and quadratic fitting (red line) are shown. Grey: individuals; black: mean of each RIL.(**B**) Residuals from the linear (SMA) fit. (**C**) Residuals from the quadratic fit.

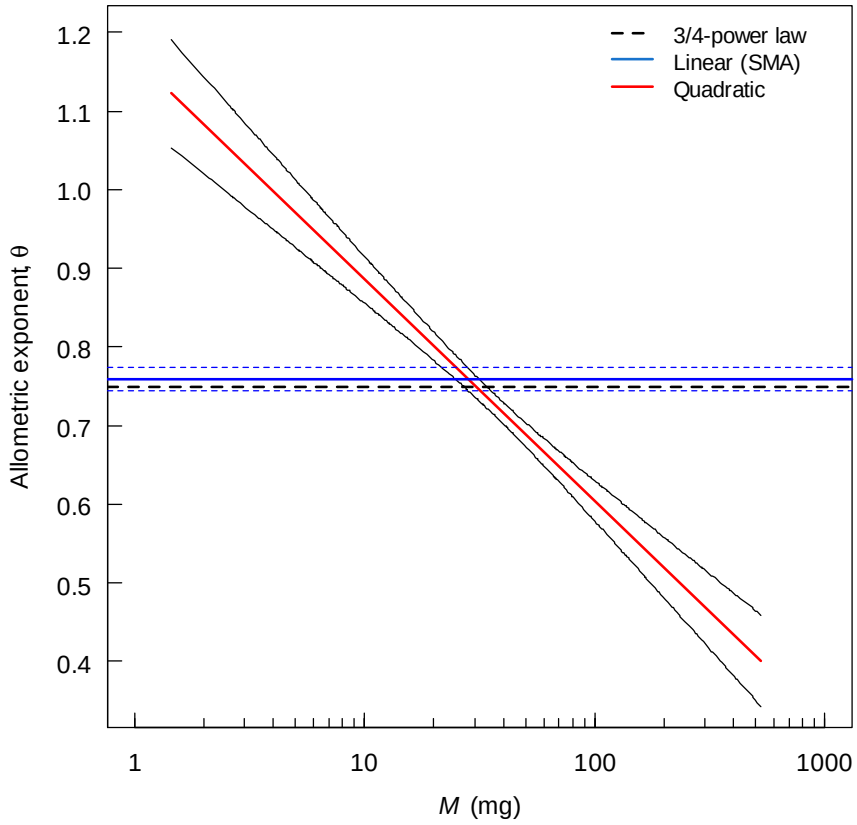

Figure S2. Slope of the allometric scaling of plant growth. Slope of the quadratic fit (red line) with 95% pointwise confidence interval (black lines), slope of the log-linear fit (blue line) with 95% confidence interval and predicted ¾-power law (dotted black line).

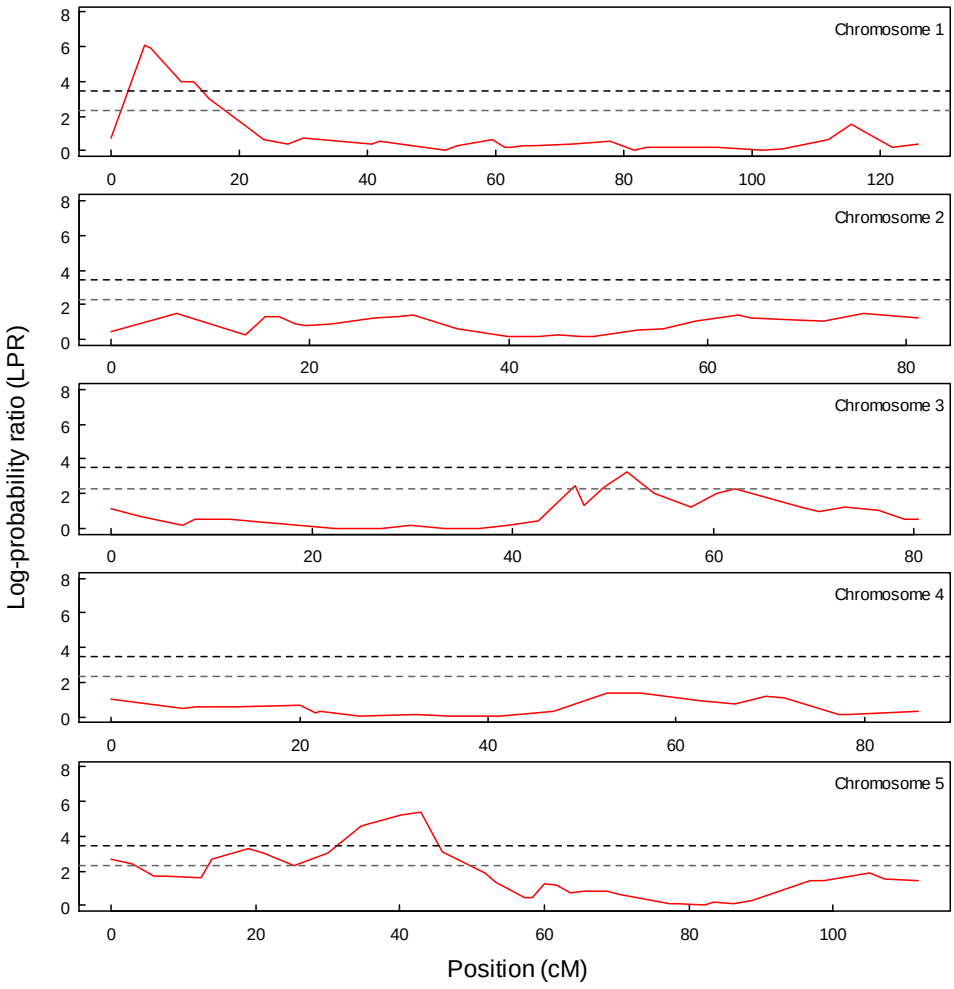

Figure S3. Relationship QTL (rQTL) of the allometric scaling of plant growth.
The rQTL analysis identifies the markers for which there is a significant difference in the standard major axis (SMA) of the relationships between growth rate and aboveground dry mass (*M*) depending on the allelic value. The figure below shows the distribution of the log-probability ratios (LPR = $-\log_{10}(P)$) from the tests of common standard major axis (SMA) at each of the 144 markers along the five chromosomes (L*er* allele versus Cvi allele). For each locus, the LPR is similar to the LOD score from the classical QTL analyses. Two significance thresholds of the LPR were calculated to account for multiple testing. The conservative Bonferroni criterion sets the threshold to $LPR_{Bonf} = -\log_{10}(\alpha/n)$, where α is the desired significance level and n the number of tests, *i.e.* the number of markers; thus for $\alpha = 0.05$, $LPR_{Bonf} = 3.46$ (red line). We also used a less conservative resampling procedure with bootstrap permutation, as proposed by Westfall and Young (1993). 1000 genotypes samples were generated at each locus and the threshold LPR_{boot} was estimated as the proportion of sampled *p*-values that is less than the original *p*-value; here $LPR_{boot} = -\log_{10}(5/1000) = 2.30$ (blue line).

Cited references

Westfall P.H. & Young S.S. (1993). On adjusting p-values for multiplicity. Biometrics, 49, 941-944.

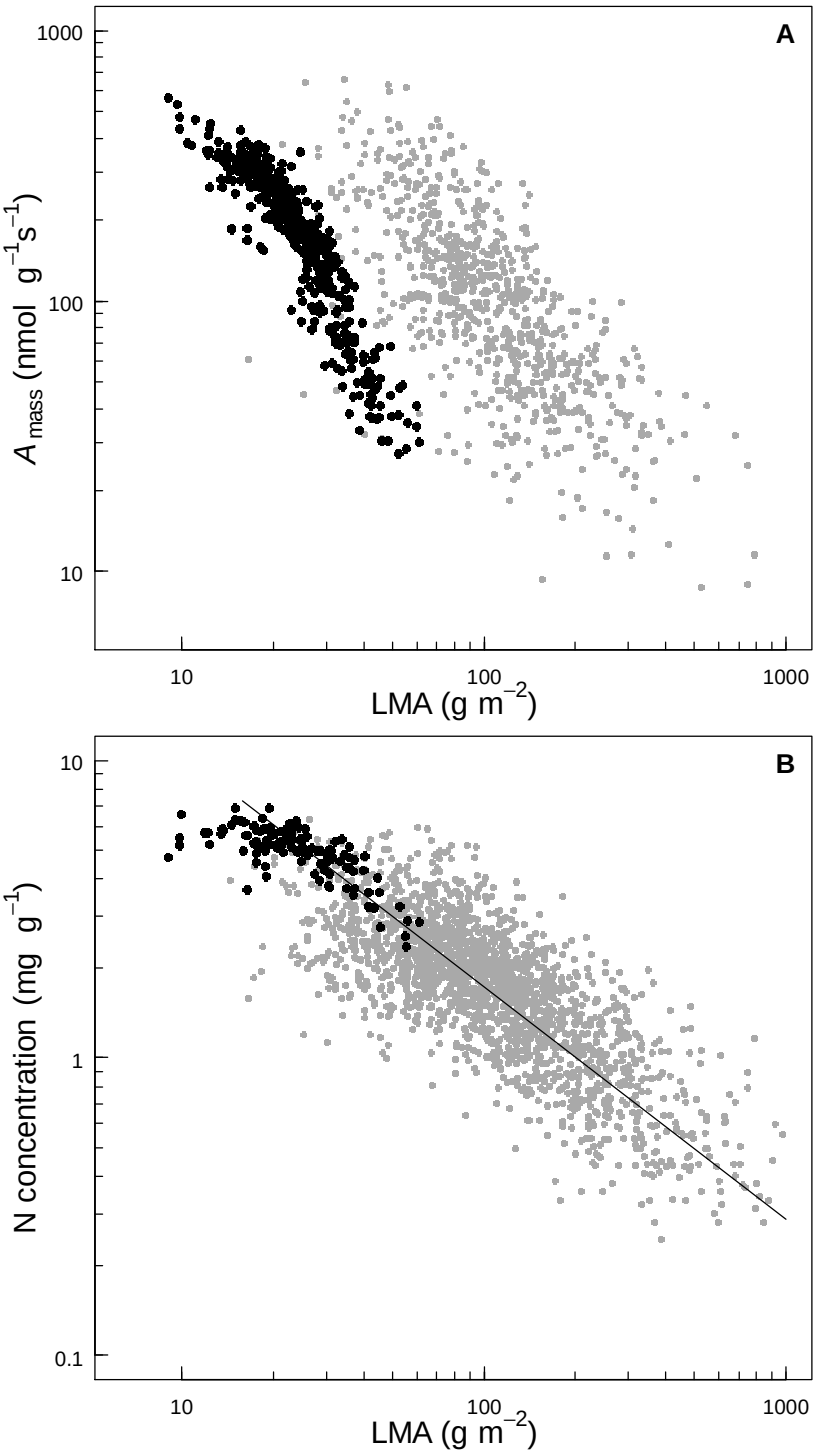

Figure S4. Comparison between intra- (*A. thaliana*, this study) and inter-specific leaf economics spectrum (LES). (A) Relationship between mass-based net photosynthetic rate and leaf dry mass per area (LMA). (B) Relationship between N concentration and LMA. Data are from the whole RIL population of this study (Experiment 1; black dots) and for the original GLOPNET dataset (grey dots).

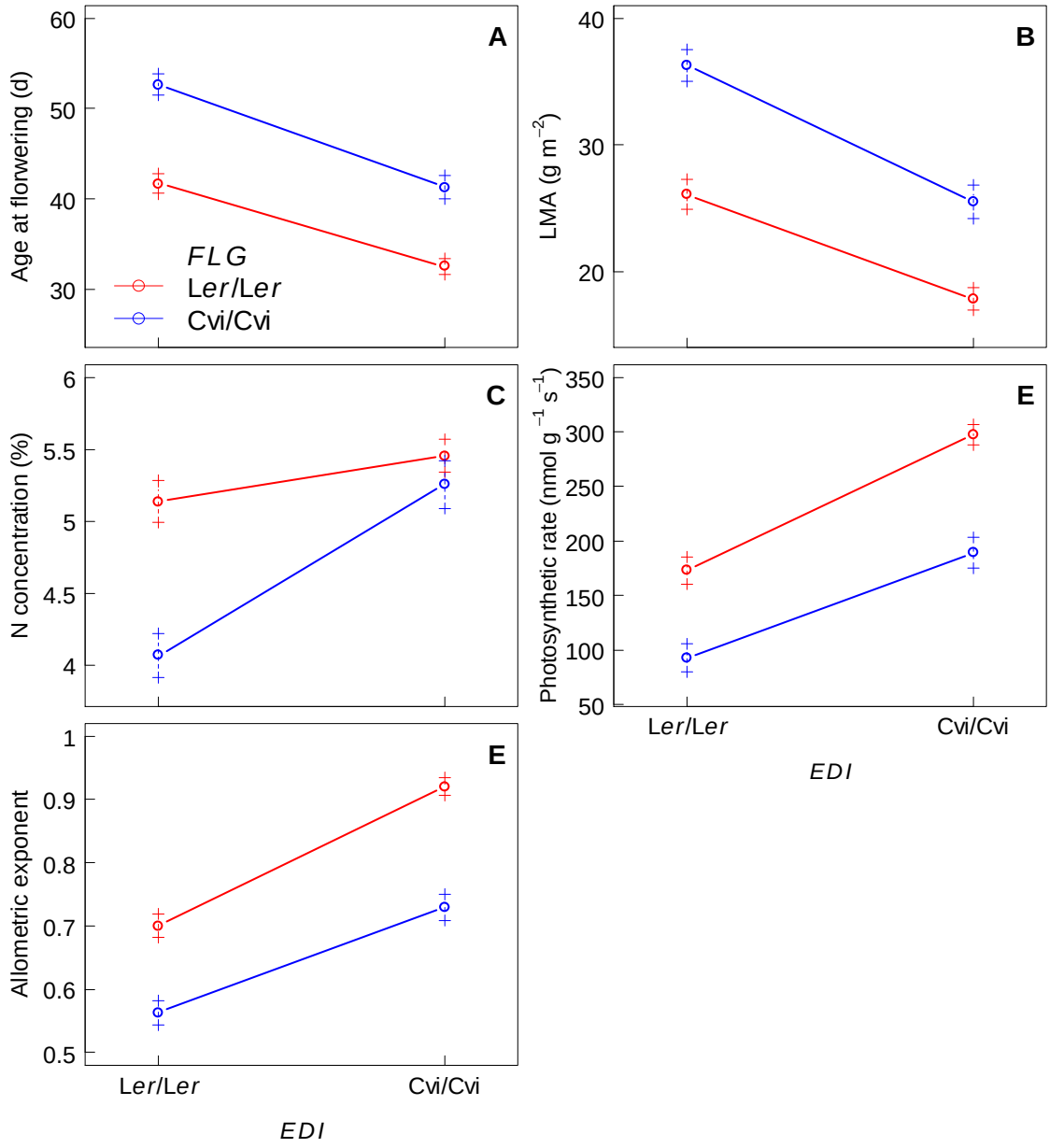

Figure S5. Phenotypic values (± SE) at *EDI* and *FLG* depicting their additive effects. L*er* (red) and Cvi (blue) parental allele at FLG. (**A**) Dry mass, (**B**) age at flowering, (**C**) leaf dry mass per area (LMA), (**D**) mass-based photosynthetic rate, (**E**) growth rate, (**F**) allometric exponent (θ_q), (**G**) N concentration. No epistatic interactions were found among traits ($P > 0.05$), except for N concentration for which the difference of *EDI* effect depending of the allele at *FLG* might indicate an epistatic interaction ($P < 0.01$). The interaction could arise from the difficulty to get good estimates of N concentration with very small samples such as the Cvi/L*er* individuals.

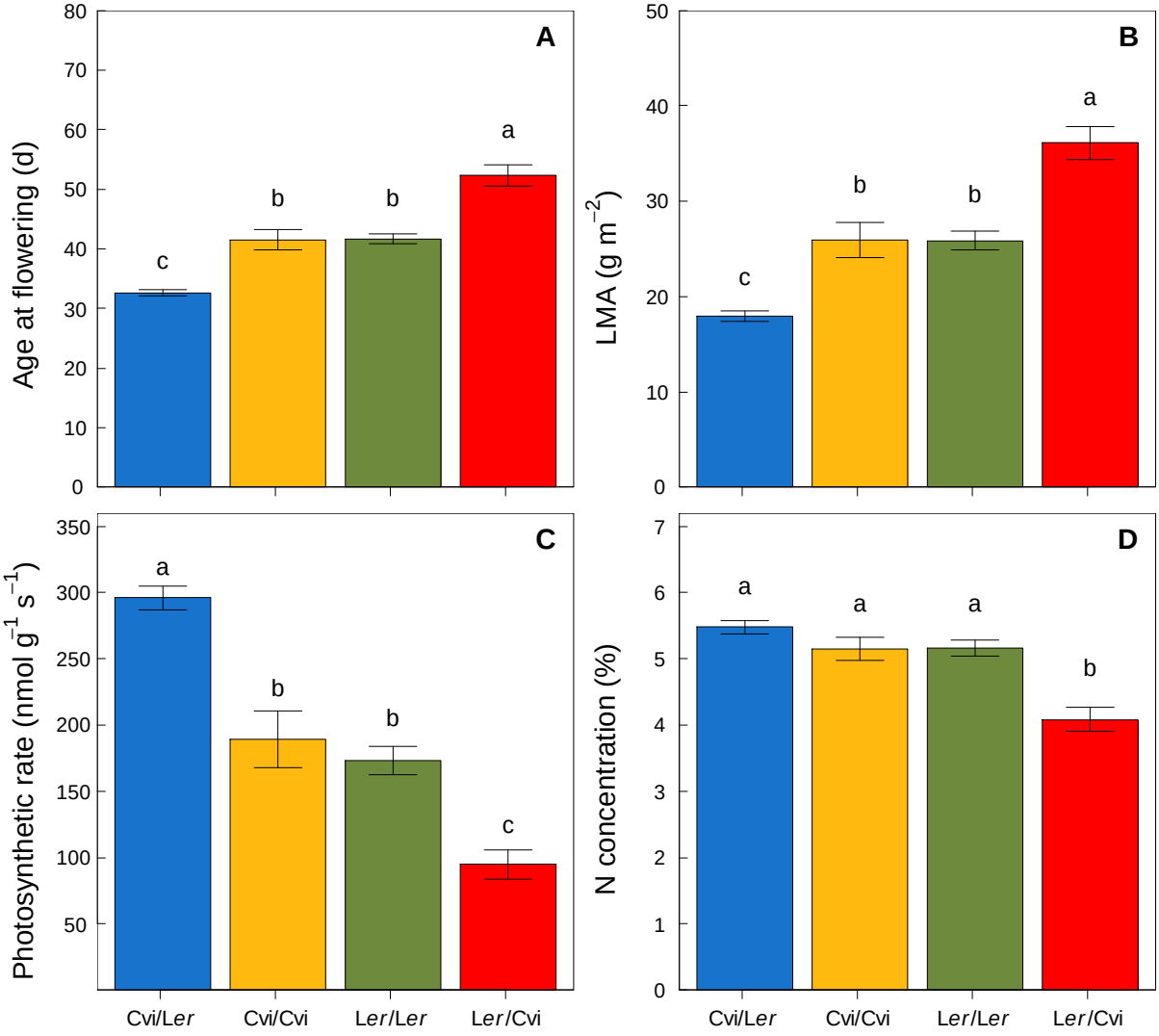

Figure S6. Mean phenotypic values of leaf economics traits depending on the allelic combination at *EDI*/*FLG*. (A) Age at flowering; (B) leaf mass per area (LMA); (C) mass-based net photosynthetic rate; (D) N concentration. Parental types Cvi/Cvi (yellow) and L*er*/L*er* (green), and recombinant types Cvi/L*er* (blue) and L*er*/Cvi (red) at the loci *EDI*/*FLG*, respectively. Different letters represent significant differences ($P < 0.01$) in post-hoc Tukey test following ANOVA. Number of RILs varies between 21 and 44 depending on the allelic combination. Data from Experiment 1.

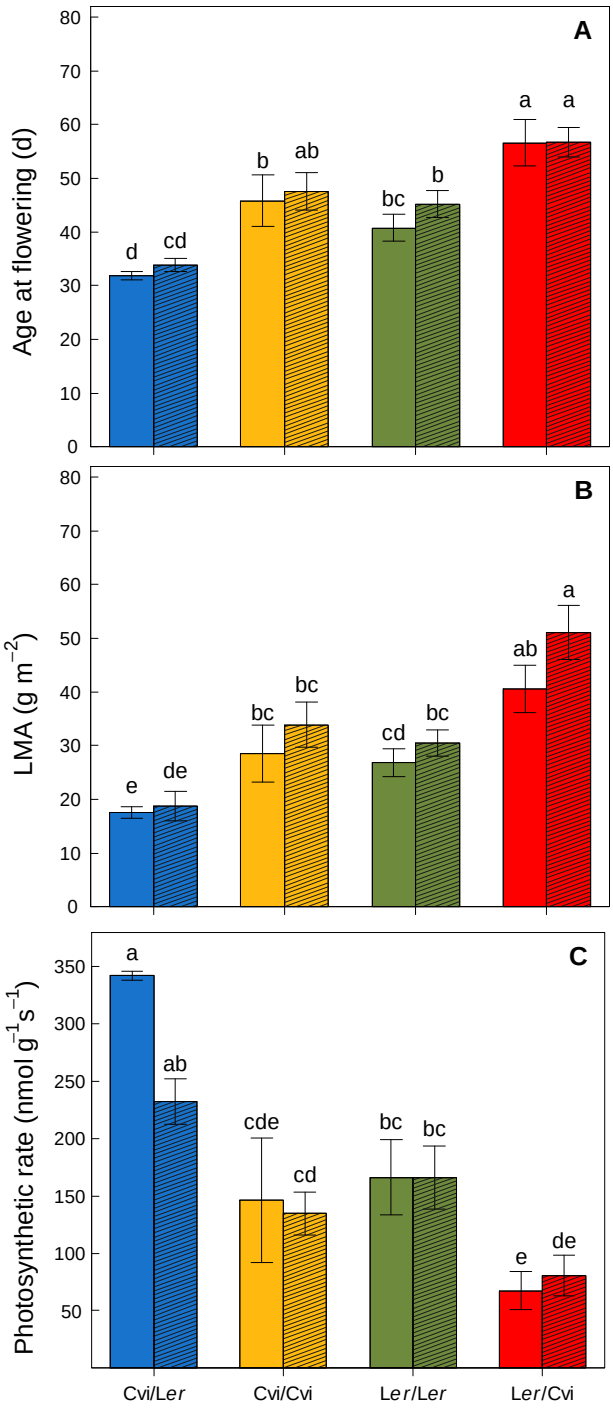

Figure S7. Mean trait values (± SE) in the 16 RILs repeated in Experiment 1 and Experiment 2. (**A**) age at flowering; (**B**), leaf mass per area (LMA); (**C**), mass-based net photosynthetic rate. Mean value of the four RILs for each allelic combination *EDI*/*FLG* from Experiment 1 (solid bars; $n = 4$) were compared to data from Experiment 2 (dashed bars; $n = 6$). Parental types Cvi/Cvi (yellow) and L*er*/L*er* (green), and recombinant types Cvi/L*er* (blue) and L*er*/Cvi (red) at the loci *EDI*/*FLG*, respectively. Different letters indicate significant differences between means following a Kruskal-Wallis test ($P < 0.05$).

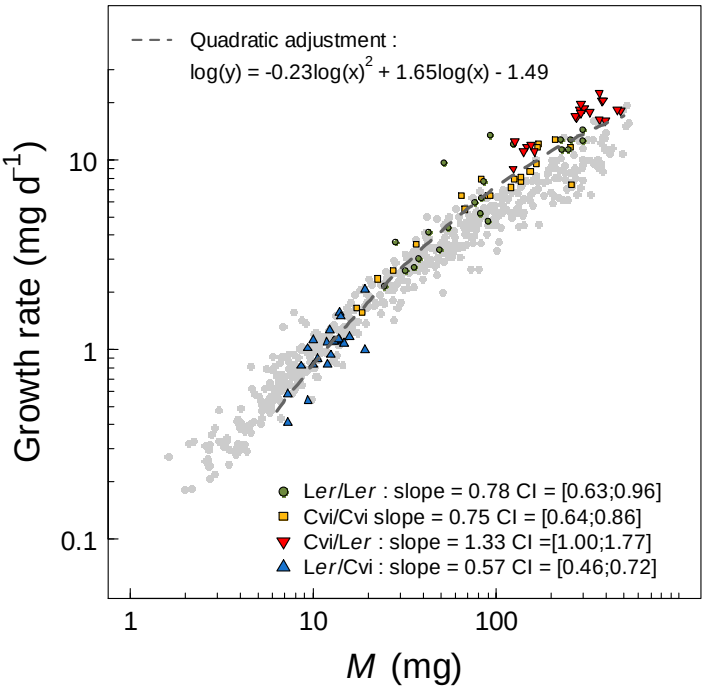

Figure S8. Allometric scaling of plant growth in the 16 RILs (n = 6) from Experiment 2. Parental types Cvi/Cvi (yellow squares) and L*er*/L*er* (green circles), and recombinant types Cvi/L*er* (blue upward triangles) and L*er*/Cvi (red downward triangle) at the loci *EDI*/*FLG*, respectively. Quadratic adjustment was performed with nls (R/stats), whereas SMA regression of each allelic combination was estimated with R/smatr and tested against those found in Experiment 1. No significant difference in the fitted allometric slope was found in the four RILs per allelic combination between Experiment 1and Experiment 2 (P = 0.06 for the four L*er*/L*er* RILs, P = 0.40 for the four Cvi/Cvi RILs, P = 0.83 for the four L*er*/Cvi RILs, P = 0.13 for the four Cvi/L*er* RILs).

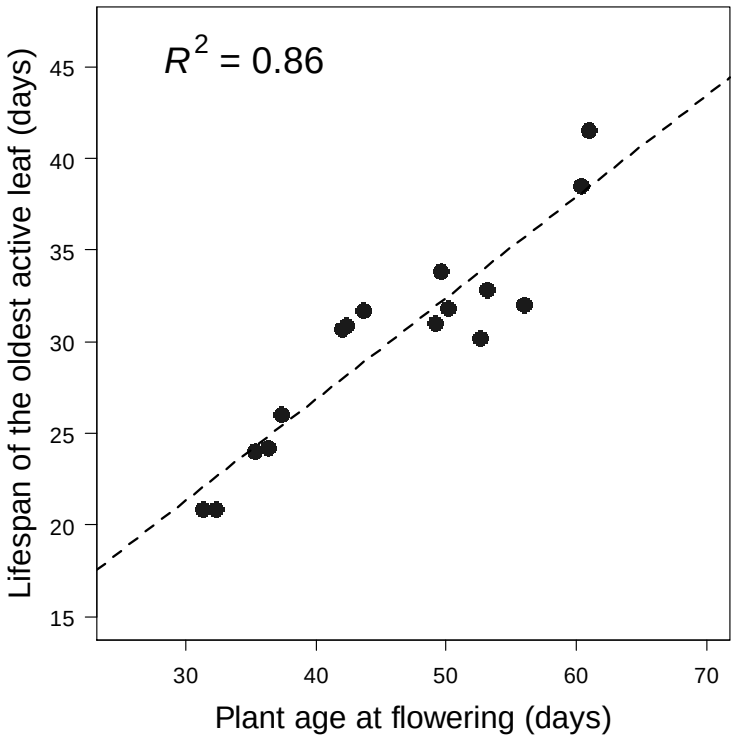

Figure S9. Correlation between flowering time and leaf longevity. Leaf longevity measured across the 16 repeated RILs in Experiment 2, as the age of the oldest photosynthetically active leaf at flowering (n = 6 for each RIL).

Manuscript #6

Genetic variability in plant allometries under combined water deficit and high temperature

François Vasseur[1], Cyrille Violle[2], Thibaut Bontpart[1], Brian J. Enquist[3,4], François Tardieu[1], Christine Granier[1] and Denis Vile[1]

[1]INRA, Montpellier SupAgro, UMR759 Laboratoire d'Ecophysiologie des Plantes sous Stress Environnementaux (LEPSE), F-34060 Montpellier, France

[2]CNRS, UMR5175, Centre d'Ecologie Fonctionnelle et Evolutive, F-34000 Montpellier, France

[3]Departement of Ecology and Evolutionary Biology, University of Arizona, 1041 E Lowell St., Tucson, Arizona, 85721, USA

[4]The Santa Fe Institute, 1399 Hyde Park Road, Santa Fe, New Mexico 87501, USA

Adapted from an article in preparation.

Abstract

Developmental and physiological changes with organismal size and temperature are key drivers of evolutionary adaptation and diversification of plant species. Although the allometric trajectories of many plant traits have been the focus of intense investigations, we lack information about: (*i*) the scaling of traits under contrasted, potentially stressful, environments, and (*ii*) the genetic architecture underlying allometric plasticity. Pleiotropy can affect trait covariations, notably allometric relationships, in multiple directions (i.e. along or perpendicular to the main axis of covariation). Here we modeled the allometries of growth, whole-plant carbon and water economy, leaf structure and life history in a population of recombinant inbred lines of *Arabidopsis thaliana* under isolated and combined high temperature and water deficit. We then examined the genetic architecture and tested the possible evolutionary outcomes of plasticity in plant allometries. Our results identify major pleiotropic loci associated with changes in allometric trajectories in interaction with the environment, and with changes in reproductive success and survival. Additionally, we found a minor pleiotropic locus that affects the economy of carbon and water, independently of plant size but dependently on the environment. Strikingly, allelic variation at this locus caused reduced reproductive success, specifically in a situation of competition for resources. Overall, our findings suggest that pleiotropy-by-environment governs the allometry of major adaptive traits, and may be important for rapid response to natural selection and breeding.

Key-words: *Arabidopsis thaliana*, genotype-by-environment interaction, QTL, trade-offs, plant economics spectrum, net photosynthesis, transpiration, water use efficiency, growth rate, metabolic scaling, life history, fitness.

Introduction

Genetic variability in organismal size and in thermal sensitivity plays a major role in the evolutionary mechanisms of plant adaptation. A theoretical approach has emerged these last decades to model and predict scaling relationships between plant form and function. Specifically, the metabolic theory of ecology (MTE) (Brown et al. 2004) has been described as one of the most significant recent theories in biology (Whitfield 2004), and it continues to feed vigorous debates in the field of ecology and evolutionary biology (e.g. Price et al. 2012). Based on the WBE model (West et al. 1997, 1999), the Metabolic Theory of Ecology (MTE) proposes that the metabolic rate (B) scales with organismal mass (M) and depends on temperature (T) as:

$$B = \beta_0 M^{b_1} F(T) \quad (1)$$

where b_1 is the scaling exponent, β_0 is a normalization constant, and $F(T)$ represents a temperature dependence function. In accordance with MTE assumption, empirical investigations showed that the central tendency of b_1 often approximates quarter powers, although for any given relationship considerable variation may exist (Price et al. 2007, Vasseur et al. 2012 = Manuscript #5). $F(T)$ is an exponentially increasing function until an optimum temperature (T_{opt}), where it decreases dramatically above T_{opt} (Johnson et al. 1942). This decrease reflects the limits of morphological and physiological plasticities to ensure sufficient coordination of the biological processes beyond a certain temperature threshold. Moreover recent findings indicate that there is no genetic variability within species in the temperature function of plant metabolism ($F(T)$) (Parent and Tardieu 2012).

Plants frequently encounter supra-optimal temperatures in the field and high temperature is often associated with water deficit. High temperature and water deficit are among the major stresses impeding plant growth and productivity and are likely key drivers of the evolution of plant form and physiology (Ackerly and Reich 1999). These two stresses act independently or interactively on plant physiology due to their direct and indirect effects on carbon fixation and water consumption (Vile et al. 2012 = Manuscript #1; Vasseur et al. 2011 = Manuscript #3). For instance, reduced transpirational water losses in response to water scarcity can diminish leaf cooling capacities and therefore enhance plant susceptibility to higher air temperature (Pantin et al., submitted = Manuscript #4). In its seminal development, MTE stated that stabilizing selection should operate on allometric coefficients (Enquist and Bentley 2012). The lack of genetic variability in $F(T)$ within species suggests that selection

could operate on the mass-related allometric coefficients, such as b_1. However, the genetic variability in allometric coefficients remains poorly investigated ((Price et al. 2012) but see (Vasseur et al. 2012 = Manuscript #5)) and we lack empirical data about the plasticity of allometric trajectories in response to changes in the environment. More importantly, we still do not know to what extent the genetic variability in plant allometries is associated with variability in the efficiency of resource utilization, reproductive success and survival.

Traits that maximize carbon fixation and water consumption are embedded in a network of dependency that limits the strategies for nutrient uptake and conservation. For instance, net photosynthesis and transpiration are both governed by exchange surfaces and stomata aperture, which results in a limited variability for water use efficiency (WUE), i.e. for the rate of carbon assimilation per unit of water loss. These traits are also allometric functions of plant size, although they do not *directly* depend on organismal temperature, i.e. $F(T)$ is a constant in the Eq. (1) applied to physiological and morphological traits. In addition, there is a fundamental trade-off between the rate of acquisition of resources and lifespan. For instance, increasing leaf longevity requires important structural investment, which is associated with (*i*) increasing leaf mass per area (LMA), but (*ii*) reducing rate of carbon fixation per unit leaf mass (Reich et al. 1997, Wright et al. 2004). Similar trade-offs have been observed between the assimilation and the conservation of many resources by vegetative organs, including nitrogen, phosphorus and water (Freschet et al. 2010, Mommer and Weemstra 2012). This global pattern of covariations between traits, hereafter referred to as the 'plant economics spectrum' (PES), is assumed to be tightly linked to variations in allometric trajectories (Bonser 2006). Supporting this idea, we reported coordinated changes in the allometric coefficient of plant growth and the PES (Vasseur et al. 2012 = Manuscript #5). The PES is assumed to be the result of tight physiological constraints on the evolution of individual characters. For instance, it has been proposed that genotypes exhibiting phenotypic variability perpendicularly to the main axis of covariation (see Figure 1) would be affected in their reproductive success (Donovan et al. 2011). Within a canopy, the ecological strategies for water and carbon economics are crucial to take advantage over competitors, but we lack data about the variability of those traits and their effects in ecologically relevant conditions. In this study, we investigated the changes in fitness components, specifically survival, reproductive success and resources use efficiency, associated to genetic variability in allometric relationships.

Using a mapping population of *Arabidopsis thaliana* cultivated under optimal conditions, we showed that a few pleiotropic genes with major effects can orchestrate the

Figure 1. Theoretical representation of the genetic effects on the allometric relationships.

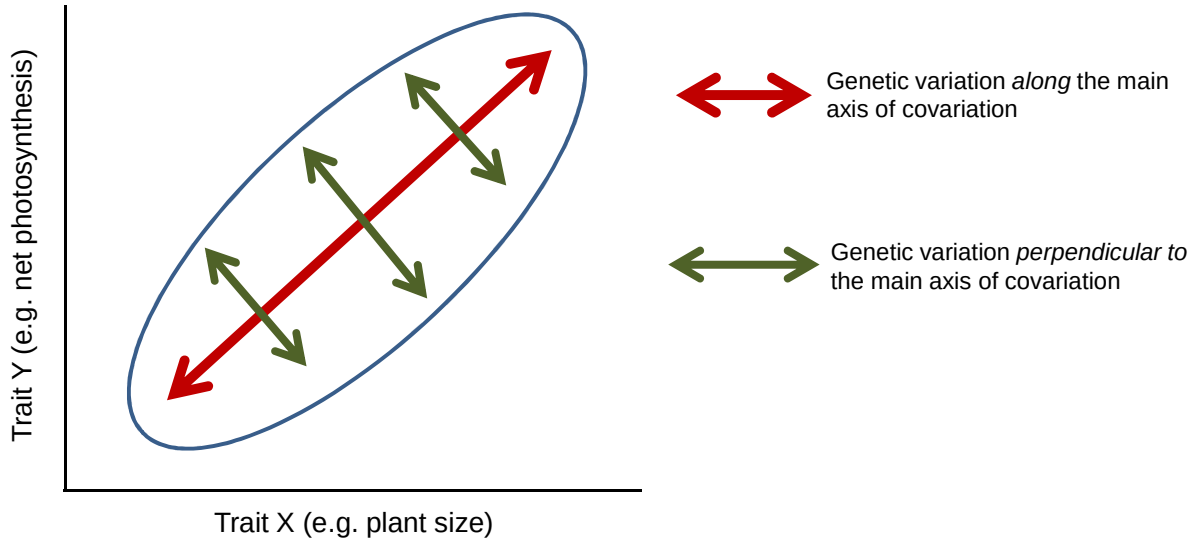

coordinated changes in major plant traits (Vasseur et al. 2012 = Manuscript #5). The evolutionary role of pleiotropy is at the core of quantitative genetics since the first observation that pleiotropic quantitative trait loci (QTL) affect the variance-covariance matrix of potentially adaptive traits, and thus, the evolution of individual characters (Walsh and Blows 2009). Using the same mapping population as in (Vasseur et al. 2012 = Manuscript #5), we used a mixed-effect modeling approach to examine how pleiotropy governs the relationships linking plant size to major functional traits in response to water deficit and supra-optimal temperature. We also estimated the probability to survive and reproduce in stressing environments. In addition, we tested introgressed lines at targeted QTL grown in fluctuating environmental conditions and in competition for light and water with relatives. We examined the seed production in these lines as a proxy of reproductive success. With this dataset, we focused on three main questions:

- How do allometric relationships vary in response to water deficit and high temperature?
- What are the genetic determinants of the variation *along* and *perpendicularly* to the allometric trajectories (see Figure 1)?
- What are the consequences of both genetic variations for plant performance, specifically in a situation of competition?

We show that allometric trajectories vary widely in response to water deficit and supra-optimal temperature. Independently of the environment, the phenotypic variation *along* allometric trajectories was genetically constrained by the effects of a few major pleiotropic QTL. Allelic variability at such QTL induced large differences in traits related to individual fitness, notably in a situation of competition with relatives. Secondly, we identified another pleiotropic QTL that generates variability *perpendicular* to the allometric trajectories dependently on the environmental conditions. Allelic variation at MSAT2.22 induced variability in the plasticity of WUE under water deficit. Strikingly, seed production in introgressed lines at MSAT2.22 was significantly affected in a situation of competition with the non-introgressed line. This later result strongly supports previous hypotheses about the evolution of the PES (Donovan et al. 2011). Our findings identify genetic variability in multiple allometric trajectories underlying plant performance with possible outcomes for natural selection.

Materials and methods

This study relies on the data from two sets of experiments. The first set includes the same four experiments than the ones described in the Manuscript #4. In this study, we added three variables to this dataset: average survival in each RIL, water use efficiency and leaf temperature. The second set includes two experiments, performed to investigate the seed production of introgressed lines at three targeted QTL. All detailed meteorological data – including daily soil water content, air temperature and VPD –, as well as all phenotypic traits measured, are available in the PHENOPSIS database (Fabre et al. 2011).

Plant material

In the first set of experiments, we used the same population of 120 recombinant inbred lines (RILs) as in Manuscript #4 and Manuscript #5. In the second set of experiments, we selected three introgressed lines that carry allelic variation at three targeted QTL (CRY2, GH.121L and MSAT2.22, respectively). Lines were chosen from the genome-wide coverage population previously developed by introgressing genomic regions from the Cvi accession into the L*er* accession (Keurentjes et al. 2007). The line LCN 1-2.5 (NASC code N717045; $CRY2_{Cvi}$) carries a Cvi fragment at the top of chromosome 1 (where the QTL CRY2 is located). LCN 5-6 (N717123; $GH.121L_{Cvi}$) carries a Cvi fragment in the middle of chromosome 5, whereas LCN 2-20 (N717091; $MSAT2.22_{Cvi}$) carries a Cvi fragment at the end of chromosome 2. The positions of the introgressions on the genetic map are provided in Figure S1.

Experiments using the RILs population

The description of the traits measured is provided in the Manuscript #4, except for leaf temperature, survival and water use efficiency (WUE). Survival was estimated for each RIL as the percent of individuals that reach reproduction among the 4 replicates of each RIL. Leaf temperature was measured with at least three random infra-red zenithal imaging (ThermaCAM^{TM} Researcher Pro 2.10, FLIR Systems AB) acquired within the automaton (Figure S2f). Images were recorded for each plant between bolting stage and first flower open. Five random spots were chosen at the surface of the rosette to estimate T_{leaf} (K). Water use efficiency (WUE, nmol mg^{-1}) was estimated as the ratio of net photosynthesis and transpiration (A / ET in Manuscript #4).

Experiments using introgressed lines

The two parental lines (L*er* and Cvi) and the three introgressed lines were grown in two different conditions: (*i*) without competition in optimal environmental conditions, and (*ii*) with competition in a fluctuating (greenhouse) environment. The experiment without competition was performed in the PHENOPSIS automaton in CTxWW (as described above for RILs, n = 10). In the competitive situation, a seed of each genotype was sown at the center of a 2 cm-spaced matrix of eight L*er* plants in a square pot (side = 8 cm), (see Figure S3; n = 10). In the greenhouse, supplemental metal halide lighting was used to extend day length to 16h, air temperature was 16.7/31.5 °C (min/max for night/day), and air humidity varied between 17% and 77%. Plants were irrigated twice a week. In both experiments, irrigation was stopped at first flower open and main flowering stem was isolated with a funnel. After plant desiccation, flowering stems were detached from the rosette, seeds were harvested and weighted.

Statistical analyses

Below T_{opt}, the temperature-dependency of the metabolic rate is described by an exponentially increasing (Boltzmann–Arrhenius) function (Gillooly et al. 2001, Brown et al. 2004, Savage et al. 2004):

$$F(T) = e^{E_a/RT} \quad (2)$$

where E_a is the average activation energy of metabolism (eV), R is the Boltzmann constant (R = 8.617 10^{-5} eV K^{-1}), and T is the temperature of the organism in Kelvin.

Irrespective of the range of temperature (i.e. below or above T_{opt}), $F(T)$ is described by the equation:

$$F(T) = \frac{Te^{\left(\frac{\Delta H_A}{RT}\right)}}{1+e^{\left[\frac{\Delta S_D}{R}\left(1-\frac{\Delta H_D}{\Delta S_D T}\right)\right]}} \quad (3)$$

where ΔHA (J mol^{-1}) is the enthalpy of activation of the considered rate and determines the curvature at low temperature (Johnson et al. 1942). In the physiologically relevant temperature range, the difference between E_a and ΔHA is within 4%, so observed values of ΔHA can be compared with the values of E_a in the literature, although the parameters cannot be rigorously interpreted in an enzymatic context (see (Parent et al. 2010, Parent and Tardieu 2012)). Following Parent and colleagues (Parent et al. 2010), we normalized observed growth rate by $F(20)$ in *Arabidopsis thaliana*. Normalization transforms the absolute measurement of growth rate in each condition to a temperature-independent value, thereby eliminating $F(T)$ in the allometric function of plant metabolism.

Table 1. Coefficients of the allometric relationships. Estimated from the mixed-model, with vegetative dry mass (*M*) as covariate. All traits centered in each environmental condition. $\mathbf{y = WD \times HT \times b_0 + WD \times HT \times b_1 M + WD \times HT \times b_2 M^2 + WD \times HT \times G}$. Traits (y) = normalized growth rate (mg d^{-1}), net photosynthesis (nmol s^{-1}), transpiration (mg d^{-1}), WUE (nmol mg^{-1}), total leaf area (mm^2), LMA (g m^{-2}), age at reproduction (days), and reproductive dry mass (mg). G: genetic effects. Optimum condition (CTxWW) used as intercept. Confidence intervals (CI) estimated with a Markov Chain Monte Carlo algorithm following 1000 permutations. The intercepts are not meaningful because the mixed-model was performed on centered data in each condition.

Trait	Effect	b_0	CI	b_1	CI	b_2	CI
Normalized growth rate	intercept	0.054	[0.037 ;0.074]	0.766	[0.743 ;0.785]	-0.146	[-0.18 ;-0.11]
	HT effect	0.022	[-0.002 ;0.045]	0.115	[0.083 ;0.146]	-0.038	[-0.078 ;0.009]
	WD effect	-0.049	[-0.073 ;-0.027]	0.031	[0.005 ;0.06]	0.133	[0.09 ;0.173]
	HTxWD effect	0.016	[-0.016 ;0.044]	-0.056	[-0.105 ;-0.019]	-0.057	[-0.106 ;0.008]
Net photosynthesis	intercept	0.086	[0.053 ;0.121]	0.602	[0.563 ;0.639]	-0.227	[-0.287 ;-0.161]
	HT effect	0.06	[0.011 ;0.106]	0.521	[0.479 ;0.591]	-0.072	[-0.155 ;0.005]
	WD effect	-0.04	[-0.088 ;0.003]	0.055	[0.001 ;0.103]	0.11	[0.034 ;0.201]
	HTxWD effect	-0.063	[-0.125 ;0.004]	-0.145	[-0.218 ;-0.058]	0.089	[-0.021 ;0.196]
Transpiration	intercept	0.003	[-0.017 ;0.024]	0.515	[0.491 ;0.537]	-0.01	[-0.048 ;0.026]
	HT effect	-0.042	[-0.069 ;-0.015]	-0.016	[-0.048 ;0.02]	0.089	[0.04 ;0.132]
	WD effect	-0.032	[-0.058 ;-0.006]	-0.068	[-0.1 ;-0.037]	0.084	[0.03 ;0.126]
	HTxWD effect	0.038	[0.003 ;0.076]	-0.12	[-0.171 ;-0.066]	-0.083	[-0.153 ;-0.023]
WUE	intercept	0.081	[0.041 ;0.124]	0.068	[0.019 ;0.11]	-0.219	[-0.305 ;-0.144]
	HT effect	0.128	[0.07 ;0.176]	0.607	[0.547 ;0.679]	-0.222	[-0.322 ;-0.126]
	WD effect	-0.039	[-0.09 ;0.016]	0.079	[0.026 ;0.145]	0.104	[0.002 ;0.205]
	HTxWD effect	-0.108	[-0.182 ;-0.033]	-0.052	[-0.142 ;0.047]	0.182	[0.042 ;0.301]
Total leaf area	intercept	0.007	[-0.004 ;0.019]	0.76	[0.75 ;0.775]	-0.019	[-0.041 ;-0.002]
	HT effect	0.018	[0.006 ;0.035]	0.113	[0.097 ;0.131]	-0.03	[-0.054 ;-0.008]
	WD effect	-0.043	[-0.054 ;-0.03]	-0.003	[-0.016 ;0.012]	0.111	[0.088 ;0.133]
	HTxWD effect	0.003	[-0.016 ;0.02]	-0.074	[-0.098 ;-0.053]	-0.025	[-0.052 ;0.006]
LMA	intercept	-0.004	[-0.017 ;0.006]	0.235	[0.221 ;0.246]	0.011	[-0.007 ;0.031]
	HT effect	-0.01	[-0.023 ;0.004]	-0.096	[-0.113 ;-0.082]	0.017	[-0.005 ;0.04]
	WD effect	0.046	[0.033 ;0.059]	0.03	[0.013 ;0.042]	-0.119	[-0.139 ;-0.094]
	HTxWD effect	-0.007	[-0.024 ;0.011]	0.076	[0.054 ;0.097]	0.031	[0.003 ;0.063]
Age at reproduction	intercept	-0.021	[-0.029 ;-0.015]	0.121	[0.119 ;0.135]	0.054	[0.043 ;0.065]
	HT effect	-0.001	[-0.007 ;0.009]	0.011	[0.005 ;0.024]	-0.006	[-0.024 ;0.002]
	WD effect	0.012	[0.005 ;0.02]	0.039	[0.03 ;0.048]	-0.029	[-0.042 ;-0.016]
	HTxWD effect	-0.004	[-0.014 ;0.006]	-0.002	[-0.016 ;0.009]	0.018	[0 ;0.036]
Reproductive dry mass	intercept	0.05	[0.02 ;0.079]	0.427	[0.394 ;0.461]	-0.131	[-0.184 ;-0.083]
	HT effect	0.05	[0.023 ;0.09]	0.111	[0.074 ;0.16]	-0.083	[-0.157 ;-0.041]
	WD effect	0.008	[-0.025 ;0.037]	-0.093	[-0.13 ;-0.059]	-0.015	[-0.065 ;0.046]
	HTxWD effect	-0.019	[-0.053 ;0.031]	-0.007	[-0.056 ;0.061]	-0.015	[-0.103 ;0.044]

Any trait *Y* can thereby be modeled as a temperature-independent function of plant mass (*M*), such as:

$$Y = \beta_0 M^{b_1} \quad (4)$$

which, on a logarithmic scale, becomes:

$$\mathrm{y} = \log(Y) = b_0 + b_1 \log(M) \quad (5)$$

where $b_0 = \log(\beta_0)$. Corrections and extensions of the initial theory have demonstrated that several measures of metabolism are quadratic functions of organismal size (Kolokotrones et al. 2010, Vasseur et al. 2012 = Manuscript #5). Thus,

$$y = \log(Y) = b_0 + b_1 \log(M) + b_2 \log(M)^2 \quad (6)$$

To investigate the variability in allometric trajectories, we fitted a mixed model to the allometric equation (6), such as:

$$y = \mathrm{W} \times \mathrm{T} \times b_0 + \mathrm{W} \times \mathrm{T} \times b_1 M + \mathrm{W} \times \mathrm{T} \times b_2 M^2 + \mathrm{G} \times \mathrm{W} \times \mathrm{T} \quad (7)$$

where b_0 is the intercept, and b_1 and b_2 are the allometric coefficients of first and second order, respectively. Watering (W) and air temperature (T) levels were treated as fixed effects, and the genotype (G) effect was treated as random effect. We used centered data within each environment to estimate the allometric coefficients, and the control treatment (CTxWW) was used as intercept. The confidence interval of each coefficient was estimated with a Markov Chain Monte Carlo (MCMC) following 1000 permutations.

We used composite interval mapping as implemented in R*qtl* to identify QTL of vegetative dry mass and functional traits within each environment. To test to what extent the variability that is perpendicular to the main axis of the PES bivariate relationships is genetically determined, we performed a quantitative genetic analysis of the residuals extracted from the loess fit of the bivariate relationships between age at reproduction, LMA, A_{mass} and ET_{mass}. To test the size-independent effects of MSAT2.22 on WUE, we also extracted the best unbiased linearized predictors (BLUPs) from the mixed-model, which represent the variability that is not explained by the covariate (i.e. *M* in interaction with T and W) but that is explained, at least in part, by the random effects (i.e. G in interaction with T and W). We tested the difference in seed production between introgressed lines, Cvi and L*er* using a non-parametric Kruskal-Wallis' test. All statistical analyses were performed using R 2.12.

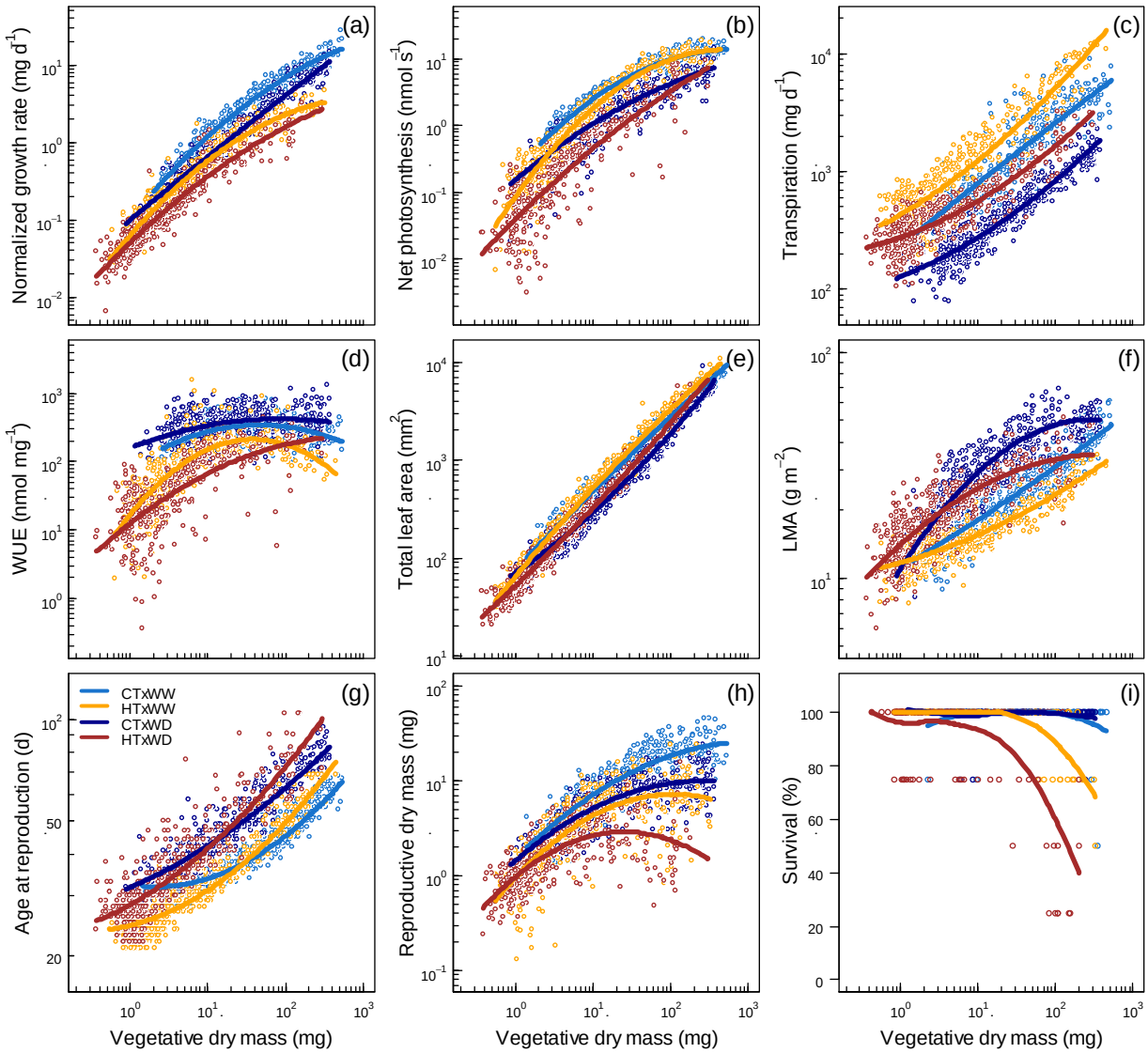

Figure 2. Allometric trajectories of major plant traits depending on the environment. (a-h) Curves fitted from the coefficients estimated with a mixed-model performed on $\log_{10}$-transformed data (not centered), from the model: $\boldsymbol{y = WD \times HT \times b_0 + WD \times HT \times b_1 M + WD \times HT \times b_2 M^2 + WD \times HT \times G}$ (see Table 1 legend). (i) Curves fitted from a loess on the mean value of each RIL. CTxWW in light blue: control temperature and well-watered (20 °C x 0.35 g H_20 g^{-1} dry soil). CTxWD in dark blue: control temperature and water deficit (20 °C x 0.20 g H_20 g^{-1} dry soil). HTxWW in orange: high temperature and well watered (30 °C x 0.35 g H_20 g^{-1} dry soil). HTxWD in brown: high temperature and water deficit (30 °C x 0.20 g H_20 g^{-1} dry soil).

Results

Mixed-model of allometric relationships

Plant traits exhibited a huge variability in all of the four combinations of water availability and air temperature (Table S1). Vegetative dry mass was significantly reduced by 63% under HT, 32% under WD, and 81% under the combination of HT and WD. From the mixed-model approach, we estimated the variability in allometric coefficients of all traits but survival, depending on the environmental conditions (Table 1, Figure 2). We could not perform a mixed-model on survival because we estimated an average value for each RIL. The loess fit revealed a decrease in the survival of the biggest plants in stressing environments, especially when HT was combined to WD (Figure 2i). It resulted in a reduction of individual replicates for vegetative and reproductive traits for the big genotypes grown in stressing environments.

The average slope of the allometric relationship of normalized growth-rate (i.e. b_1, the first-order allometric coefficient) was 0.77 in CTxWW, 0.80 in CTxWD, 0.89 in HTxWW and 0.86 in HTxWD (Table 1). There was a significant convex curvature in this relationship, as illustrated by the negative second-order term in CTxWW (b_2 = -0.15, Table 1). The significant second-order term b_2 indicated that the local slope (i.e. the derivative of the allometric function) varied with plant size. The convex curvature of the allometric scaling of growth rate was not significantly affected by HT, but was significantly reduced by WD (+0.13), leading to a linear relationship in CTxWD (Figure 2a). Net photosynthesis exhibited similar allometric trajectories than growth rate (Figure 2b). The average allometric slope was 0.60 in CTxWW and it was significantly increased by stressing conditions. The convex curvature was not affected by HT but reduced under WD (+0.11). Inversely, the allometric trajectory of transpiration (Figure 2c) exhibited no curvature in CTxWW, but a concave curvature in stressing conditions with a significant temperature-by-water availability interaction (Table 1). The average slope was significantly reduced by WD in interaction with HT. As a consequence of the opposite curvatures in the allometric relationships of net photosynthesis and transpiration, WUE exhibited a strongly convex allometric trajectory in all conditions. The bell-shaped trajectories illustrate the decrease in the local allometric slope as dry mass increases, specifically in stressing conditions (b_2 varies from -0.44 in HTxWW, to -0.12 in CTxWD, Figure 2d). The allometric relationship of total leaf area exhibited a weak curvature (Figure 2e), but it was significantly affected by HT and WD in opposite direction (-0.03 and +0.11, respectively). As predicted by MTE, the average allometric slope of total leaf

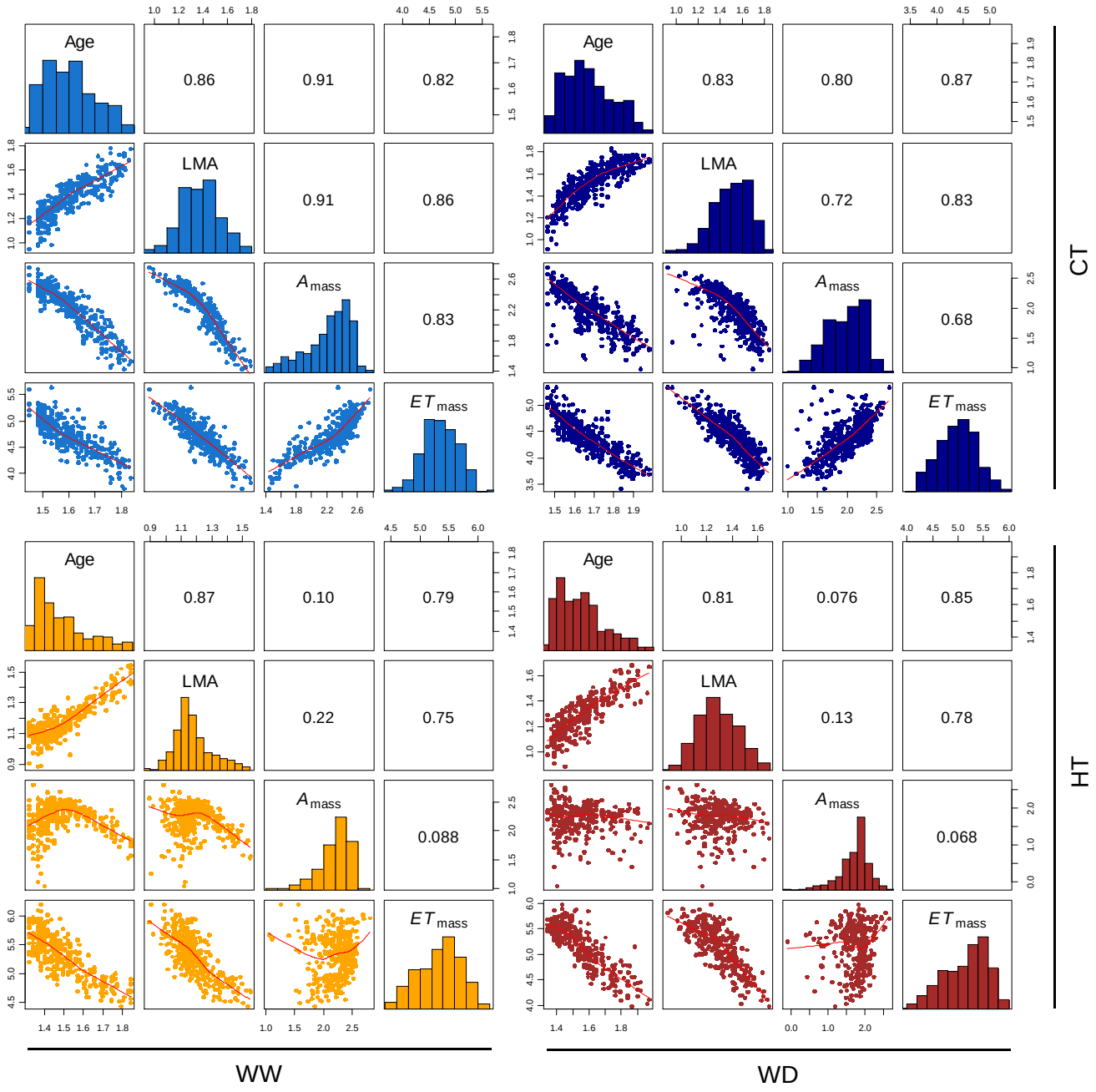

Figure 3. The plasticity of the PES to water deficit and high temperature. Bivariate relationships, on a $\log_{10}$ scale, between age at reproduction (Age, days), leaf mass per area (LMA, g m^{-2}), mass-based net photosynthetic rate (A_{mass}, nmol s^{-1} g^{-1}), and mass-based transpiration rate (ET_{mass}, mg d^{-1} g^{-1}). CTxWW in light blue: control temperature and well-watered (20 °C x 0.35 g H_20 g^{-1} dry soil). CTxWD in dark blue: control temperature and water deficit (20 °C x 0.20 g H_20 g^{-1} dry soil). HTxWW in orange: high temperature and well watered (30 °C x 0.35 g H_20 g^{-1} dry soil). HTxWD in brown: high temperature and water deficit (30 °C x 0.20 g H_20 g^{-1} dry soil). Pearson's coefficients of correlation are displayed in upper diagonals. Red curve is fitted from a loess adjustment.

area approximated ¾ (b_1 = +0.76 in CTxWW), although it increased significantly under HT (+0.11), in interaction with WD (+0.04). Leaf mass per area (LMA) exhibited a different allometric trajectory depending on water availability (Figure 2f). The allometric relationship was linear in WW but convex in WD (both under CT and HT). Increase in LMA with plant size was reduced by water depletion, whatever the air temperature. The average slope of the allometric relationship of LMA approximated ¼ (b_1 = +0.23 and +0.24 in CTxWW and HTxWD, respectively), although it was significantly decreased under HT (-0.10) and increased under WD (+0.03) with significant interactive effect of HT and WD. Age at reproduction exhibited a concave allometric trajectory in all conditions (Figure 2g, Table 1). However, in stressing environments age at reproduction increased less dramatically with size than in optimum condition (b_2 varied between +0.05 in CTxWW, +0.04 in HTxWW, +0.02 in CTxWD, and +0.03 in HTxWD). The average allometric slope was significantly increased both by WD and HT (b_1 = +0.12 in CTxWW; b_1 = +0.17 in HTxWD, no significant interaction). The allometric relationship of reproductive dry mass exhibited a convex curvature, specifically in stressing conditions (Table 1; Figure 2h). This illustrates a reduced reproductive allocation in both the smallest and biggest plants in supra-optimal temperature and limited water availability.

The plasticity of water and carbon economics

Next, we investigated the pattern of covariations between life history traits and the traits that reflect the functional strategies of carbon and water economics across the four environments. In each environment, age at reproduction and LMA covaried positively (Figure 3), and together negatively covaried with mass-based transpiration rate (ET_{mass}) Mass-based net photosynthetic rate (A_{mass}) decreased with LMA and age at reproduction under CT (both in WW and WD) but not under HT (both in WW and WD). Thus, in CT plants are characterized by either a 'fast' strategy of carbon and water economics (i.e. high photosynthetic/transpiration rates and low age at reproduction/LMA), or a 'slow' strategy of carbon and water economics (i.e. low photosynthetic/transpiration rates and high age at reproduction/LMA). In other words, the economy of carbon was strongly dependent of the thermal conditions. A significant effect of air temperature was also found on the covariation between A_{mass} and ET_{mass}. This illustrated the strong plasticity of WUE to air temperature (see Figure 1d). We also observed important residual variability in all relationships, which suggested possible genetic effects independent of the main axis of covariation.

Table 2. QTL of plant size and percentage of genetic variation explained within each environment. Percent (%) of variability from the QTL analysis performed on vegetative dry mass (log_{10}-transformed data) within each environment. Name: closest molecular marker to the LOD score peak. All QTL are significant ($P < 0.05$). Position along chromosome (chr) and confidence intervals (CI) estimated with a Markov Chain Monte Carlo algorithm following 1000 permutations.

Marker	chr	position [CI]	CTxWW	CTxWD	HTxWW	HTxWD
CRY2	1	6 [3-8]	38.3	30.5	21.4	25.4
BH.180C	5	16 [12-20]	10.7	10.6	20.2	14.5
GH.121L	5	39 [35-42]	17.6	18.6	25.5	23.3
BF.168L	5	100 [92-105]	4.8			
Total			80.8	74.9	83.9	79.4

Table 3. Variance components (%) beyond allometric relationships. Components of the size-independent variance (%) attributable to genetic effects (G), and genotype-by-environment effects (GxT, GxW and GxTxW for genotype-by-temperature, genotype-by-watering and genotype-by-temperature-by-watering, respectively) extracted from the mixed-model of each allometric relationships (see legend of Table 1).

Trait	G	GxT	GxW	GxTxW
Normalized growth rate	0.9	10.1	4.8	0.0
Net photosynthesis	0.0	3.9	0.5	9.1
Transpiration	2.2	4.4	0.0	0.0
WUE	0.0	4.0	2.1	4.8
Total leaf area	18.9	9.9	2.4	2.2
LMA	13.7	10.4	2.8	2.7
Age at reproduction	29.4	8.6	2.9	0.0
Reproductive dry mass	16.0	11.3	1.5	7.0

Table 4. Variance components (%) of the residuals of the PES attributable to MSAT2.22. Age at reproduction (days), leaf mass per area (LMA, g m^{-2}), mass-based net photosynthetic rate (A_{mass}, nmol s^{-1} g^{-1}) and mass-based transpiration rate (ET_{mass}, mg d^{-1} g^{-1}). Residuals extracted after fitting a loess between each pair of traits (see Figure 2). ANOVA significance levels: *** = P < 0.001; ** = P < 0.01; * = P < 0.05; . = P < 0.1.

x-trait	y-trait	CTxWW	CTxWD	HTxWW	HTxWD
Age at reproduction	LMA	2.4 .	11.3 ***	1.4 NS	0.8 NS
	A_{mass}	0.3 NS	7.4 **	2.7 .	0.3 NS
	ET_{mass}	13.2 ***	19.7 ***	9.7 ***	2.3 NS
LMA	A_{mass}	2.5 .	2.5 .	0.1 NS	0.3 NS
	ET_{mass}	15.7 ***	20.0 ***	5.2 *	1.0 NS
A_{mass}	ET_{mass}	3.5 *	5.3 *	0.6 NS	1.6 NS

Genetic variability in plant allometries

QTL analysis revealed few pleiotropic loci that account for the most of the variability in vegetative dry mass within each environment (Table 2), as well as for the correlated traits (Figure S4). Specifically, four pleiotropic QTL ($P < 0.001$) were identified and together explained 81% of the variability in plant size under control conditions (Table 2). Three of them were also identified under stress and explained more than 70% of plant size variability (Table 2): CRY2 at the top of chromosome 1, and BH.180C and GH.121L two epistatic QTL at the top and middle of chromosome 5, respectively). As previously observed in optimum conditions (Vasseur et al. 2012 = Manuscript #5), the additive effects of the two major QTL, CRY2 and GH.121L, generated extreme phenotypes notably characterized by very large and very small sizes in the recombinant types (i.e. in L*er*/Cvi and Cvi/L*er*, respectively; Figure S5). Because of pleiotropic effects, CRY2 and GH.121L controlled the bivariate changes in both allometric relationships and traits related to the PES. Moreover, because allometric relationships were generally not log-linear in our conditions (b_2 significantly different from zero), the allelic variability at these major QTL was associated to variability in the allometric coefficients (e.g. in the local slope), depending on the environment.

The mixed-model approach revealed that, beyond the variability in plant traits generated by the size-effect of the major pleiotropic QTL described above, there was still an important variance component (of the residuals) that was attributable to genetic variability (Table 3). An important part of the variability of life history and morphological traits (i.e. age at reproduction, reproductive dry mass, total leaf area, and LMA; 13.7% < G < 29.4%) was attributable to genetic (G) effects only, independently of size and environmental effects (Table 3). A non-negligible part of the size-independent variability in these traits was also attributable to genetic effects that depended on the thermal condition (8.6% < GxT < 11.3%). However, a very low part of the genetic variability depended on the water availability (1.5% < GxW < 2.9%) or on the interaction of water and temperature levels (0% < GxTxW < 7%). For the physiological traits (i.e. normalized growth rate, net photosynthesis, transpiration and WUE), there was almost no genetic variability independently of the environment (0% < G < 2.2%; Table 3), and a weak, but non negligible, part that depended on temperature (GxT = 10.1% for normalized growth rate), or on temperature in interaction with water availability (GxTxW = 9.1% for net photosynthesis).

We then investigated the genetic architecture underlying the variability in plant traits that was independent of plant size. We found that the locus MSAT2.22 was associated with (*i*) the variability in the plasticity of the residuals of the relationships between the traits from the

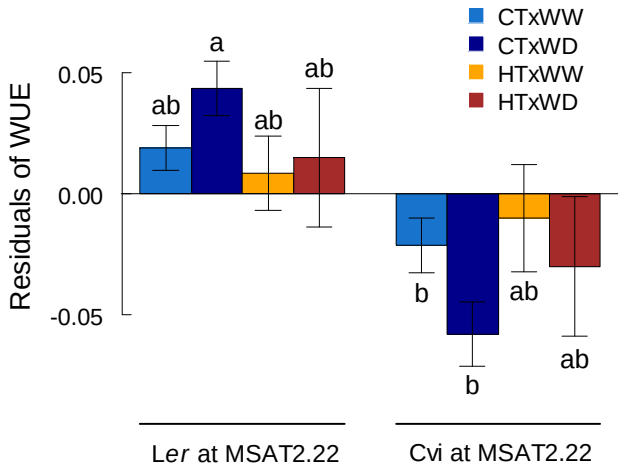

Figure 4. Effect of MSAT2.22 on the residuals of the allometry of WUE. Residuals extracted from the allometric mixed-model (see legend of Table 1). ANOVA significance: $P < 0.05$. CTxWW in light blue: control temperature and well-watered (20 °C x 0.35 g H_20 g^{-1} dry soil). CTxWD in dark blue: control temperature and water deficit (20 °C x 0.20 g H_20 g^{-1} dry soil). HTxWW in orange: high temperature and well watered (30 °C x 0.35 g H_20 g^{-1} dry soil). HTxWD in brown: high temperature and water deficit (30 °C x 0.20 g H_20 g^{-1} dry soil).

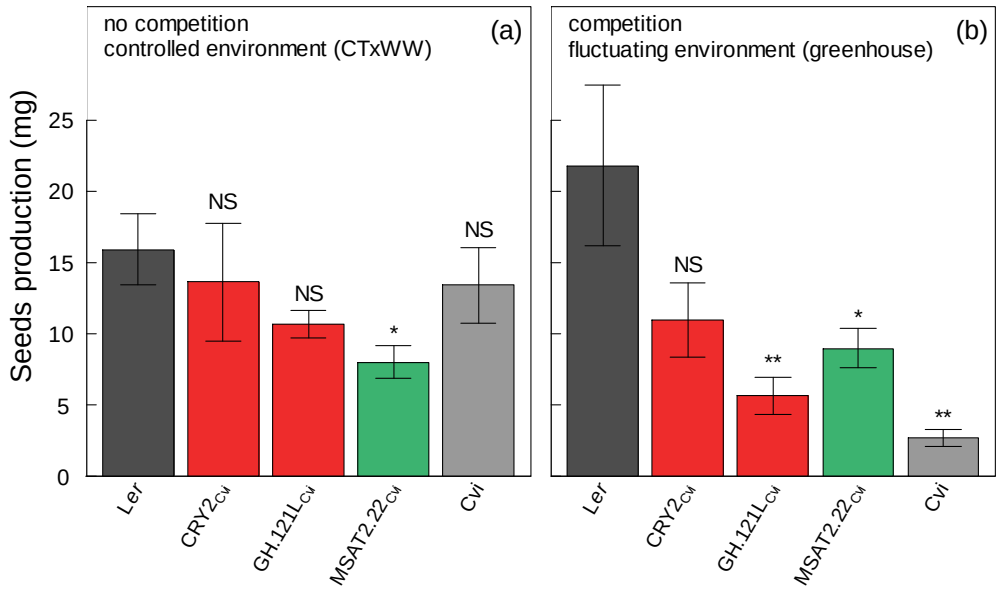

Figure 5. Reproductive success of introgressed lines in different situations. (a) Total mass of seeds produced by plant without competition, in optimum condition (CTxWW). (b) Total mass of seeds produced by plant in a competitive situation with the L*er* parent, and in fluctuating environment (greenhouse). $CRY2_{Cvi}$: NIL introgressed with Cvi allele at CRY2. $GH.121L_{Cvi}$: NIL introgressed with Cvi allele at GH.121L. $MSAT2.22_{Cvi}$: NIL introgressed with Cvi allele at MSAT2.22. Kruskal-Wallis significance levels: *** = P < 0.001; ** = P < 0.01; * = P < 0.05; ° = P < 0.1.

PES (Table 4, Figure S6), and (*ii*) the variability in WUE attributable to size-independent GxTxW effects (Table 3). Specifically, in each environmental condition but HTxWD, MSAT2.22 affected the residuals of the relationship between ET_{mass} and age at reproduction ($P < 0.001$; Table 4), and the residuals of the relationship between ET_{mass} and LMA, ($P < 0.05$; Table 4). In CTxWD, MSAT2.22 also significantly affected the relationships between (*i*) LMA and age at reproduction, (*ii*) A_{mass} and age at reproduction, and (*iii*) A_{mass} and ET_{mass} (all $P < 0.05$). The residuals of the allometry of WUE were also significantly different according to L*er* or Cvi allele at MSAT2.22 in CTxWD, but not in the other conditions ($P < 0.05$; Figure 4, Figure S7). Therefore, MSAT2.22 generates variability in WUE independently of plant size or age, but this variability depended on the environment, specifically on water availability.

Test for fitness of targeted genotypes in specific conditions

We examined the reproductive success of three lines previously generated to carry introgressed QTL of Cvi into L*er* background ($CRY2_{Cvi}$, $BH.121L_{Cvi}$ and $MSAT2.22_{Cvi}$). When plants were grown in optimum conditions (CTxWW) and without competition, only $MSAT2.22_{Cvi}$ displayed a significant reduction in seed production compared to the L*er* parental accession ($P < 0.05$; Figure 5a). When grown under competition in a fluctuating environment (greenhouse), all three lines displayed a reduced seed production compared to L*er* (Figure 5b; Figure S3). The reproductive success of Cvi decreased significantly in a competitive situation with L*er* ($P < 0.05$), whereas the reproductive success of L*er* was not significantly affected. The extreme position along allometric relationships of $CRY2_{Cvi}$ and $BH.121L_{Cvi}$ lines had different consequences for reproductive success in a competitive situation. The reproductive success was not significantly affected in small/fast growing plants ($P > 0.05$ for $CRY2_{Cvi}$), but it was significantly decreased in large/slow growing plants ($P < 0.05$ for $BH.121L_{Cvi}$). Our results also showed that the negative effect on WUE of the Cvi allele at MSAT2.22 was associated with a significant decrease in reproductive success whatever the environment and the competitive situation (both $P < 0.05$).

Discussion

Allometric variations support MTE predictions

In our modeling approach, we used temperature-normalized growth rate to eliminate $F(T)$ in Eq. (1), and thus, to perform a linear mixed-model on the mass-dependent allometric function. By doing so, we assumed the parameters of $F(T)$, such as T_{opt} and the activation

enthalpy ΔH_A, constant for all genotypes in our population. This initial assumption was supported by a recent meta-analysis among 18 plant species, which showed a lack of genetic variability for the parameters of $F(T)$ within species and closely related species (Parent and Tardieu 2012). This finding was interpreted as the consequence of very slow evolution of the thermal sensitivity of metabolic and developmental rates in plants. Nonetheless, this finding also suggests that the mechanisms of rapid adaptation could be targeted on the phenotypic variability in plant physiology and morphology. Consequently, we expect genetic variability in the mass-dependent allometric coefficients of major plant traits, specifically in the allometric slopes illustrated by b_1 and b_2. In strong accordance with the MTE predictions, in optimum conditions (CTxWW), total leaf area and temperature-normalized growth rate scaled to vegetative dry mass with a slope that approximates ¾ (for both b_1 = 0.76, Table 1), and LMA scaled to vegetative dry mass with a slope that approximates ¼ (b_1 = 0.23). However, environmental conditions significantly affected traits values and allometric coefficients. This result supports the evolutionary assumptions of MTE (West et al. 1999, Vasseur et al. 2012 = Manuscript #5) that plasticity in allometric slope exists, but stabilizing selection operates to fix the value around the canonical ¾ slope in optimum conditions. Moreover, the allometric relationships were generally not linear, meaning that the local slope (i.e. the derivative of the allometric function) changed as plant size increased among genotypes within each environment. Therefore, different plant sizes were associated to different functional strategies characterized by multiple allometric coefficients.

Major pleiotropic QTL to the origin of a Dobzhansky-Muller incompatibility?

The syndrome of Dobzhansky-Muller is related to the phenomenon of speciation between genetically close organisms (Coyne and Orr 2004). The syndrome describes how the interaction between the allelic mutations from two parental genotypes is deleterious for the development of the hybrids. Abundant literature has redundantly identified the rare alleles at CRY2 and GH.121L of the *Arabidopsis* accessions Cvi and L*er*, respectively, as pleiotropic hotspots involved in many molecular and physiological processes in different environmental conditions (e.g. (Alonso-Blanco et al. 1999, Borevitz et al. 2002, Fu et al. 2009, Mendez-Vigo et al. 2010)). Furthermore, previous works have demonstrated that the effects of CRY2 and GH.121L reflect pleiotropy at a single locus rather than several closely linked loci (e.g. El-Assal et al. 2001, Vasseur et al. 2012 = Manuscript #5). L*er* and Cvi are originated from contrasted geographic locations: central Europe and Cape Verde Islands, respectively. Due to

the peculiar climatic conditions in which Cvi has evolved, this accession is strongly divergent from the *A. thaliana* taxon, and has sometimes been described as "*almost* another species than *Arabidopsis thaliana*" (C. Becker, personal communication). Our results showed that the allelic variability between L*er* and Cvi at CRY2 and BH.121L generated plants that strongly differ in size, and consequently in their allometric trajectories, although in average HT and WD induced a reduction of plant size whatever the allelic combination. The RILs that carry recombined allelic combinations at CRY2/BH.121L (i.e. L*er*/Cvi and Cvi/L*er*) exhibited extreme size, and, thus, extreme allometric trajectories. In optimum condition, we previously demonstrated that these extreme phenotypes deviate from the canonical ¾ slope of metabolic allometry (Vasseur et al. 2012 = Manuscript #5). Many evidences in the present study further indicated that the parental allelic combinations exhibit highly performing phenotypes. Indeed, the bell-shaped curvature of reproductive allometry, while closely flat in optimum condition, was more pronounced under WD and HT, which implies a strong decrease in reproductive allocation, specifically in small genotypes and also, but to a lower extent, in big genotypes. Similarly, WUE exhibited optimality in intermediate phenotypes. This is particularly true in HTxWW because of an important decrease in the WUE of the small RILs that carry Cvi/L*er* combination at CRY2/GH.121L. At the opposite, the large RILs that carry L*er*/Cvi combination at CRY2/GH.121L suffered dramatically of HT and WD. In the most stressing condition (HTxWD), survival until reproduction was decreased up to 75% in the biggest plants. As last evidence, the mass of seeds produced in the large introgressed line ($GH.121L_{Cvi}$) that carries non-native allelic combination (i.e. L*er*/Cvi at CRY2/GH.121L) was significantly reduced in competition under fluctuating environment. Our findings are consistent with the negative effect of CRY2 on ovule fertilization reported in literature (Alonso-Blanco et al. 1999). Moreover, our findings support previous evidences about the enhanced performance of intermediate size/age at reproduction in natural populations of *Arabidopsis thaliana* (Metcalf and Mitchell-Olds 2009). Therefore, while innocuous in their native genetic background, the interaction between the L*er* and Cvi alleles at major pleiotropic QTL generates deleterious phenotypes with low fitness. Strikingly, a cross between L*er* and Cvi results in 50% of the offspring with reduced survival, performance and fertility. One may suppose that this incompatibility reflects a Dobzhansky-Muller syndrome, in which the additive effects of Cvi and L*er* alleles at CRY2/GH.121L decrease the fitness of the offspring in the L*er* x Cvi population, although they are not deleterious in their native genetic backgrounds. The accumulation of mutations at major pleiotropic genes in the Arabidopsis populations from the Cape Verde Islands and from Eastern Europe may reduce in

the capacity of the Cvi and L*er* hybrids to propagate in natural conditions. It strongly supports the idea that Cvi is "*almost* another species than *Arabidopsis thaliana*".

Escaping from the PES: genetic variability meets evolutionary constraints

The functional trade-offs illustrated by the covariation between age at reproduction (a proxy of lifespan), leaf structure and carbon fixation have been extensively described (Reich et al. 1997, Wright et al. 2004, Bonser et al. 2010), but the plasticity of these relationships have not been investigated, except at the interspecific level (Atkinson et al. 2010). Here, we demonstrated strong effects of temperature and water availability on the covariations underlying the economy of carbon and water within a population of genetically-related individuals. Strikingly, mass-based net photosynthetic rate decreases with plant size, LMA and age at reproduction in sub-optimal, but not in supra-optimal, temperature, whatever the watering condition. Similarly to what have been proposed for the responses to WD (Tardieu et al. 2011), this result suggests that metabolic rate decreases dramatically above T_{opt} (~ 26.5 °C in *A. thaliana*) because the physiological acclimations to maximize carbon fixation and water conservation do not support the coordination of biological processes at supra-optimal temperature. This deleterious imbalanced trade-off between carbon gain and water conservation is reflected by the allometry of WUE, which was, in average, decreased by HT (note that, inversely, WD tended to increase WUE). Moreover, the decrease was enhanced in the smallest and biggest plants that exhibit the extreme strategies for water and carbon economics.

A central question about physiological trade-offs concerns their evolution. Specifically, it remains unclear why some phenotypes are not observed. For instance, why did not we find big/early flowering plants, or small/late flowering plants? There are two ways to explain why such trait combinations do not exist: (*i*) natural selection could eliminate unfit or poorly performing phenotypes; and (*ii*) genetic constraints could limit the genetic variability that is perpendicular to the major axis of correlation. Using empirical data from different species, Donovan and colleagues (Donovan et al. 2011) recently advocated that selection is likely the major determinant of covariations between the traits of the PES at the leaf level (i.e. the 'leaf economics spectrum'). However in the present study, selection is only targeted on a sufficient seeds production in classical laboratory conditions to allow the propagation of RILs (Alonso-Blanco et al. 1998). Thus, our results demonstrated that the positions in the phenotypic space are constrained to an axis of covariation not by natural selection, but by the pleiotropic effects of major QTL, such as CRY2 and GH.121L. However, the optimum performance for the

intermediate parental allelic combinations supports the idea that the position along the PES could be the indirect outcome of stabilizing selection on allometric coefficients.

In accordance to previous works (McKay et al. 2003, Hausmann et al. 2005), we reported the effect of MSAT2.22 on the plasticity of WUE to WD. Strikingly, we demonstrated that MSAT2.22 generates variability that is perpendicular to the allometric trajectory of carbon and water economics. MSAT2.22 displayed modest effects that depend on the environmental conditions, specifically on the water availability. Hence, this result suggests that escaping from the PES is genetically possible, but only to a weak extent and under certain environmental conditions. MSAT2.22 was associated with a significant decrease in reproductive success with or without competition. Unfortunately, we do not know whether the genetic variability could generate very early/big plants (or very late/small plants) that are unable to reproduce in laboratory conditions. Nonetheless, our findings strongly support the Donovan's hypothesis that escaping from the PES would be associated to a reduced fitness. In this context, it is difficult to explain why the Cvi allele at MSAT2.22 has been maintained in the *Arabidopsis* populations of the Cape Verde Islands. One may hypothesized that the L*er* allele at MSAT2.22 was the result of a punctual, beneficial, genetic mutation that propagated after the divergence of Cvi and L*er* accessions. Overall, our data indicate that the PES is shaped by genetic constraints limiting the phenotypic variability in many directions. This result is consistent with the findings of Dorn and Mitchell-Olds (Dorn and Mitchellolds 1991) who reported low genetic variability perpendicular to the axis of covariation between age and size at reproduction. Within the range of reachable trait-trait combinations, evolutionary forces may operate to eliminate the genotypes that exhibit dramatically altered allometric trajectories. Such evolutionary outcome is a promising avenue, but it needs to be tested in the field with natural plant populations.

Conclusion

In this study, we found strong plasticity in the allometric relationships of many adaptive traits. This plasticity was generated by few pleiotropic QTL with presumably major influence for the mechanisms of plant adaptation. We identified QTL that govern variations *along* the allometric trajectories, and that consequently strongly impact plant performance depending on the environmental conditions. In addition, we identified a QTL that governs the variability *perpendicularly* to the allometric trajectories of water use efficiency. The evolutionary role of this QTL needs to be tested in natural conditions and with different accessions. If confirmed,

this QTL would also be a promising target for breeders, specifically in a global warming world.

Acknowledgements

We thank M. Dauzat, A. Bédié, F. Bouvery, J. Pasquet-Kok, J. Bresson, C. Balsera, and G. Rolland for technical assistance with the PHENOPSIS platform and their help during experiments. F.V. was funded by a CIFRE grant (ANRT, French Ministry of Research) supported by BAYER Crop Science (contract 0398/2009 – 09 42 008).

References

Ackerly, D. D. and P. B. Reich. 1999. Convergence and correlations among leaf size and function in seed plants: a comparative test using independent contrasts. American Journal of Botany **86**:1272-1281.

Alonso-Blanco, C., H. Blankestijn-de Vries, C. J. Hanhart, and M. Koornneef. 1999. Natural allelic variation at seed size loci in relation to other life history traits of *Arabidopsis thaliana*. Proceedings of the National Academy of Sciences of the United States of America **96**:4710-4717.

Alonso-Blanco, C., A. J. M. Peeters, M. Koornneef, C. Lister, C. Dean, N. van den Bosch, J. Pot, and M. T. R. Kuiper. 1998. Development of an AFLP based linkage map of L*er*, Col and Cvi *Arabidopsis thaliana* ecotypes and construction of a L*er*/Cvi recombinant inbred line population. Plant Journal **14**:259-271.

Atkinson, L. J., C. D. Campbell, J. Zaragoza-Castells, V. Hurry, and O. K. Atkin. 2010. Impact of growth temperature on scaling relationships linking photosynthetic metabolism to leaf functional traits. Functional Ecology **24**:1181-1191.

Bonser, S. P. 2006. Form defining function: interpreting leaf functional variability in integrated plant phenotypes. Oikos **114**:187-190.

Bonser, S. P., B. Ladd, K. Monro, M. D. Hall, and M. A. Forster. 2010. The adaptive value of functional and life-history traits across fertility treatments in an annual plant. Ann Bot **106**:979-988.

Borevitz, J. O., J. N. Maloof, J. Lutes, T. Dabi, J. L. Redfern, G. T. Trainer, J. D. Werner, T. Asami, C. C. Berry, D. Weigel, and J. Chory. 2002. Quantitative trait loci controlling light and hormone response in two accessions of *Arabidopsis thaliana*. Genetics **160**:683-696.

Brown, J. H., J. F. Gillooly, A. P. Allen, V. M. Savage, and G. B. West. 2004. Toward a metabolic theory of ecology. Ecology **85**:1771-1789.

Coyne, J. A. and H. A. Orr. 2004. Speciation. Sinauer Associates, Inc, Sunderland, MA.

Donovan, L. A., H. Maherali, C. M. Caruso, H. Huber, and H. de Kroon. 2011. The evolution of the worldwide leaf economics spectrum. Trends in Ecology & Evolution **26**:88-95.

Dorn, L. A. and T. Mitchell-olds. 1991. Genetics of *Brassica-Campestris* .1. Genetic constraints on evolution of life-history characters. Evolution **45**:371-379.

El-Assal, S. E. D., C. Alonso-Blanco, A. J. M. Peeters, V. Raz, and M. Koornneef. 2001. A QTL for flowering time in Arabidopsis reveals a novel allele of *CRY2*. Nature Genetics **29**:435-440.

Enquist, B. J. and L. P. Bentley. 2012. Land Plants: New Theoretical Directions and Empirical Prospects. Pages 164-187 Metabolic Ecology. John Wiley & Sons, Ltd.

Fabre, J., M. Dauzat, V. Negre, N. Wuyts, A. Tireau, E. Gennari, P. Neveu, S. Tisne, C. Massonnet, I. Hummel, and C. Granier. 2011. PHENOPSIS DB: an information system for *Arabidopsis thaliana* phenotypic data in an environmental context. BMC Plant Biol **11**:77.

Freschet, G. T., J. H. C. Cornelissen, R. S. P. van Logtestijn, and R. Aerts. 2010. Evidence of the 'plant economics spectrum' in a subarctic flora. Journal of Ecology **98**:362-373.

Fu, J., J. J. Keurentjes, H. Bouwmeester, T. America, F. W. Verstappen, J. L. Ward, M. H. Beale, R. C. de Vos, M. Dijkstra, R. A. Scheltema, F. Johannes, M. Koornneef, D. Vreugdenhil, R. Breitling, and R. C. Jansen. 2009. System-wide molecular evidence for phenotypic buffering in Arabidopsis. Nature Genetics **41**:166-167.

Gillooly, J. F., J. H. Brown, G. B. West, V. M. Savage, and E. L. Charnov. 2001. Effects of size and temperature on metabolic rate. Science **293**:2248-2251.

Granier, C., L. Aguirrezabal, K. Chenu, S. J. Cookson, M. Dauzat, P. Hamard, J. J. Thioux, G. Rolland, S. Bouchier-Combaud, A. Lebaudy, B. Muller, T. Simonneau, and F. Tardieu. 2006. PHENOPSIS, an automated platform for reproducible phenotyping of plant responses to soil water deficit in *Arabidopsis thaliana* permitted the identification of an accession with low sensitivity to soil water deficit. New Phytologist **169**:623-635.

Hausmann, N. J., T. E. Juenger, S. Sen, K. A. Stowe, T. E. Dawson, and E. L. Simms. 2005. Quantitative trait loci affecting delta^{13}C and response to differential water availibility in *Arabidopsis thaliana*. Evolution **59**:81-96.

Johnson, F. H., H. Eyring, and R. W. Williams. 1942. The nature of enzyme inhibitions in bacterial luminescence: Sulfanilamide, urethane, temperature and pressure. Journal of Cellular and Comparative Physiology **20**:247-268.

Keurentjes, J. J., L. Bentsink, C. Alonso-Blanco, C. J. Hanhart, H. Blankestijn-De Vries, S. Effgen, D. Vreugdenhil, and M. Koornneef. 2007. Development of a near-isogenic line population of *Arabidopsis thaliana* and comparison of mapping power with a recombinant inbred line population. Genetics **175**:891-905.

Kolokotrones, T., V. Savage, E. J. Deeds, and W. Fontana. 2010. Curvature in metabolic scaling. Nature **464**:753-756.

McKay, J. K., J. H. Richards, and T. Mitchell-Olds. 2003. Genetics of drought adaptation in *Arabidopsis thaliana*: I. Pleiotropy contributes to genetic correlations among ecological traits. Molecular Ecology **12**:1137-1151.

Mendez-Vigo, B., M. T. de Andres, M. Ramiro, J. M. Martinez-Zapater, and C. Alonso-Blanco. 2010. Temporal analysis of natural variation for the rate of leaf production and its relationship with flowering initiation in *Arabidopsis thaliana*. J Exp Bot **61**:1611-1623.

Metcalf, C. J. and T. Mitchell-Olds. 2009. Life history in a model system: opening the black box with *Arabidopsis thaliana*. Ecology Letters **12**:593-600.

Mommer, L. and M. Weemstra. 2012. The role of roots in the resource economics spectrum. New Phytologist **195**:725-727.

Parent, B. and F. Tardieu. 2012. Temperature responses of developmental processes have not been affected by breeding in different ecological areas for 17 crop species. New Phytologist **194**:760-774.

Parent, B., O. Turc, Y. Gibon, M. Stitt, and F. Tardieu. 2010. Modelling temperature-compensated physiological rates, based on the co-ordination of responses to temperature of developmental processes. J Exp Bot **61**:2057-2069.

Price, C. A., B. J. Enquist, and V. M. Savage. 2007. A general model for allometric covariation in botanical form and function. Proc Natl Acad Sci U S A **104**:13204-13209.

Price, C. A., J. S. Weitz, V. M. Savage, J. Stegen, A. Clarke, D. A. Coomes, P. S. Dodds, R. S. Etienne, A. J. Kerkhoff, K. McCulloh, K. J. Niklas, H. Olff, N. G. Swenson, and J. Chave. 2012. Testing the metabolic theory of ecology. Ecology Letters.

Reich, P. B., M. B. Walters, and D. S. Ellsworth. 1997. From tropics to tundra: Global convergence in plant functioning. Proceedings of the National Academy of Sciences of the United States of America **94**:13730-13734.

Savage, V. M., J. F. Gilloly, J. H. Brown, and E. L. Charnov. 2004. Effects of body size and temperature on population growth. Am Nat **163**:429-441.

Tardieu, F., C. Granier, and B. Muller. 2011. Water deficit and growth. Co-ordinating processes without an orchestrator? Curr Opin Plant Biol **14**:283-289.

Vasseur, F., C. Violle, B. J. Enquist, C. Granier, and D. Vile. 2012. A common genetic basis to the origin of the leaf economics spectrum and metabolic scaling allometry. Ecology Letters **15**:1149-1157.

Walsh, B. and M. W. Blows. 2009. Abundant genetic variation plus strong selection = multivariate genetic constraints: a geometric view of adaptation. Annual Review of Ecology Evolution and Systematics **40**:41-59.

West, G. B., J. H. Brown, and B. J. Enquist. 1997. A general model for the origin of allometric scaling laws in biology. Science **276**:122-126.

West, G. B., J. H. Brown, and B. J. Enquist. 1999. The fourth dimension of life: fractal geometry and allometric scaling of organisms. Science **284**:1677-1679.

Whitfield, J. 2004. Ecology's big, hot idea. PLoS Biol **2**:e440.

Wright, I. J., P. B. Reich, M. Westoby, D. D. Ackerly, Z. Baruch, F. Bongers, J. Cavender-Bares, T. Chapin, J. H. C. Cornelissen, M. Diemer, J. Flexas, E. Garnier, P. K. Groom, J. Gulias, K. Hikosaka, B. B. Lamont, T. Lee, W. Lee, C. Lusk, J. J. Midgley, M. L. Navas, U. Niinemets, J. Oleksyn, N. Osada, H. Poorter, P. Poot, L. Prior, V. I. Pyankov, C. Roumet, S. C. Thomas, M. G. Tjoelker, E. J. Veneklaas, and R. Villar. 2004. The worldwide leaf economics spectrum. Nature **428**:821-827.

Supporting Information

Table S1. General statistics of the phenotypic traits. LMA : leaf mass per area, A_{mass}: mass-based net photosynthetic rate, ET_{mass}: mass-based transpiration rate. ANOVA significance levels: *** = P < 0.001; ** = P < 0.01; * = P < 0.05; ° = P < 0.1.

Trait	min	max	mean	G	W	T	WxT
Vegetative dry mass (mg)	0.370	529.8	43.5	***	***	***	NS
Age at reproduction (d)	21.0	104.0	40.3	***	***	***	*
Total leaf area (cm^2)	0.212	108.0	11.0	***	***	***	NS
Reproductive dry mass (mg)	0.130	45.7	6.55	***	***	***	*
LMA ($g\ m^{-2}$)	5.989	69.0	23.9	***	***	***	***
Normalized growth rate ($mg\ d^{-1}$)	0.006	28.2	1.94	***	***	***	***
A_{mass} ($nmol\ s^{-1}\ g^{-1}$)	0.769	947.4	148.5	***	***	***	***
ET_{mass} ($g\ d^{-1}\ g^{-1}$)	2.695	1580.9	162.5	***	***	***	***
WUE ($nmol\ mg^{-1}$)	0.360	1587.7	231.9	***	NS	***	***

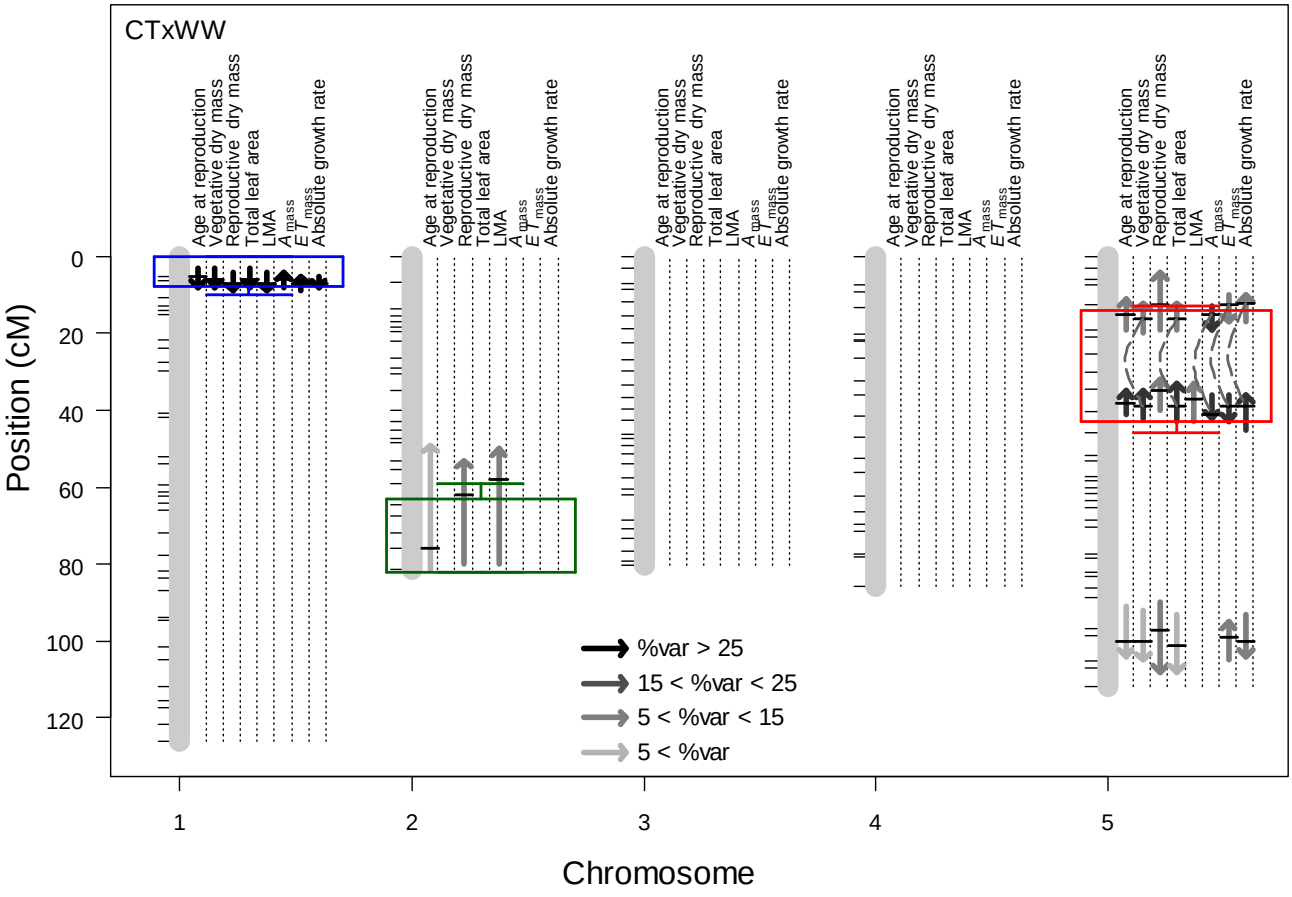

Figure S1. Positions of genomic introgressions in introgressed lines. Positions of the three introgressed lines are provided in (Keurentjes et al. 2007) and reported on the genetic map where the QTL of the functional traits in CTxWW were reported (from Figure S5a). Blue: $CRY2_{Cvi}$, red: $GH.121L_{Cvi}$, and green: $MSAT2.22_{Cvi}$.

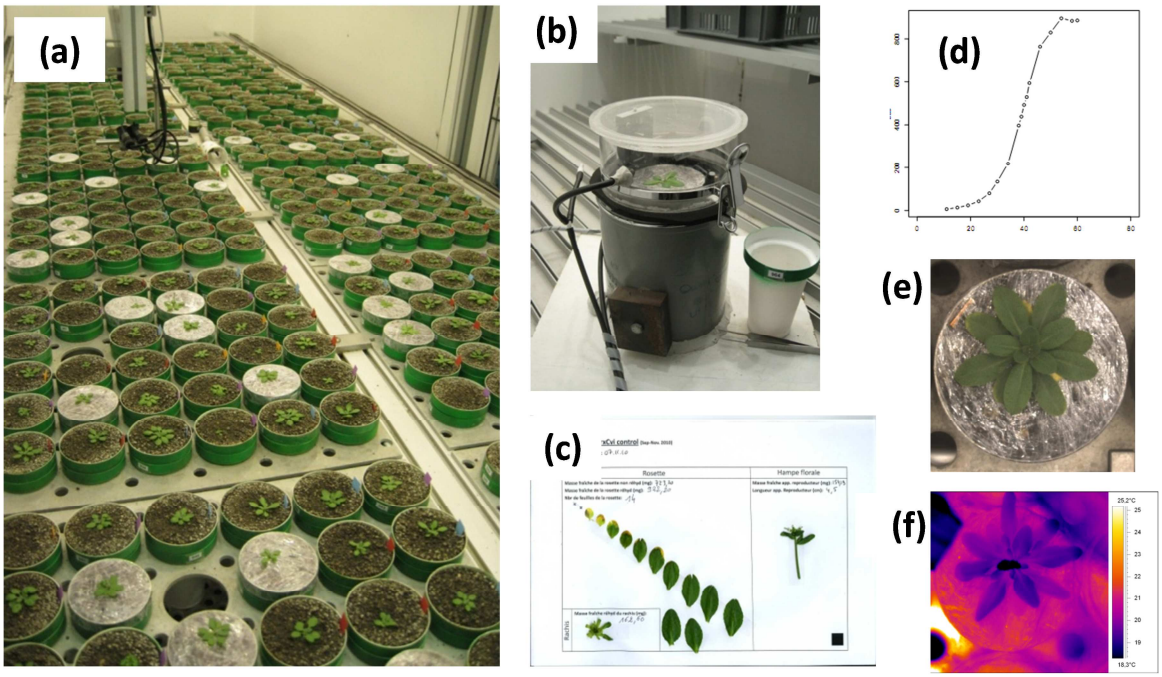

Figure S2. The PHENOPIS facility and the experimental procedures. (a) The PHENOPSIS automaton in Montpellier (France) (Granier et al. 2006). (b) Whole-plant chamber for analyzing gas exchange with CIRAS 2 analyzer (PP systems). (c) Total leaf area scanned at flowering to measure total leaf area. (d) Example of growth curve fitted from 2-3 days with zenithal images. (e) Example of zenithal images acquired from the PHENOPIS automaton. Soil was filled with plastic film to prevent water loss from the soil. (f) Example of infra-red image acquired from the PHENOPSIS automaton.

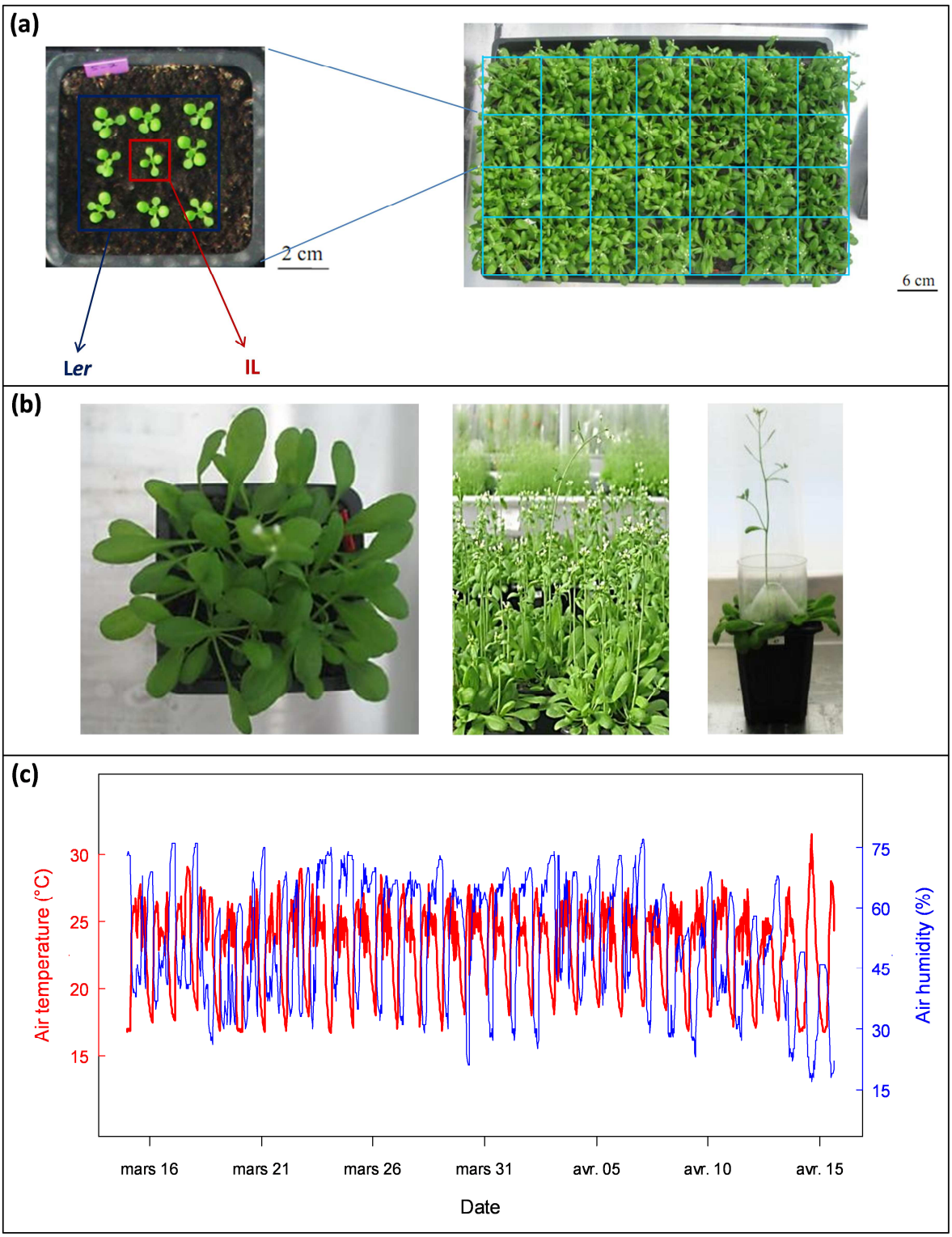

Figure S3. Experimental procedure to estimate reproductive success in competition. (a) Five genotypes were grown within a matrix of eight plants (L*er* accession): the two parental accessions L*er* and Cvi, and the three introgressed lines (IL): $CRY2_{Cvi}$, $GH.121L_{Cvi}$, and $GH.121L_{Cvi}$. (b) At first flower open, the flowering stem of the tested genotype was isolated with a funnel, and irrigation was stopped. All seeds of each plant were harvested when dried (~ 3 weeks later). (c) Plants were grown in greenhouse under fluctuating air temperature and humidity, and soil humidity (data not shown).

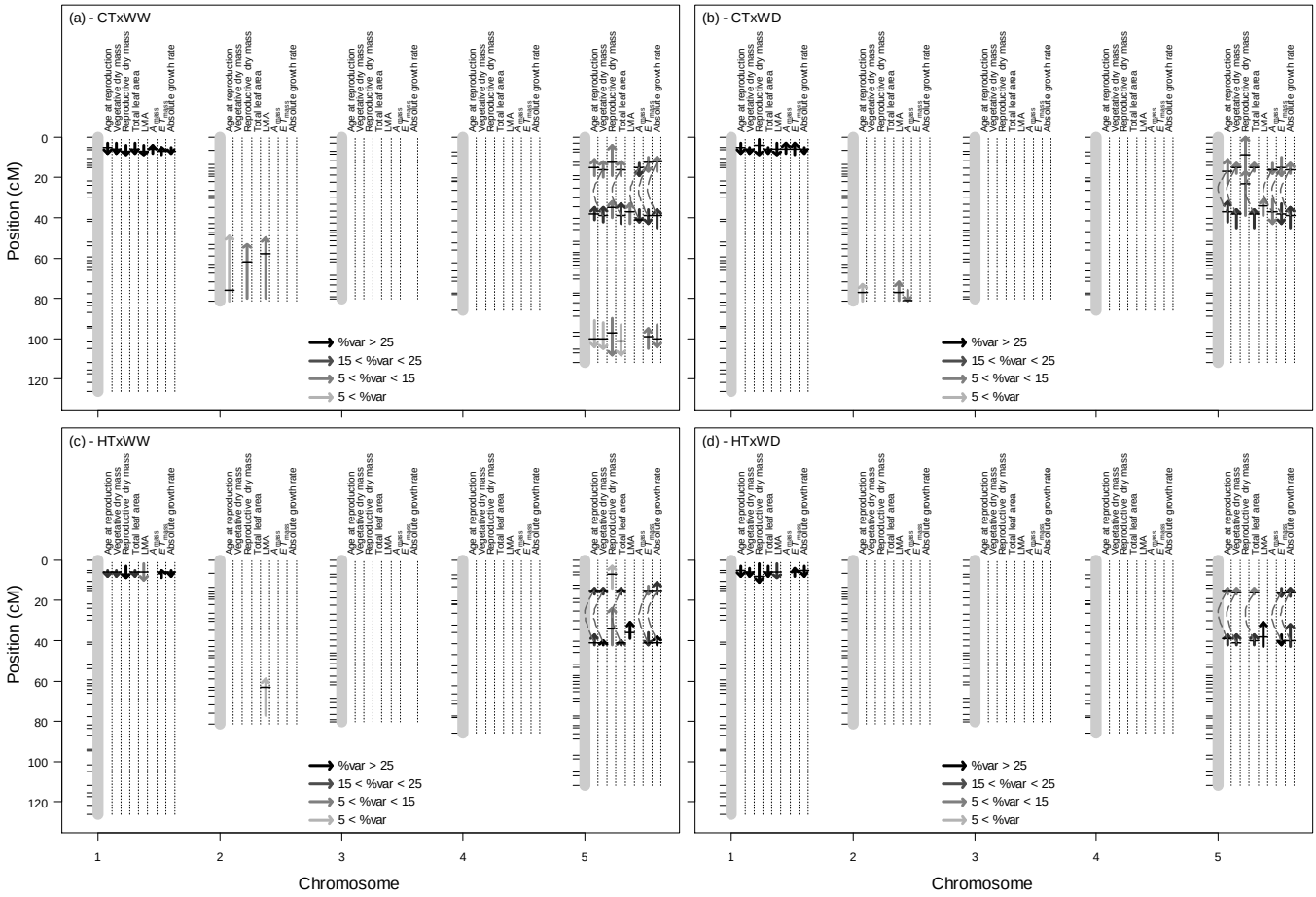

Figure S4. QTL analysis of the phenotypic traits within the four environments. (a) CTxWW: control temperature and well-watered (20 °C x 35 g H_20 g^{-1} dry soil). (b) CTxWD: control temperature and water deficit (20 °C x 20 g H_20 g^{-1} dry soil). (c) HTxWW: high temperature and well watered (30 °C x 35 g H_20 g^{-1} dry soil). (d) HTxWD: high temperature and water deficit (30 °C x 20 g H_20 g^{-1} dry soil). From column 1 to 8: age at reproduction (days), vegetative dry mass (mg), reproductive dry mass (mg), total leaf area (cm^2), leaf mass per area (LMA, g m^{-2}), mass-based net photosynthetic rate (A_{mass}, nmol s^{-1} g^{-1}), mass-based transpiration rate (ET_{mass}, mg d^{-1} g^{-1}), and absolute growth rate (mg d^{-1}). Arrows length represents confidence interval and arrows color represents the percent of variability explained by each QTL (< 5% to > 25%: lighter grey to black, respectively). Arrows direction represents the effect of Cvi allele against L*er* allele. Dashed lines represent significant epistatic interactions between QTL ($P < 0.05$).

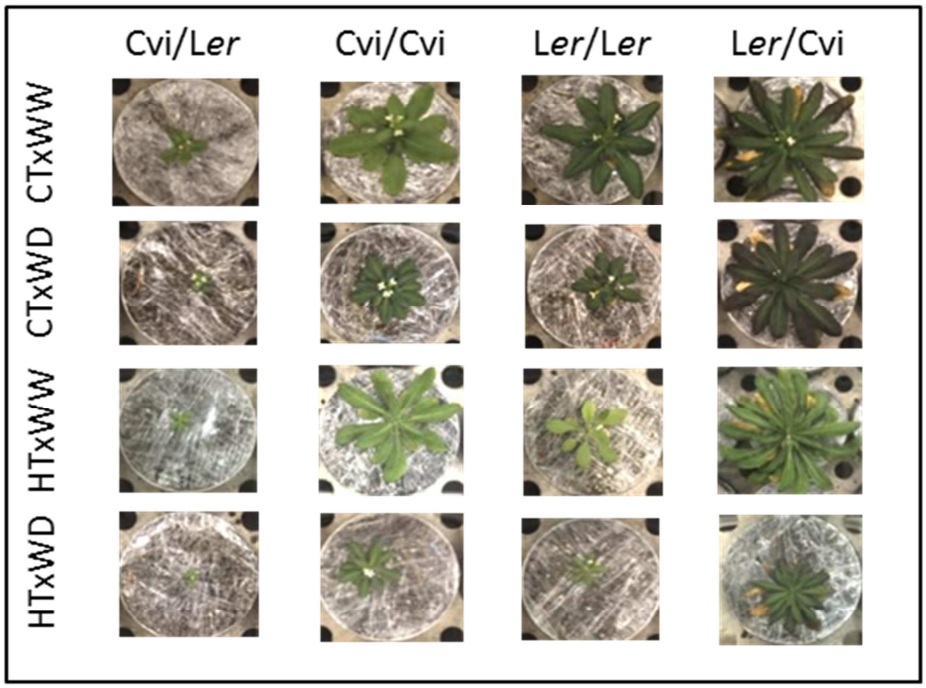

Figure S5. Examples of phenotypes in RILs according to their allelic combination at CRY2/GH121L. Allelic combination depends on the allele (L*er* or Cvi) at two major pleiotropic QTL: CRY2/GH.121L. All images were taken at the same stage (first flower open).

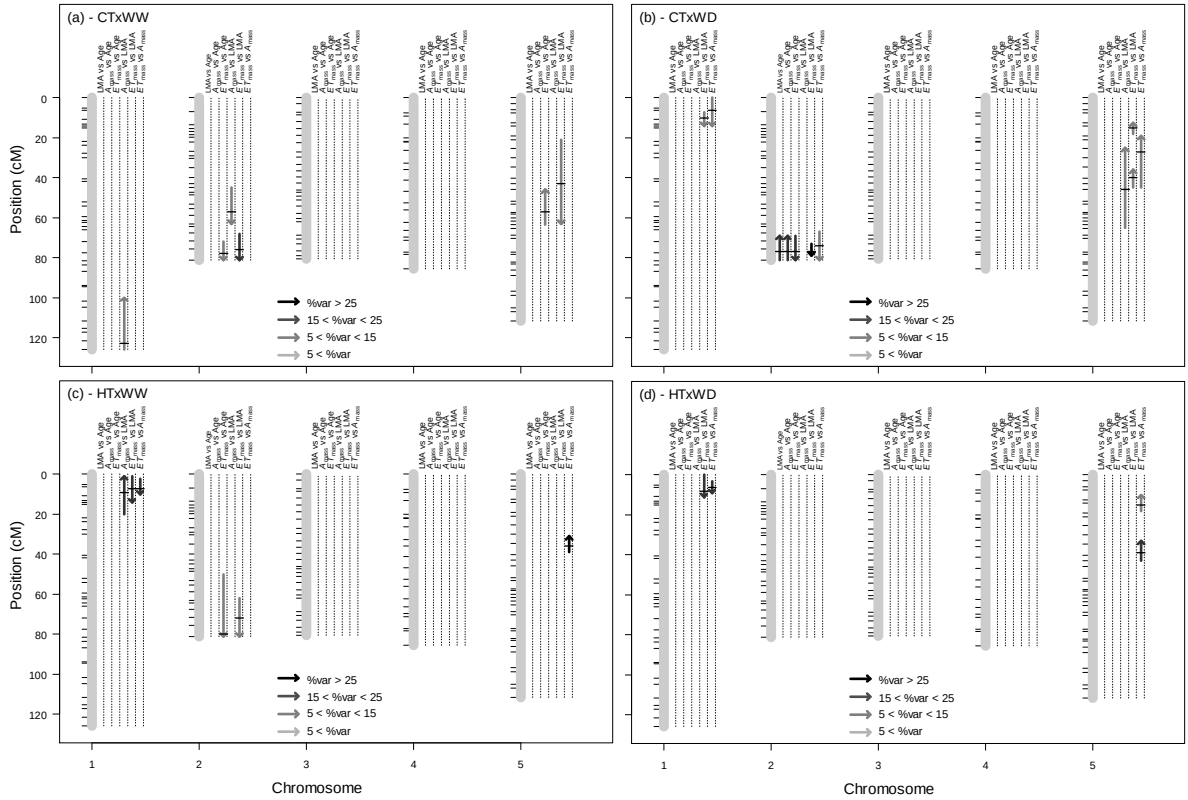

Figure S6. QTL analysis of the residuals of the PES. The residuals of each bivariate relationship were extracted from a loess fit (see Figure 2). From column 1 to 6: LMA (leaf mass per area, g m^{-2}) versus Age (age at reproduction, days), A_{mass} (mass-based net photosynthetic rate, nmol s^{-1} g^{-1}) versus Age, ET_{mass} (mass-based transpiration rate, mg d^{-1} g^{-1}) versus Age, A_{mass} versus LMA, ET_{mass} versus LMA, and ET_{mass} versus A_{mass}. (a) CTxWW: control temperature and well-watered (20 °C x 35 g H_20 g^{-1} dry soil). (b) CTxWD: control temperature and water deficit (20 °C x 20 g H_20 g^{-1} dry soil). (c) HTxWW: high temperature and well watered (30 °C x 35 g H_20 g^{-1} dry soil). (d) HTxWD: high temperature and water deficit (30 °C x 20 g H_20 g^{-1} dry soil). Arrows length represents confidence interval and arrows color represents the percent of variability explained by each QTL (< 5% to > 25%: lighter grey to black, respectively). Arrows direction represents the effect of Cvi allele against L*er* allele. Dashed lines represent significant epistatic interactions between QTL ($P < 0.05$).

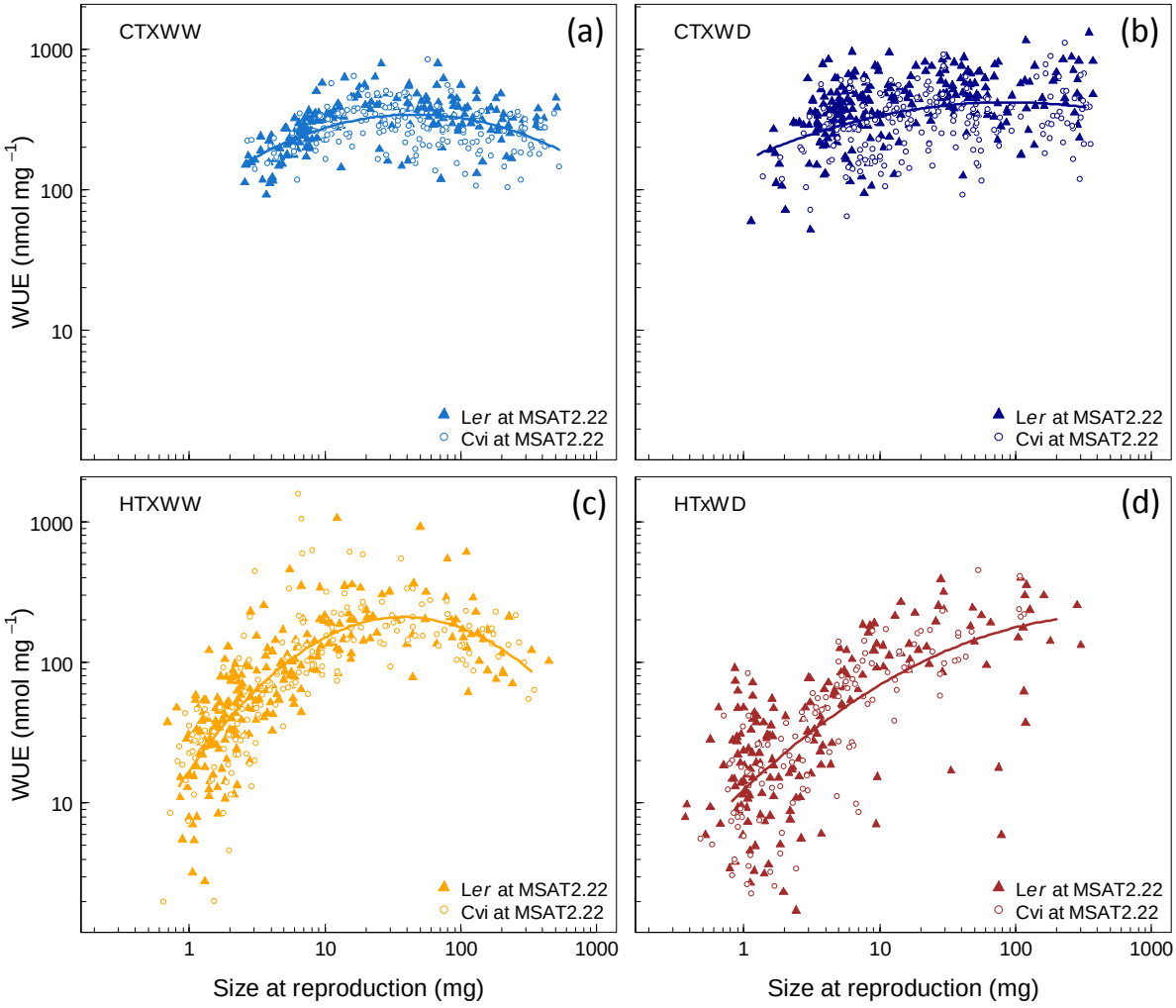

Figure S7. Allometry of WUE according to the allele at MSAT2.22. (a) CTxWW: control temperature and well-watered (20 °C x 0.35 g H_20 g^{-1} dry soil). (b) CTxWD: control temperature and water deficit (20 °C x 0.20 g H_20 g^{-1} dry soil). (c) HTxWW: high temperature and well watered (30 °C x 0.35 g H_20 g^{-1} dry soil). (d) HTxWD: high temperature and water deficit (30 °C x 0.20 g H_20 g^{-1} dry soil). Filled triangle: L*er* allele at MSAT2.22. Empty circle: Cvi allele at MSAT2.22.

Conclusion générale

Au cours de cette thèse nous avons décrit les réponses intégrées d'*Arabidopsis thaliana* à deux contraintes environnementales majeures : le déficit hydrique et les hautes températures. Nos résultats ont permis à la fois de mettre en évidence la forte plasticité phénotypique des plantes à ces deux stress, et d'en cartographier le déterminisme génétique. En accord avec les résultats de la littérature (Ludwig-Muller et al. 2000, Aguirrezabal et al. 2006, Parent and Tardieu 2012), les traitements appliqués ici ont été néfastes, autrement dit ont représenté un stress, pour l'ensemble des génotypes cultivés. Ceci est illustré par la diminution de la taille des organes végétatifs et reproducteurs en condition de stress, ainsi que par l'augmentation de la mortalité sur une partie de la population de lignées recombinantes. Nous avons mis en évidence que les hautes températures et le déficit hydrique ont des effets additifs sur de nombreux traits liés au développement et à l'histoire de vie, alors qu'ils ont des effets interactifs sur les traits physiologiques liés à la fixation du carbone. Par ailleurs, les résultats indiquent que tous les génotypes présentent les mêmes réponses développementales aux stress mais des réponses physiologiques très variables. A l'origine de cette variabilité, des gènes pléiotropes gouvernent le développement de la plante indépendamment de l'environnement tandis que d'autres induisent des réponses physiologiques variables suivant les conditions. Ainsi, nous avons montré que la gestion de l'eau est fortement liée à la taille et à l'âge de la plante, ce qui implique que ces traits partagent le même déterminisme génétique. En revanche, les réponses différentes du métabolisme carboné nous ont permis de trouver des QTL associés à des variations d'efficience d'utilisation de l'eau en réponse aux stress hydrique et thermique.

Les gènes et les QTL pléiotropes impliqués dans la régulation du développement sont à l'origine de variation forte dans la taille des plantes au stade reproducteur. L'analyse des relations allométriques nous a permis de proposer un modèle conceptuel dans lequel la pléiotropie des gènes majeurs du développement serait à l'origine des contraintes évolutives opérant sur les principaux processus physiologiques et métaboliques. Selon ce modèle, la fixation d'allèles résulterait de la sélection des individus présentant la relation métabolisme/taille la plus favorable dans des conditions environnementales données. Les relations allométriques varient significativement en réponse à la température et à la disponibilité en eau, et présentent des signes d'optima pour de nombreux traits adaptatifs. Les allèles rares de Cvi et L*er* aux gènes *CRY2* et *HUA2* sont à l'origine de stratégies

fonctionnelles très variables, caractérisées par des variations allométriques importantes associées à des différences de performance et de succès reproducteur. Les effets délétères de l'association de *CRY2* et *HUA2* sur les performances des descendants du croisement L*er* x Cvi semblent indiquer un certain degré d'incompatibilité génétique entre les deux accessions parentales. Si les effets additifs de *CRY2* et *HUA2* pourraient être limités à cette population, les mécanismes génétiques mis en jeu sont en théorie applicables à l'ensemble des plantes vasculaires. L'accumulation de mutations à des gènes majeurs du développement pourrait être à l'origine des phénomènes de spéciation résultant de l'isolement génétique des populations naturelles. Tester ces mécanismes dans de multiples populations naturelles est indispensable. Les centaines d'accessions d'*Arabidopsis thaliana* récemment séquencées offrent un matériel de choix dans une telle perspective (e.g. Horton et al. 2012). De plus, les progrès fulgurants en matière de séquençage permettent d'envisager de développer très rapidement ce genre d'approches sur d'autres espèces (Galvao et al. 2012).

Parmi les QTL impliqués dans la régulation des processus physiologiques indépendamment du développement, MSAT2.22 contrôle l'efficience d'utilisation de l'eau selon sa disponibilité dans le sol. Ce locus offre des perspectives encourageantes pour l'amélioration des espèces cultivées face aux changements climatiques actuels. Dans les approches de génétique directe, la première étape visant à déterminer la ou les mutations responsables de l'effet d'un QTL s'appuie sur la réduction progressive de l'intervalle de confiance par recombinaison et/ou introgression. Basée sur cette approche, une étude a récemment identifié un gène codant un facteur de transcription responsable de l'effet de MSAT2.22 sur la ramification des parties végétatives indépendamment de la floraison (Huang et al. 2012). Cette étude rapporte aussi la variabilité naturelle présente à ce locus dans les populations *d'A. thaliana*. Dans les futures recherches, la valeur adaptative de ce QTL et du ou des gènes causaux devra être examinée dans d'autres génotypes, ainsi que dans d'autres situations environnementales, afin d'en évaluer l'universalité ou les limites. L'exportation des connaissances génétiques développées sur les espèces modèles aux espèces d'intérêt agronomique demeure une étape clef souvent difficile à franchir en amélioration des plantes. Cette difficulté peut être illustrée par l'absence d'effet d'*ERECTA* sur la variabilité phénotypique observée dans notre étude sur la population L*er* x Cvi. Ce gène, qu'une mutation dans l'accession parentale L*er* (Landsberg *erecta*) rend non fonctionnel, code un récepteur kinase dont précédentes études ont montré l'implication dans la prolifération et la différenciation cellulaire des organes aériens en lien avec de nombreux processus physiologiques comme l'efficience d'utilisation de l'eau (Masle et al. 2005, van Zanten et al.

2009, Tisne et al. 2011). L'absence d'effet d'*ERECTA* est l'occasion de souligner plusieurs points importants relatifs à l'analyse génétique de caractères quantitatifs.

D'une part, les différences entre nos résultats et ceux de la littérature peuvent provenir du matériel génétique utilisé. Les effets d'*ERECTA* pourraient par exemple dépendre d'interactions épistatiques avec d'autres gènes, et donc de la variabilité allélique associée à ces gènes. De plus, les interactions épistatiques peuvent elles-mêmes dépendre de l'environnement dans lequel les plantes se développent (Gibson and Dworkin 2004). La variabilité des effets génétiques selon les populations et selon les environnements est en cours d'investigation au LEPSE. Les premiers résultats suggèrent que les effets d'*ERECTA* dépendraient d'interactions épistatiques variables selon la disponibilité en eau dans le sol (données non présentées). D'autre part, les différences entre certains résultats de la littérature et les nôtres peuvent s'expliquer par le type de mesures. Par exemple dans l'étude de Masle et al. (2005), l'efficience d'utilisation de l'eau a été estimée à l'aide de la discrimination isotopique du carbone, et de la mesure des échanges gazeux sur une feuille mature. La discrimination isotopique du carbone a été utilisée chez de nombreuses espèces (Farquhar and Richards 1984, Farquhar et al. 1989, Condon et al. 2002, Brendel et al. 2008) ; elle permet d'estimer l'efficience d'utilisation de l'eau intégrée sur des pas de temps longs. Cependant, la contribution des échanges gazeux du sol, en contact permanent avec les feuilles de la rosette, pourrait fausser les mesures chez *A. thaliana*. Dans notre étude, nous avons utilisé le rapport entre la photosynthèse et la transpiration. La mesure de la transpiration, intégrée sur plusieurs jours, prend en compte les phénomènes possibles de compensation entre la gestion de l'eau au cours de la journée et au cours de la nuit. Des différences génotypiques de transpiration diurne et nocturne ont d'ailleurs été mises en évidence dans la thèse. Par ailleurs, les mesures de photosynthèse ont été réalisées sur plante entière, prenant ainsi en compte la géométrie des organes dans l'espace et la structure des feuilles de la rosette. De précédents travaux au LEPSE ont remarqué l'absence d'effet d'*ERECTA* sur la structure du mésophylle malgré des effets importants sur la structure de l'épiderme (données non présentées). En accord avec une étude récente (Flexas et al. 2012), ces résultats suggèrent que la photosynthèse serait principalement sous la dépendance du mésophylle, et donc moins affectée par les effets génétiques, comme ceux d'*ERECTA*, opérant sur les cellules épidermiques et les stomates. Une perspective de cette thèse est de décortiquer l'importance relative du mésophylle et des stomates dans les échanges d'eau et de carbone avec l'air à la base des processus de croissance végétale. Enfin, la mesure des plantes au même stade, et non au même âge, nous a permis d'intégrer la variation des traits au cours de l'ontogénie. Les relations allométriques de

la photosynthèse et de la transpiration suggèrent que la mesure de ces caractères à la fin du cycle de développement reflète l'état physiologique imposé par la taille et l'âge. En particulier, cette mesure prend en compte le recouvrement des organes végétatifs à l'origine de contraintes fortes sur les stratégies d'acquisition et de conservation de l'eau et du carbone. Par ailleurs la dynamique de croissance d'une plante est intimement liée à la durée de son cycle. En conséquence, les gènes identifiés comme impactant la croissance à un âge donné sont généralement des gènes pléiotropes impliqués dans le développement et l'histoire de vie (Granier et al., en préparation). De manière générale, l'absence d'effet d'*ERECTA* dans nos mesures de l'efficience d'utilisation de l'eau souligne l'importance de comprendre les phénomènes de compensation dans le temps et dans l'espace pour ne pas surestimer la valeur adaptative d'un gène ou d'un QTL (Tardieu 2012). De plus, ces différences illustrent les problèmes qui peuvent être rencontrés en vue de la validation fonctionnelle d'un gène.

Les mécanismes causaux à l'origine de la coordination des réponses phénotypiques aux facteurs abiotiques sont complexes à élucider. Des méthodes statistiques permettent d'estimer les liens de causalité entre plusieurs variables corrélées (Shipley 2000), mais leur application aux relations non linéaires observées dans cette étude nécessite des développements qui seront prochainement envisagés. Nos résultats suggèrent que les trajectoires évolutives des plantes seraient orientées vers la maximisation de la fixation du carbone, plutôt que vers la régulation thermique des feuilles par la transpiration. De plus l'étude des relations allométriques indique que les contraintes structurales imposées par la taille sur l'interception de la lumière ont des conséquences fortes sur la performance des plantes, en particulier en réponse au stress. Le stress hydrique n'est cependant pas associé à une dégradation du métabolisme carboné, comme le montre l'augmentation de l'efficience d'utilisation de l'eau. Métabolique ou hydrique, la cause de l'impact de la sécheresse sur la performance des plantes est un sujet de débat chez les écophysiologistes (Sala 2009, Hummel et al. 2010, McDowell 2011, Muller et al. 2011). Les données acquises ne permettent pas de déterminer les mécanismes moléculaires liant le statut carboné à la réponse coordonnée des plantes face aux facteurs abiotiques. Ces mécanismes devraient être abordés à partir d'une analyse détaillée des variations ontogéniques de chacun des caractères (Pantin et al. 2012), ainsi que par une étude des gènes et des voies métaboliques impliqués (Baerenfaller et al. 2012). Les résultats acquis durant cette thèse pourraient permettre de paramétrer des modèles mécanistes qui simuleraient l'ensemble des processus impliqués et leurs interactions.

Les données acquises durant cette thèse ont permis de caractériser la coordination des processus physiologiques et développementaux face aux facteurs abiotiques. Paradoxalement,

la diversité des stratégies fonctionnelles n'est déterminée que par un nombre restreint de gènes ou de QTL dont l'action diffère selon les caractères et selon les conditions environnementales. Dans un contexte agronomique, nos résultats suggèrent que des améliorations significatives de performance en condition de stress thermique peuvent être attendues en orientant les recherches vers l'analyse des relations entre métabolisme carboné, taille, et architecture des variétés agronomiques. La modélisation des relations allométriques assistée d'un phénotypage approprié dans différents scenarios climatiques est une étape déterminante pour piloter l'utilisation des génotypes les mieux adaptés morphologiquement à certains types d'environnements. Cette étude et les approches qui y sont développées encourageront peut-être de futures investigations pour évaluer les implications écologiques et les applications agronomiques des gènes et des mécanismes identifiés.

Références

Aguirrezabal, L., S. Bouchier-Combaud, A. Radziejwoski, M. Dauzat, S. J. Cookson, and C. Granier. 2006. Plasticity to soil water deficit in *Arabidopsis thaliana*: dissection of leaf development into underlying growth dynamic and cellular variables reveals invisible phenotypes. Plant Cell and Environment **29**:2216-2227.

Baerenfaller, K., C. Massonnet, S. Walsh, S. Baginsky, P. Buhlmann, L. Hennig, M. Hirsch-Hoffmann, K. A. Howell, S. Kahlau, A. Radziejwoski, D. Russenberger, D. Rutishauser, I. Small, D. Stekhoven, R. Sulpice, J. Svozil, N. Wuyts, M. Stitt, P. Hilson, C. Granier, and W. Gruissem. 2012. Systems-based analysis of Arabidopsis leaf growth reveals adaptation to water deficit. Mol Syst Biol **8**:606.

Brendel, O., D. Thiec, C. Scotti-Saintagne, C. Bodénès, A. Kremer, and J.-M. Guehl. 2008. Quantitative trait loci controlling water use efficiency and related traits in *Quercus robur L.* Tree Genetics & Genomes **4**:263-278.

Condon, A., R. Richards, G. Rebetzke, and G. Farquhar. 2002. Improving intrinsic water-use efficiency and crop yield. Crop Science **42**:122-131.

Farquhar, G., K. Hubick, A. Condon, and R. Richards. 1989. Carbon isotope discrimination and water-use efficiency. Stable isotopes in ecological research 21-46.

Farquhar, G. and R. Richards. 1984. Isotopic composition of plant carbon correlates with water-use efficiency of wheat genotypes. Functional Plant Biology **11**:539-552.

Flexas, J., M. M. Barbour, O. Brendel, H. M. Cabrera, M. Carriquí, A. Díaz-Espejo, C. Douthe, E. Dreyer, J. P. Ferrio, J. Gago, A. Gallé, J. Galmés, N. Kodama, H. Medrano, Ü. Niinemets, J. J. Peguero-Pina, A. Pou, M. Ribas-Carbó, M. Tomás, T. Tosens, and C. R. Warren. 2012. Mesophyll diffusion conductance to CO_2: an unappreciated central player in photosynthesis. Plant Science **193–194**:70-84.

Galvao, V. C., K. J. Nordstrom, C. Lanz, P. Sulz, J. Mathieu, D. Pose, M. Schmid, D. Weigel, and K. Schneeberger. 2012. Synteny-based mapping-by-sequencing enabled by targeted enrichment. Plant Journal **71**:517-526.

Gibson, G. and I. Dworkin. 2004. Uncovering cryptic genetic variation. Nat Rev Genet **5**:681-690.

Horton, M. W., A. M. Hancock, Y. S. Huang, C. Toomajian, S. Atwell, A. Auton, N. W. Muliyati, A. Platt, F. G. Sperone, B. J. Vilhjalmsson, M. Nordborg, J. O. Borevitz, and J. Bergelson. 2012. Genome-wide patterns of genetic variation in worldwide *Arabidopsis thaliana* accessions from the RegMap panel. Nature Genetics **44**:212-216.

Huang, X., S. Effgen, R. C. Meyer, K. Theres, and M. Koornneef. 2012. Epistatic natural allelic variation reveals a function of AGAMOUS-LIKE6 in axillary bud formation in Arabidopsis. The Plant Cell Online **24**:2364-2379.

Hummel, I., F. Pantin, R. Sulpice, M. Piques, G. Rolland, M. Dauzat, A. Christophe, M. Pervent, M. Bouteillé, and M. Stitt. 2010. Arabidopsis plants acclimate to water deficit at low cost through changes of carbon usage: an integrated perspective using growth, metabolite, enzyme, and gene expression analysis. Plant Physiology **154**:357-372.

Ludwig-Muller, J., P. Krishna, and C. Forreiter. 2000. A glucosinolate mutant of Arabidopsis is thermosensitive and defective in cytosolic Hsp90 expression after heat stress. Plant Physiology **123**:949-958.

Masle, J., S. R. Gilmore, and G. D. Farquhar. 2005. The *ERECTA* gene regulates plant transpiration efficiency in Arabidopsis. Nature **436**:866-870.

McDowell, N. G. 2011. Mechanisms linking drought, hydraulics, carbon metabolism, and vegetation mortality. Plant Physiology **155**:1051-1059.

Muller, B., F. Pantin, M. Génard, O. Turc, S. Freixes, M. Piques, and Y. Gibon. 2011. Water deficits uncouple growth from photosynthesis, increase C content, and modify the relationships between C and growth in sink organs. Journal of Experimental Botany **62**:1715-1729.

Pantin, F., T. Simonneau, and B. Muller. 2012. Coming of leaf age: control of growth by hydraulics and metabolics during leaf ontogeny. New Phytologist **196**:349-366.

Parent, B. and F. Tardieu. 2012. Temperature responses of developmental processes have not been affected by breeding in different ecological areas for 17 crop species. New Phytologist **194**:760-774.

Sala, A. 2009. Lack of direct evidence for the carbon-starvation hypothesis to explain drought-induced mortality in trees. Proc Natl Acad Sci U S A **106**:E68; author reply e69.

Shipley, B. 2000. Cause and correlation in Biology: A user's guide to path analysis, structural equations and causal inference. Cambridge Unversity Press.

Tardieu, F. 2012. Any trait or trait-related allele can confer drought tolerance: just design the right drought scenario. J Exp Bot **63**:25-31.

Tisne, S., F. Barbier, and C. Granier. 2011. The *ERECTA* gene controls spatial and temporal patterns of epidermal cell number and size in successive developing leaves of *Arabidopsis thaliana*. Ann Bot **108**:159-168.

van Zanten, M., L. B. Snoek, M. C. Proveniers, and A. J. Peeters. 2009. The many functions of *ERECTA*. Trends Plant Sci **14**:214-218.

Annexes

Manuscript #7

Genetic variability in plant architecture allows the maintenance of water use efficiency under high temperature

François Vasseur[1], Florent Pantin[1,2] and Denis Vile[1]

[1]INRA, Montpellier SupAgro, UMR759 Laboratoire d'Ecophysiologie des Plantes sous Stress Environnementaux (LEPSE), F-34060 Montpellier, France

[2]Department of Cell and Developmental Biology, John Innes Centre, Norwich Research Park, Colney, Norwich, NR4 7UH, United Kingdom

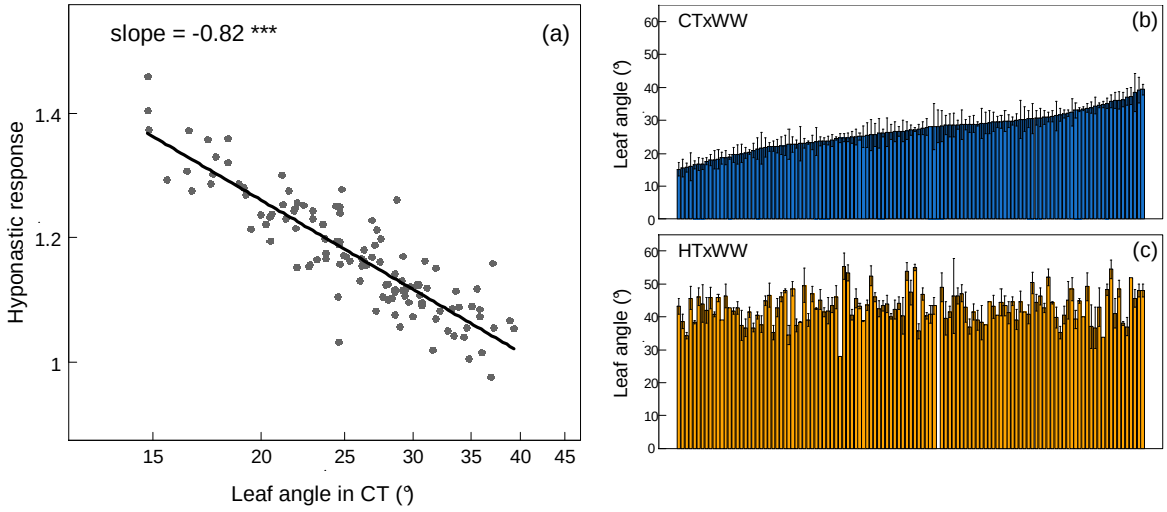

Figure 1. Variability in leaf angle and hyponastic response in the RILs population. (a) Relationship between leaf angle in control temperature (CT = 20 °C) and the hyponastic response induced by high temperature (HT = 30 °C). Hyponastic response = $\log_{10}$ (leaf angle in HT) / $\log_{10}$ (leaf angle in CT). Each point is the mean value of each of the 120 lines (n= 4). ANOVA significance: *** $P < 0.001$. (b) Mean leaf angle of each line in CT (n = 4). (c) Mean leaf angle of each line in HT (n = 4).

Correspondence

Plants have evolved physiological mechanisms to alleviate the deleterious effects of abiotic stresses. High temperature (HT) exposure is among the most detrimental constraints occurring in the field. Changes in leaf orientation, associated with coordinated changes in several others leaf functional properties, are observed in many species under HT (van Zanten et al. 2010b). In *Arabidopsis thaliana*, a similar architectural plasticity, including erected leaves, is observed after exposure to supra-optimal temperature, low light, and spectral composition of light enriched in far-red wavelengths (van Zanten et al. 2010b). This set of morphological changes, referred to as the hyponastic response, is associated to an increase in transpiration rate and thus, in heat dissipation under HT (Crawford et al. 2012). In addition, the hyponastic response allows photosynthetic tissue to reach light in a situation of competition for light (both within and between individuals) (van Zanten et al. 2010b). Therefore, the architectural plasticity has been recently hypothesized to be the result of evolutionary forces on leaf cooling and/or carbon gain capacities (Vasseur et al. 2011, Crawford et al. 2012). However, we lack evidences about to what extent the genetic variability in HT-induced hyponastic response is associated to variability in the traits that maximize carbon gain and water consumption. The present study suggests that genetically-driven hyponastic response can improve the maintenance of water use efficiency (WUE, i.e. the amount of carbon fixed per unit of water lost) under stressing thermal conditions.

We grew a population of 120 recombinant inbred lines (RILs) of *Arabidopsis thaliana* under two thermal conditions. As in most experimental studies (Saidi et al. 2011, Vasseur et al. 2011, Vile et al. 2012), control air temperature (CT) was set to 20 °C, whereas HT was set to 30 °C. This HT level has been identified to be the basal thermotolerance, that is the highest temperature tolerated by a plant that has never encountered previous HT, of the *Arabidopsis* accession Col-0 (Ludwig-Muller et al. 2000). In all individuals, the average angle between leaf and soil, and the leaf temperature were recorded with lateral and infra-red imaging, respectively (see supporting materials and methods). Strikingly, a lower variability in leaf angle was observed in HT than in CT (angles vary between 15 ° and 40 ° in CT, and between 28 ° and 55 ° in HT). This is explained by the higher hyponastic response exhibited in the plants with the smallest leaf angle in CT (Figure 1). We modeled leaf angle with a mixed-model approach ($\text{Leaf angle} = T_{air} \times T_{leaf} + \text{G} + \text{G} \times T_{air}$), using leaf temperature (T_{leaf}, °C) as a continuous covariate, air temperature (T_{air}, °C) as a fixed effect and genotype (G) as a random effect (Supporting materials and methods).

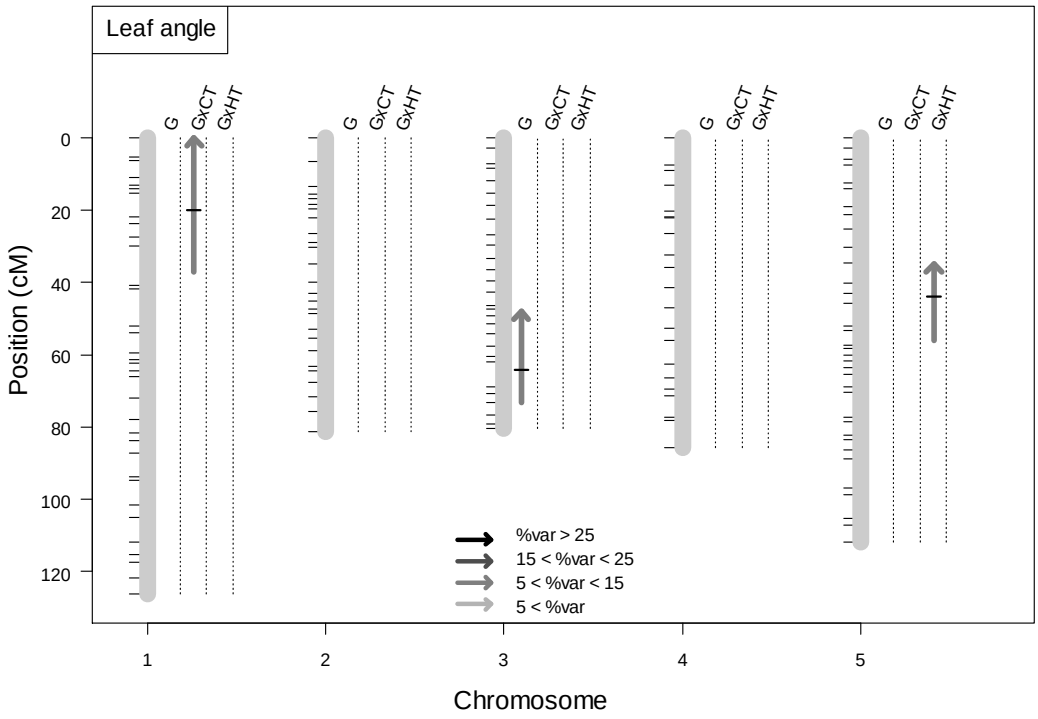

Figure 2. QTL for leaf angle depending on leaf temperature. Analysis performed on the best linearized unbiased predictors (BLUPs) of the genetic effects (G) and of the genotype-by-temperature effects (GxCT and GxHT) on leaf angle, extracted from the mixed-model performed on all individuals (see supporting materials and methods).

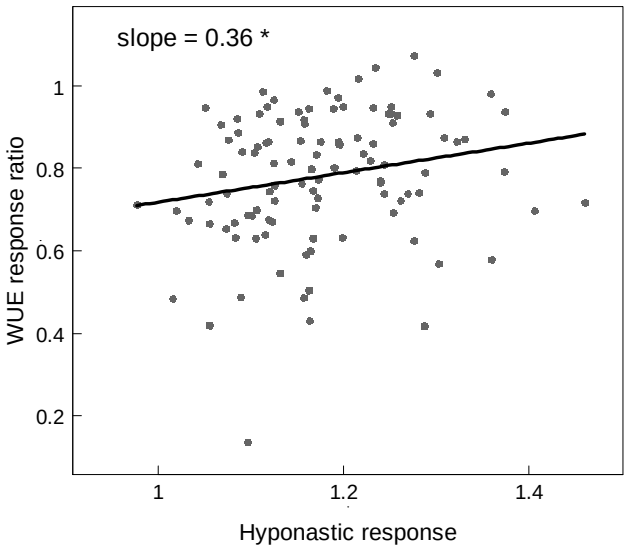

Figure 3. Relationship between hyponastic response and WUE maintenance. WUE (nmol CO_2 mg^{-1} H_2O) is estimated as the ratio between net photosynthesis (nmol CO_2 s^{-1}) and transpiration (mg H_2O s^{-1}). WUE response ratio = $\log_{10}$ (WUE in HT) / $\log_{10}$ (WUE in CT). Hyponastic response = $\log_{10}$ (leaf angle in HT) / $\log_{10}$ (leaf angle in CT). Each point is the mean value of each of the 120 lines (n= 4). ANOVA significance: * P < 0.05.

On one hand, evolutionary assumptions about the HT-induced hyponasty (Vasseur et al. 2011, Crawford et al. 2012) posit that there is genetic variability for this morphological response. Mixed-model revealed a significant interaction between air temperature and leaf temperature (Table S1). In average, the 10 °C-increase in air temperature lead to only +1.66 ° on leaf angle, and 7.2% of the variance in leaf angle was attributable to genetic effects (G) independently of the environment. Nonetheless, 35.4% of the variance in leaf angle was attributable to genotype-by-environment interactions (GEI). The analysis revealed one quantitative trait loci (QTL) for the G effects, and two QTL for the GEI (Figure 2). Such genetic variability is consistent with the previous findings of van Zanten and colleagues. These authors reported that ethylene-induced hyponastic growth in *Arabidopsis thaliana* was controlled by the *ERECTA* gene (van Zanten et al. 2010a). Although *ERECTA* did not drive HT-induced hyponastic response in our data, the QTL identified for the genetic variability in hyponastic response (GEI) overlapped pleiotropic QTL previously described to drive important differences in plant performance, notably on the rate of carbon fixation and on relative growth rate (Vasseur et al. 2012).

On the other hand, evolutionary assumptions also posit that variations in individuals' hyponastic responses are associated to variations in individuals' performance. It is advanced that HT-induced hyponasty occurs to enhance cooling capacity through an increase in transpiration rate (Crawford et al. 2012). In addition, it is also proposed that hyponasty may be the result of an impaired carbon status under HT, similarly to the shade avoidance syndrome observed under low light intensity (Vasseur et al. 2011). Thus, the temperature-mediated changes in plant architecture are hypothesized to be governed by the global trade-off between carbon gain and water conservation (Pantin et al., in prep.). Here, we found a significant positive correlation between the hyponastic response and the response ratio of WUE (Figure 3), which results in a shared genetic underpinning as highlighted by the QTL analysis of the response ratio of WUE (Table S2). Hence, genotypes with the smallest leaf angle under CT were the most plastic in their architecture, and the exhibited the lower decrease in WUE under HT.

Water and carbon balances are major determinants of plant growth and productivity (Ciais et al. 2005, Pantin et al. 2012). Our results demonstrate that the maintenance of water use efficiency in stressing environment is genetically linked to the plasticity in plant architecture. Overall, our findings suggest that manipulating the tight relationship between carbon gain and water consumption through the engineering of plant architecture is a promising avenue to improve plant performance in a warming world.

References

Ciais, P., M. Reichstein, N. Viovy, A. Granier, J. Ogee, V. Allard, M. Aubinet, N. Buchmann, C. Bernhofer, A. Carrara, F. Chevallier, N. De Noblet, A. D. Friend, P. Friedlingstein, T. Grunwald, B. Heinesch, P. Keronen, A. Knohl, G. Krinner, D. Loustau, G. Manca, G. Matteucci, F. Miglietta, J. M. Ourcival, D. Papale, K. Pilegaard, S. Rambal, G. Seufert, J. F. Soussana, M. J. Sanz, E. D. Schulze, T. Vesala, and R. Valentini. 2005. Europe-wide reduction in primary productivity caused by the heat and drought in 2003. Nature **437**:529-533.

Crawford, A. J., D. H. McLachlan, A. M. Hetherington, and K. A. Franklin. 2012. High temperature exposure increases plant cooling capacity. Current Biology **22**:R396-397.

Ludwig-Muller, J., P. Krishna, and C. Forreiter. 2000. A glucosinolate mutant of Arabidopsis is thermosensitive and defective in cytosolic Hsp90 expression after heat stress. Plant Physiology **123**:949-958.

Pantin, F., T. Simonneau, and B. Muller. 2012. Coming of leaf age: control of growth by hydraulics and metabolics during leaf ontogeny. New Phytologist **196**:349-366.

Saidi, Y., A. Finka, and P. Goloubinoff. 2011. Heat perception and signalling in plants: a tortuous path to thermotolerance. New Phytologist **190**:556-565.

van Zanten, M., L. Basten Snoek, E. van Eck-Stouten, M. C. Proveniers, K. U. Torii, L. A. Voesenek, A. J. Peeters, and F. F. Millenaar. 2010a. Ethylene-induced hyponastic growth in Arabidopsis thaliana is controlled by *ERECTA*. Plant Journal **61**:83-95.

van Zanten, M., T. L. Pons, J. A. M. Janssen, L. A. C. J. Voesenek, and A. J. M. Peeters. 2010b. On the relevance and control of leaf angle. Critical Reviews in Plant Sciences **29**:300-316.

Vasseur, F., F. Pantin, and D. Vile. 2011. Changes in light intensity reveal a major role for carbon balance in Arabidopsis responses to high temperature. Plant Cell and Environment.

Vasseur, F., C. Violle, B. J. Enquist, C. Granier, and D. Vile. 2012. A common genetic basis to the origin of the leaf economics spectrum and metabolic scaling allometry. Ecology Letters **15**:1149-1157.

Vile, D., M. Pervent, M. Belluau, F. Vasseur, J. Bresson, B. Muller, C. Granier, and T. Simonneau. 2012. Arabidopsis growth under prolonged high temperature and water deficit: independent or interactive effects? Plant Cell and Environment **35**:702-718.

Supporting information

Supporting materials and methods

Plant material

We used a population of 120 recombinant inbred lines (RILs), previously generated from a reciprocal cross between two parental *Arabidopsis thaliana* accessions: Landsberg *erecta* (L*er*) and Cape Verde Islands (Cvi) (Alonso-Blanco et al. 1998).

The PHENOPSIS facility (Granier et al. 2006) maintains constant growing environment and allows for the precise temporal monitoring and automated measurements of 504 potted plants (Supporting Figure S1). We performed two experiments with the same 122 genotypes (120 RILs, n = 4; 2 parental lines, n = 8). In the first experiment, control air temperature (CT) was set to 20/17 °C day/night, while in the second, high temperature (HT) was set to 30/25 °C. VPD was maintained at 0.7-0.8 kPa both under CT and HT. Soil water content was controlled before sowing to estimate the amount of dry soil and water in each pot. Subsequent changes in pot weight were due to changes in water status. Soil water content was maintained at 0.35 g H_20 g^{-1} dry soil with a modified one-tenth-strength Hoagland solution. Pot weight was automatically adjusted to reach the target soil water content by weighing and watering each individual pot every day.

Leaf angle was estimated with three lateral images of each individual. The angle α (°) between the two youngest fully expanded leaves was measured with image analysis software (ImageJ). Leaf angle with soil surface was estimated as: 90 - (α / 2) (Figure S2). Leaf temperature was measured with at least three random infra-red zenithal imaging (ThermaCAM^{TM} Researcher Pro 2.10, FLIR Systems AB) from the PHENOPSIS automaton. Images were recorded for each plant between bolting stage and first flower open. Five random spots were chosen at the surface of the rosette to estimate T_{leaf} (°C) (Figure S3).

Whole-plant water loss was measured at reproductive stem emergence (bolting stage) by daily weighing of the pots over four consecutive days. Soil evaporation was prevented by sealing the soil surface with four layers of a plastic film. The transpiration rate (E, mg H_2O d^{-1}) was estimated as the slope of the linear regression between pot weight and time. Net photosynthetic rate (A, nmol CO_2 s^{-1}) was determined at the canopy level after removal of the reproductive stem (see Vasseur et al. (2012)). Water use efficiency (WUE, nmol mg^{-1}) is estimated as A / E. The response ratio of WUE was estimated as $\log_{10}$(WUE in HT) / $\log_{10}$ (WUE in CT).

Statistical analyses

After log10-transformation of the data (to ensure normalization of the residuals), we fitted the mixed model: $Leaf\ angle = T_{air} \times T_{leaf} + G + G \times T_{air}$, where Tleaf (°C) is average leaf temperature recorded with infra-red imaging (see above) and treated as continuous covariate, Tair is the average air temperature in the PHENOPSIS automaton during the considered experiment (20 °C and 30 °C for CT and HT, respectively) considered as fixed effect. The genotypic (G) and genotypic-by-temperature (GxTair) effects were treated as random. The confidence interval of each coefficient was estimated with a Markov Chain Monte Carlo (MCMC) following 1000 permutations. We used composite interval mapping as implemented in Rqtl to identify i) the QTL that are responsible of the variability in the best linearized unbiased predictors (BLUPs) of both G and GxTair, and ii) QTL that are responsible of the variability in the response ratio of WUE All statistical analyzes were performed using R 2.12.

Table S1. Mixed-model on leaf angle. Mixed model performed on leaf angle after $\log_{10}$-transformation of the data, as: . The confidence interval of each coefficient was estimated with a Markov Chain Monte Carlo (MCMC) following 1000 permutations.

Fixed effects	intercept	1.333	[1.220;1.439]
	T_{air}	0.523	[0.206;0.688]
	T_{leaf}	0.004	[-0.002;0.011]
	T_{leaf}xT_{air}	-0.012	[-0.0193;0.0004]
Variance components (%)	G	7.3	
	GxT	36.7	

Table S2. QTL analyses of the hyponastic response and of the response ratio of WUE.

Traits	Marker	Chr	Position (cM)	% var
BLUPs G Leaf angle	FD.98C	3	63 [50-69]	12.2
BLUPs GxCT Leaf angle	EC.66C	1	21 [0-38]	8.2
BLUPs GxHT Leaf angle	AD.129L	5	44 [35-56]	8.0
Response ratio WUE	AXR-1	1	8 [0-12.9]	26.5
	DF.184L	5	29 [25-38]	15.6

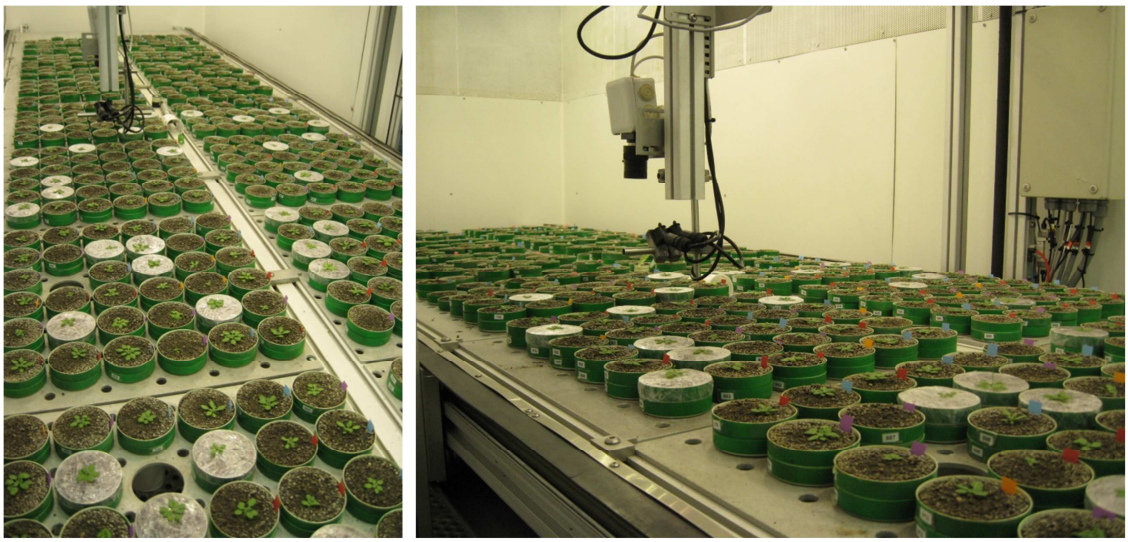

Figure S1. The PHENOPSIS automaton in Montpellier (France).

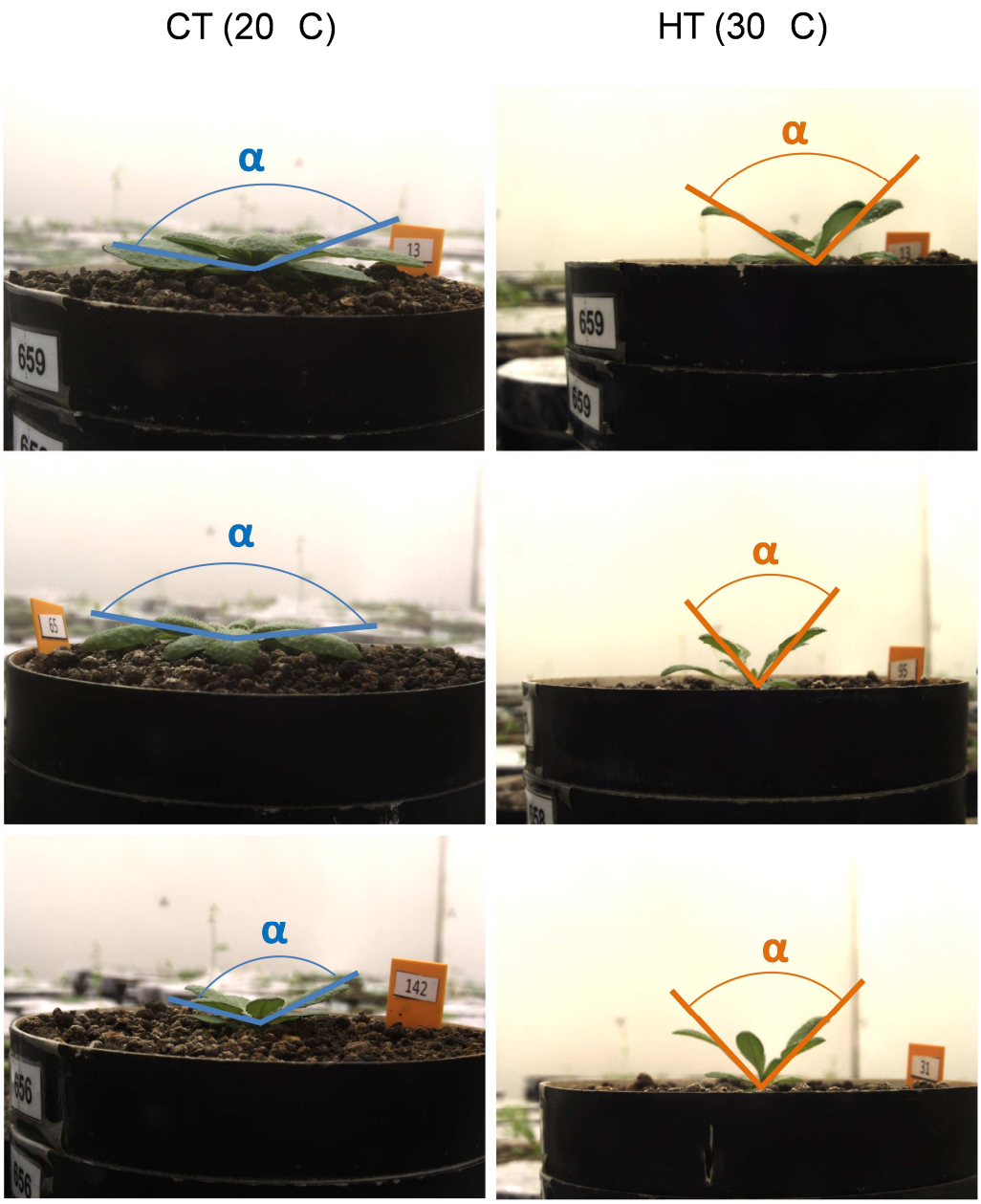

Figure S2. The angle α (°) between the two youngest fully expanded leaves was measured with image analysis software (ImageJ). Leaf angle with soil surface was estimated as: 90 - (α / 2).

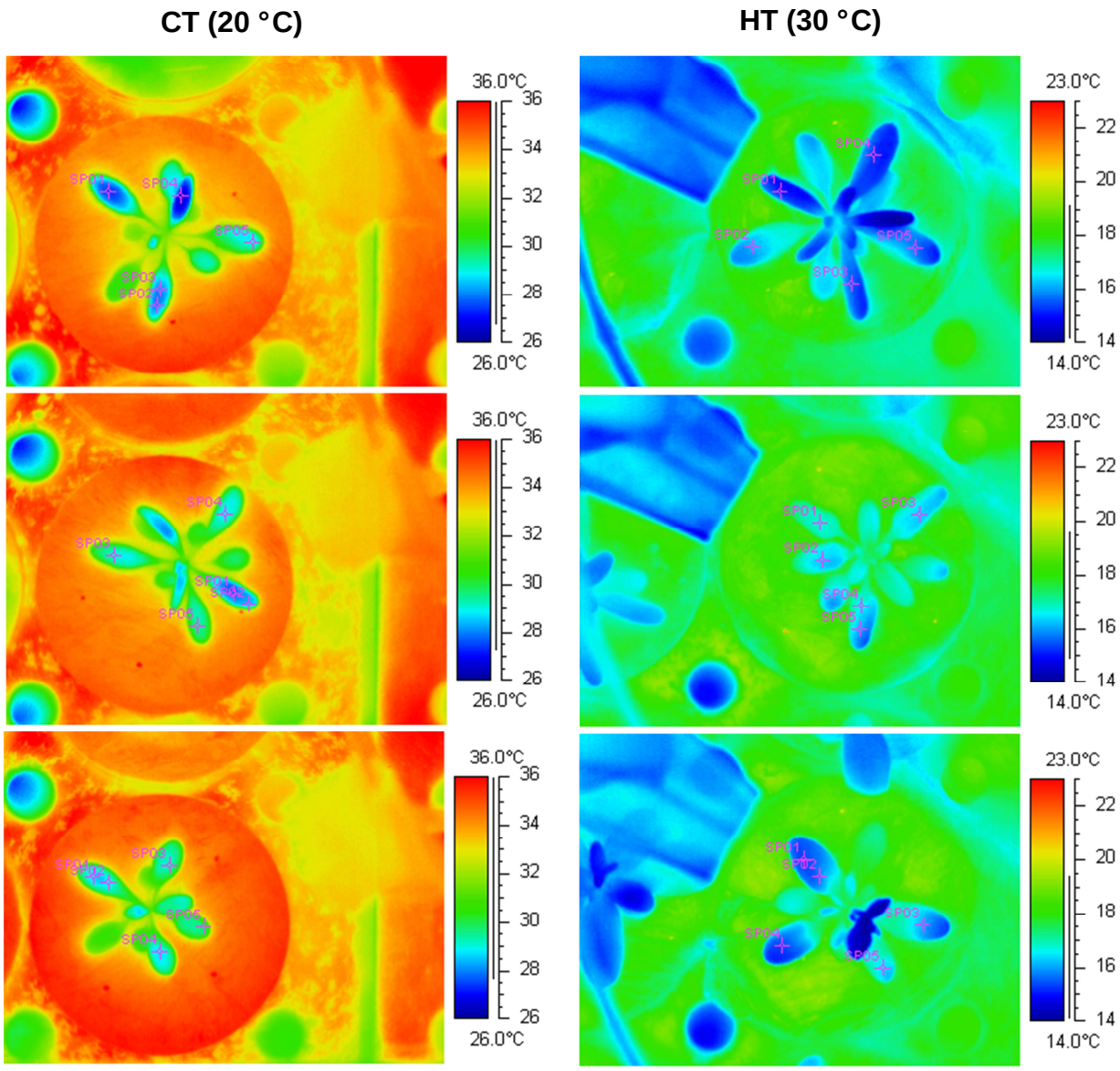

Figure S3. Infra-red imaging recorded for each plant between bolting stage and first flower open. Five random spots (for each image: sp01 to sp05) were chosen at the surface of the rosette to estimate T_{leaf} (°C).

Manuscript #8

Venation networks and the leaf economics spectrum in *Arabidopsis thaliana*

Benjamin Blonder[1], François Vasseur[2], Cyrille Violle[1,3], Brian J. Enquist[1,4], Christine Granier[2] and Denis Vile[2]

[1]Department of Ecology and Evolutionary Biology, University of Arizona, 1041 E Lowell St, Tucson, Arizona, 85721, USA

[2]Laboratoire d'Ecophysiologie des Plantes sous Stress Environnementaux (LEPSE), INRA, Montpellier SupAgro, F-34060, Montpellier, France

[3]Centre d'Ecologie Fonctionnelle et Evolutive, CNRS, UMR5175, F-34000, Montpellier, France

[4]The Santa Fe Institute, 1399 Hyde Park Road, Santa Fe, New Mexico, 87501, USA

Article in preparation

Abstract

The leaf economics spectrum (LES) describes strong interspecific relationships between multiple functional traits that determine carbon and nitrogen fluxes in vascular plants. The mechanistic and evolutionary origins of these patterns have been controversial, though a recent model has proposed that the physiology of leaf venation networks controls multiple LES correlations. Here we test the hypothesis that genetic variation in minor vein density is associated with coordinated phenotypic variation in LES traits. We study a large set of ecotypes, mutants, recombinant inbred lines and near isogenic lines of *Arabidopsis thaliana* known to be associated with LES trait variation. We show that 1) leaf minor vein density is highly variable between these genotypes, and 2) that variation in vein density successfully predicts the sign of correlations with carbon assimilation rate, leaf lifespan, leaf mass per area, and nitrogen content, in line with theory. Our results indicate that venation networks are an important linkage between physiological and evolutionary processes in the LES. If this genetic basis for the LES extends to other species then our results may provide targets for improving yields in agriculturally important plants.

Key-words: Leaf economics spectrum, venation network, vein density, genetic constraint.

Introduction

The leaf economics spectrum (LES) describes correlations between multiple leaf traits including carbon assimilation rate (Am), lifespan (LL), mass-per-area (LMA) and nitrogen content (Nm) (Wright *et al.* 2004). These patterns are found globally and across all vascular plant taxa (Reich et al. 1997, Wright et al. 2005). Despite the importance of the LES in constraining plant strategies and terrestrial nutrient fluxes, its mechanistic origin has been unclear. Models for the origin of the LES have focused on resource use optimization and leaf physiology. Approaches include maximization of carbon gain (Kikuzawa 1995), sometimes under nitrogen availability constraints (Mcmurtrie and Dewar 2011), or in optimal allocation of resources to structural tissues (Shipley *et al.* 2006) or venation networks (Blonder *et al.* 2011).

An evolutionary perspective could provide a deeper understanding of processes generating the LES, but linkages between genes and leaf physiology have been limited. Recently, (Donovan *et al.* 2011) made a meta-analysis showing that the LES is primarily the result of natural selection against certain combinations of traits. This study suggests a limited role for the genetic constraints that could limit the independent variability of correlated traits, and, thus, directly shape the LES covariations. However the study was not able to find much empirical data able to identify relevant selection gradients or genes. However, (Vasseur *et al.* 2012) recently showed that in *Arabidopsis thaliana*, a small set of pleiotropic genes at two loci (*EDI* and *FLG*) do underlie multiple LES correlations. This study provides a key advance by identifying a common genetic basis for the LES, as had been previously hypothesized (Chapin *et al.* 1993). A key issue is now to understand the physiological effects of these genes, because the LES is inherently a physiological pattern.

Here we focus on assessing the role of leaf venation networks for the LES (Blonder *et al.* 2011). The importance of venation networks to leaf functioning is becoming widely recognized (Brodribb *et al.* 2010). All species with megaphyll leaves share a similar vascular architecture (Roth-Nebelsick et al. 2001, Brodribb et al. 2010), with veins providing water transport, carbon transport, mechanical support, and herbivory defense at the cost of a large carbon investment. A recent model (Blonder *et al.* 2011) proposes that the venation network cannot simultaneously optimize all these functions, leading to a constrained spectrum of leaf trait combinations. A key trait is minor vein density (VD; mm-1). In this model, higher VD increases water transport capacity (Brodribb *et al.* 2007), leading to higher Am that is also associated with high Nm. Optimal flow considerations mean higher VD decreases leaf

thickness and therefore damage resistance (Noblin *et al.* 2008), leading to lower LMA and LL. These hypothesized tradeoffs lead to trait correlations with the correct magnitude and sign, suggesting that venation networks are one of the proximal physiological mechanisms generating the LES. These results are consistent with an evolutionary paradigm in which 1) a small number of genes constrain vascular patterning, 2) the geometry of the resulting venation network coordinates multiple LES trait values, and 3) natural selection acts on non-optimal trait combinations, further limiting ranges of trait values and ordinating species along the spectrum. Thus, for example, leaves with low VD and high thickness could exist but would have low Am and high LMA, leading to a negative carbon balance. Such a paradigm has not been empirically assessed but would be consistent with the role for natural selection proposed by Donovan et al., and the identification by Vasseur et al. of a common genetic basis constraining phenotypic variability in LES traits.

Here we test the hypothesis that genes that control the geometry of the venation network also control the coordination of traits in the LES. We predict that 1) the genes known to underly the LES will be associated with changes in VD, and 2) genetic variability in VD will lead to recapitulation of the LES, such that an increase (decrease) in VD will be simultaneously correlated with higher (lower) Am and Nm, and lower (higher) LMA and LL. We assessed these predictions using multiple genotypes of the model plant *A. thaliana*. We assembled a dataset (Table 1) including a) five natural ecotypes with native ranges distributed across the Northern Hemisphere, b) sixteen recombinant inbred lines (RILs) generated by crossing two ecotypes from contrasting environments, c) five near isogenic lines varying from wildtype only at loci previously identified to underly the LES, d) five knockout mutants, of which three lost functioning in genes found within the above loci, and two lost auxin sensitivity, causing vascular patterning defects. We grew replicates of each genotype under tightly controlled environmental conditions and used a high-throughput phenotyping system (Granier *et al.* 2006) to study variation in VD, LMA, Am, Nm, and flowering time (a proxy for LL).

Materials and methods

Plant material

We selected five *A. thaliana* ecotypes originating in multiple environments (Col-0 and Col-4, from Germany; Cvi-0, from the Cape Verde Islands; L*er*-2, L*er*-4, from irradiated seeds from Poland) (Alonso-Blanco et al. 1998). We also selected a subset of 16 RILs from a L*er* x Cvi population (Alonso-Blanco et al. 1998). The phenotypes of these RILs span the

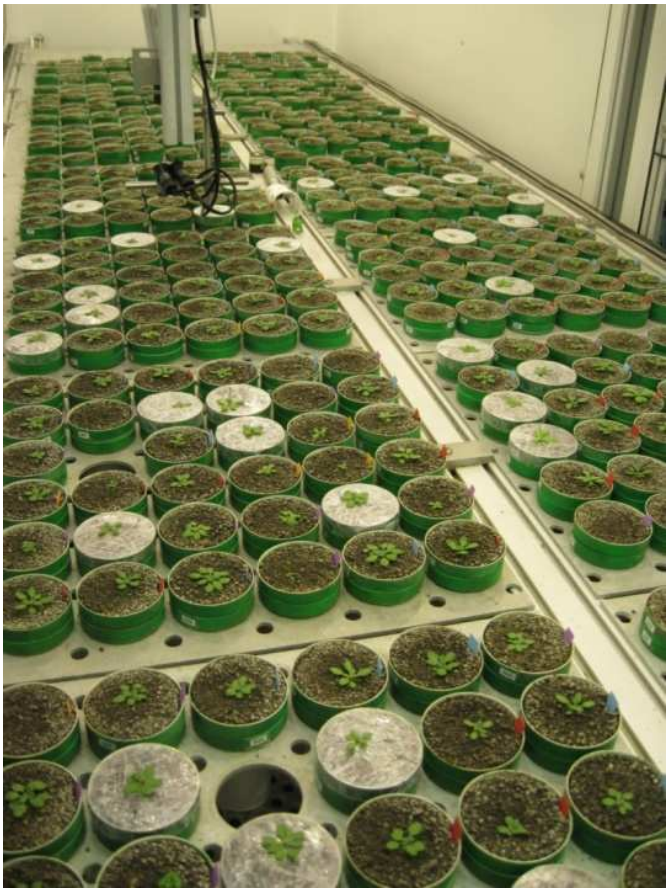

Figure 1. The PHENOPSIS automated phenotyping platform can grow several hundred *A. thaliana* plants under tightly-controlled conditions.

range of leaf trait values previously observed for a larger set of RILs (Vasseur *et al.* 2012). We also selected five NILs developed by introgressing Cvi into L*er* (Keurentjes *et al.* 2007) in order to assess the *EDI* and *FLG* loci, which are known to have multiple pleiotropic effects on the LES. NILs 1-2.13, 1-2.5 and 1-3 carry introgressions of chromosome 1 associated with the *EDI* locus. NILs 5-7 and 5-8 carry introgressions of chromosome 5 associated with the *FLG* locus. We also selected three knockout mutants for genes (CRY2, encoding a blue-light receptor (El-Assal *et al.* 2001), and *HUA2*, encoding a transcription factor in the AGAMOUS pathway (Doyle *et al.* 2005)) known to be implicated in the *EDI* and *FLG* loci (Doyle *et al.* 2005). Mutants *cry2-1* (Col-4 background) and *fha-1 (*likely Ler-0 background[1]) describe loss of function in *CRY2*, while mutant *hua2-4* describe loss of function in *HUA2* (Col-0 background). Finally, we also selected two knockouts mutants for the *AXR1* gene that confers resistance to auxin, a hormone necessary for vascular patterning (Alonso-Peral et al. 2006, Scarpella et al. 2010). Mutants *axr1-3* and *axr-12* (both likely Col-0 background) are associated with incomplete vascular development and lower VD.

Growing conditions

We used the PHENOPSIS automated growth chamber facility (Granier *et al.* 2006) to grow and phenotype the plants (Figure 1a). The facility can maintain constant environmental conditions and automatically monitor multiple traits. This study extends the dataset and methods of Vasseur et al. 2012 (Experiment 2, described fully in that publication's Appendix 1). For this study we grew a total of 198 plants (n=7.0±2.2 s.d. per mutant, 6.4±0.5 per NIL, 5.4±0.7 per RIL, and 9.0±2.9 per ecotype).

Trait measurements

All traits were collected on the first day of flowering after removing flowering stems. Flowering date was used as an accurate proxy for LL (day) (Vasseur *et al.* 2012). To measure whole-plant photosynthesis, we used a whole-plant chamber designed for *A. thaliana* and connected to an infrared gas analyzer (CIRAS 2; PP Systems, Amesbury, MA, USA). Before making measurements we sealed the surface of the soil with plastic film to eliminate carbon fluxes from soil respiration. A zenithal camera determined projected leaf area. We then determined Am (nmol g-1 s-1) as the whole-plant rate divided by the product of projected leaf area and LMA. To calculate LMA and other traits, we first harvested each rosette. We then wrapped the rosette in moist paper and kept it at 4°C overnight to fully rehydrate the leaves. The oldest non-senescing and fully expanded leaf was then stored in a vial at -80°C to be later

[1] http://arabidopsis.info/StockInfo?NASC_id=108

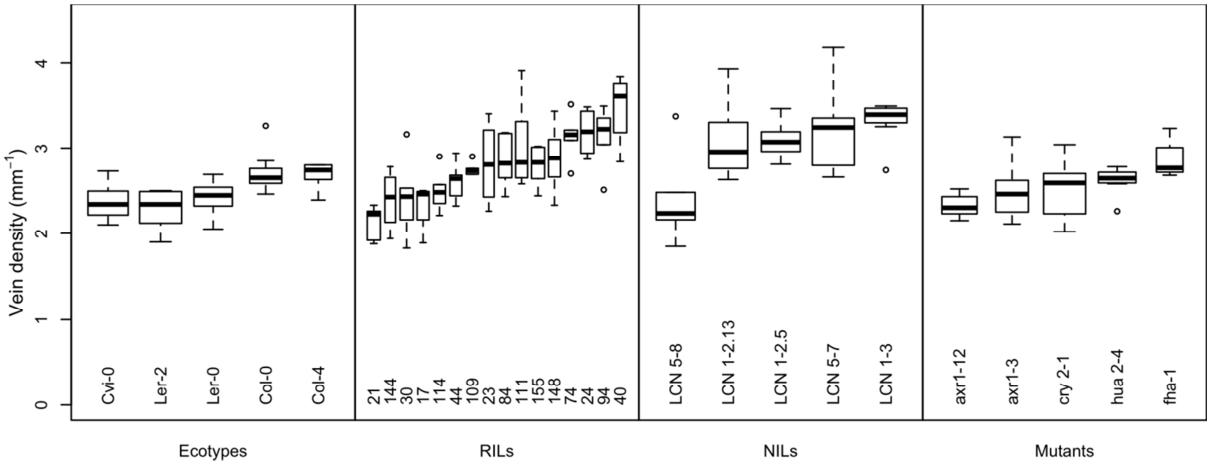

Figure 2. Vein density is variable between *A. thaliana* genotypes, whether generated between ecotypes, recombinant inbred lines generated from crosses between ecotypes, or near isogenic lines or mutants generated to target loci associated with the LES.

measured for VD. For all remaining leaves, leaf area was obtained by digitally scanning each leaf with its petiole removed. These leaves were then dried at 65 °C for 72 hours and weighed to determine dry mass. LMA (g m^{-2}) was then determined as the total dry mass divided by the total leaf area. Vein density was obtained by a chemical clearing process and subsequent digital imaging and hand-tracing (Figure 1b). Leaves were defrosted and cleared in a solution of 0.5% safranin in ethanol for seven days, then rinsed in a series of ethanol, 1:1 ethanol:toluene, and toluene before slide-mounting in the toluene-based Permount resin. After curing for three days, slides were back-illuminated and imaged using a dissecting microscope (SZX12, Olympus) and digital camera (T2i, Canon). Final image resolution was 195 pixels per millimeter. A contrast limited adaptive histogram equalization was applied to the red channel of each image to improve image quality. Using an image-editing program (GIMP, GNU) we hand-traced the boundary of each leaf and all veins. We measured total leaf area and total vein length using a custom program (MATLAB, MathWorks). VD (mm-1) was then calculated as total vein length divided by leaf area. All traits were measured on each individual, except Nm, which for cost reasons was measured only on a subset of leaves. For ecotypes, mutants, and NILs, a random subset of individuals were chosen (n = 6-15 per category) for measurements of Nm. For RILs, genotype-mean Nm values were obtained (n = 19) from plants grown under identical conditions in Experiment 1 of Vasseur et al. 2012. In all cases, Nm (g/g) was determined on dried leaves (both lamina and petiole) by mass spectrometry (EA20000, Eurovec; Isoprime, Elementar, Cheadle, UK).

All statistical analyses were performed on $\log_{10}$-transformed trait values to meet normality assumptions of statistical tests. All analyses were conducted in R. Standardized major axis regressions were made with the 'smatr' package and power analyses with the 'pwr' package.

Results

We determined if variation in genotype previously described to vary in LES traits was associated with variation in VD. Absolute ranges for VD fell between 1.8 and 4.2 mm^{-1} (Figure 2). We found significant variation between ecotypes (ANOVA, $F_{4,40} = 6.2$, $P = 0.006$) and between RILs (ANOVA, $F_{15,70} = 7.0$, $p < 10^{-8}$). We next assessed the NILs, and found that every line for the *EDI* locus (LCN 1-2.13, LCN 1-2.5, and LCN 1-3) had significantly different VD from the parent, L*er*-0 (t-tests, all $P < 0.01$). For the *FLG* locus, the LCN 5-7 line had significantly different VD than the parent ($P = 0.003$) but the LCN 5-8 line did not ($P = 0.72$). Finally, we assessed mutants for the genes identified in Vasseur et al. (2012) in the

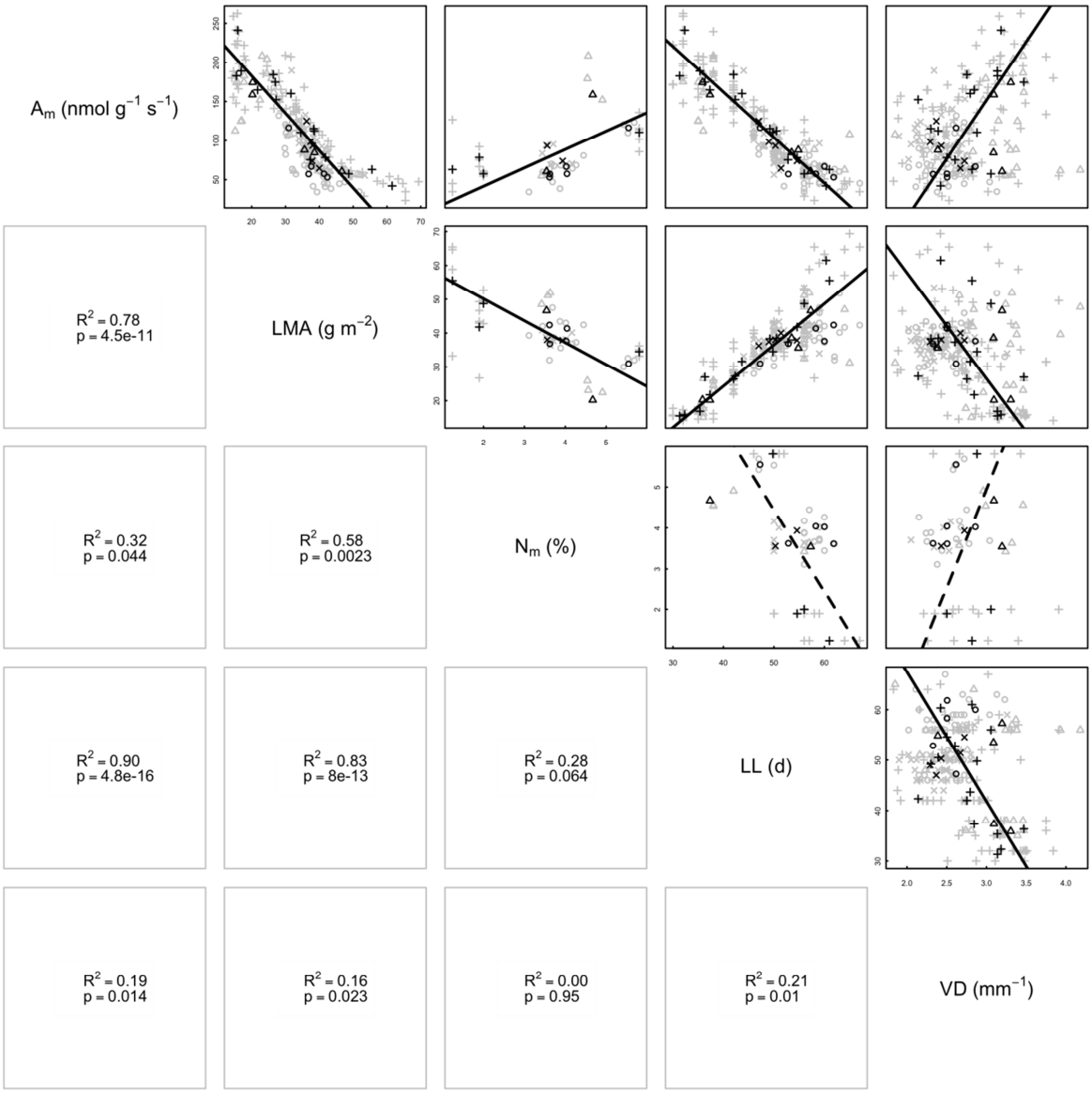

Figure 3. The leaf economics spectrum, as seen for different *A. thaliana* genotypes, is also coordinated with variation in vein density. Pairwise relationships between traits are shown, with lines indicating standard major axis regressions on genotype-mean data. (solid, $P < 0.05$; dashed, not significant). Gray points indicate individual leaves; black points, genotype means. Symbols indicate genotype category: circles, mutants; triangles, NILs; pluses, RILs, crosses, ecotypes. Regression statistics are shown in the lower panel for each pairwise relationship.

same way. For the *CRY2* knockout, *fha-1* was different from its L*er*-0 background (P = 0.01) but *cry2-1* was not different from its Col-4 background (P = 0.18). For the *HUA2* knockout, *hua2-4* was not different from its Col-0 background (P = 0.39). We also tested two mutants directly affected in their venation network because of an impairment of hormonal communication in the *AXR1* gene. We found that *axr1-12* had different VD than its Col-0 background (P = 0.003) and we failed to find a difference for *axr1-3* (P = 0.21).

We next assessed the role of venation networks in the LES (Figure 3) by determining if these genotypes associated with variation in VD also generated LES-like patterns. We first established that the LES was found between genotypes: we found that the signs of all pairwise correlations between Am, LMA, Nm, and LL that are described by the interspecific LES (Wright *et al.* 2004) were recapitulated when pooling all genotypes (binomial test, P = 0.015[2]). All pairwise correlations between Am, LMA, Nm, and LL were significant (standard major axis regressions, all $P < 0.05$, $R^2 > 0.28$). We next determined if VD was also correlated with LES traits. We found that VD was significantly correlated with Am, LMA, and LL (standard major axis regressions, all $P < 0.05$, $R^2 > 0.16$) but was not with Nm (p = 0.95). The sign of the three significant correlations was consistent with model predictions (binomial test p(3|n=4,s=1/2) =0.31). We finally determined if the effects of VD were variable by category. Principal component analysis showed that for all categories, VD dominated the second-most important axis, explaining 19-27% of total trait variation (Figure S1).

We also assessed the role of other venation network traits in the LES. We calculated the mean distance between veins (d; mm), the loopiness of the network (ξ; areoles mm^{-2}), as well a dimensionless shape index (SI=VD x d) that describes the elongation of areoles. These additional traits were correlated with LES traits but also highly correlated with VD (Figure S2). This result suggests that within this species, only one metric of the venation network is sufficient to characterize variation in LES traits.

[2] For c variables there are $n = \binom{c}{2}$ unique pairwise correlations. If the probability of correctly predicting the sign of a correlation is s, then the binomial probability of making at least k correct predictions is $p(k \mid n,s) = \sum_{i=k}^{n} \binom{n}{i} s^n (1-s)^{n-i}$. Smaller p values indicate successful predictions that are less likely to occur by chance. Assuming four LES variables ($c = 4$), equiprobable states ($s = 0.5$) and all correct predictions (k=n), then P = 0.015.

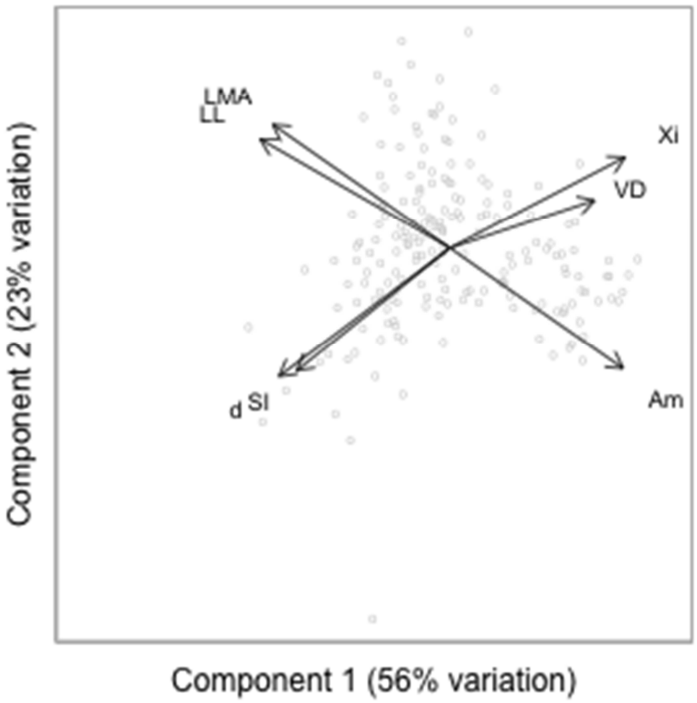

Figure S2. Principal components analysis of multiple vein traits and LES traits. Analysis was made on a correlation matrix of log10 transformed values. Points show individuals of multiple genotypes. Additional vein traits distance (d), loopiness (ξ, drawn as Xi on the plot), and SI (shape index) fall along the same axis as VD. As in Figure S1, Nm was omitted from the analysis because of limited data.

Discussion

Our study makes a link between evolutionary and functional bases of the LES through venation networks. We showed that multiple natural and artificial sources of genetic variation that are associated with LES trait variation are also associated with variation in VD; moreover, in this range of genotypes, the relationship between VD and LES traits is largely consistent with theory (Blonder *et al.* 2011). Thus the genes underlying vascular patterning appear to have coordinated effects on multiple leaf functional traits. Contrary to the hypothesis of (Donovan *et al.* 2011), our findings are consistent with the idea that the LES is mainly shaped by genetic constraints, and not by natural selection. While the shared genetic determinism of the traits related to the LES does not allow independent variability (i.e. to 'get out of the spectrum'), it does allow different positions along the spectrum. However, this does not preclude the possibility for natural selection to operate *within* the LES. Therefore, the allelic frequency at the relevant genes may vary between populations, or species, depending on the environmental conditions. Although this idea remains to be tested, variation in venation network geometry does appear to be strongly associated with variation in climate, both within and across species (ref my paleoclimate and aspen papers, if we can publish them in time).

It is important to note while venation networks provide a key understanding of the LES, they do not provide a complete understanding. In this study, VD explained at most 20 to 30% of the variation in LES traits. Variation in other aspects of leaf physiology that may be developmentally independent or not linked to the genes identified here may also be important (e.g. for structural investment (Shipley *et al.* 2006), stomatal patterning, Rubisco synthesis, etc.). Thus, this study is only the first step towards a synthetic understanding of the multiple genetic causes of LES trait variation which may include models beyond what we tested here (Shipley et al. 2006, Mcmurtrie and Dewar 2011).

Some of our null results (e.g. no significant difference in VD between a vascular patterning mutant and wildtype) also may be due to low statistical power. For an effect size of 0.5 (reasonable given the difference in means and error variances observed in these results) and a power of 0.9 (i.e. a 10% chance of incorrectly deciding there is no difference in VD), a sample size of approximately 80 would be required for these two-sided t-tests. Sample sizes for ecotypes, mutants, and NILs, were never larger than 12. However the significant differences we did find are likely to represent true genetic effects on VD.

VD is a simple trait that may not fully encapsulate the role of leaf venation networks in plant functioning. For example, it does not measure other traits that influence hydraulic conductance and total carbon cost, such as variation in mesophyll thickness (Brodribb *et al.* 2007), or variation in vein width (Sack *et al.* 2012). Leaf area (Brodribb *et al.* 2010) and its coordination with vein density (Sack *et al.* 2012) may also be highly important to the LES, because of the competing size-dependent demands of hydraulics and metabolism (Pantin *et al.* 2011) as well as energy balance (Nicotra *et al.* 2011), A recent model has identified some of the couplings between these traits that may modulate the role of venation networks in the LES (ref to my aspen paper if we can publish in time). However, a more detailed assessment of cellular physiology was beyond the scope of this study.

Building on the work of (Vasseur *et al.* 2012), this study identifies a role in vascular development for the *EDI* and *FLG* loci, as well as for the *AXR1* and *CRY2* genes and potentially the *HUA2* gene. Further work may elucidate the molecular or developmental mechanisms coupling these genes to leaf venation network geometry, which (with the exception of *AXR1* (Alonso-Peral *et al.* 2006)) remain unknown. Decades of study have yielded many more vascular patterning mutants in *A. thaliana* than were studied here (Perez-Perez et al. 2002, Scarpella et al. 2010). Generally, vascular development follows patterns of auxin concentration and is therefore sensitive to variation in genes that modulate production/inhibition of auxin or sensitivity to it (Donner and Scarpella 2009). Determining if the genes described above, as well as others at the *EDI*/*FLG* loci, are implicated in these pathways would further assess the hypotheses proposed here. Moreover a broader study of vascular patterning mutants and their functional traits could provide a more comprehensive test of the ideas proposed here.

The LES is fundamentally a global interspecific pattern, so understanding the generality of these results for other species is a critical but unresolved issue. Many vascular plant species have vastly different life histories than *A. thaliana*, and it is plausible that multiple genetic pathways are responsible for convergence in functioning. Synapomorphies for leaf vascular architecture fall deep in the Embryophyte tree (e.g. high angiosperm VD arising ~100 Mya (Roth-Nebelsick et al. 2001, Boyce et al. 2009)), which would be consistent with a common genetic basis. However, VD and other LES traits can also vary greatly within recently evolved clades (Carlquist 1959, Givnish et al. 2005, Dunbar-Co et al. 2009), suggesting that there is available genetic variation, not necessarily of common origin, in many species. Genetic work in more species will be necessary to resolve this issue. However the advantages of studying *A. thaliana* - fully known genome, rapid growth, and small size - are

not relevant for nearly all other species. We suggest that the most progress could be made with agricultural species. Here, genomes are better known, growth is generally fast, and progress understanding LES tradeoffs could lead to potentially controversial applications for crop physiology and plant breeding.

References

Alonso-Blanco, C., A. J. M. Peeters, M. Koornneef, C. Lister, C. Dean, N. van den Bosch, J. Pot, and M. T. R. Kuiper. 1998. Development of an AFLP based linkage map of Ler, Col and Cvi Arabidopsis thaliana ecotypes and construction of a Ler/Cvi recombinant inbred line population. The Plant Journal **14**:259-271.

Alonso-Peral, M. M., H. Candela, J. C. del Pozo, A. Martinez-Laborda, M. R. Ponce, and J. L. Micol. 2006. The HVE/CAND1 gene is required for the early patterning of leaf venation in Arabidopsis. Development **133**:3755-3766.

Blonder, B., C. Violle, L. P. Bentley, and B. J. Enquist. 2011. Venation networks and the origin of the leaf economics spectrum. Ecology Letters **14**:91-100.

Boyce, C. K., T. J. Brodribb, T. S. Feild, and M. A. Zwieniecki. 2009. Angiosperm leaf vein evolution was physiologically and environmentally transformative. Proceedings of the Royal Society B **276**:1771-1776.

Brodribb, T., T. Feild, and G. Jordan. 2007. Leaf maximum photosynthetic rate and venation are linked by hydraulics. Plant Physiology **144**:1890.

Brodribb, T. J., T. S. Feild, and L. Sack. 2010. Viewing leaf structure and evolution from a hydraulic perspective. Funct Plant Biol **37**:488-498.

Carlquist, S. 1959. Vegetative Anatomy of Dubautia, Argyroxiphium, and Wilkesia (Compositae). Pacific Science **13**:195-210.

Chapin, F. S., K. Autumn, and F. Pugnaire. 1993. Evolution of suites of traits in response to environmental stress. American Naturalist **142**:S78-S92.

Donner, T. and E. Scarpella. 2009. Auxin-transport-dependent leaf vein formation. Botany **87**:678-684.

Donovan, L. A., H. Maherali, C. M. Caruso, H. Huber, and H. d. Kroon. 2011. The evolution of the worldwide leaf economics spectrum. Trends in Ecology & Evolution **26**:88-95.

Doyle, M. R., C. M. Bizzell, M. R. Keller, S. D. Michaels, J. Song, Y.-S. Noh, and R. M. Amasino. 2005. HUA2 is required for the expression of floral repressors in Arabidopsis thaliana. The Plant Journal **41**:376-385.

Dunbar-Co, S., Margaret J. Sporck, and L. Sack. 2009. Leaf Trait Diversification and Design in Seven Rare Taxa of the Hawaiian Plantago Radiation. International Journal of Plant Sciences **170**:61-75.

El-Assal, S. E. D., C. Alonso-Blanco, A. J. M. Peeters, V. Raz, and M. Koornneef. 2001. A QTL for flowering time in Arabidopsis reveals a novel allele of CRY2. Nature Genetics **29**:435-440.

Givnish, T. J., J. C. Pires, S. W. Graham, M. A. McPherson, L. M. Prince, T. B. Patterson, H. S. Rai, E. H. Roalson, T. M. Evans, W. J. Hahn, K. C. Millam, A. W. Meerow, M. Molvray, P. J. Kores, H. E. O'Brien, J. C. Hall, W. J. Kress, and K. J. Sytsma. 2005. Repeated evolution of net venation and fleshy fruits among monocots in shaded habitats confirms a priori predictions: evidence from an ndhF phylogeny. Proceedings of the Royal Society B **272**:1481-1490.

Granier, C., L. Aguirrezabal, K. Chenu, S. J. Cookson, M. Dauzat, P. Hamard, J.-J. Thioux, G. Rolland, S. Bouchier-Combaud, A. Lebaudy, B. Muller, T. Simonneau, and F. Tardieu. 2006. PHENOPSIS, an automated platform for reproducible phenotyping of plant responses to soil water deficit in Arabidopsis thaliana permitted the identification of an accession with low sensitivity to soil water deficit. New Phytologist **169**:623-635.

Keurentjes, J. J. B., L. Bentsink, C. Alonso-Blanco, C. J. Hanhart, H. B. D. Vries, S. Effgen, D. Vreugdenhil, and M. Koornneef. 2007. Development of a near-isogenic line population of

Arabidopsis thaliana and comparison of mapping power with a recombinant inbred line population. Genetics **175**:891-905.

Kikuzawa, K. 1995. The Basis for Variation in Leaf Longevity of Plants. Vegetatio **121**:89-100.

Mcmurtrie, R. E. and R. C. Dewar. 2011. Leaf-trait variation explained by the hypothesis that plants maximize their canopy carbon export over the lifespan of leaves. Tree Physiology **31**:1007-1023.

Nicotra, A. B., A. Leigh, C. K. Boyce, C. S. Jones, K. J. Niklas, D. L. Royer, and H. Tsukaya. 2011. The evolution and functional significance of leaf shape in the angiosperms. Functional Plant Biology **38**:535-552.

Noblin, X., L. Mahadevan, I. A. Coomaraswamy, D. A. Weitz, N. M. Holbrook, and M. A. Zwieniecki. 2008. Optimal vein density in artificial and real leaves. Proceedings of the National Academies of Sciences **105**:9140-9144.

Pantin, F., T. Simonneau, G. Rolland, M. Dauzat, and B. Muller. 2011. Control of leaf expansion: a developmental switch from metabolics to hydraulics. Plant Physiology **156**:803-815.

Perez-Perez, J., J. Serrano-Cartagena, and J. Micol. 2002. Genetic analysis of natural variations in the architecture of Arabidopsis thaliana vegetative leaves. Genetics **162**:893.

Reich, P., M. Walters, and D. Ellsworth. 1997. From tropics to tundra: Global convergence in plant functioning. Proceedings of the National Academies of Sciences **94**:13730-13734.

Roth-Nebelsick, A., D. Uhl, V. Mosbrugger, and H. Kerp. 2001. Evolution and function of leaf venation architecture: A review. Annals of Botany **87**:553-566.

Sack, L., C. Scoffoni, A. Mckown, K. Frole, M. Rawls, J. Christopher Havran, H. Tran, and T. Tran. 2012. Developmentally based scaling of leaf venation architecture explains global ecological patterns. Nature Communications **3**:837.

Scarpella, E., M. Barkoulas, and M. Tsiantis. 2010. Control of Leaf and Vein Development by Auxin. Cold Spring Harbor Perspectives in Biology **2**.

Shipley, B., M. J. Lechowicz, I. Wright, and P. B. Reich. 2006. Fundamental trade-offs generating the worldwide leaf economics spectrum. Ecology **87**:535-541.

Vasseur, F., C. Violle, B. Enquist, C. Granier, and D. Vile. 2012. A common genetic basis to the origin of the leaf economics spectrum and metabolic scaling allometry. Ecology Letters **15**:1149-1157.

Wright, I., P. Reich, J. Cornelissen, D. Falster, P. Groom, K. Hikosaka, W. Lee, C. Lusk, U. Niinemets, J. Oleksyn, N. Osada, H. Poorter, D. Warton, and M. Westoby. 2005. Modulation of leaf economic traits and trait relationships by climate. Global Ecology and Biogeography **14**:411-421.

Wright, I., P. Reich, M. Westoby, D. Ackerly, Z. Baruch, F. Bongers, J. Cavender-Bares, T. Chapin, J. Cornelissen, and M. Diemer. 2004. The worldwide leaf economics spectrum. Nature **428**:821-827.

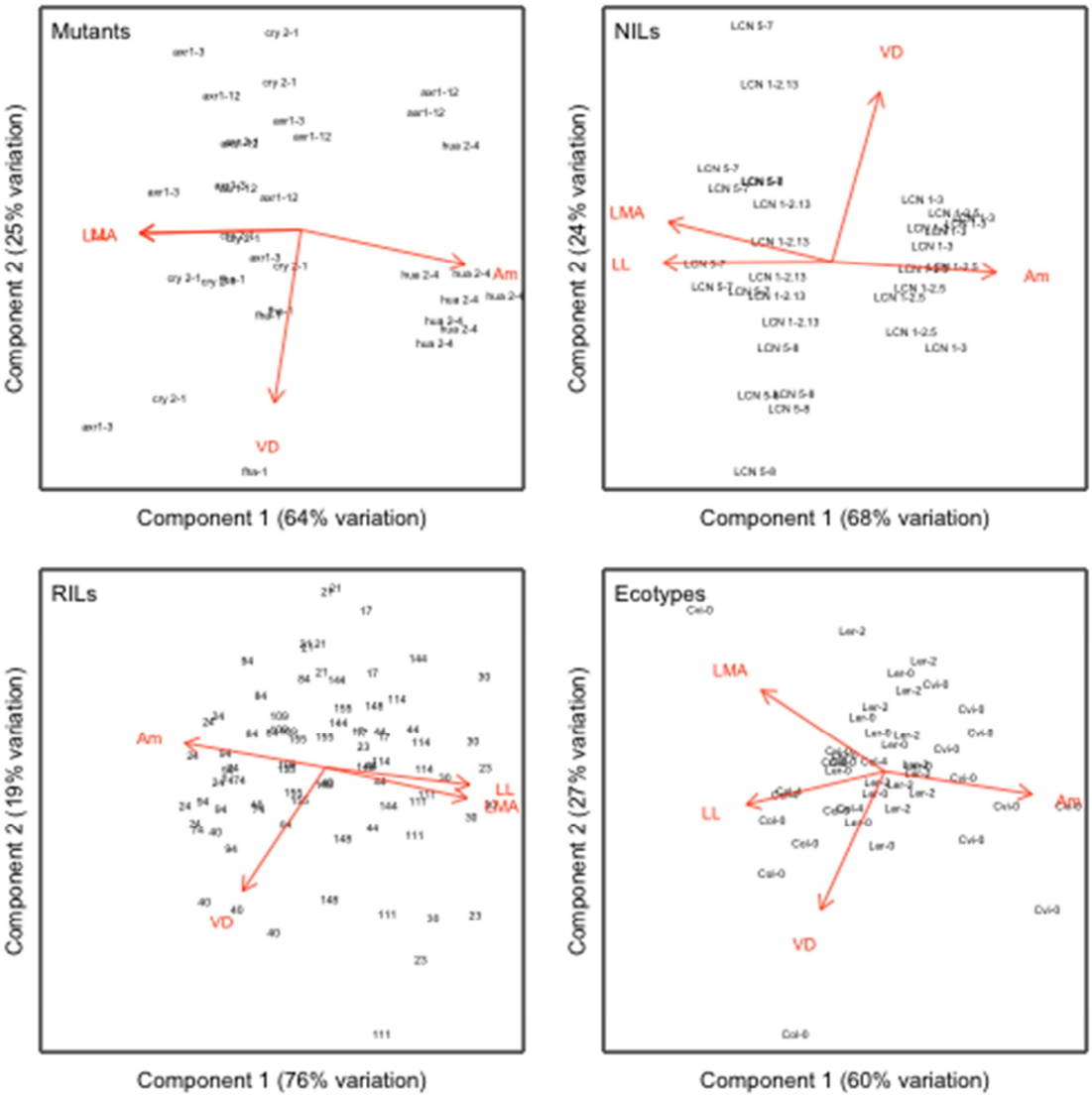

Figure S1. Principal components analysis of correlations between log_{10} transformed leaf traits. Nm was omitted from the analysis because many genotypes were not assayed for this trait. Each point represents an individual of one genotype.